AGARD-LS-207

AGARD

ADVISORY GROUP FOR AEROSPACE RESEARCH & DEVELOPMENT
7 RUE ANCELLE, 92200 NEUILLY-SUR-SEINE, FRANCE

AGARD LECTURE SERIES 207

System Implications and Innovative Applications of Satellite Navigation

(les Applications nouvelles offertes par la navigation par satellite et leurs incidences au niveau systèmes)

The material in this publication was assembled to support a Lecture Series under the sponsorship of the Mission Systems Panel of AGARD and the Consultant and Exchange Programme of AGARD presented on 1-2 July 1996 in Paris, France, 4-5 July 1996 in Rome, Italy, 8-9 July 1996 in Madrid, Spain and 11-12 July 1996 in St. Petersburg, Russia.

NORTH ATLANTIC TREATY ORGANIZATION

Published June 1996

Distribution and Availability on Back Cover

AGARD-LS-207

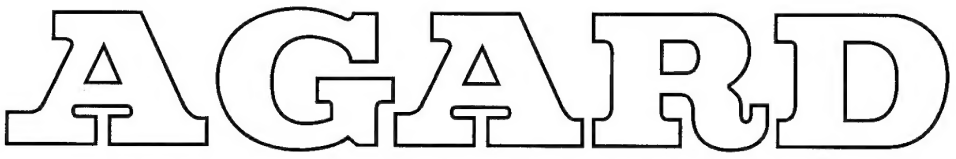

ADVISORY GROUP FOR AEROSPACE RESEARCH & DEVELOPMENT
7 RUE ANCELLE, 92200 NEUILLY-SUR-SEINE, FRANCE

AGARD LECTURE SERIES 207

System Implications and Innovative Applications of Satellite Navigation

(les Applications nouvelles offertes par la navigation par satellite et leurs incidences au niveau systèmes)

The material in this publication was assembled to support a Lecture Series under the sponsorship of the Mission Systems Panel of AGARD and the Consultant and Exchange Programme of AGARD presented on 1-2 July 1996 in Paris, France, 4-5 July 1996 in Rome, Italy, 8-9 July 1996 in Madrid, Spain and 11-12 July 1996 in St. Petersburg, Russia.

North Atlantic Treaty Organization
Organisation du Traité de l'Atlantique Nord

DISCLAIMER NOTICE

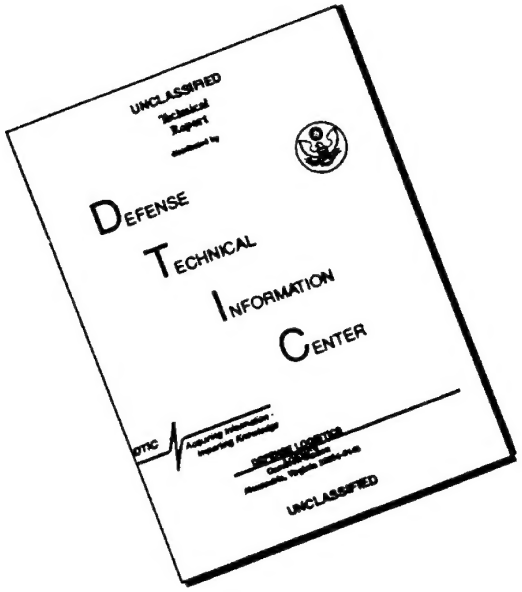

THIS DOCUMENT IS BEST QUALITY AVAILABLE. THE COPY FURNISHED TO DTIC CONTAINED A SIGNIFICANT NUMBER OF PAGES WHICH DO NOT REPRODUCE LEGIBLY.

The Mission of AGARD

According to its Charter, the mission of AGARD is to bring together the leading personalities of the NATO nations in the fields of science and technology relating to aerospace for the following purposes:

- Recommending effective ways for the member nations to use their research and development capabilities for the common benefit of the NATO community;
- Providing scientific and technical advice and assistance to the Military Committee in the field of aerospace research and development (with particular regard to its military application);
- Continuously stimulating advances in the aerospace sciences relevant to strengthening the common defence posture;
- Improving the co-operation among member nations in aerospace research and development;
- Exchange of scientific and technical information;
- Providing assistance to member nations for the purpose of increasing their scientific and technical potential;
- Rendering scientific and technical assistance, as requested, to other NATO bodies and to member nations in connection with research and development problems in the aerospace field.

The highest authority within AGARD is the National Delegates Board consisting of officially appointed senior representatives from each member nation. The mission of AGARD is carried out through the Panels which are composed of experts appointed by the National Delegates, the Consultant and Exchange Programme and the Aerospace Applications Studies Programme. The results of AGARD work are reported to the member nations and the NATO Authorities through the AGARD series of publications of which this is one.

Participation in AGARD activities is by invitation only and is normally limited to citizens of the NATO nations.

Published June 1996

ISBN 92-836-1038-5

Printed by Canada Communication Group
45 Sacré-Cœur Blvd., Hull (Québec), Canada K1A 0S7

System Implications and Innovative Applications of Satellite Navigation

(AGARD LS-207)

Executive Summary

The Global Positioning Satellite System (GPS) is now operational and GLONASS will soon be declared operational. Meanwhile, INMARSAT has announced its intent to expand its services to include navigation signals broadcast from geostationary satellites, and several industrial organizations plan to provide commercial, satellite-based, navigation services.

With prospects for reliable worldwide service becoming a reality, the technical and financial barriers to innovative applications are being overcome.

Given the possibilities available to civil and military aircraft, aircrew no longer need aeronautical documentation in order to attain their points of destination, in particular in regions where the aeronautical infrastructure remains rudimentary. Moreover, pilots will be able to land, or at least achieve the required minima, without the aid of air traffic control approach assistance.

This Lecture Series, sponsored by the AGARD Mission Systems Panel and implemented by the Consultant and Exchange Programme, will provide, prior to the entry into service of this new mode of navigation:

- an appreciation of the technical, operational and performance features of satellite-based navigation including the signal-in-space the user equipment for GPS, GLONASS, and integrated GPS/GLONASS implementations;
- an assessment of the quality of service that has been achieved and an introduction to projected service enhancements.

The introductory lecture will provide an overview of satellite-based navigation and some of the imaginative uses to which it has already been put. The application of satellite signals to precision approach and landing for civil aviation and for determination of vehicle attitude (orientation) will be featured in the following lectures. Other topics include:

- the quality monitoring of user's navigation solutions;
- the integration of satellite navigation with inertial measurements and high-precision relative and differential positioning.

Les implications pour les systèmes des applications nouvelles de la navigation par satellite

(AGARD LS-207)

Synthèse

Le Système de Navigation GPS est à présent opérationnel et le GLONASS va bientôt l'être également. En attendant, INMARSAT a annoncé son intention d'étendre ses services dans le but d'inclure la diffusion des signaux de navigation en provenance des satellites géostationnaires et, parallèlement, plusieurs organisations industrielles prévoient de fournir des prestations de service en matière de navigation afin de répondre aux besoins commerciaux.

Avec les perspectives d'un service fiable de couverture mondiale, les barrières financières et techniques pour les applications nouvelles seront maîtrisées.

Compte tenu des possibilités offertes aux aéronefs civils et militaires, les équipages pourront s'affranchir de documentations aéronautiques pour atteindre leurs points de destination, en particulier dans les régions où l'infrastructure aéronautique reste rudimentaire. De surcroît, les pilotes seront en mesure d'atterrir, ou du moins atteindre les minimas requis, sans l'aide de moyens de contrôle et de percée.

Ce Cycle de Conférences, présenté dans le cadre du programme des consultants et des échanges, sous l'égide du Panel AGARD des systèmes de conduite de mission, a pour objet, avant la mise en service de ce nouveau mode de navigation, de présenter:

- une appréciation de la réalité des performances opérationnelles et techniques de la navigation par satellite en tenant compte de la propagation des ondes dans l'espace, des récepteurs pour le GPS, le GLONASS, ainsi que de la mise en œuvre du système intégré GPS/GLONASS;
- l'évaluation de la qualité du service qui a été accomplie et une introduction à des prestations de service accrues pour l'avenir.

L'introduction fournit un aperçu de la navigation par satellite et quelques utilisations imaginatives qui ont déjà été réalisées. Les applications, pour l'Aviation Civile, des signaux en provenance des satellites pour les approches et atterrissages de précision et pour la définition du positionnement des véhicules, sont décrites dans la suite de la conférence. En outre, d'autres sujets abordent:

- la qualité de réception des sytèmes d'aide à la navigation;
- l'intégration de la navigation par satellite des systèmes inertiels, au positionnement de grande précision et différentiel.

Contents

List of Authors/Speakers

Lecture Series Director: Dr. Richard Greenspan
Draper Laboratory M/S 30
555 Technology Square
Cambridge, MA 02139-3563
USA

Dr. Yuri I. BAZAROV
State Scientific & Research Institute
for Navigation and Hydrography
Russian Ministry of Defence
41 Codgevennai Street
St. Petersburg 199106
Russia

Dr. Jacques BESER
3S Navigation
23141 Plaza Pointe Drive
Laguna Hills
California 92653
USA

Prof. Frank van GRAAS
Avionics Engineering Center
School of Electrical Engineering
and Computer Science
361 Stocker Center
Athens, Ohio 45701
USA

Dr. Gérard LACHAPELLE
Department of Geomatics Engineering
The University of Calgary
2500 University Drive NW
Calgary, Alberta
T2N 1N4
CANADA

Mr. Richard E. PHILLIPS
The Charles Stark Draper Laboratory
555 Technology Square
Cambridge, MA 02139-3563
USA

Dr. George T. SCHMIDT
The Charles Stark Draper Laboratory
555 Technology Square
Cambridge, MA 02139-3563
USA

GLOBAL NAVIGATION SATELLITE SYSTEMS

Richard L. Greenspan
Draper Laboratory
Cambridge, MA 02139

ABSTRACT

The Global Navigation Satellite System (GNSS) is the visionary goal for a world-wide utility that will ultimately provide reliable and dependable navigation and timing services to civil and national users. The enabling technology is firmly rooted in operational satellite navigation systems that have been developed for military use, including the Global Positioning Satellite System (GPS) and the Global Navigation Satellite System (GLONASS) developed in the USA and in Russia, respectively. However, the rapid acceptance into operational use by the civil community of even the degraded performance levels that have already been made available has exposed the need for additional features, as well as opportunities to exploit secondary features of the existing signals to deliver improved services. Although these additional features will be provided initially as augmentations to the existing systems, the GNSS, in whatever form it eventually takes, remains the end point toward which governments, international service providers, industry, and user groups are planning.

This introductory lecture provides an overview of the means by which individual design features of Satellite Navigation Systems are seen to satisfy the mission requirements for specific user groups, and it sets the context for the other presentations in this Lecture Series. This presentation is organized from the viewpoint of the users of the Satellite Navigation Services; it also includes a review of some applications of these services that were not even remotely anticipated by their original designers. Most of this discussion is based on the Global Positioning Satellite System.

1.0 INTRODUCTION

The development of navigation satellites dates to the late 1950s following the launch of "Sputnik," and the subsequent realization that since the orbit of that satellite could be determined from observations of the Doppler shift on the signals it broadcast as received at precisely surveyed terrestrial stations, then one should be able to determine one's own position by means of the Doppler on signals received from a navigation satellite in a well determined orbit. This led researchers at the *Applied Physics Laboratory* of *Johns Hopkins University* to propose the TRANSIT satellite navigation system, which was subsequently developed by them under funding from the U.S. Navy [1]. However, the lineage of terrestrial radio-navigation aids dates further back into the 1930's when researchers in Great Britain, Germany, and the United States conceived of the means to navigate by determining lines-of-position to fixed radio transmitters [2,3]. However, even the most optimistic extension of these pioneering techniques would not provide the services that are routinely expected by today's navigation users. The following remarks provide an overview of the ways that *user requirements* influence the architecture, operational practices, service levels, and features of satellite navigation systems.

To date, the providers of satellite navigation services have been military agencies for whom concerns about the high cost of development and acquisition activities, as well as the ongoing costs for Operation and Maintenance (O&M) of the system have been mitigated by National Security considerations and by institutional support from the civil community (most notably, the Federal Aviation Administration (FAA) in the United States). However, the reluctance of civil authorities of other nations to rely on a system that is controlled by military agencies of a foreign government has led to the search for an international civil GNSS for which issues of assured civil control, cost of ownership, and cost recovery are layered on the specification of the technical attributes of the system that will ultimately be designed.

1.1 Service Requirements for a GNSS

The first operational navigation satellite system was the United State's Navy Navigation Satellite System (TRANSIT). Initial funding was received in December 1958, and operational use began in January 1964. TRANSIT was designed to provide periodic navigation fixes to the U.S. ballistic missile-carrying submarine fleet. These position updates were used to reset the ships' inertial navigation system to counteract the cumulative effects of gyroscopic drift and anomalous gravity. TRANSIT was the means by which these updates could be made in all weather, remote from land beacons, and with enough stealth for the submarine to avoid detection by hostile forces.

TRANSIT provided the following attributes of a GNSS:

- *24-hour daily operation in all weather.*
- *Acceptable (for its mission) 2-dimensional positioning accuracy.*

However, it had the following deficiencies for adoption as a more widespread navigation service. The position updates were not *continuous*--there was up to an average of 100 minutes between successive satellite passes,* and *vehicle dynamics* were a concern because each position fix required observation of the satellite signals over 10 to 16 minutes. Therefore, TRANSIT was not well suited for users who needed

*All TRANSIT satellites broadcast narrowband signals on the same frequencies in the UHF band. The number of operational satellites was therefore usually set at five to avoid in-band interference between signals from two satellites. The limited number of active satellites is the reason that fixes were available only intermittently.

Paper presented at the AGARD MSP Lecture Series on "System Implications and Innovative Applications of Satellite Navigation", held in Paris, France from 1-2 July 1996; Rome, Italy from 4-5 July 1996; Madrid, Spain from 8-9 July 1996 and St. Petersburg, Russia from 11-12 July 1996, and published in LS-207.

continuous, instantaneous position fixes, such as aircraft and land vehicles that were not equipped with state-of-the-art inertial systems to dead reckon accurately in between satellite fixes. Nevertheless, TRANSIT rapidly became a mainstay for maritime navigation after civil user equipment came on the market, and it later enjoyed some popularity in land-survey applications. Operational support for TRANSIT by the U.S. Navy is scheduled to be discontinued in 1996.

GPS and GLONASS are current realizations of satellite navigation systems that provide *additional* benefits to their users compared to TRANSIT in the following respects:

- *CONTINUITY: There are enough GPS and GLONASS satellites, in carefully determined orbits, to guarantee continuous availability of position fixes with a specified accuracy.*
- *USER DYNAMICS: Positioning is based on time difference-of-arrival for ranging to four or more satellites. Under normal operating conditions, high-quality measurements to all these satellites can be made once per second (faster in some applications). When a higher output rate is required for high dynamics vehicles, it can be provided as the output of an integrated GPS/inertial navigation processor.*
- *ACCURACY: The three-dimensional navigation accuracy of the GPS Precise Positioning Service (PPS) is specified as 15.0 meters spherical error probable (SEP). (SEP is the radius of a sphere centered on "truth" into which half of repeated position estimates are expected to fall). Operational experience with current Block IIA GPS satellites indicates that the SEP being realized is typically 8.0 meters or less; improvements projected for implementation with Block IIF GPS satellites are expected to reduce the SEP for PPS users to 5.0 meters or less by 2010. (See LECTURE 4.)*
- *COST: Holding the cost of GPS user equipment for military aircraft to less than $10,000 was a goal set by the GPS Joint Program Office (JPO) at its inception in 1974 [4]. That goal was achieved. What was not expected was the rapid drop in the cost of hand-held military equipment to about $1200 per set (in large volumes) that was driven by the intense interest of the civil community in GPS. Hand-held civil-user sets are now available from consumer catalogs at prices lower than for television sets, washing machines, stereo receivers, and other mass-market consumer products.*

Despite these advances over the prior satellite technology, neither GPS nor GLONASS alone can satisfy other emerging requirements of civil users. Foremost among these are the requirements for:

- *SIGNALS INTEGRITY: which is the means to ensure that a user does not incorporate measurements from any satellite within a fixed interval (often taken as 10 seconds) of the onset of a failure of that satellite to provide a signal that satisfies nominal quality limits [5].*
- *SIGNALS AVAILABILITY: which is the fraction of time that a user will see enough healthy satellites, in a favorable viewing geometry, to ensure that the nominal system-level performance is available. In this context, "favorable" is measured by the geometric dilution of precision (GDOP) associated with the satellites that are visible above a specified elevation threshold [6].*

Signals integrity may be reported via the GNSS itself, or it may be determined within individual user equipments that track more than the minimum number of satellites needed to form a navigation solution. The technical literature reflects active interest in such Receiver Autonomous Integrity Monitoring (RAIM) schemes [7-9]. **LECTURE 8** in this series addresses that topic. However, increasing attention is being paid to augmenting the navigation satellite constellation with geosynchronous communications satellites that will broadcast INTEGRITY advisories immediately after any satellite failure is detected by terrestrial monitor stations [6, 10, 11].

In this regard, note that INTEGRITY was not a requirement in the development of GPS or GLONASS. Today's GPS satellites are "uploaded" once per day with messages, including satellite "health" indicators. Although the interval between uploads could be reduced to 12 hours (or less, using alternate upload stations), the 10-second goal is not realizable using the current constellation. However, the Block IIR satellites that will be launched beginning late in 1996 will have an intersatellite communication link (cross-link ranging) that will allow messages uploaded to one satellite to be relayed to the other satellites. When this capability is fully implemented, **and if** the means to detect and upload timely health advisories is added to the GPS Control Segment, then GPS may meet the integrity challenge without further augmentation. However, it is not expected that all GPS satellites will be Block IIR (or follow on) models until after 2002. Thus, there is an interest in interim augmentation techniques (e.g., WAAS [11]) using commercial satellites such as INMARSAT [12] that will provide desired levels of signals integrity sooner; perhaps as early as 1998. Meanwhile, U.S. military aircraft that fly within national airspace controlled by civil aviation authorities will also have to meet civil integrity requirements; therefore, the incorporation of RAIM in the upgrade of the standard GPS user equipment for military aircraft (MAGR) has been contracted for development.

The military designers of GPS did not set as stringent a requirement on the "AVAILABILITY" of a GPS navigation solution as the civil community. The military is willing to tolerate solutions with "poor" DOP (e.g., PDOP > 6.0) as long as they occur in less than about 1 percent of navigation trials, whereas the civil aviation community looks for availability at greater than the 99.9999 level.

The only way that the availability criterion for civil aviation will be met starting from a base of 24 GPS satellites is to augment the constellation available to users. **(See LECTURE 10.)** The introduction of user equipment that can track both GPS and GLONASS satellites is one approach to meet that goal. As noted above, another approach is to add satellites that broadcast GPS-like signals from geostationary

orbits. A variant of this approach that may be less costly is based on the observation that the greatest need for "availability" is when using satellites for precision landing of aircraft. In those circumstances, the placement of terrestrial "pseudolites" in the vicinity of airports might serve multiple functions for improving satellite visibility, uploading integrity messages, and contributing to the effective use of carrier-phase differential GPS for positioning with decimeter accuracy or better [13,14]. **(See LECTURE 7.)**

Proposals for the "augmentation" of GPS and GLONASS constellations have surfaced another feature desired by civil users that was not designed into these systems. Neither GPS nor GLONASS is intended to carry 2-way communications message traffic. In fact, one virtue of the military user equipment is that it is passive. However, if satellite-based positioning is coupled with a reporting capability, then the basis for an "automatic dependent surveillance" system is established, whereby satellite navigation also contributes to Air Traffic Control. Although there has been discussion of this feature, and some feasibility demonstrations [15], the institutional "pull" to provide the service has been relatively weak.

1.2 GPS System Design

In the following remarks, we demonstrate how the stated requirements on GPS [16] contributed to the design of the operational system. The designers of a GNSS will eventually revisit these decisions in the context of new requirements and the relaxation of other requirements that are unique to the military mission (such as selective availability, antispoofing (message encryption), nuclear hardening, and provisions for secondary payloads).

1.2.1 Constellation

The basic requirement of GPS users is that enough satellites are *visible* and arranged with the proper *geometric relation* to each terrestrial user such that accuracy goals for positioning are met when their time-delay measurements are within nominal accuracy limits. In general, the lower the satellite orbital altitude, the more satellites are needed to give any desired level of geometric strength to the navigation solution. The situation to be avoided is one in which the four (or more) satellites used in the navigation solution all lie on one plane. For example, a satellite system composed solely of equatorial geostationary satellites would have good visibility (except in polar regions) but would not be able to resolve one component of the users coordinates.

The selection of a satellite constellation is driven by the cost of launching enough satellites to ensure good visibility in the region of operations. Launch costs for low-earth orbit (LEO) are relatively low, but substantially more satellites are needed compared to higher orbits. Another strong argument against using LEO satellites is that they are visible for relatively short periods, and the user equipment must be able to distinguish and track a large number of satellites moving with high relative acceleration when they are in the user's field of view. This forces user equipment to implement relatively large tracking loop bandwidths, which, in turn, reduces the measurement signal-to-noise ratio (SNR) and the measurement quality, and also increases the possibility of a "loss of lock."

GPS satellites in 12-hour ("sidereal") inclined circular orbits, at about 10,900 nautical miles altitude have the attractive attribute that these orbits repeat twice daily at any terrestrial location (with about 4 minutes offset caused by the difference between the solar day and the sidereal day). This is a particularly nice feature for experimenters who want repeatability of test conditions. (In fact, the constellation was configured during the development phase to give the maximum useful daily visibility at the GPS test site in Arizona.) In general, the number of satellites, the inclination of their orbits, and the number of orbital planes reflect an optimization among a number of factors including launch costs, opportunities for launch, and ground coverage (GDOP).

Maximizing the visibility of satellites argues that each satellite antenna should provide full earth coverage (28-degree main beam width). The GPS antenna beamwidth is actually about 50 percent wider (about 43 degrees at L1), so that some energy can be received by users who would otherwise be shadowed by the Earth. The antenna beam is also tapered to deliver approximately constant power to terrestrial users at nadir out to the satellite horizon [17].

1.2.2 Signal Structure

The GPS satellites broadcast signals have the following features:

- *Signals from different satellites create the least possible mutual interference at each user set.*
- *The measurement SNR exceeds a threshold value.*
- *The widest signaling bandwidth is available to make the most precise time delay measurements.*

1.2.2.1 Multiple Access

Signal design for GPS is a classical example of a multiple-access communication application in which all satellites share the available signaling bandwidth. The leading alternatives separate signals either in time slots (TDMA), in frequency slots (FDMA), or by code division (CDMA).

TDMA can satisfy all three requirements listed above, but suffers from a relatively high ratio of peak-to-average transmitted power, which reduces the efficiency of the satellite transmitter (more prime power must be provided). In addition, the time slots allocated to each satellite have to be designed to prevent interference between signals received by any user. The resulting time offset between signals received from different satellites can be large enough to degrade the navigation solution for high dynamics users. An equivalent effect was seen in some early versions of single-channel sequential GPS receivers.

FDMA with pseudorandom phase shift keying is the choice for GLONASS. **(See LECTURE 2.)** It can satisfy the first two requirements, but since the uncertainty of the basic ranging

measurement is (inversely) proportional to the bandwidth occupied by the ranging signal, it is inherently less precise than either TDMA or CDMA signals that occupy the same frequency allocation. FDMA is most attractive in that the signals broadcast by **all** satellites can be identical (except for their frequency slot), thereby simplifying the design of the satellite electronics and the code generation function of the user equipment. However, the receiver must provide parallel processing channels for the different satellite frequency slots. (This was believed by GPS designers to cause a significant cost penalty compared to CDMA). Other benefits of the FDMA approach are that efficient use of satellite prime power is made because the ratio of peak-to-average transmitted power is unity and the signals are continuous, so coherent integration can be applied to increase the measurement SNR and to resolve small differences in Doppler shift (i.e., to make precise carrier phase (velocity) measurements).

GPS receivers distinguish satellite signals by their unique phase and code modulated carrier structure (CDMA). The codes were selected after an exhaustive search procedure to minimize the maximum interference one satellite will create for the reception of signals from another satellite over the whole range of delay and delay rate differences. The CDMA signals are continuous and their peak-to-average transmitter power ratio is unity. They are similar to FDMA signals in that coherent integration can be applied to build up the measurement SNR and to resolve small Doppler differences.

1.2.2.2 Frequency Allocation

Other features of the GPS (and GLONASS) signals are: 1) the selection of an L-band frequency allocation; 2) the identical modulation of two widely separated carrier tones for the purpose of measuring the excess propagation delay at L-band, caused by the passage of the satellite signals through the ionosphere; 3) the independent modulation of coarse acquisition and precision ranging signals in quadrature on these carriers; and 4) the modulation of low bandwidth data to be used in forming the GPS navigation solutions on the CDMA modulated carriers.

The L-band frequency allocation(s) for satellite navigation were available, and relatively few high-power radio services that might interfere with navigation signals were active in that band as of 1973. In addition, the carrier frequency is high enough that the directional (earth coverage) antenna on the satellite can be realized within the diameter of the spacecraft. Compared to UHF bands used for TRANSIT, the propagation effects of excess ionospheric delay and variability of that delay are smaller, and the sensitivity of L-band to attenuation from atmospheric water vapor is less than at higher microwave frequencies as well as is the free-space propagation loss for omnidirectional user antennas. For these reasons, L-band was an attractive compromise choice. In fact, it is so attractive to other servic es that by the 1990s, the mobile radio industry has petitioned for L-band frequency allocations that might potentially interfere with satellite navigation services. (GLONASS signals will move to a slightly lower frequency band as a preventative measure.)

1.2.2.3 Signal Power

The strongest GPS signal received at the surface of the earth is specified to be the L1 C/A code signal at -160 dBW [17]. This signal is approximately 30 dB weaker than receiver noise in the broadcast signal bandwidth. The GPS receiver separates the modulated GPS signal from the background noise by a cross-correlation process that collects all of the GPS energy in a narrow bandwidth (a few Hz) while retaining only about half of thermal noise added by the receiver in that small bandwidth. The post-correlation SNR is typically in the range of 38 to 42 dB in a 1-Hz bandwidth.

It seems intuitively reasonable that GPS users could gain further benefit versus receiver noise or interfering signals (intentional or unintentional) if the power transmitted by each satellite were increased. This option is not realizable because the power received by terrestrial GPS users is limited by international agreements on spectrum utilization, and by the fact that low-cost user equipment is provided with omnidirectional antennas to receive signals from satellites at arbitrary elevation and azimuth.

The international agreement (International Telecommunication Union (ITU)) specifies that satellite broadcasts in the frequency band from 1.525 GHz to 2.5 GHz shall produce a power density flux of no more than -154 dBW/meter^2 in any 4-kHz bandwidth [18]. This is to prevent interference to terrestrial line-of-sight microwave communication links that operate in that band. Now, the effective receiving area of an omnidirectional antenna at the GPS L1 frequency is -25.4 dB relative to 1 meter^2. If the C/A code GPS power is -160 dBW into a 1.023-MHz bandwidth , the maximum GPS power density flux in a 4-kHz bandwidth is:

$$-160 \text{ dBW } -34.1 \text{ dB} + 25.4 \text{ dB/m}^2 = -158.7 \text{ dBW/m}^2$$

According to this calculation, the C/A code margin versus the ITU specification is only 4.7 dB. Block IIA satellites have actually been broadcasting C/A signals that are received into a 0-dB gain antenna at about -157 dBW, which is 3 dB higher than the specified value; hence, the operating margin versus the ITU Specification is reduced to less than 2 dB for those satellites. This indicates that there is little margin for further increases in the power broadcast by GPS satellites. In another interference control action, the GPS broadcast signal is filtered to limit emissions in several frequency bands used by radio astronomers [19].

1.2.3 Satellite Control and Operations

The mission of the GPS Control Segment is to monitor the satellite constellation, disseminate timely data on satellite performance to GPS users, and to take all required actions to maintain the availability of nominal system performance to these users. The most visible actions of the Control Segment have been the daily uploads of GPS data messages to each satellite. Experience has shown that the specified system performance can be met on this upload schedule, even though more frequent uploads could be made. Several

factors are converging to drive a reconsideration of that policy.

- *Interest in reducing navigation errors to support precision delivery of GPS-assisted weapons.*
- *The introduction of cross-link ranging on Block IIR satellites.*
- *The requirement for military aircraft equipped with GPS to satisfy "signals integrity" requirements for operations in CONUS. This is a new need that was not anticipated during the initial design of the system.*

The first item focuses attention on measurements that show that the GPS user's error budget is dominated by systematic errors in the broadcast ephemeris. Foremost among these is unmodeled satellite clock drift. This observation is the basis for recent proposals to improve the point positioning accuracy of GPS PPS users by refreshing the downlinked satellite data on the order of a few hours or less [20,21]. The second item addresses one means to implement more frequent message uploads, and the last factor gives further motivation for taking actions that enable the GPS system to satisfy a new operational requirement without recourse to large investments in system augmentations.

1.3 Signals Exploitation

GPS was primarily viewed as a point positioning system. The fact that user velocity could also be determined from line-of sight RF carrier (Doppler) measurements using the same equations that relate user position to line-of-sight time delay measurements was understood, and the performance level for velocity measurement accuracy was set at 0.1 meters/second for each axis.

However, the exploitation of carrier-based measurements initially received little visibility in military applications, perhaps because the carrier tracking loops were viewed as being particularly vulnerable to loss-of-lock in high dynamics or by signals interference. The carrier-tracking loop was viewed primarily as the source of "velocity aiding" to the code-tracking loop, by which means the code loop bandwidth could be reduced. In addition, most aircraft installations coupled GPS with an Inertial Navigation System that was intended to "aid" the code loops whenever the carrier loop lost lock. **(See LECTURE 6.)**

However, by the early 1980s, various civil and military organizations had demonstrated that carrier-phase measurements were the key to attitude determination using interferometric processing of GPS signals received at two or more antennas **(See LECTURE 5)**, and to the positioning of one receiver relative to another with accuracies on the order of a few hundredths of the L-band wavelength. It was also realized that the same cancellation of "common mode" errors that underlay relative positioning using carrier phase measurements also worked to allow relative positioning at the 1- to 5-meter level using code delay measurements. This concept for "Differential GPS" (DGPS) was immediately and aggressively adopted by the civil community as a countermeasure to "selective availability," and serves as the basis for emerging industries that provide "differential corrections" to their GPS customers. By these means, the civil community can provide its members with (relative) positioning services that are comparable to or better than the point positioning accuracy provided to "authorized" military users of GPS. **(See LECTURE 9.)**

The gist of these remarks is that the GPS signals in space support a wide range of applications, some of which were not envisaged by the system designers, and some of which the GPS operators may regret. It is incumbent on designers of a future GNSS to anticipate the uses to which their signals will be put, and to take early action to foster those applications.

At this point, we move on to discuss some of the innovative uses for a GNSS. The discussion is based on some emerging applications of GPS that are already identified.

2.0 APPLICATIONS OF GPS

GPS currently provides precise, repeatable position, velocity, and time to properly equipped users at any time, in any location having line-of-sight visibility to four or more satellites, and under all but the most severe weather conditions. The evolution of this service to a GNSS that is fully accessible to all civil users is the vision that drives the world-wide community of users and service providers. Although GPS and GLONASS owe their existence to military sponsorship, they incorporate features that are so attractive that sales in the civil market will exceed military sales by an order of magnitude by the year 2000 [22].

2.1 High-Precision Applications

Carrier-tracking measurements on GPS signals typically resolve the line-of-sight delay to each satellite to within one-hundredth of a cycle (absent interference). This corresponds to an equivalent ranging precision of about 2 millimeters. However, these carrier-phase measurements are ambiguous; the integer number of wavelengths in each observable is undetermined. By the early 1980s, surveyors realized that these "ambiguities" could be resolved for closely-spaced, stationary antennas with an acceptable amount of observation time and computational burden. This initiated the development of centimeter-level relative positioning that finds its expression in the applications listed below.

2.1.1 Survey and Geographic Information Systems

The survey community has provided the greatest drive toward developing high-precision, high-accuracy relative positioning by means of carrier-phase DGPS. The earliest demonstrations of these techniques for static positioning were done by MIT and Draper Laboratory [23,24] under sponsorship of the U.S. Air Force Geophysics Laboratory in 1980-1982, and by JPL [25,26]. Counselman (MIT) demonstrated the use of interferometric processing of GPS signals to determine vector baselines defined by the phase-centers of GPS antennas. His measurements introduced the use of broad-band cross-correlation values of these signals, which were sampled and processed using Very Long Baseline Interferometry (VLBI) instrumentation previously developed for the radio astronomy community. MacDoran (JPL) did

similar work independently. At the same time, the Draper Laboratory group, with the collaboration of Counselman, demonstrated the first use of post-correlation carrier-phase interferometry.

These earliest experiments implemented a "connected element interferometer," in which signals from each antenna were processed using a common clock. Interferometry evolved through the 1980s to measure widely spaced baselines; the "double-differencing" technique was developed to suppress the effect of individual clocks on the observables, and attention shifted to developing the means to resolve "carrier-phase ambiguities" for long static baselines [27,28]. Contemporary research is extending those techniques to dynamically changing baselines, under the rubric of "kinematic DGPS" [29,30]. The payoff of these techniques for surveying is to reduce the time and cost of each survey.

A major attraction of GPS for surveyors or agencies responsible for Geographic Information Systems (GIS) development is that it is readily adapted to operations in rough terrain in which "traditional" techniques involving line-of sight methods are awkward or impossible (e.g., locating hazards or resources in bodies of water).

2.1.2 Civil Aviation

Civil aviation authorities have been exploring the use of GPS navigation in all phases of flight. GPS is now approved as a "primary means" of navigation in oceanic and remote areas [11], and is on the way to that certification for en-route and terminal area navigation. Administrative actions are being taken to realize these goals [31 - 35].

The leading edge of contemporary activity to apply GPS in civil aviation deals with the most stringent requirements for Precision Approach and Landing. GPS is being shown capable of providing height information that is accurate to better than 7 inches as required for Category III Autoland operations. Several techniques involving beacons or pseudolites, or retransmission of GPS signals from repeaters located in the vicinity of airport runways have been evaluated [36-38]. The rapid pace for insertion of GPS into operational use by the aviation community has been unprecedented.

2.1.3 Agriculture

The commercial success of satellite navigation signifies the emergence of a new era in which submeter-level accuracy is seen as a revenue enhancer and an enabling technology in applications that have traditionally been technology averse. Most notable in this regard are the applications of precision navigation to agriculture. Industry and universities are pioneering the development of equipment with which fields are ripped and furrows are plowed, seeded, and cultivated using machinery that is navigated by DGPS along preplanned trajectories to accuracies of a few millimeters [39-41]. Other innovative applications to farming and animal husbandry include the automated dispensing of pesticides and hazardous chemicals from aircraft without the need to place humans at risk on the ground, and tracking livestock as well as wild animals [42].

2.2 Attitude Determination

It was noted in the earliest demonstrations of GPS interferometry that vector baselines were being determined. It follows that, if the baseline length (magnitude) is known in advance, then the orientation of the baseline is determined from the interferometric measurements [43]. This observation was responsible for interest in applying GPS attitude determination in circumstances where inertial techniques would be unavailable (e.g., in space) or too costly. However, most researchers soon discovered that their devices did not achieve the "noise-limit" for measurement accuracy [44-46]. The common wisdom today is that the individual carrier-phase measurements are limited by multipath distortion to a few centimeters. The search is on for ways to reduce these effects. (**See LECTURE 5.**) Some progress has been made in using signal processing to limit multipath errors; the ultimate solution may involve a combination of improved carrier-phase estimation techniques *and* careful selection of the measurements that are incorporated in the attitude determination to suppress those that are most corrupted by multipath.

2.3 Timing

The discussion to this point has emphasized the uses of GPS in navigation and control applications. However, GPS is the means by which unprecedented synchronization of remote clocks can be implemented. AT&T in the United States has used GPS to synchronize its network timing nodes for several years, and other telecommunications service providers are investigating that application [47,48]. We have even heard that some producers of (rock) concert videos have been using GPS to time-tag recordings at individual microphones to simplify post-concert sound mixing. The technical "quality" of power on some distribution grids is another beneficiary of the inexpensive means to synchronize measurements at widely separated locations [49]. Unique military applications of precise timing are also numerous, including time-tagging signal intercepts for radio emitter location, as an element of security systems, and as an element of LPI systems design.

2.4 Vehicular Applications

One limitation of GPS is that the signals can be obstructed by terrain, foliage, or by cultural objects, such as tunnels or buildings in an urban environment or in mountainous terrain. When the signal masking is intermittent, the integration of GPS with other sensors may provide the "flywheel" to maintain satisfactory performance until the signals are reacquired. For example, vehicles traveling along defined roads can combine odometers with electronic maps to provide satisfactory navigation during GPS outages. Similar instrumentation offers a solution to outages in tunnels; few drivers need to know their position to within GPS accuracy in those circumstances. The true benefit of these other sensors is likely to be to limit the growth of navigation errors during the outage to an amount for which

rapid reacquisition of GPS is available when the vehicle clears the outage.

Other vehicular applications of GPS include precise positioning reports for calling emergency services to an accident, a remote fire, or to a rescue scene. The military equivalent of these applications is battlefield medical triage, in which GPS provides the locations of the wounded whose need for medical attention is prioritized by the medics.

2.5 Unusual Applications

In addition to the obvious application of GPS to surveying, GIS, aircraft and ships navigation, and military applications, the civil community has been aggressively using GPS in novel ways. Some of the interesting applications of GPS reported in the last few years include:

- *Resource Management and Conservation:*
  - The locations of individual Redwood trees in Sequoia National Forest were determined and compiled into a Forestry data base [50].
  - Wild animals are tracked and their habits are determined using miniature GPS and communications equipment [51].
  - The evolution of oil spills has been tracked with GPS equipped buoys [52].
  - Ocean drilling is aided by the use of GPS to position the drill platform precisely at previously explored locations [53].
  - Treasure hunters or scientists can accurately return to productive locations on an otherwise featureless ocean.
  - Archaeologists can do rapid surveys in rough terrain that is difficult to survey by conventional means.
- *Vehicular Navigation:*
  - GPS combined with electronic maps informs drivers who are not familiar with a particular neighborhood [54].
  - GPS combined with an interrogate/respond system is the basis for automatic determination (and collection) of tolls on limited-access highways, bridges, and tunnels [55].
  - DGPS-based vehicles can precisely navigate robotic equipment for hazardous missions such as nuclear waste disposal, mine disposal, pesticide and fertilizer dispersion [56].
  - Dispatch of emergency equipment [57].
  - Monitoring locations of vehicle fleets. For example, bus riders may be provided precise information about the next arriving bus, or trucks can be rerouted to avoid hazards or to gain some economic advantage [58].
- *Athletics and Recreation*
  - GPS is being used to assist golfers by determining the precise yardage to the next hole. Once can speculate about public acceptance of a GPS guided golf-ball *but the enabling technology is not too far beyond today's means.*
  - GPS has been used in glider competitions to prove that pilots have complied with route requirements [59].
  - Hikers and campers can benefit from GPS when venturing into unfamiliar territory [60].
  - Fishermen can return to unmarked waters where fishing has previously been good.

3.0 CONCLUSION

The long-term trend in GPS user equipment is towards reduced volume, weight, power consumption, and cost. Sets will become more competent, using redundancy management to eke the most reliable navigation solutions from available satellite observations, and they will be embedded into larger systems whose primary purpose is not navigation. The GPS/GNSS technology will become so common that, to paraphrase the words of Bradford Parkinson, who was the first director of the GPS JPO:

> *"As the applications expand, GNSS will touch every citizen of the world in ways that even today, are not yet fully appreciated [61]."*

In fact, the day is likely to arrive when GNSS is so routinely integrated into daily life that the paradoxical situation arises that Navigation "disappears" as an active intellectual discipline, whereas its practice flourishes in applications that are transparent to the user.

REFERENCES

1. Parkinson, B.W. et al., "A History of Satellite Navigation," NAVIGATION, Vol. 42, No. 1, Spring 1995, pp. 109 - 164.
2. Stuart, D.M., "The Omnidirectional Range," Aero Digest, June 15, 1945.
3. Williams, J.E.D., "From Sails to Satellites," Oxford University Press, Oxford, England, 1992. Chapter 12, SONNE/CONSOL, pp. 224 - 225.
4. [Ed.] Parkinson, B.W., Spilker, J.J. et al., "Global Positioning System: Theory and Applications," AIAA, Washington D.C., January 1996, p. 9.
5. Brown, A. K., "Civil Aviation Integrity Reqirements for the GPS," NAVIGATION, Vol. 32, No. 1, Spring 1988, pp. 23 - 40.
6. Phlong, W.S., Elrod, B.D., "Availability Characteristics of GPS and Augmentation Alternatives," NAVIGATION, Vol. 40, No. 4, Winter 1993/94, pp. 409 - 428.
7. Brown, R.G., Hwang, P.Y.C., "GPS Failure Detection by Autonomous Means within the Cockpit," NAVIGATION, Vol. 33, No. 4, Winter 1986/87, pp. 335 - 353.

8. Brown, R.G., "A Baseline RAIM Scheme and a Note on the Equivalence of Three RAIM Methods," Proceedings of ION National Technical Meeting, (San Diego California) Institute of Navigation, Washington D.C., Jan. 27-29, 1992, pp. 127 - 138.

9. Misra, P., et al., "RAIM of GPS and GLONASS," NAVIGATION, Vol. 40, No. 1, Spring 1993, pp. 87 - 104.

10. Kinal, G.V., Sing, J.P., "An International Geostationary Overlay for GPS and GLONASS," NAVIGATION, Vol. 37, No. 1, Spring 1990, pp. 81 - 94.

11. Lundberg, O. , "Waypoints for Radio Navigation in the 21st Century," Proceedings ION GPS-94, (Salt Lake City, UT) Institute of Navigation, Alexandria VA, Sept. 20 - 24, 1994, pp. 3- 15.

12. Loh, R., et al., "The U.S. Wide Area Augmentation System (WAAS)," NAVIGATION, Vol. 42, No. 3, Fall 1995, pp. 435 - 465.

13. Klein, D., Parkinson, B.W., "The Use of Pseudo-Satellites for Improving GPS Performance," NAVIGATION, Vol. 31, No. 4, Winter 1984/85, pp. 303 - 315.

14. Cobb, H.S., Cohen, C., Parkinson, B.W., "Theory and Design of Pseudolites," Proceedings, ION National Technical Meeting, (San Diego, CA) Institute of Navigation, Alexandria VA, Jan. 24-26, 1994, pp. 69 - 75.

15. Bayliss, E., et al., "Aircraft Surveillance Based on GPS Position Broadcasts from Mode-S Beacon Transponders," Proceedings ION GPS-94, (Salt Lake City, UT) Institute of Navigation, Alexandria VA, September 20 - 24, 1994, pp. 939-950.

16. op. cit. (Ref. 4) pp. 29 -31.

17. Anon., "Interface Control Document GPS-ICD-200, with IRN-200B-PR001," Department of the Air Force (U.S.) , July 1, 1991.

18. Anon., "Protection of Terrestrial Line of Sight Radio-Relay System Against Interference," ITU, CCIR - Report 941.

19. Ponsonby, J.E.B., "Spectrum Management and the Impact of the GLONASS and GPS Satellite Systems on Radio Astronomy," JOURNAL, Royal Institute of Navigation, Vol. 44, No. 3, 1992.

20. Butts, J., Shank, Capt. C., "Navigation Message Correction Tables: A Proposal," Proceedings, ION National Technical Meeting, (Anaheim, CA), Institute of Navigation, Washington DC, January 18-20, 1995, pp. 97 - 104.

21. Brottlund, B., Harris, C., Shank, Capt. C., Navigation Message Correction Tables: On-Orbit Results," Proceedings ION Annual Meeting (Colorado Springs, CO) Institute of Navigation, Alexandria VA, June 5 - 7, 1995, pp. 413 - 428.

22. Anon. "The Global Positioning System, A Shared National Asset," National Academy Press, Washington DC, 1995.

23. Counselman, C.C. III, et al., "Accuracy of Relative Positioning by Interferometry with GPS: Double-Blind Test Results," Proceedings of the Third International Geodetic Symposium on Satellite Doppler Positioning, New Mexico State University, Las Cruces, NM, Feb. 8 - 12, 1982, pp. 1173 - 1176.

24. op. cit. (Ref 23) Greenspan, R.L., et al., "Accuracy of Relative Positioning by Interferometry with Reconstructed Carrier GPS: Experimental Results", pp. 1177 - 1196.

25. op. cit. (Ref 23) MacDoran, P.F., et al, "SERIES; Satellite Emission Range Inferred Earth Surveyor," pp. 1143 - 1164.

26. MacDoran, P.F., et al., "Codeless GPS System for Positioning of Offshore Platforms and 3D Seismic Arrays," NAVIGATION Vol. 31, No. 2, SUMMER 1984, PP. 57 - 69.

27. op. cit. (Ref 23) Hatch, R., "The Synergism of GPS Code and Carrier Measurements," pp. 1213 - 1232.

28. Remondi, B.W., "Performing Centimeter-Level Surveys in Seconds with GPS Carrier Phase: Initial Results," NAVIGATION, Vol. 2., No. 4, Winter 1985/86, pp. 386 - 402.

29. Wong, R.V.C., Schwartz, K.P., Cannon, M.E., "High Accuracy Kinematic Positioning by GPS-INS," NAVIGATION, Vol. 35, No. 2, Summer 1988, pp. 275 - 288.

30. Hwang, Patrick Y.C., "Kinematic GPS for Differential Positioning: Resolving Integer Ambiguities on the Fly," NAVIGATION, Vol. 38, No. 1 Spring 1991, pp. 1 - 16.

31. Kelly, R.J., Davis, J.M., "Required Navigation Performance for Precision Approach and Landing with GNSS Application," NAVIGATION, Vol. 41, No. 1, Spring 1994, pp. 1 - 30.

32. Anon., "RTCA Task Force Report on the Global Navigation Satellite System (GNSS) Transition and Implementation Strategy," Prepared by RTCA/TF-1, Sept. 1992.

33. Anon., "User Requirements for Future Communications, Navigation, and Surveillance, Including Space Technology Applications," RTCA/DO-193, Sept. 1986.

34. Anon., "Airborne Supplemental Navigation Equipment Using the Global Positioning System (GPS) ," Federal Aviation Administration, TSO C-129, Dec. 10, 1992.

35. Wullschleger, V., et al., "Curved Precision Approach Flight Tests with GPS Integrated into a State-of-the-Art-Avionic Suite," Proceedings ION GPS-92, (Albuquerque, NM) Institute of Navigation, Washington DC, Sept. 16 - 18, 1992, pp. 363 - 371.

36. van Graas, F., Diggle, D.W., Hueschen, R.M. "Interferometric GPS Flight Reference/Autoland System: Flight Test Results," Proceedings ION GPS-93 (Salt Lake

City, UT) Institute of Navigation, Alexandria VA, Sept. 22-24, 1993, pp. 855-870.

37. Cohen, C.E. et al., "Real-Time Flight Test Evaluation of the GPS Marker Beacon Concept for Category III Kinematic GPS Precision Landing," Proceedings of ION GPS-93, (Salt Lake City, UT), Institute of Navigation, Alexandria VA, Sept 22-24, 1993, pp. 841 - 849.

38. Cohen, C.E., et al., "Preliminary Results of Category III Precision Landing with 110 Automatic Landings of a United Boeing 737 Using GNSS Integrity Beacons," Proceedings ION National Technical Meeting, Anaheim, CA, Jan. 18 - 20, 1995, pp. 157 - 166.

39. Palmer, R.J., "Techniques of Navigating in a Farm Field," NAVIGATION, Vol. 36, No. 4, Winter 1989-90, pp. 337 - 344.

40. LaChapelle, G., et al., "GPS System Integration and Field Approaches in Precision Farming," NAVIGATION, Vol. 41, No. 3, Fall 1994, pp. 323-336.

41. Dedes, G., Goad, C., "Real Time Centimeter Level GPS Positioning of Cutting Blades and Earth Moving Equipment," Proceedings ION National Technical Meeting, (San Diego, CA) Institute of Navigation, Alexandria VA, Jan. 24 - 26, 1994, pp. 69 - 75.

42. Roberts, G., "A Low-Power Portable Post-Processed DGPS Package for Precise Position-Logging of Sheep on Hill Pastures," Proceedings, ION GPS-93, (Salt Lake City, UT) Institute of Navigation, Alexandria VA, Sept. 22 - 24, 1993, pp. 1141 - 1148.

43. Brown, A.K., "Interferometric Attitude Determination Using the GPS: A New Gyrothrodolite," Proceedings, Third International Geodetic Symposium on Satellite Doppler Positioning, New Mexico State University, Las Cruces NM, Feb. 8 - 12, 1982, pp. 1289 - 1304.

44. van Graas, F., Braasch, M., "GPS Interferometric Attitude and Heading Determination: Initial Flight Test Results," NAVIGATION, Vol. 38, No. 4, Winter 1991/92, pp. 297 - 316.

45. Cohen, C.E., Parkinson, B.W., McNally, B.D., "Flight Tests of Attitude Determination Using GPS Compared Against an Inertial Navigation Unit," NAVIGATION, Vol. 41, No. 1, Spring 1994, pp. 83 - 98.

46. Kruczynski, L., Li., C.P., "Using GPS to Determine Vehicle Attitude," Proceedings ION GPS-88 (Colorado Springs, CO) Institute of Navigation, Washington D.C., Sept. 19 - 23, 1988, pp. 139 - 146.

47. Butterline, E., Abate, J.E., Acampette, G.P., "Timing a National Telecommunication Network Using GPS ," Oral Presentation at ION GPS-92, (Albuquerque, NM) Institute of Navigation, Washington D.C., Sept. 16-18, 1992.

48. Allan, D., Kusters, J., Gifford, R., "Civil GPS Timing Applications," Proceedings ION GPS-94, (Salt Lake City, UT) Institute of Navigation, Alexandria, VA, Sept. 20 - 24, 1994, pp. 25 - 32.

49. Wilson, R.E., Sterlina, P.S., "GPS Synchronized Power System Phase Angle Measurements," Proceedings ION GPS-93, (Salt Lake City, UT) Institute of Navigation, Alexandria VA, Sept . 22 - 24, 1993, pp. 1149 - 1155.

50. Johanssen, S., "GPS in Swedish Forestry," Proceedings ION GPS-94, (Salt Lake City, UT) Institute of Navigation, Alexandria VA, Sept. 20 - 24, 1994, pp. 79 - 83.

51. Rogers, A.R., Anson, Peter, "Animal-Borne GPS: Tracking the Habitat," GPS World, Vol. 5, No. 7, July 1994, pp. 20- 32.

52. Lehr, W.J., Simecek-Beatty, D., "Slick Work: GPS Stalks the Oil Spill," GPS World, Vol. 5, No. 9, Sept. 1994, pp. 20-29.

53. Saether, K.H., et al., "Towing the Troll: Positioning a North Atlantic Gas Platform," GPS World, Vol. 6, No. 10, Oct. 1995, pp. 20-32.

54. Krakiwsky, E.J., Bullock, J.B., "Smart Vehicles: Digital Data-Putting GPS on the Map," GPS World, Vol. 5, No. 5, May 1994, pp. 43-46.

55. Albrecht, U., Widl, A., Weber, G., "Electronic Toll Collection Based on GPS," Proceedings ION GPS-94, (Salt Lake City, UT) Institute of Navigation, Alexandria VA, Sept. 20 - 24, 1994, pp. 205 - 209.

56. Wendling, M.A., Wade, C.D., "Rad Rover: GPS Visits the Hot Spots," GPS World, Vol. 5, No. 5, May 1994, pp. 20 - 26.

57. Lacy, N., Cameron, M., "Mayday in the Rockies: Colorado's GPS-Based Emergency Vehicle Location System," GPS World, Vol. 6, No. 10, Oct. 1995, pp. 40 - 47.

58. Braun, M., Remer, M., "Travelink: Getting Minneapolis to Work on Time," GPS World, Vol. 6, No. 10, Oct. 1995, pp 48 - 52.

59. Blackburn, A., "A Soaring Success: World-Classs Gliders Chart Winning Routes with GPS," GPS World, Vol. 6, No. 7, July 1995, pp. 26 - 34.

60. Wolper, J., et al., "Multisensor GPS-Based Recreational Trail Mapping," (Salt Lake City, UT) Proceedings ION GPS-94, Institute of Navigation, Alexandria VA, Sept. 20 - 24, 1994, pp. 237 - 244.

61. Parkinson, B.W., "Overview," "Global Positioning System," Vol. 1, Institute of Navigation, Washington D.C., 1980, p.1.

Introduction to

Global Navigation Satellite System

Dr. Y. Bazarov

State Scientific and Research Institute for Navigation and Hydrography,
Ministry of Defence

Codgevennai st. 41, St. Petersburg, 199106, Russia

SUMMARY

Russian Global Navigation Satellite System (GLONASS) is a space-based positioning, velocity, and time system. In this lecture the evolution of GLONASS towards opertional status is presented.

The operational constellation, the constellation maintenance plan and replenisment policy, coverage and dilution of precision factors are described along with Russian National Policy for user access to the service.

The lecture addresses the characteristics of GLONASS broadcast signals in space including modulation technique, code structure, message content and formats, Navigation accuracy achieved by GLONASS users, differential technique, user equipment performance, future GLONASS upgrades and applications of GLONASS in Commonwealth of Independent States are described.

1. GLONASS HISTORY

Global navigation satellite system is the system of the second generation in the row of the navigation satellite systems in Russia. Development and design of GLONASS bigan in the mid of 1970s, and the first satellite was launched in October 12, 1982 (COSMOS 1413). The Russian experts who were ingaged in design of GLONASS represent all the major institutes and enterprises that have taken part in designing and building of GLONASS, including the Russian Space Agency (RSA), the Military Space Forces (MSF), Scientific and Manufacturing Association of Applied Mechanics (SMA AM), the Scientific Research Institute of Space Device Engineering (SRI SDE), the Russian Institute of Radionavigation and Time (RIRT), the Central Scientific Research Institute of Machine Building and the Moscow Aviation Institute.

GLONASS was originally envisioned as being able to satisfy naval requirements for coordinate/time support.

Its the first task now is to provide continuous global navigation/time support to an unlimited number of military users on land, in the air, at sea, or in space.

In line with its military nature, the Russian Ministry of Defense is both the principal user and the owner of GLONASS. Within the Ministry of Defense responsibility for GLONASS policy and operation falls under the Military Space Forces. MSF have management responsibility for the GLONASS areas outlined below:
- System Control Center
- Master System Time Clock
- Command and Tracking Stations
- Quantum-optical tracking stations.

There is one more important division in MSF - Coordinated Research and Information Center (CRIC). The center is designed to answer user questions regarding to:
- information about GLONASS status;
- information about healthy and unhealthy GLONASS satellites;
- information about coming launches;
- information about system almanac;
- information about coorperation between Russia and other countries for augmentation of GLONASS;
- information of commercial applications and civilian use of GLONASS signal.

Within MSF CRIC supervises over the following problems:
- integrated use of GLONASS and GPS NAVSTAR (coordination of the time scales and coordinate systems);
- access to GLONASS use of national and foreign users.

The second task of GLONSS is to provide civilian users with navigation and time information.

While the military retains ultimate control of the GLONASS, use of GLONASS for civilian applications is the providence of RSA. Within RSA, GLONASS issues and policy are the responsibility of the Department of Space Apparatus for Communications, Navigation and Geodesy.

Under MSF oversight, overall program direction and technical and design support services are provided by a large number of Russian space and electronics enterprises. The GLONASS systems integrator is SMA AM, located in Krasnoyarsk. This enterprise is also the GLONASS spacecraft designer and is responsible for all space segment research and development. Ground segment research and development is the responsibility of Scientific and Manufacturing Association of Space Device Engineering (SMA

Paper presented at the AGARD MSP Lecture Series on "System Implications and Innovative Applications of Satellite Navigation", held in Paris, France from 1-2 July 1996; Rome, Italy from 4-5 July 1996; Madrid, Spain from 8-9 July 1996 and St. Petersburg, Russia from 11-12 July 1996, and published in LS-207.

SDE), situated in Moscow. SMA SDE also designs and builds some subsystems, the command and tracking station, and the phase control equipment, develops user equipment.

The Russian Institute of Radionavigation and Time (St. Petersburg), designs and supports the synchronization of master clock system, maintains satellite and earthbased time and frequency standards, and develops user equipment. Research and development of user equipment are performed by SMA AM also. The Central Scientific Research Institute of Machine Bulding (Moscow) and the Moscow Aviation Institute (MAI) also conduct research and development for various system elements as consultants to the primary enterprises involved.

The Internavigation Committee was set up in 1985 to negotiate and enforce civilian navigation agreements. As GLONASS was never originally intended to be used for civilian purposes, the Committee was not expected to play a role in determining system requirements. As civilian interest has grown, however, the Committee has played a more substantial role in negotiating and coordinating international policy and agreements.

In 1992 INTERNAVIGATION Interdepartmental Commission was founded with task to support civilian use of radionavigation systems and GLONASS first of all in Russia. A year later the Radionavigation Intergovermmental Council was organized with the same task but within Commonwealth of Independent States (CIS).

International use of GLONASS time and navigation signals has also steadily increased. In May 1987 GLONASS data was integrated with other sources as part of the Earth rotation parameters determination service. In 1988 at the meeting of the International Civil Aviation Organization the Russian government offered free use of GLONASS signals worldwide. A similar offer was made at the meeting of the International Maritime Organization (IMO) in the same year.

In September 1993 President Boris Yeltsin offically proclaimed GLONASS as an operational system. Now the system is the backbone of the Russian Radionavigation Plan / 1 /.

2. GROUND SEGMENT

GLONASS is composed of three segments: a ground control segment; a space segment; and a user segment. GLONASS Ground Control Segment in shown in Fig. 1.

Ground Segment Elements

The Ground Based Control Complex measures and predictis individual satellite ephemeris, monitoring of navigation signals. It also controls the uplink of predicted ephemeris and phase data to each GLONASS satellite as well as information regarding the orbits of all 24 satellites. i.e., the sistem almanac. Synchronization among satellite time standards, the central synchronizer, and the Universal Time Coordinated (UTC), and satellite telemetry, tracking and control of satellite onboard systems are also performed by the Ground Based Control Complex.

The Ground-Based Control Complex (GBCC) includes the following six elements:
- System Control Center (SCC);
- Central Synchronizer;
- Command and Tracking Stations (CTS), i.e., Ground-Based Tracking Stations;
- Phase Control System (PCS);
- Quantum-Optical Tracking Stations (QOTS);
- Navigational Field Control Equipment.

The System Control Center, a military complex run by MSF is located in Golitsino, about 70 kilometers southwest of Moscow, schedules and coordinates the work of all system functions, while the central synchronizer forms standard system time signals and relays them to the Phase Control System.

Ground Based Tracking Stations measure individual satellite trajectories and uplink required control and secondary information to the satellite onboard computer. Trajectory tracking is carried out every 10 to 14 orbits. Tracking involves three-five measurement sessions each lasting 10 to 15 minutes. Range to the satellite is measured by radar with a maximum error of between two and three meters. These radar ranges are periodically calibrated using a laser ranging device at the Quantum Optical Tracking Stations. Each satellite carries laser reflectors specifically for this purpose.

The Phase Control System monitors satellite transmitted signals. The received ranging signals are compared with a reference signal of a highly stable frequency standard (relative error approximately 10^{-13}) by the Phase Control System. This comparison results in pseudorange $S(t) = R(t) + A(t)$, where $R(t)$ is the range from the ground station to the satellite; $A(t)$ is the sum caused by the phase difference between the satellite frequency standards and those at the ground station. Because $S(t)$ is a measured quantity and allowing for a maximum error of $R(t)$, the value of $A(t)$ can be determined with an error of about three to four meters. Measuring the resulting errors, or $A(t)$ allows prediction of the size of $A(t+T)$ and, correspondingly, of correction to the satellite ranging signal which is then uploaded by the ground station to correct any variations in the satellite time standard. This comparison of each satellite range signal phases is carried out at least on a daily basis. $A(t+T)$ prediction error is dependent on the satellite frequency standard stability and the $A(t+T)$ prediction procedure.

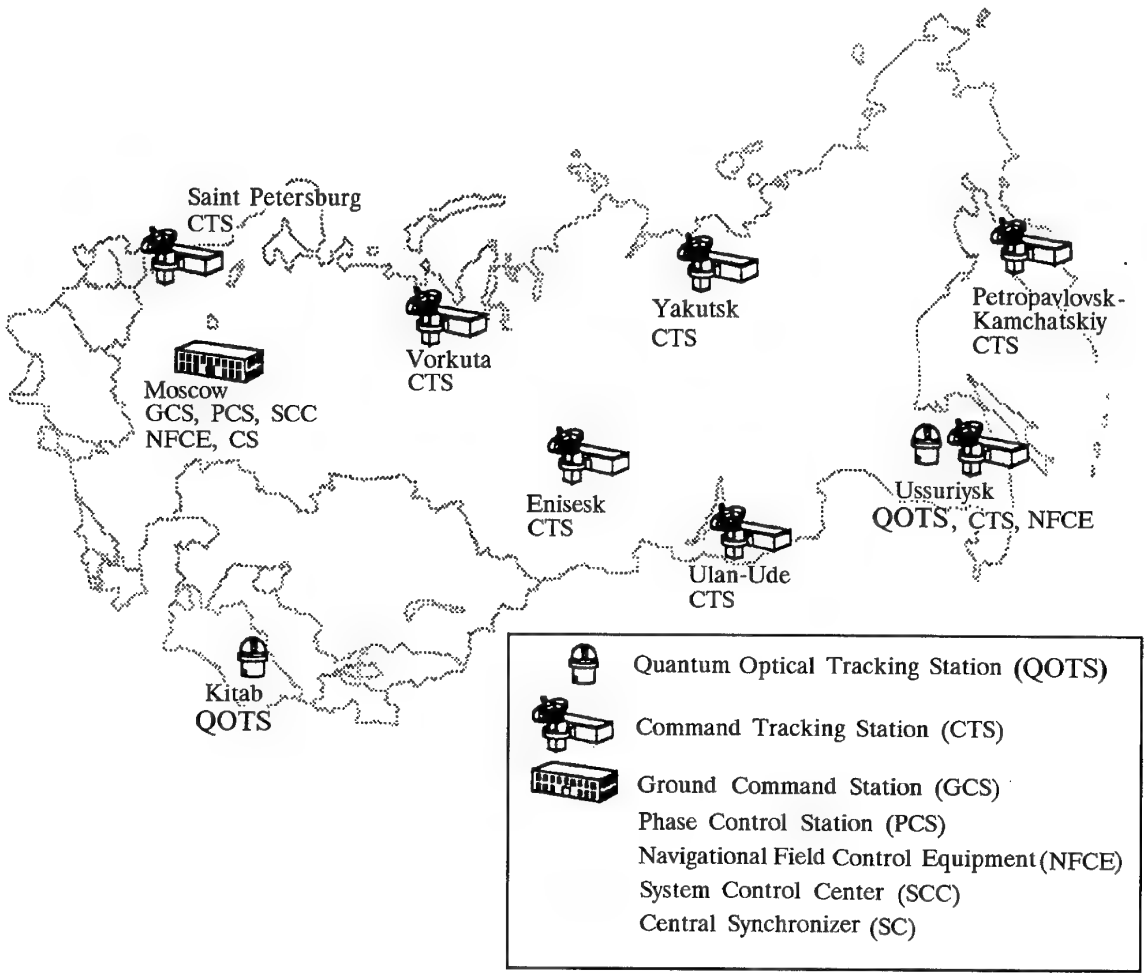

Fig. 1
GLONASS Ground Control Segment

Ranging signal corrections are predicted within 24 hours in advance and uploaded along with ephemeris information. Onboard time scale synchronization parameters are renewed twice a day. Therefore, phase error of the satellite ranging signals can lead to a pseudorange measurement error of at most five to six meters.

To ensure GLONASS system accuracy input of satellite ephemeris information is required. Data from remote tracking stations are used to compute ephemeris, synchronize range signal phases, and control GLONASS signal emissions.

Any interruption in the normal operation of the ground segment decreases the accuracy of GLONASS signals. Tests have shown that the onboard frequency standard can maintain acceptable accuracy (one part in $5x10^{-13}$) for no more than two to three days of autonomous operations. Although the satellite central processor is capable of 30 days of autonomous operations, this variability in the time standard is the limiting component for autonomous GLONASS operations.

Laser Tracking Stations

In the last 20 years SRI SDE has developed three different laser satellite tracking systems or Quantum Optical Tracking Stations. This includes the GEOIK Laser Ranging System, the Etalon QOTS, and the Maidanak QOTS. In total, 20 such complexs were built in the former Soviet Union.

The GEOIK stations serve as a part of the GEOIK geodetic system, which was used to define Earth coordinate systems and Earth gravitational field models. These models formed the basis for precise calculation of GLONASS satellite orbits. Etalon QOTS and Maidanak QOTS laser stations are used to calibrate radar measurements and orbit determination of the GLONASS system. These stations use second generation systems and are being upgraded to third generation systems.Detailed specifications of these third generation military systems remain classified.

Second generation Etalon QOTSs are able to measure the position of satellites visible in reflected solar light down to stellar magnitudes of less than 13 up to a maximum altitude of 20,000 kilometers. Range errors based on a 15 second averaging interval are about 1.5-2 cm and between 2 and 3 arc seconds in angular position.

In southern Uzbekistan a multi-functional quantum-optical complex has been set up on Maidanak Mount. The Maidanak QOTS system is capable of measuring ranges to an object up to an altitude of 40,000 kilometers and down to a visible stellar magnitude of 16. Maximum error of satellite angular coordinate determination does not exceed 1-2 arc seconds in operative mode and 0.5 arc seconds in non-operative mode with measurements not longer than 15 minutes. Maximum ranging error is not more than 1.5-1.8 cm. and the error of the fix to the UTC scale is not more than ± 1 μ second.

Ephemeris Corrections

Ephemeris information received from a satellite is tied to the closest 30-minute time signal. The maximum expected errors in this information are:

30-60 meters and 1-3 mm/s along the orbit.
20-40 meters and 4-8 mm/s in laterally and
5-12 meters and 1-3 mm/s along the radius.

3. GLONASS SATELLITE

A GLONASS satellite is a pressurized, hermetically sealed container. The antenna support subassembly is attached to one end of the container. The subassembly in turn carries the Earth sensor, laser corner reflectors, a 12-element navigation signal antennae, and various communiction antenna. The solar panels, engines, portion of the attitude control system, and the thermal control system are attached to the pressurized section.

Each satellite includes six onboard systems specified below.

- Onboard navigation and control complex;
- Attitude control system;
- Correction system;
- Thermal control system;
- Power supply system;
- Onboard Clock.

Onboard Navigation Complex

The onboard navigation complex is the heart of the satellite. It is composed of a navigational information forming unit, an onboard synchronizer, a memory unit, a receiver, and navigation transmitters. The complex operates in one of two modes: recording mode, or subsequent retransmission of navigational information mode. In the recording mode navigational information is uplinked to the satellite and then stored in onboard memory. Under normal conditions corrected navigational data are uplinked to the satellite every orbit.

The onboard navigation complex contains the information-logical complex(ILC). The ILC has three primary functions: first it records information about satellite ephemeris and the system almanac uplinked from the ground stations; second, it handles time signal formation and reproduction of navigational frames for system users; third, the ILC performs regular diagnosis of the status of the onboard navigation complex.

Onboard Control Complex

The onboard control complex manages the operational mode of each GLONASS satellite. A ranging subsystem, an onboard control unit, and a telemetry processing and control system are contained within this subassembly.

The onboard control complex records navigational information and transmits telemetry data, as well as controlling and regulating satellite power distribution.

The ranging system provides satellite range measurement information directly when queried.

Attitude Control System

The attitude control system performs initial orientation of the satellite and maintains proper orientation throughout the life of the satellite. This process begins immediatly after satellite separation from the launch vehicle. Using the satellite onboard propulsion system, the attitude control system stabilizes the satellite and dampens any gross oscillations. After taking the desired orbital position, the attitude control system points the solar arrays towards the sun and the spacecraft longitudinal axis points the antenna subassembly towards the Earth.

The magnitude of the Earth and Sun orientation error is no greater than three-five degrees, respectively.

Maneuvering System

The maneuvering system initially places the spacecraft in its assigned orbital plane position. It also maintains the satellite latitude argument and controls the satellite thruster system. Each GLONASS satellite has 24 orientational thrusters of 10 grams thrust each and two position correction thrusters of 500 grams thrust each.

Thermal Control System

The thermal control system regulates the satellite internal temperature. The spacecraft design, especially its orientation and heat discharge value, allows use of a louvered gas thermal-control system that employs the external surface of the pressurized container as a radiator. Heat dissipation regulation is carried out by a series of louvers, opening or closing the outlet to the radiator, depending on the internal gas temperature. An internal fan circulating the gas dissipates the heat from individual devices.

Power Supply System

The power supply system, composed of a solar cell, storage battery, control relays and a voltage regulator, provides electrical power to onboard spacecraft equipment. The initial power output of the solar cell is 1600 watts, with an area of 17.5 square meters. When illuminated by the sun the solar array charges the storage battery, which in turn provides power to the satellite equipment when the satellite is in shadow. The storage battery has a discharge capacity of 70 Amp-hours.

In 1982 GLONASS became the first Russian satellite to be built with nickel-hydrogen batteries. Recent experience and testing have extended battery life and have been the primary factor in extending satellite lifetime to a minimum of five years.

Onboard Clocks

The onboard clock is the most critical element of the GLONASS satellite. It is the long-term stability and predictability of modern atomic clocks that make the concept of navigation satellite systems possible.

Initial work on Atom-Ray of Frequency Standards–atomic clocks – began in Russia in 1957 at IRE AN USSR and now called RIRT. RIRT has developed several clocks, first based on a rubidium gas cell and more recently based on cesium.

The GLONASS clocks have been a steady improvement in frequency variation (initially $5x10^{-11}$ peak-to-peak, then progressing to better than $1x10^{-11}$), temperature stability (from $2x10^{-12}$ - per degree centigrade to better than $2x10^{-13}$), and operational lifetime (from 5,000 hours to better than 18,000 hours).

Future GLONASS plans call for development of fequency standards increasingly better than $1x10^{-12}$. To meet these technical requirements an Atom Ray Tube with light pump and detection is under development. Test examples were produced in 1993. Serial production is scheduled to begin not later then 1997. Further development work is underway to extend the service life of this standard to 70,000 hours.

4. GLONASS CONSTELLATION

4.1. Number of satellites and their orbits

The orbital constellation of the GLONASS system consists of 24 navigational satellites (ST), eight in each three orbital planes. Orbit altitude is 18840 - 19940 km; orbit inclination is 64°8±0°3; orbit eccentricity is 0±0.01. The orbital planes are located every 120 degrees relative to the absolute longitude of the ascending node. The orbital planes are numbered 1, 2, and 3 in increasing order in the direction of the Earth rotation. The STs of the first orbital plan are asigned system numbers from 1 to 8, the Sts of the second orbital plane - from 9 to 16, and the Sts of the third orbital plane - from 17 to 24. The system numbers of the ST in the orbital planes increase in the direction opposite the motion of the ST.
The nominal values of the absolute longitudes of the ascending nodes of the ideal orbital planes, recordered at 0000 hours official Moscow time on January 1, 1983, are equal to 251°15'00" + 120° (i-1), where i is the number of the orbital plane (i=1, 2, 3).

The nominal angle between adjacent STs in a plane is equal to 45°.

The average rate of precession of the orbital planes is minus $0.59251x10^{-3}$ rad/day.

The ideal values of the arguments of latitude of the ST with system numbers j = N + 8 and j = N + 16 differ from the arguments of latitude of the ST with system

numbers j = N and j = N + 8 respectively, by plus 15°, where N = 1, ... 8 and had the following value at 0000 hours official Moscow time on January 1, 1983:

$$145°26'37" + 15° (27 - 3j + 25j^*),$$

where j is the system number of the ST (j = 1, 2,...,24);

$J^* = E\left\{\frac{j-1}{8}\right\}$ is the integral part of $\left\{\frac{j-1}{8}\right\}$

The interval of the repeatability of the ST routes and zones of radio visibility of the ST by ground equipment is 17 turns (7 days 23 hours 27 minutes 28 seconds).

The draconitic orbital period of the ST is 11 hours 15 minutes 44 ± 5 seconds.

The maximum drifts of the ST relative to its ideal position in orbit do not exceed ± 5° for a five-year period of employment / 2 /.

The ballistic structure of GLONASS constellation is shown in the Fig. 2.

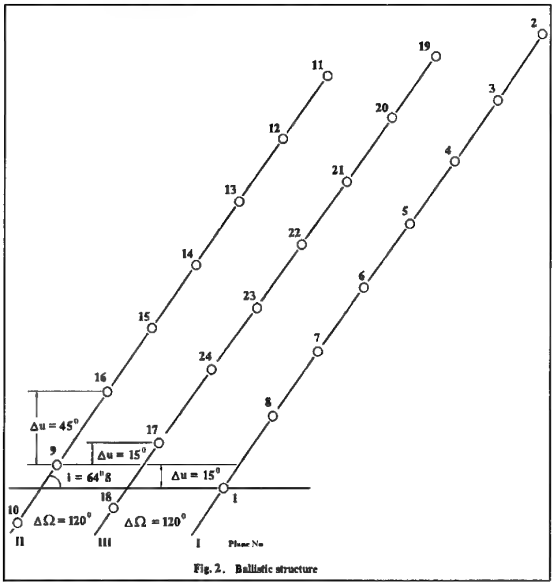

Fig. 2. Ballistic structure

4.2. Constellation Maintenance and Replenishment Policy

Based on the perfomance of all 24 satellites, GLONASS controllers will determine the "best" 21 to activate. The remaining three will be held for back-up or in reserve. Periodically, the "mix" will be evaluated and, if necessary, a new "best" set of 21 will be defined. When necessary to maintain system accuracy, three new satellites will be launched and used either to replace malfunctioning satellites or held in reserve for future use.

Concurrently, the ground segment is being expanded to handle all 24 satellites. As new capabilities are added, additional satellites are launched to supplement the full constellation.

GLONASS satellites are launched three at a time from the Baikonur Cosmodrome in Kazakhstan by a Proton launch vehicle. Initially, the spacecraft enters an intermediate 200 km circular orbit. From there they are transferred to an elliptical orbit with an apogee of 19100 km. After perigee correction, the satellite enter a circular 19100 km orbit. Each satellite has its own orbital correction engines for final insertion into the designated orbital slot. On average, satellite launch, positioning, and checkout period does not exceed 25 days.

A single satellite failure once the permanent system of 21 operationl and three spare satellites is established would not lower the system design probability of successful fix determination below 94.7 percent. There are provisions to activate either a back-up satellite from available on-orbit satellite reserves, or to prepare three new satellites for launch (one replacement satellite and two others for future orbital reserves). The maximum launch preparation time for these new satellites is 650 hours per set of three.

4.3. Coverage and Dilution of Precision

Ballistic configuration of GLONASS constellation was chosen with use of two criteria:
- minimum of maximum user errors in the all fields of GLONASS usage duaring all the time of the system function;
- minimum of orbital planes in the system.

The result of the calculation with these criteria brings to three planes. Under these conditions the coverage and the average Dilution of precision were calculated and are shown in the Table 1 and in the Fig. 3 / 3 /.

Table 1

The coverage and the average Dilution of Precision of GLONASS (24 satellites)

Characteristics	Number of satellites (N)					
	4	5	6	7	8	9
P	1	1	1	1	0.91	0.58
HDOP	1.41	1.26	1.15	1.03	0.95	0.89
VDOP	2.0	1.75	1.70	1.61	1.60	1.55
TDOP	1.13	1.03	1.03	0.95	0.93	0.91
DOP (R, T)	2.67	2.42	2.26	2.12	2.07	1.99

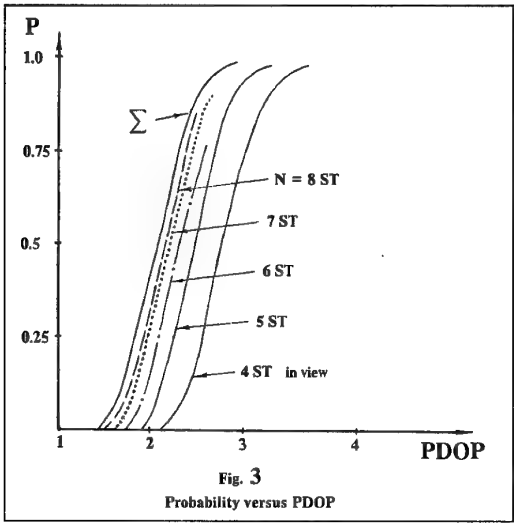

Fig. 3
Probability versus PDOP

The probability when the user has no less than four satellites in view is equal to 1, HDOP has range from 0.89 to 1.41 worldwide, DOP (R,T) ranges from 1.99 to 2.67.

4.4. Error Budgets

Inaccuracies in determination of user position are caused by the environment in navigation parameters are measured and by the process carried out by the user equipment to estimate the position. One sourse of variable error is associated with satellite motion relative to the user. This causes a change of the geodynamic factor and may necessitate a change from tracking one group of satellites to tracking another group with a better relative geometry.

To obtain repeatable, accurate results, the second factor requires that allowances would be made for additional signal delay while the signal propagates through the atmosphere. This can be done either by use of secondary information and an atmosphere model in the user equipment or by measuring two frequencies.

A passive mode of position determination, the third factor, necessitates synchronization of all time standards of all satellites. Highly stable time standards with error rates that are between 10^{-13} and 10^{-14} and transmission of onboard time-standard corrections provide such synchronization.

The error sources and magnitudes noted in Table 2 are tipical for civil GLONASS accuracies.

Three factors dictate the design of GLONASS equipment and the ability to obtain position in the space: the motion of navigational satellites, the high altitude of a satellite orbit, and the need for a passive technique to fix position. The first factor requires knowledge of the satellite coordinates, their velocities and accelerations at the moment of measurement. This is determined by the processing unit of the user equipment based on satellite ephemeris data broadcast by the satellite.

Table 2

Civil GLONASS Error Sources

Error Source	Error (meters)	
	1 s Averaging Time	10 s Averaging Time
Satellite Errors	9.2	9.2
User Errors: Ionosperic Delay Compensation	10	10
Tropospheric Delay Compensation	2	2
Receiver Noise and Resolution	15	5
Multipath	3	1
Others	1.5	1
System UERE (one sigma)	20.6	14.7

4.5 GLONASS Integrity

GLONASS integrity is carried out by Autonomus Monitiring System (AMS) onboard the satellite and by Ground Navigational Field Control Equipment (GNFCE). When AMS detects failure the bit "1" in the sign Bn is transmitted in the radionavigation signal. It means for user that this satellite is unhealthy for navigation. The failure is detected within the time which not exceeds one minute.

When GNFCE detects the failure of the satellite the Ground Command Station loads bit "0" in the sign Cn for unhealthy satellite onboad all satellites.

In this case the information about unhealthy satellite can be transmitted to user within the time which not exceeds 16 hours. Sign Bn is transmitted in operative information and sign Cn - in nonoperative information / 2 /.

5. SIGNALS IN SPACE

5.1. Carrier Frequencies

The radio signals of satellites of the GLONASS occupy in the L-band of radio frequencies: the L1 band ranges from 1602.5625 to 1615.5 MHz in steps of 0.5625 MHz, while the L2 band ranges from 1246.4375 to 1256.5 MHz in steps of 0.4375 MHz . The nominal values of the carrier frequencies of the navigational radio signals of the satellites are determined by the following expressions:

$$f_1 = f_{01} + K\Delta f_1$$
$$f_2 = f_{02} + K\Delta f_2$$

K-0,1 2,...,24-number of the carrier frequency;
f_{01} - 1602 MHz; f_{02} - 1246 MHz;
$K\Delta f_1$ - 562.5 kHz. $K\Delta f_2$- 437,5 kHz.

The number K = 0 is not used by users of the GLONASS, and is intended for checking standby satellite in orbit when making up the orbital grouping of the system. Distribution of numbers K = 1, 2, ..., 24 among the satellites of the system n = 1, 2, ..., 24 is contained in the system almanac (nonoperative information in the navigational data).

L1 and L2 frequencies of each satellite are coherent and generated by common standard of frequency.

But now the change of frequency band for GLONASS is foreseen. The change will be carried out by stages.

Stage 1 (from present moment up to 1998)

Lettered frequencies (1610,6...1613,8 MHz) with K = 16, 17, 18, 19, 20 will not be used at all.

Lettered frequencies with K = 13, 14, 21 will be used with limitation.

GLONASS satellites with K = 0, ..., 12 will have the oppotunity to emit lettered frequencies with K = (-7, ..., -1).

It is supposed that satellites launched at this stage will be equiped with filters which decrease the level of the outband emission in the frequency band 1660...1670 MHz upto the level which meets Recommendation ITU-R 769.

Stage 2 (1998 - 2005)

Satellites will use unlimitted lettered frequencies with K = 0, ..., 12.

Lettered frequency with K = 13 will be used with limitation.

It is supposed that satellites launched at this stage will be equiped with filters which decrease the level of the outband emission in the frequency band 1660...1670 MHz upto the level which meets Recommendation ITU-R 769.

Stage 3 (from 2005)

At this stage the lettered frequencies will be used with K = (-7, ..., +6) only but lettered frequencies with K = +5 and +6 will be used limitedly during short period of time (for example, during replenishment) / 2 /.

It is supposed that satellites launched at this stage will be equiped with filters which decrease the level of the outband emission in the frequency bands 1610,6...1613,8 MHz and 1660...1670 MHz upto the levels which meet Recommendation ITU-R 769.

5.2. Modulation Technique

The characteristics of the modulating navigational signal transmitted by each satellite of the GLONASS are determined below based on its structure and method of formation.

The modulating navigational signal is obtained by mod 2 summation of three binary signals of the following:
1. the ranging code, transmitted at a rate of 511 kbit/s;
2. the sequence of data, transmitted at a rate of 50 bit/s;
3. the meander oscillation, transmitted at a rate of 100 bit/s.

The binary sequence thus obtained is then used to modulate the carrier oscillation of the L-band.

5.3. Code Structure

5.3.1. Structure of the ranging code

L1 and L2 signals are modulated by a 5.11 MHz precision (P) code and simulteneously L1 is modulated by a 0.511 MHz coarse (C) code. The binary signals are formed by a P-code or C-code which is modulo-2 added to L1 in phase quadrature (only P is present on

L2). The P-code is pseudorandom (PR) sequence with a period of one second.

The ranging code of coarse signal is a PR sequence of the maximum length of the shift register and has the following characteristics: nominal repetition period 1 ms, nominal symbol transmission rate 511 kbit/s.

The range PR sequence (RPRS) is taken from the 7-th bit of the 9-bit shift register. The code of the initial state of the shift register corresponds to the presence of "1" in all bits of the register.

The initial symbol in the period of the PR signal is the 1-st symbol in the group 111111100, nominally repeating every 1 ms. The resultant polynomial, which corresponds to the shift register forming the range code, has the following form :

$$G(x)= 1 + x^5 + x^9.$$

The simplified structure diagram of forming range code and synchroimpulses of navigation radio signal given in Fig. 4.

5.3.2. Structure of the sequence of data

The sequence of data transmitted from each satellite is shaped in the form of continuously following two-second lines. The first part of each line has a duration of 1.7 s and is intended for the transmission of digital information. The second part of each line has a duration of 0.3 s and is intended for transmission of the binary code of time mark.

The first part of the data line is the binary sequence obtained by mod 2 summation of two binary sequences:
1. the sequence of symbols of digital information in relative code with a symbol of 20 ms;
2. meander with a symbol duration of 10 ms.

The binary code of the time mark is a shortened binary PR sequence of 30 symbols long with a symbol duration of 10 ms. The PR time mark sequence is described by the resultant polynomial

$$g(x) = 1 + x^3 + x^5$$

and has the form:

11111000110111010100001001011O

The first symbol of the digital information in each two-second line is always "0". It is "empty" and supplements the shortened time mark PRS of the previous line to the complete (unshortened) PR sequence.

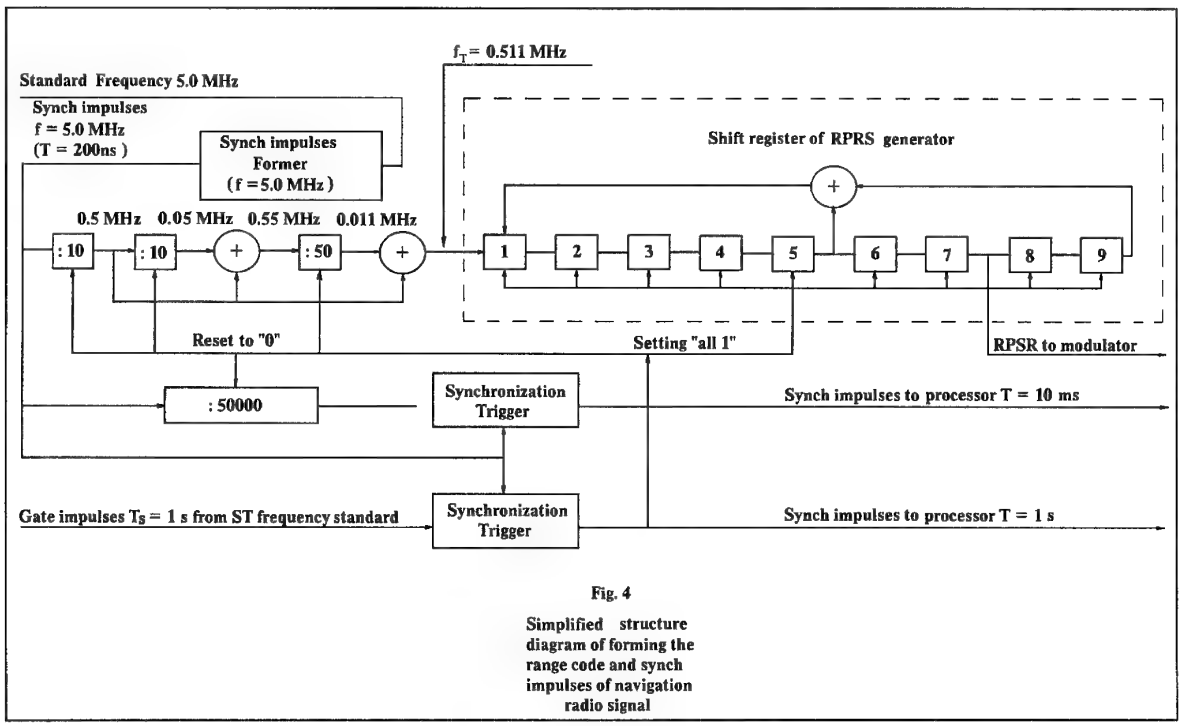

Fig. 4

Simplified structure diagram of forming the range code and synch impulses of navigation radio signal

The simplified structure diagram of forming sequence data is given in Fig. 5.

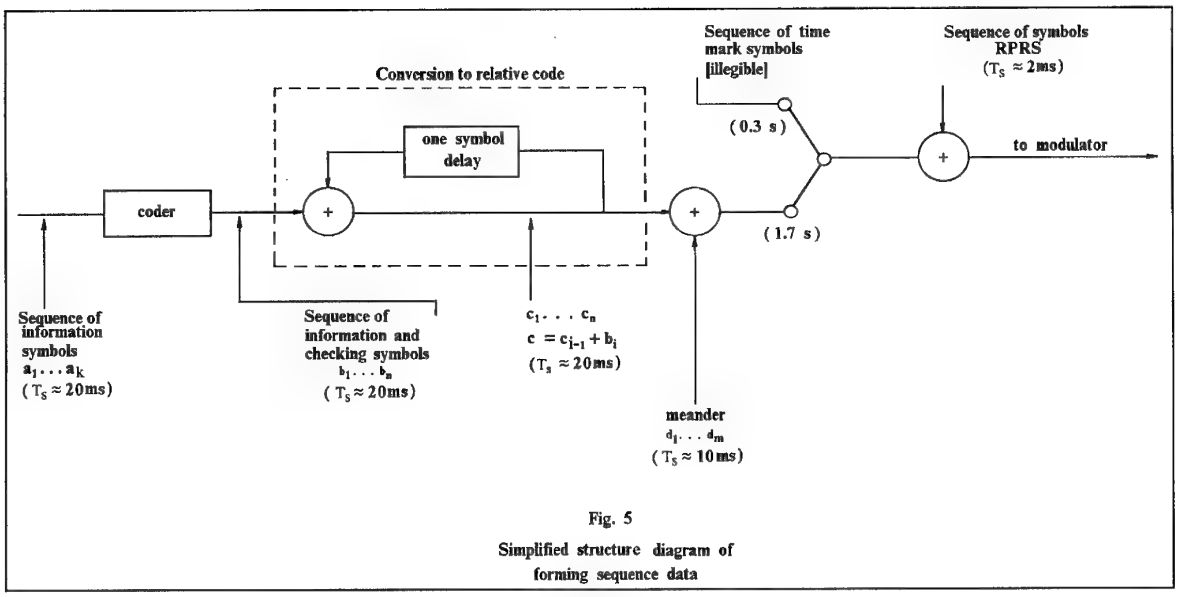

Fig. 5

Simplified structure diagram of forming sequence data

In the emitted navigational radio signal the boundaries of the two-second lines, the boundaries of the symbols of the digital information, the boundaries of the meander symbols, the boundaries of the time mark PRS symbols, and the boundaries of the RPRS symbols are synchronized among themselves; the boundaries of the meander symbols and those of the symbols of digital information coincide with the front edges of the initial RPRS symbols. The back edge of the last time mark PRS symbol in the emitted navigational radio signal is a time mark and corresponds to the moment of time that differs from the beginning of the 24-hour period, Moscow decree time, by an integer number of even seconds in the time scale of the satellite.

The time ratios between the synchimpulses of the modulating navigational signal and the range code of the RPRS are given in Fig. 6.

The process of forming data sequence transmitted in the radio signal is explained in Fig. 7.

5.4. Message Content and Formats

The digital information (DI) transmitted by each satellite includes operational and nonoperative DI.

Operative DI pertains to a given satellite, and contains:

- the time marks and their values of time of the satellite;
- shift of the time scale of the satellite relative to the time scale of the GLONASS. They also contain a value which characterizes the relative difference between the emitted radionavigation signal carrier frequency and a nominal value;
- the ephemeries information.

Nonoperative DI contains the system almanac,which includes:
- data of the state of all satellites of the system (state almanac)(less accurate than the operative information);
- the shift of the time scale of each satellite relative to the scale of the GLONASS (phase almanac);
- parameters of orbits of all satellites of the system (orbit almanac);
- correction to the time scale of the GLONASS system.

As previously noted, the navigational message is transmitted by the strings with a duration of 2 seconds each. Fifteen strings make up a 30-second information frame in which the entire volume of operative information related to a specific moment of a given satellite orbital position and part of the nonoperative information are transmitted. The overall volume of the system almanac is transmitted in five successive frames constituting a superframe with a duration of 2.5 minutes. A detailed description of the superframe is quoted in the "Interface Control Document" (3d version).

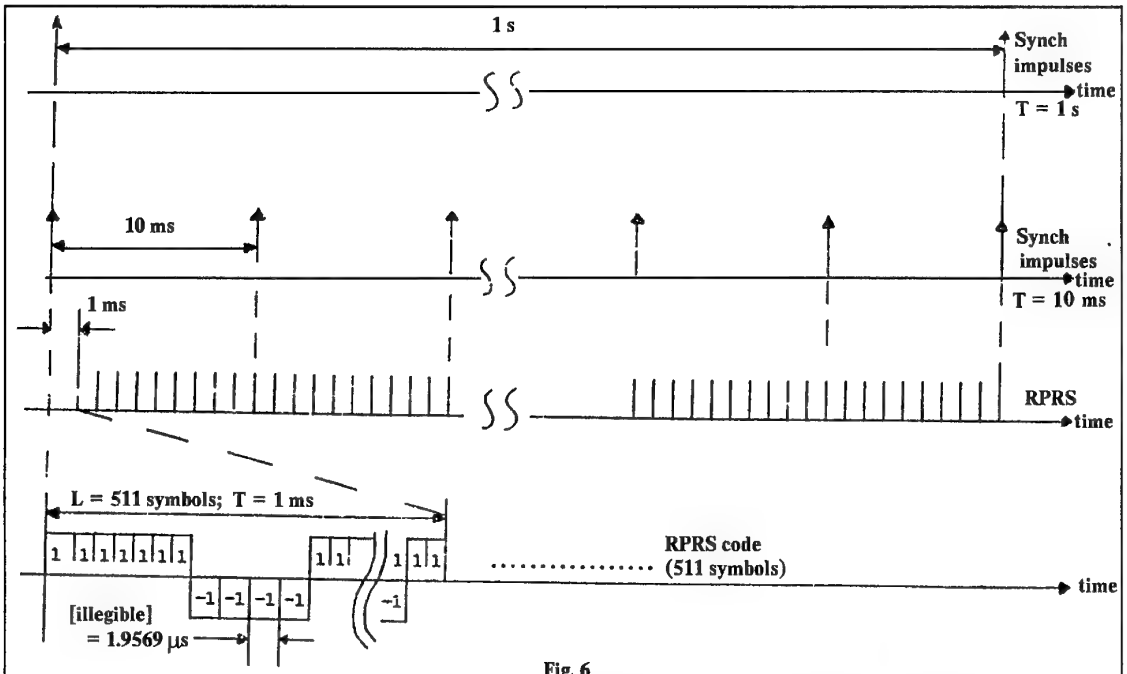

Fig. 6

Time relationship between synch impulses of modulating navigational signal and range code

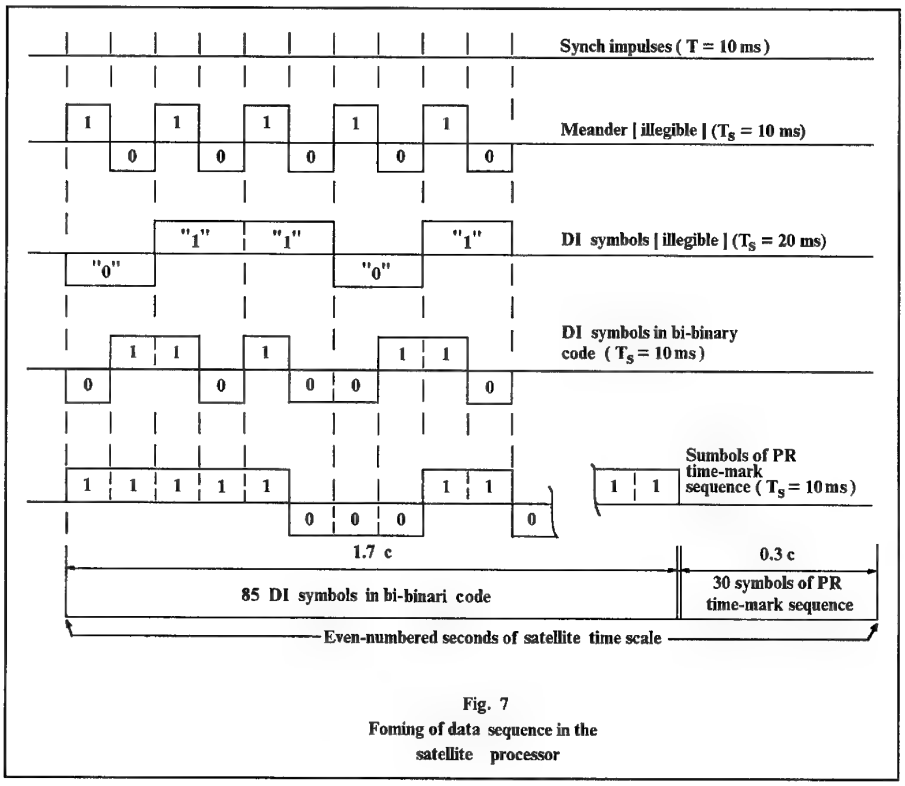

Fig. 7

Foming of data sequence in the satellite processor

The structure of superframe is shown in Fig. 8.

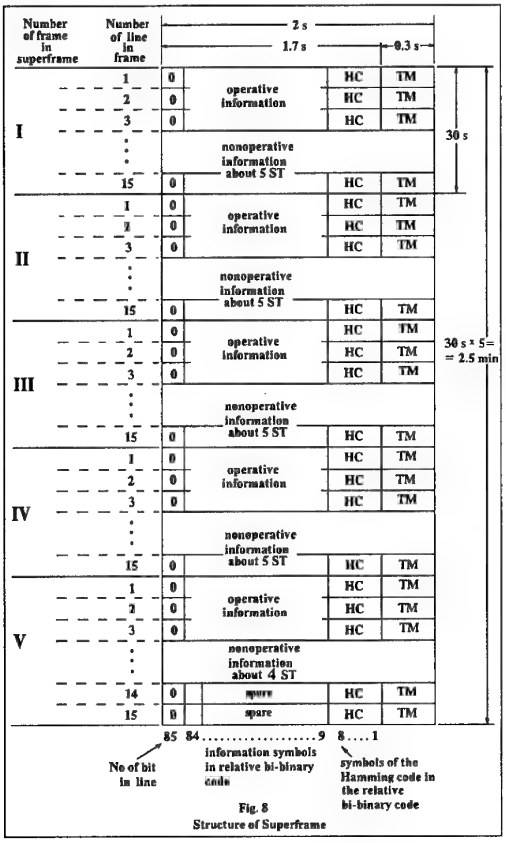

Fig. 8
Structure of Superframe

The structure of Navigation frame is given in Fig. 9.

Below are given the letter designations, used in Fig. 9, for the parameters of the ephemerides and their content:
Word m - number of line in the navigatonal frame.

Word t_k - the time of the beginning of the frame within the current 24-hour period, calculated in the scale of onboard time, is represented in the following form:
the 5 high-order bits indicate the number of integer hours which have passed since the beginning of the current 24-hour period;
the 6 middle-order bits indicate the number of integer minutes which have passed from the moment of the beginning of the current hour;
the low-order bits indicate the number of seconds in the current minute to the start of the frame;
the beginning of the 24-hour period of onboard time of the satellite coincides with the beginning of the next superframe;

Word B_n - contains 3 bits; the user equipment analyzes the high-order bit of this word, a "1" in which indicates the fact of the unfitness of this satellite for carrying out measurement sessions; the second and the third bits of this word are not analyzed by the user equipment.

Word t_b - the time within the current 24-hour period by the Moscow decree time, which includes the operational information transmitted in the frame; the discreteness of representation of t_b is 15 minutes; the operational information is replaced at moments of time that are multiple of 30 or 60 minutes on the time scale of the satellite.

Word П1 - sign of replacement of operational information; the sign communicates the value of the time interval between values of Δt_b (min) in this and the previous frame; signs 00, 01, 10 and 11 have the corresponding values of Δt_b equal to 0, 30, 45 and 60 min.

Word П2 - sign of replacement t_b is the sign of odd parity ("1") or even parity ("0") of the orbital number (b) of the 30- (60) minute current interval of time which midpoint is given by the numerical value of word t_b.

Word П3 - the sign, state "1" of which means that in this frame the almanac is transmitted for 5 satellites of the system, and state "0" means that in this frame the almanac is transmitted for 4 satellites.

Word $\gamma_n(t_b)$ - the relative difference at moment of time t_b of the forecast value of the carrier frequency of the emitted navigational radio signal of the n-th satellite from the nominal value

$$\gamma_n(t_b) = \frac{f_n(t_b) - f_{Hn}}{f_{Hn}}$$

where $f_n(t_b)$ - forecast value of the carrier frequency of the emitted navigational radio signal of the n-th satellite, taking into account gravitational and relativistic effects at moment of time t_b;
f_{Hn} - nominal value of the carrier frequency of the navigational radio signal of the n-th satellite.

Word $\tau_n(t_b)$ - shift of the time scale of the n-th satellites t_n relative to the time scale of the system t_s and is equal to the phase shift of the RPRS of the emitted navigational radio signal of the n-th satellite relative to the system reference signal at moment of time t_b, expressed in units of time (s)

$$\tau_n(t_b) = t_s(t_b) - t_n(t_b)$$

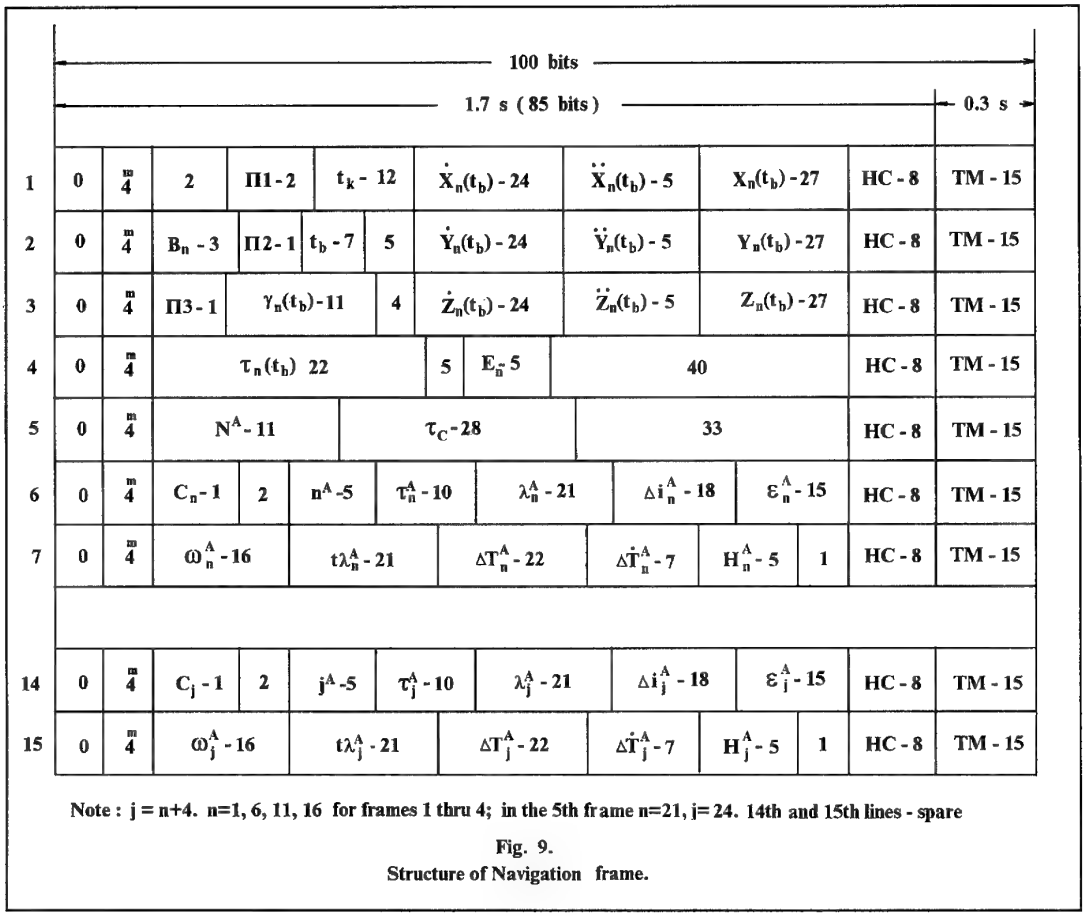

Note : j = n+4. n=1, 6, 11, 16 for frames 1 thru 4; in the 5th frame n=21, j= 24. 14th and 15th lines - spare

Fig. 9.
Structure of Navigation frame.

Parameters of Satellite Ephemerides are shown in Table 3.

Table 3

Parametrs of Satellite Ephemerides

Parameter *	No of bits **	Value of low order bit	Range of value	Unit of measurement
m	4 ***	1	0...15	dimensionless
t_k	5 6 1	1 1 30	0...23 0...59 0;30	hours minutes seconds
t_b	7	15	15;30...1425	minutes
$\gamma_n(t_b)$	11	2^{-40}	$\pm 2^{-30}$	dimensionless
$t_n(t_b)$	22	2^{-30}	$\pm 2^{-9}$	seconds
$X_n(t_b), Y_n(t_b), Z_n(t_b)$	27	2^{-11}	$\pm 2.7*10^4$	kilometers
$\dot{X}_n(t_b), \dot{Y}_n(t_b), \dot{Z}_n(t_b)$	24	2^{-20}	± 4.3	km/sec
$\ddot{X}_n(t_b), \ddot{Y}_n(t_b), \ddot{Z}_n(t_b)$	5	2^{-30}	$\pm 6.2*10^{-9}$	km/sec ^{2}
E_n	5	1	0...31	24 hr period

Notes:
* Numerical values of parameters are presented as a sign of a number and its modulus: the + sign corresponds to the zero symbol, and symbol one corresponds to the - sign. The sign of the number (+ or -) occupies the high order bit.
** See Fig. 9 which shows the arrangement of bits in the navigation frame.

Words $X_n(t_b)$, $Y_n(t_b)$, $Z_n(t_b)$ - coordinates of the n-th satellite in the rectangular Greenwich geocentric coordinate system at moment of time t_b .

Words $\dot{X}_n(t_b)$, $\dot{Y}_n(t_b)$, $\dot{Z}_n(t_b)$ - components of the velocity vector of the n-th satellite in the rectangular Greenwich geocentric coordinate system at moment of time t_b.

Words $\ddot{X}_n(t_b)$, $\ddot{Y}_n(t_b)$, $\ddot{Z}_n(t_b)$ - components of the acceleration of the n-th satellite in the rectangular. Greenwich coordinate system at moment of time t_b caused by the action of the Moon and Sun.

Word E_n - characterizes the "age" of the operational information - time interval which has passed from the moment of calculating (loading) the operational information to moment of time t_b for the n-th satellite; word E_n is formed on board the satellite.

Data of the system almanac.
The almanac (nonoperative information) includes: data on the time scale of the system, data on the time scale of each satellite, and also data on the orbit elements and the technical state of the all satellites of the system.

The number of bits, the value of the low-order bit, the range of values, and units of measurement of the parameters of the almanac are given in Table 4.
In the words which numerical values can take both positive and negative values, the high-order bit is the sign, the symbol "0" corresponds to the "plus" sign, and symbol "1" - to the "minus" sign.

Below are given the letter designations, used in Fig. 9, for the parameters of the almanac (see Table 4), and their meanings are explained:

Word τ_C - correction to the time scale of the system relative to the time scale in which the ephemerides and the parameters of synchronization of the satellite are calculated. Correction τ_C is given at the beginning of day with number N^A.

Word N^A - number of calendar days within the four year period beginning with a leap year, to which corrections τ_C and the data of the system almanac are corresponded (orbit almanac and phase almanac).

Word n^A - conventional number of satellite in the system.

Word H^A_n - letter of the carrier frequency of the navigational radio signal emitted by a satellite with number n^A.

Table 4

Parametrs of System Almanac

Parameter*	No of bits **	Value of low order bit	Range of value	Unit of measurement
τ_c	28***	2^{-27}	±1	seconds
N^A	11	1	0....1461	24 hr period
n^A	5	1	1...24	dimensionless
$H^A{}_n$	5	1	1...24	dimensionless
$\lambda^A{}_n$	21***	2^{-20}	+1	half-cycle
$t^A{}_n$	21	2^{-5}	0...44100	seconds
$\Delta\lambda^A{}_n$	18***	2^{-20}	±0.067	half-cycle
$\Delta T^A{}_n$	22***	2^{-9}	$\pm 3.6*10^3$	s/orbit
$\Delta T^A{}_n$	7***	2^{-14}	$\pm 2^{-8}$	s/orbit
$\varepsilon^A{}_n$	15	2^{-20}	0...0.03	dimensionless
$\omega^A{}_n$	16***	2^{-15}	±1	half-cycle
$\tau^A{}_n$	10***	2^{-18}	$\pm 1.9*10^{-3}$	seconds
$C^A{}_n$	1	1	0...1	dimensionless

Notes:

* Numerical values of parameters are presented as a sign of a number and its modulus: the + sign corresponds to the zero symbol, and symbol one corresponds to the - sign. The sign of the number (+ or -) occupies the high order bit.

** See Fig. 9 which shows the arrangement of bits in the navigation frame.

*** The parameters indicated by this symbol have a range of values which coincides with a maximum value taking into account of the value of the low order bit.

Word $\lambda^A{}_n$ - Greenwich longitude of the first (within a day with number N^A) ascending orbital node of a satellite with number n^A.

Word $t^{A\lambda}{}_n$ - the closest time to the beginning of a day with number N^A of the day's first ascending node of the orbit of satellite with number n^A.

Word $\Delta i^A{}_n$ - correction to the average value of orbit inclination for a satellite with number n^A at moment $t^{A\lambda}{}_n$ (the average of orbit inclination is taken as 63°).

Word $\Delta T^A{}_n$ - correction to the average value of the draconitic time period of a satellite with number n^A at moment $t^{A\lambda}{}_n$ (average value T of the draconitic time period of a satellite is taken as 43200 s).

Word $\dot{\Delta T}^A{}_n$ - rate of change of the draconitic time period of a satellite with number n^A.

Word $\varepsilon^A{}_n$ - orbit eccentricity of a satellite with number nA at moment of time $t^{A\lambda}{}_n$.

Word $\omega^A{}_n$ - argument of perigee of orbit of a satellite with number n^A at moment of time $t^{A\lambda}{}_n$.

Word $\tau^A{}_n$ - rough value of the shift in the time scale of a satellite with number n^A relative to the system time scale for moment of time $t^{A\lambda}{}_n$, equal to displacement of the RPRS of the emitted navigational radio signal relative to the nominal position, expressed in units of time.

Word $C^A{}_n$ - generalized criterion of the state of a satellite with number n^A at moment of establishment of nonoperational information (orbit and phase almanacs); a value of the criteroin of C_n - 0 indicates unfitness of the satellite for use in sessions of navigational determinations, and a value of the criterion C_n = 1 shows that the satellite is healthy.

GLONASS time

The GLONASS time is established by the monitoring and control subsystem (MCS) and is referenced to the scale of Universal Coordinated Time UTC(SU). The time scale of the GLONASS is the time scale of the system central synchronizer (SCS) which is part of the MCS. The MCS of the GLONASS must control the system time scale so that it would differ from the UTC(SU) scale by no more than 1 ms.

All GLONASS satellites are equiped with cesium frequency standard. The accuracy of mutual synchronization between satellites is equal to 20 nc (rms).

The time scale of each satellite is periodically compared with that of the SCS. The error of the ST time scale relative to SCS does not exceed 10 ns at the moment of measurements. The navigation message contains the necessary information (corrections) which enables the user to "tie" its own time scale to the UTC(SU) time scale. The accuracy of this information is such as to make it possible to carry out "tieing" of the user's time to UTC(SU) with a maximum error of + 1 ms and to SCS time with error which is less than 100 ns.

The coordinate system

The ephemerides transmitted by each satellite of the GLONASS as part of the operational information describe the location of the phase center of the transmitting antenna of the satellite in the Earth-centred Earth-fixed geodetic system PE-90 (Parameters of the Earth, 1990), given as follows:

COORDINATE ORIGIN - located at the center of mass of the Earth;

Z AXIS - directed towards the mean north pole in the mean epoch 1900-1905, as defined in resolutions of the International Astronomical Union and the International Association of Geodesy;

X AXIS - lies in the plane of the terrestrial equator of the epoch 1900-1905, plane XOZ is parallel to the mean Greenwich meridian and defines the position of the zero point of the adopted system of longitude reckoning;

Y AXIS - supplements the geocentric rectangular coordinate system to the rigth.

The geodetic latitude B of point M is defined as the angle between the normal to the surface of an ellipsoid and the equatorial plane; the geodetical longitude L - the angle between the plane of the prime meridian and the plane of the meridian passing through point M (positive direction of reckoning longitudes - from the prime meridian eastwards); geodetic height H - the distance along the normal to the surface of an ellipsoid to point M.

5.5. EIRP/Antenna Footprint

Each satellite must emit a navigational radio signal with a minimum level such that the power of the radio signal received at the output of an isotropic, linearly polarized antenna of a user located on the earth surface and observing this satellite at an elevation angle of 5 degrees would be no less than minus 161 dBW.

In Fig. 10 the antenna footprint is shown. The dependence of minimum signal power level versus of elevation angle of ST was calculated taking into account the following assumptions:

- the loss of signal power at the output of the receiver isotropic linear polarized user antanna is less than 3 dB;
- the ST is above 5 degree mask angle;
- the loss of signal power when signal propagates through atmosphere is less than 2 dB;
- the error of ST angle orientation is less than 1 degree.

All signals transmitted by a given satellite must be coherently formed by the onboard frequency standard generater. All digital signals must be synchronized with the transmitted ranging PR signal by transmission rate.

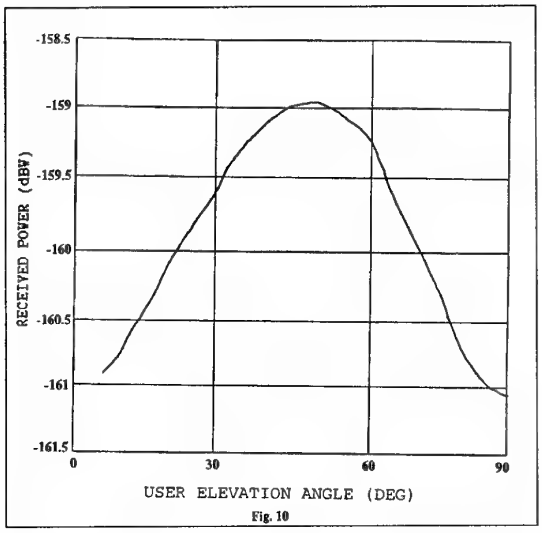

Fig. 10

The navigational radio signal emitted by each satellite of the GLONASS must have right-hand circular polarization. The ellipticity over the field must be no worse than 0.7 in the sector of the angle of radiation of +19 degrees relative to the axis of symmetry of the radiation pattern of the onboard satellite antenna.

6. USER PERFORMANCE

6.1. National Policy on Access or Use

The Russian Federation has repeatedly made statements about the possibility of the unlimited civilian use of its global navigation satellite system. This position was officially confirmed on 7 March 1995 in Act No.237 of the Govemment of the Russian Federation "On execution of work for the application of the global navigation satellite system GLONASS in the interests of civil users". It contains the directive to ensure the beginning of its full operation in 1995 (24 satellites). It is emphasized in this Act that the system is meant for providing FREE long-term service for national and civil foreing users in accordance with existing commitments.

The Ministries of Transport and Defence, together with the Russian Space Agency and some other agencies concerned, have been instructed to set up the Co-ordination Council for ensuring the use of the GLONASS by the civilians.

It is planned to prepare and publish documents, which will determine the order of operation and use of the GLONASS, including the necessary documents to be presented to IMO, ICAO, and also to set up an information service to notify all users.

The Ministry of Transport is instructed by the above Act to implement the necessary measures in IMO and ICAO, meant for introducing the GLONASS for the sake of its recognition by the above mentioned international organizations.

6.2. Civil users

There is no Selective Availability in GLONASS. It makes GLONASS very attractive for civilian applications.

Civilian design specifications of GLONASS coordinate and velocity determination for moving objects are less than 100 meters by planar coordinates, 150 meters by altitude and 15 centimeters per second by velocity vector components. Designed accuracy of time determination for user is within 1 millisecond to UTC(SU) but is less than 100 ns to GLONASS time. GLONASS tests have demonstrated civil accuracies significantly better than specified: 20 meters in horizontal plane, 20 meters in altitude, and between 3 and 5 centimeters per second in velocity.

The navigation user equipment conducts noninterrogational measurements of the radio navigation parameters such as pseudorange and radial pseudo-velocity to four (three) satellites of the system simultaneously or consecutively, depending on the channels of the equipment. Using measurements and the digital information transmitted by each ST, the user coordinates and the components of its velocity vector are determined, and the user time scale is "tied" to the GLONASS time scale.

Extrapolation of ephemeris information from the last time tag to the moment of signal measurement is performed by the user equipment using a Runge-Kutta integration of the satellite motion equations in the elliptical spheroid in the Greenwich coordinate system. Extrapolation errors on a 15-minute interval should not exceed 1 meter and 1 mm/s in each of the three coordinate directions.

The last generation of user equipment can recieve and process the information from GLONASS and GPS and calculate combined fixes. As a rule the future user equipment will measure carrier phase in addition to pseudoranges.

Many different types of GLONASS user equipment have been manufactured. The Tables 5,6 presented illustrate some of the capabilities of the user equipment. No attempt has been made to make this tables complete and exhaustive summary. The current total number of GLONASS users (both civil and military) is approximately 1500.

Table 5.

Brands and Main Characteristics of Russian User Equipment
(1-st generation)

Receiver Trade Name	Shkiper	Gorn-M	Daman-M	Period	Reper*	SNS-85
Developer	SRI SDE	RIRT	RIRT	RIRT	SRI SDE	RIRT
Mass ,kg	21.5	29.8	32.5	15.5	5	15
Channels, #	1	1	1	1	6	1
Frequency bands, #	1	2	2	1	1	1
Position (3σ ,m)	100	30-50	100	300	0.02	100-150
Velocity (3σ ,cm/s)	10				3-5	20-30
Differential mode (2σ,m)	-	-	-	-	1-4	-
Time to first fix, s	174	240	180	300	60-180	240
User type	naval	airborne	ground	ground	PACG**	airborne

* - equipment works with both GLONASS and GPS system
** - PACG - Principal Administration of Cartography and Geodesy

Table 6

Brands and Main Characteristics of Russian User Equipment
(2-nd generation)

Receiver Trade Name	Shkiper-M*	ASN-21*	Inter-A*	Zver-M*	Briz*	Gnom-M*
Developer	SRI SDE	RIRT	STC Interna vigation	RIRT	SRI SDE SMA AM	SRI SDE
Mass, kg	4.5	2.5	2.3	3.5	2	3
Channels, #	6	4	12	6	12	6
Frequency bands ,#	1	1	1	1	1	1
Position (3σ, m)	45	100	75	45	60	75
Velocity (3σ, cm /s)	7.5	200	80	200	-	10
Differential mode (2σ , m)	2-10	TBD	TBD	7-10	-	4-10
Time to first fix ,s	60-180	300	120	180	100	60-180
User type	naval	airborne	airborne	naval	handheld	airborne

* - equipment works with both GLONASS and GPS system

Glonass user equipment is designed to provide contionuous and accurate coordinate-time support worldwide.

Current user equipment can be categorized among four basic types:
- One-channel equipment, capable of receiving its navigation signal from four satellites alternately and used by users not needing fast position determination;

- Two-channel equipment, capable to receive signals from three chosen satellites alternately and having a longer fix time;
- Four-channel equipment, capable to receive signals from 4 satellites simultaneously thereby providing the shortest time to fix;
- 12-14 channel equipment, capable to receive navigation signals from 6-8 GPS satellites and from 6 GLONASS satellites.

"The Federal Program (draft) of GLONASS use in interests of civilian users" projects future user volume which is shown in Table 7 / 4 /.

Table 7

Type of user	Total number of users		
	Total	among them	
		1996-2001	2001-2005
1. Aircraft users	4200	500	3700
2. Marine and river users	24800	12400	12400
3. Land users	68100	32300	35800
Total	97100	45200	51900

6.3. Military users

All branches of the Russian military use GLONASS positioning signals. In particular, the Russian navy uses the GLONASS for submarine and ship navigation and weapon guidance, the air force uses it in aircraft and helicopter navigation, and the army uses it to determine troop location on the battlefield / 5 /.

Typical military user equipment provides: position, time, distance covered since last reference point, distance to next reference point, time of arrival at next reference point, and recommended route to next reference point.

7. DIFFERENTIAL SERVICE

To increase the GLONASS fix accuracy the differential positioning techniques are used. These techniques eliminate set of system errors. To conduct differential positioning using GLONASS data, a reference station and a radio-link must be available. Position corrections are computed at the reference station and then they are broadcast to the user. Thus, the correction signals are valid only in a limited region around the station, which determines the operational area of the differential system. Three levels of diferential subsystems will be used in Russia. They are: local, regional and wide area. On average, the use of GLONASS differential techniques results to an accuracy improvement of 1.3-1.7 times at ranges of about 1.500-2.000 km, 2-3 times at ranges of about 400-600 km, and 4-6 times at ranges of about 200-300 km.

Development of a differential system must overcome several practical problems:
- Development of reference station equipment and its subsequent geodetic referencing;

- Development of differential user equipment software;
- Development of various differential data links.

SRI SDE has developed the reference station which calculates the differencial pseudorange corrections for both systems (GLONASS, GPS). It tracks 8 GLONASS and 8 GPS satellites. One station was bought by one of the German company and was tested in 1993-1994.

The results were very good. The user can determine its position with use of corrections with accuracy less than 2 m. At the same time the reference station determined the system time with error less than 25 ns / 6 /.

Radio links do not currently exist to transmit the differential corrections to users. The Zver-M reference station and maritime radiobeacon as the first step will be capable to calculate and transmit GLONASS and GPS differential corrections. Now this equipment is being manufactured by Russian Institute of Radionavigation and Time.

A working-group of the Internavigation Committee (members from RIRT, State Scientific Research Institute for Navigation and Hydrography MD, SRI SDE and Central Scientific Recearch Institute of Marine Fleet) developed proposals to extend the RTCM standard to provide the use of GLONASS in differential mode, and the possible joint use of both satellite systems in differential mode. The following tenets were taken into account during development of the proposals:

- International cooperation on the joint use of NAVSTAR and GLONASS;
- There is standard developed by the SC-104 RTCM. This standard is complete and logical; it is compatible with GPS signal structure and has already been introdused into serial equipment by foreing manufacturers;
- The NAVSTAR and GLONASS signals and secondary information frame are not unified (each system uses different Earth models and time scales). It is necessary to develop messages compatible with recommended by SC-104 RTCM ;
- The simplicity of software for reference station and user equipment, using unification of formats of correcton information.

32 radiobeacon transmitters and refrence stations will be installed along Russian coast. Site listings of Russian radiobeacons and reference stations were submitted to IALA in January 1995.

RTCM Special committee SC-104 developed recommendations "RTCM RECOMMENDED STANDARDS FOR DIFFERENTIAL GNSS (GLOBAL NAVIGATION SATELLITE SYSTEMS) SERVICE", future version 2.2, in which all GLONASS massage types are described / 7 /. The differential GPS/GLONASS corrections which will be broadcast by Russian Lighthouse service via radiobeacon data link are given in Table 8 / 8 /.

Table 8

Minimum message types

GPS message type number	Title	GLONASS message type number
1	Differential GNSS corrections (full set of satellites)	31
3	Reference station parameters	32
5	Constellation health	33
6	Null frame	(34 , N=0 or N=1)
7	Radio beacon almanacs	35
9	Sub-set differential GNSS corrections (This may replace Types 1, 31)	34 (N>1)
16	Special message	36

Today the transmission of differential corrections is carried out in accordence with Recommendation ITU-R M.823 / 9 /.

8. FUTURE GLONASS DEVELOPMENT

GLONASS is full operational now. Two to three launches of three satellites each year will be required to maintain the system. As part of a continuing improvement program, a small number of these satellites will contain new modifications of equipment which will be tested. The overall GLONASS system improvement plan is to be conducted in several stages.

The first stage (1995-1998) will include the development of an improved GLONASS satellite with a 5-year active life-span. The current GLONASS satellite has a mass of approximately 1.300 kg, but mass is expected to be increased to 1.480 kg during the first upgrade, mostly due to increased fuel loading. Minor modifications to the GLONASS Proton launch system will be required to put into orbit .these heavier satellites.

Along with increasing lifetime of the onboard systems, the satellite will have a better attitude control system, thus improving the accuracy of the ephemeris calculation. In addition, an improved onboard clock will provide more stable time signals.

Other planned system upgrades will include an improved phase control system and new high performance ground based computers. The final results of these planned modifications will improve positioning accuracy to 50 m in the horizontal plane, 70 m in vertical plane, and 0.1 cm/s in velocity. Time accuracy will be increased to within 100 ns of system time, and to within 1 ms of the GOSETALON time scale. In addition, differential corrections with respect

to UTC and the system time scales of GPS and GLONASS are planned to be relayed by the GLONASS system.

Ground tests of these upgrades are underway now. The first launch of 5 year lifetime satellites is planned in 1996 and the full replacement of satellites will be completed by 2000.

The second stage (after 2000) of GLONASS development foresees launches of the GLONASS-M satelites. This upgrade will provide the system with more autonomous satellites.

Transition from GLONASS satellite to GLONASS-M satellite foresees autonomus satellite operation for up to 60 days without degradation of the accuracy. This task will be carried out if each satellite will have the capability to make intersatellite measurements, which would allow to calculate satellite ephemeris and time-and-frequency corrections onboard satellite without ground support.

The GLONASS-M satellite will have the additional equipment for intersatellite measurements in the optical and radio frequency bands. The intersatellite communication link will be installed to broadcast navigation data. Special electronic equipment (SEE) will be used for intersatellite measurements to determine ephemeris and phase synchronization of each satellite. Onboard optical measurements would significantly reduce the problem of satellite selfpositioning, but they would require that satellites have an inertial coordinate system integrated with their onboard GLONASS satellite reciever equipment or other electronic equipment. Laser signals could either be reflected by a corner reflector (passive scheme) or would switch on a laser transmitter through a receiving device (active scheme). Results of mutual measurements can be relayed by a special radio link from one satellite to another and used for mutual position processing. Tied into one constellation they would be an accurate inertial coordinate system which will be corrected with the use of stellar observations.

The parameters measured by SEE are: pseudo-range with an accuracy of 1 m (3 rms error), optical range with an accuracy of 0.1 m (3 rms error), and angular coordinates in respect to the stars with an accuracy of 1 arc second.

The GLONASS-M system will provide:
- continuous, efficient, and accurate positioning fix of an unlimited number of users in any region of the world and any part of air and space at altitudes up to 40.000km;
- air traffic control;
- continuous efficient time and heading determination (fix accuracies within: 10-15 m, 0.01 m/s, and 15 arc sec in heading);
- relay to users the difference between the GLONASS-M time scale and the standard time scale, with an error less than 20-30 ns (3 rms error) / 5 /.

Errors in the extrapolation of the Earth's rotation irregularity (which are 30-40 m/s (rms deviation) in 60 days) are the main factor impeding 60-day complete ephemeris support autonomy. When converted to ephemeris, these errors result to satellite position errors between 45 and 70 meters. It is expected that addition of an autonomous orbital configuration system aboard the GLONASS-M satellite will increase the satellite's mass to approximately 2.000 kg.

The GLONASS-M Groud Control System will be based on the present GLONASS control center. An Automatic Measuring/Computing System and mobile command and tracking equipment will be operational by the Fall of 2000.

The designers of GLONASS-M system maintain that satellite clock instability will be about 10^{-13}, and in future the value of $5x10^{-14}$, is attainable. Stability of the ground clock as expected will be about 10^{-14}.

The main obstacle to increase high accuracy is the creation of compact, very stable frequency generators, and their installation on space vehicles and systems. A space experiment is currently being prepared to test very stable hydrogen frequency generators. The experiment is being conducted in cooperation with German and Swiss specialists. The project is called "H-Maser in space".

9. FORMER SOVIET UNION SUPPORT TO CIVIL USERS

Application for GLONASS within the CIS

According to Interstate Program adopted by Act of Council of CIS Heads of Governments in April 15, 1994 GLONASS is the principal system of navigational and geodetic survey support of different CIS users. Ukraine and Belorus are the most active republics in development and manufacturing of GLONASS, GLONASS/GPS user equipment.

Scientific Research Institute KVANT (Kiev, Ukraine), Radiodevice plant ORIZON (Smela, Ukraine) develop reference stations for marine and airborne applications and integration GLONASS/GPS receiver equipment.

Plant Izmeritel (Novopolotsk, Belorus) has manufactured several GLONASS/GPS reference stations in cooperation with SRI SDE (Moscow, Russia).

The other CIS republics finance the Russian developers and manufacturers of user equipment according to share tenet.

Creation of GLONASS, GLONASS/GPS marine, airborne, geodetic, handheld user equipment and differential subsystems are supported. The main efforts are applied to develop and manufacture the GLONASS/GPS user equipment. Besides, Ukraine develops integrated user equipment which use radiosignals of ground and satellite navigation systems.

ACKNOWLEDGEMENT

The author would like to thank his co-worker O.Nikitin who has helped him to prepare and form this lecture.

REFERENCE

1. State Scientific Technical Program "Russian Radionavigation Plan", 1993.

2. Global Navigation Satellite System (GLONASS), Interface Control Document, 3d version, MSF, Moscow, 1995.

3. Shabshaevich, V.S. and other authors, Net Satellite Radionavigation Systems, Moscow, Radio and Communication, 1993, p. 367.

4. Federal Program of Global Navigation Satellite System use in interests of Civilian Users, Draft, 1995.

5. Russia's Global Navigation Satellite System, edited by ANSER, Arlington, VA, USA, 1994.

6. Lechner W., Vorsmann P. Combined GPS, GLONASS, INS Equipment on Base of Raw Data - The first test results of experiment emission, Proceeding of Conference, Krasnoyarsk Politechnical Institute, September 1992.

7. RTCM Recommended Standards for Differential GNSS (Global Navigation Satellite Systems) Service, Third Draft, Future version 2.2, 1995.

8. Broadcast Standard for Russian DGPS/DGLONASS Ligthause Service of HDoNO MD, St.Petersburg, HDoNO MD, 1996.

9. Recommendation ITU-R M.823, Draft, Technical Characteristics of Differential Transmissions for Global Navigation Satellite System from Maritime Radio Beacons in the Frequency Band 283.5 - 395 kHz in Region 1 and 285 - 325 kHz in Regions 2 and 3, Document 8/1027-E, 26 July 1995, ITU, GENEVA, 1995.

INTEGRATED GPS/GLONASS USER EQUIPMENT.

By

Jacques Beser, Ph.D.

3S NAVIGATION
23141 Plaza Pointe Drive
Laguna Hills, CA 92653
(714) 830-3777

ABSTRACT

Integrated GPS/GLONASS receivers offer better availability, performance and integrity than GPS-only receivers. In this lecture, the GPS and GLONASS systems are compared and the advantages and difficulties associated with their combined use are discussed. The 3S Navigation R-100 series of receivers is used as a model to discuss the various receiver components and functions, including the antenna, RF/IF unit, tracking module, measurement generation and navigation solution generation. The R-100 architecture is described as well as that of the GNSS-200, which is more compact and the latest GPS/GLONASS receiver produced by 3S Navigation. Air, sea and ground results are presented. These include results for both the R-100 series as well as the GNSS-200. Stand-alone as well as differential performance are discussed.

1.0 INTRODUCTION

Two satellite-based navigation systems are now fully deployed, the U.S. GPS and the C.I.S. GLONASS. Each consists of up to 24 satellites. Although there are several similarities between these systems, the characteristics of each are sufficiently different to affect operations. Specifically, the GLONASS 3-plane versus GPS 6-plane constellation and the differing inclinations offer distinct availability features as a function of latitude, with GLONASS favoring the extreme latitudes while GPS favors the mid latitudes. This effect gets more pronounced as mask angles increase. A receiver able to operate with both GPS and GLONASS would offer the best of both worlds, with one system making up for the limitations of the other.

The added availability of GLONASS satellites would not only increase the number of visible satellites, which is the case at any location, but would provide satellites at higher elevations than achievable with GPS alone.

In addition to the added number of satellites and improved geometry, providing improved access and therefore safety margin, a GPS/GLONASS receiver is affected by Selective Availability (SA) only to the extent that GPS satellites are being used for navigation. If GLONASS-only receiver operation is selected, there is no SA and therefore 10 to 15 m (1σ) accuracy is achievable. This is significant, as baseline GPS with SA yields 50 m (1σ) horizontal accuracy, and requires a differential implementation for better accuracy. But this involves ground

Paper presented at the AGARD MSP Lecture Series on "System Implications and Innovative Applications of Satellite Navigation", held in Paris, France from 1-2 July 1996; Rome, Italy from 4-5 July 1996; Madrid, Spain from 8-9 July 1996 and St. Petersburg, Russia from 11-12 July 1996, and published in LS-207.

stations and data links, thereby increasing complexity and cost.

In addition, the GLONASS P code is currently not encrypted and provides civilian users with an accuracy comparable to the GPS Y code.

This paper addresses the advantages of integrated GPS/GLONASS navigation and describes the major components and functional requirements of an integrated GPS/GLONASS receiver. Performance data are presented for both stand-alone and differential operations.

2.0 BACKGROUND

Satellite-based navigation systems are ideally suited for navigation. They do not require locally-based ground equipment and provide all weather 24 hour-a-day availability. Optimal performance is achieved through the integrated use of GPS and GLONASS in a single receiver.

2.1 GPS/GLONASS Comparison

The U.S. Navstar Global Positioning System (GPS) is a space-based navigation system that provides the user with precise position, velocity and time information on a 24-hour basis in all-weather conditions and at any point on the globe. The system consists of a space segment, a control segment and a user segment (Ref.1). The space segment consists of 21 satellites and 3 active spares in six 12-hour orbits. The orbits are at an altitude of 20,180 Km with an inclination of 55 degrees. Each satellite continuously broadcasts a message containing precise information relative to its own position (ephemeris) and clock accuracy and less precise information relative to the position of the other satellites in the constellation (almanac). The control segment consists of monitor stations and a master control station. The monitor stations transmit satellite tracking data to the master control station, which determines the satellite orbital parameters and communicates them to the satellites for retransmission to the users. The user segment consists of the equipment necessary to track the satellites and derive position, velocity and time from the information received from the satellites as well as from other user vehicle systems.

The potential unauthorized use of this source of very precise navigational information has prompted the DoD to intentionally contaminate the satellite signals and to provide authorized users with the necessary information to recover the original signal. This contamination is called Selective Availability (SA) and results in only 100 m (2 drms) horizontal accuracy for unauthorized users. This is insufficient for many civilian applications. Given the current DoD policy to provide the full GPS accuracy to only a limited number of users, mostly the military, the civilian community devised a variation of the system, called Differential GPS (DGPS), to allow for an assured, uninterrupted level of accuracy. Briefly stated, differential GPS takes advantage of the fact that a substantial portion of the GPS error budget consists of slowly changing biases which are correlated both in time and distance between receivers. If two receivers are operating simultaneously at different locations and the location of one of them is known, correction terms to its real time measurements can be generated from this position knowledge and applied to the other receiver measurements. However, the need for dual receivers and for data link capabilities at both locations increase cost and complexity.

The GPS satellite signal uses two carrier frequencies in the L band, 1575.42 MHZ (L1) and 1227.6 MHZ (L2).

Each of these signals is modulated by either or both of a 10.23 MHZ precision (P) signal (aka Precise Positioning Service, PPS) and/or a 1.023 MHZ coarse/acquisition (C/A) signal (aka Standard Positioning Service, SPS). The binary signals are formed by a P-code or a C/A-code which is modulo-2 added to 50 bps data. The P and C/A signals are then modulo-2 added to L1 in phase quadrature (only P is present on L2). The P code is a pseudo random sequence with a period of one week, while the C/A code is a unique Gold code with a period of 1 msec. GPS receivers duplicate the P and/or C/A codes and the transmission time is determined by measuring the offset that is to be applied to the locally generated code to synchronize it with the code received from the satellite. Since the P code has a wider bandwidth, it is more difficult to acquire than the C/A code, but provides better accuracy and additional anti-jam protection. For an authorized user, operation with the P-code typically provides an unfiltered accuracy of about 16 m (1σ) while the C/A-code typically provides an unfiltered accuracy of about 32 m (1σ).

The Global Navigation Satellite System (GLONASS) (Ref.2,3,4,5,6,7) is similar to the GPS in that it is a space-based navigation system providing global, 24 hour-a-day, all weather access to precise position, velocity and time information to a properly equipped user. It consists of 24 satellites in 3 orbital planes at 19,100 Km altitude, corresponding to an 11 h 15 min. period. Orbital inclination is 64.8 degrees, as opposed to the 55 degrees of GPS. As will be discussed later, this has a significant impact on operations at high latitudes. As with GPS, each GLONASS satellite continuously broadcasts its own precise position as well as less precise position information for the entire constellation. But the transmitted data is in the form of Earth-Centered-Earth-Fixed (ECEF) coordinates and extrapolation terms, as opposed to orbital parameters, as is the case for GPS. The GLONASS control segment is similar in purpose and function to its GPS counterpart, although less is known about it in the West, as compared to GPS. The user segment consists of the equipment necessary to track the GLONASS satellites and derive position, velocity and time from the satellite data and measurements.

Each GLONASS satellite uses two carrier frequencies in the L band, which, contrary to the GPS implementation, are different for each satellite. The L1 band ranges from 1602.5625 MHz to 1615.5 MHz in jumps of 0.5625 MHz, while the L2 band ranges from 1246.4375 MHz to 1256.5 MHz in jumps of 0.4375 MHz. Each of these signals is modulated by either or both of a 5.11 MHZ precision (P) signal and/or a 0.511 MHZ coarse/acquisition (C/A) signal. The binary signals are formed by a P-code or a C/A-code which is modulo-2 added to 50 bps data. The P and C/A signals are then modulo-2 added to L1 in phase quadrature (only P is present on L2). The P code is a pseudo random sequence with a period of one second, while the C/A code is a pseudorandom sequence with a period of 1 msec. Contrary to GPS where all codes are unique to a specific satellite, a single GLONASS code is used for all satellites. GLONASS receivers duplicate the P and/or C/A codes and the transmission time is determined by measuring the offset that is to be applied to the locally generated code to synchronize it with the code received from the satellite. For unauthorized users, the accuracy achievable with GLONASS is actually superior to that achievable with GPS since there is no Selective Availability implementation on GLONASS.

In an effort to reduce the bandwidth utilized by GLONASS as well as to reduce interference in the

radioastronomy band, the GLONASS operators have formulated a transitional frequency plan as follows: until 1998, frequency channels 13 through 21 will be avoided as much as possible by implementing an antipodal configuration, in which two satellites in the same plane and separated by 180 degrees broadcast on the same frequency. From 1998 to 2005, all channels above 13 will not be used, with channel 13 used as little as possible. Beyond 2005, the band will be shifted from 0,12 to -7,+6.

The current GPS/GLONASS frequency utilization is shown in Figure 2-1.
A summary of the GPS and GLONASS characteristics is presented in Table 2-1.

2.3 GLONASS Data Messages

Figures 2-2 through 2-5 present the structure and content of the GLONASS navigation data messages broadcast by the satellites and modulated on the C/A and P codes.

As shown on Figure 2-2, the C/A code message structure consists of a superframe of 2.5 minutes containing 5 frames of 30 seconds each. Each frame consists of 15 lines, each 2 seconds long. All frames contain the ephemeris and clock data for the broadcasting satellite as well as the almanac for 5 satellites (except frame 5 which only contains almanac for 4 satellites). The detailed data content is presented in Figure 2-3.

TABLE 2-1. GPS AND GLONASS CHARACTERISTICS

GPS	GLONASS
* Spread Spectrum System	* Spread Spectrum System
* Code Division Multiplexing	* Frequency Division Multiplexing
* 24 Satellites in Six Planes . Approx. 12 h Orbit. Period . 54 Degrees Inclination	* 24 satellites in three Planes . Approx. 11h 15 min. Period . Approx. 65 Degrees Inclination
* C/A and P(Y) Codes	* C/A and P Codes
* Selective Availability	* No Selective Availability
* Satellite Broadcast Orbital Parameters Updated Every Hour	* Satellite Broadcast ECEF Position, Velocity, Accel. Updated Every 30 minutes
* WGS-84 ECEF Frame	* PZ-90 ECEF Frame
* GPS Time Synchronized with UTC (USNO)	* GLONASS Time Synchronized with UTC (SU)

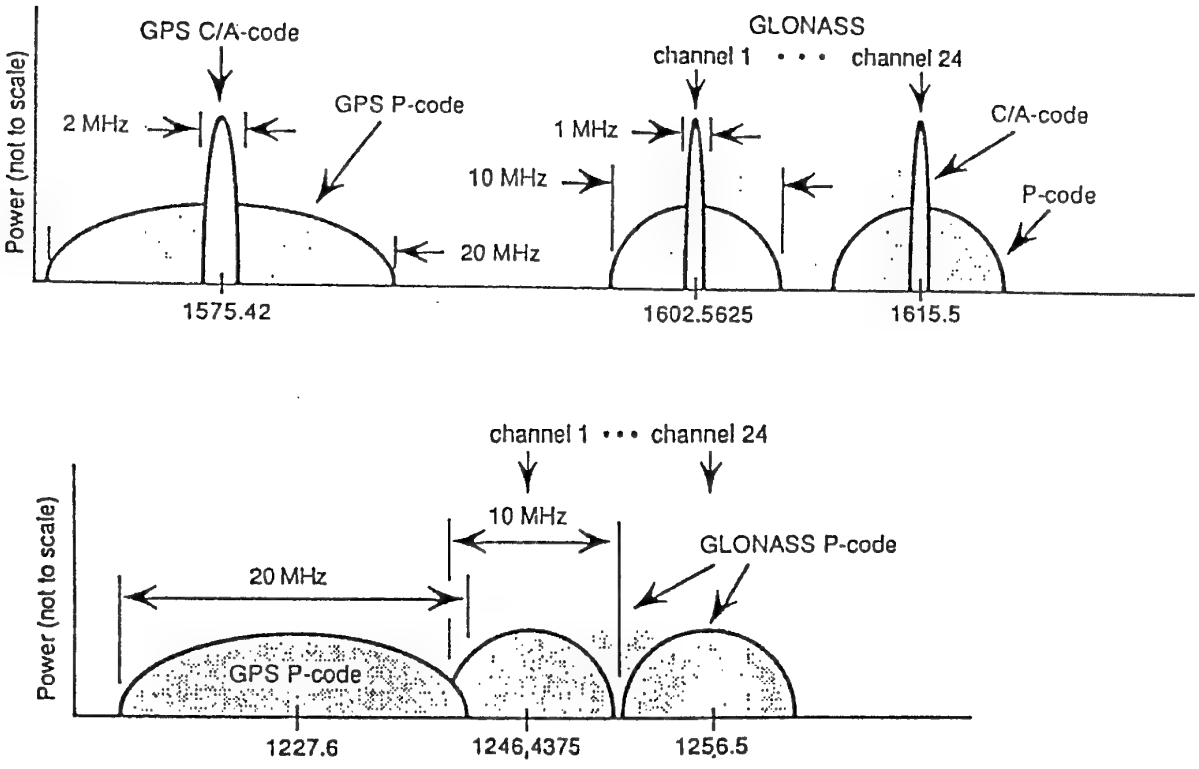

FIGURE 2-1. GPS/GLONASS FREQUENCY UTILIZATION

For the P code data, as shown on Figure 2-4, the superframe has a 12 minutes duration, and consists of 72 frames of 10 seconds duration. Each frame consists of 5 lines, each 2 seconds long. Each frame contains the ephemeris and clock information for the broadcasting satellite as well as one third of the almanac information for one satellite, requiring therefore 72 frames for the entire 24 satellites constellation.

3.0 ADVANTAGES OF DUAL GPS/GLONASS SYSTEM

In this section, the advantages of combined GPS/GLONASS operation are briefly reviewed. More details can be found in reference 7.

3.1 Faster Acquisition Time

A faster acquisition time can be achieved in the cold start mode, as more satellites are visible at any given time and location, thereby increasing the probability of acquisition.

3.2 Better Coverage in Obstructed Environment

This is one of the primary advantages of the dual implementation. Especially for applications where it is essential that tracking be continuous even when surrounded by buildings, trees or mountains, the increased constellation will greatly enhance operational capability.

Figure 3-1 illustrates the advantage of combined operation in New-York city, assuming a 45 degree mask angle.

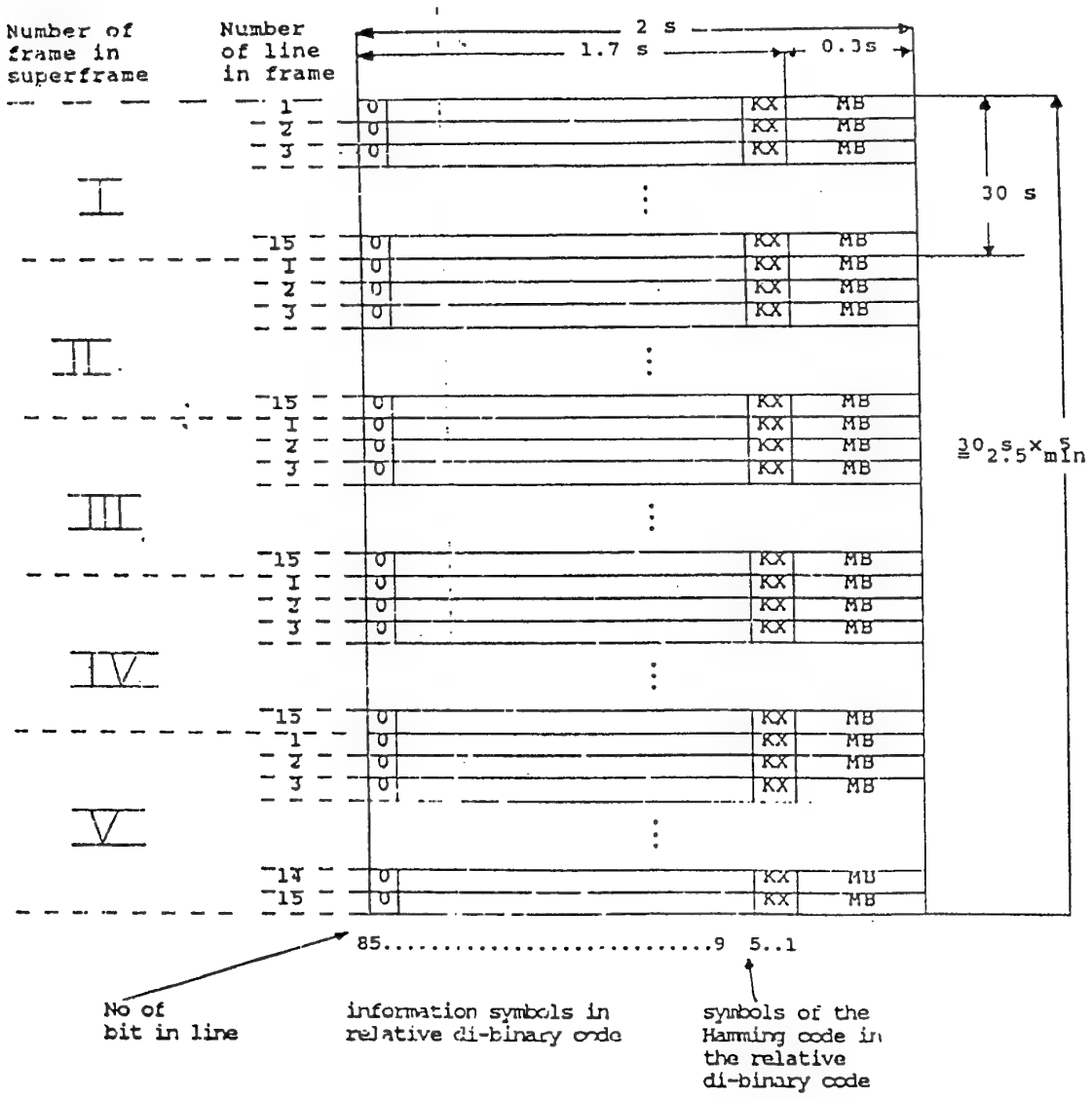

FIGURE 2-2. C/A CODE NAVIGATION MESSAGE FRAME STRUCTURE

3.3 Improved Accuracy

This section first addresses system accuracy at the measurement level. Position accuracy is then obtained by multiplying measurement accuracy by PDOP.

3.3.1 Measurement Accuracy

A pseudorange measurement error budget is presented in Ref.7 for a GPS C/A code receiver. If one also factors in the Selective Availability (SA) contributions, the projected Standard Positioning Service (SPS) horizontal accuracy is 100 meters (2drms). This approximately leads to 50 meters (1σ) and considering an HDOP of 2.0 we obtain a measurement accuracy of 25 meters.

A similar error budget is not available for the GLONASS system. An MIT Lincoln Laboratory paper (Ref.8) determined via measurement sampling and analysis that GLONASS measurement accuracy was 7 meters (1σ). Closer inspection of the work done on this paper indicates that mean values (i.e. 50% probabilities) were used instead of the RMS values. A better estimate for the range accuracy would therefore be 8.75 meters, or about the SPS GPS accuracy available without SA implemented.

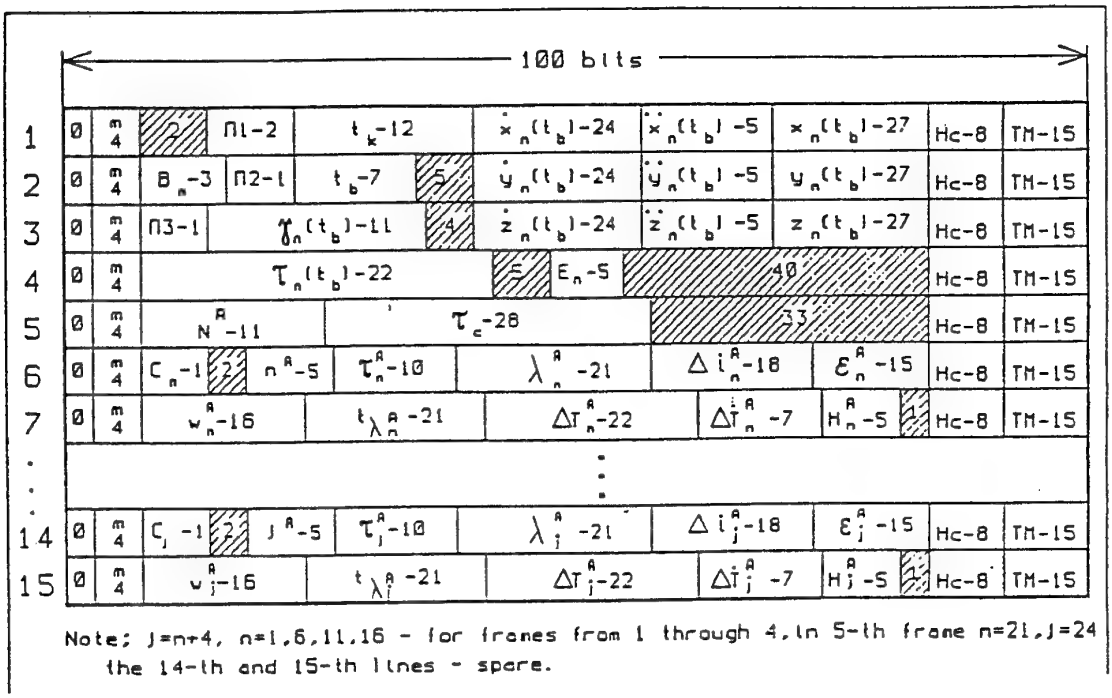

FIGURE 2-3. C/A CODE NAVIGATION MESSAGE STRUCTURE

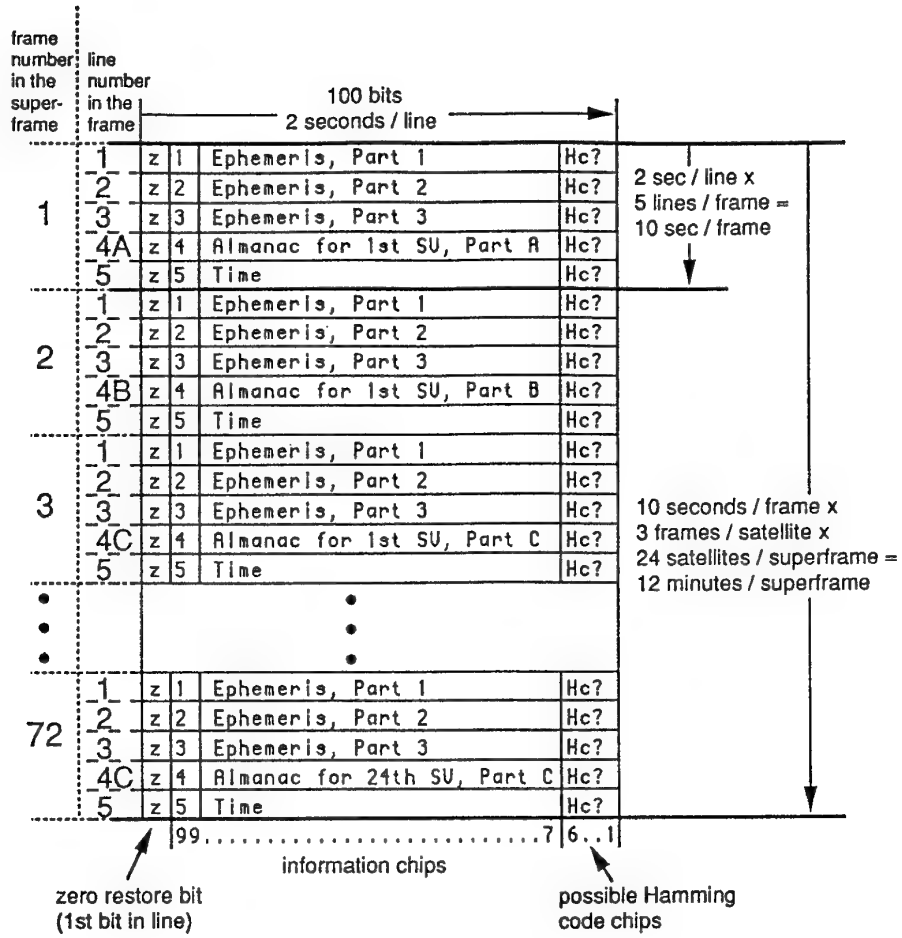

FIGURE 2-4. P CODE NAVIGATION MESSAGE FRAME STRUCTURE

The GLONASS measurement accuracy of 8.75 meters is quite attractive compared with the commercial GPS measurement accuracy of 25 meters.

3.3.2 Dual Operation Accuracy Issues

The major software issue relating to dual GLONASS/GPS operations has to do with timing. Specifically, in a GPS-only or GLONASS-only configuration, all measurements include a receiver clock error with respect to either GPS or GLONASS time, whichever system is being used. As this error is common to all measurements, it will only affect the time estimate and not the position or velocity estimates.

In the case of dual operation, some measurements will include a receiver-to-GPS clock error, while others will include a receiver-to-GLONASS clock error. Clearly, the relation between the GPS and GLONASS time references has to be known for acceptable position accuracies to be achieved. The following brief analysis clarifies the issue.

A GPS pseudorange measurement can be represented as:

$$PR_{GPS} = R + c(\delta tR_{GPS} - \delta t_{SVGPS}) + \delta atmos + noise$$

where:

PR_{GPS} is a GPS PR measurement,

δtR_{GPS} is the receiver clock error with respect to GPS time,

δt_{SVGPS} is the GPS satellite clock error with respect to GPS time,

$\delta atmos$ are the atmospheric delay errors (iono and tropo).

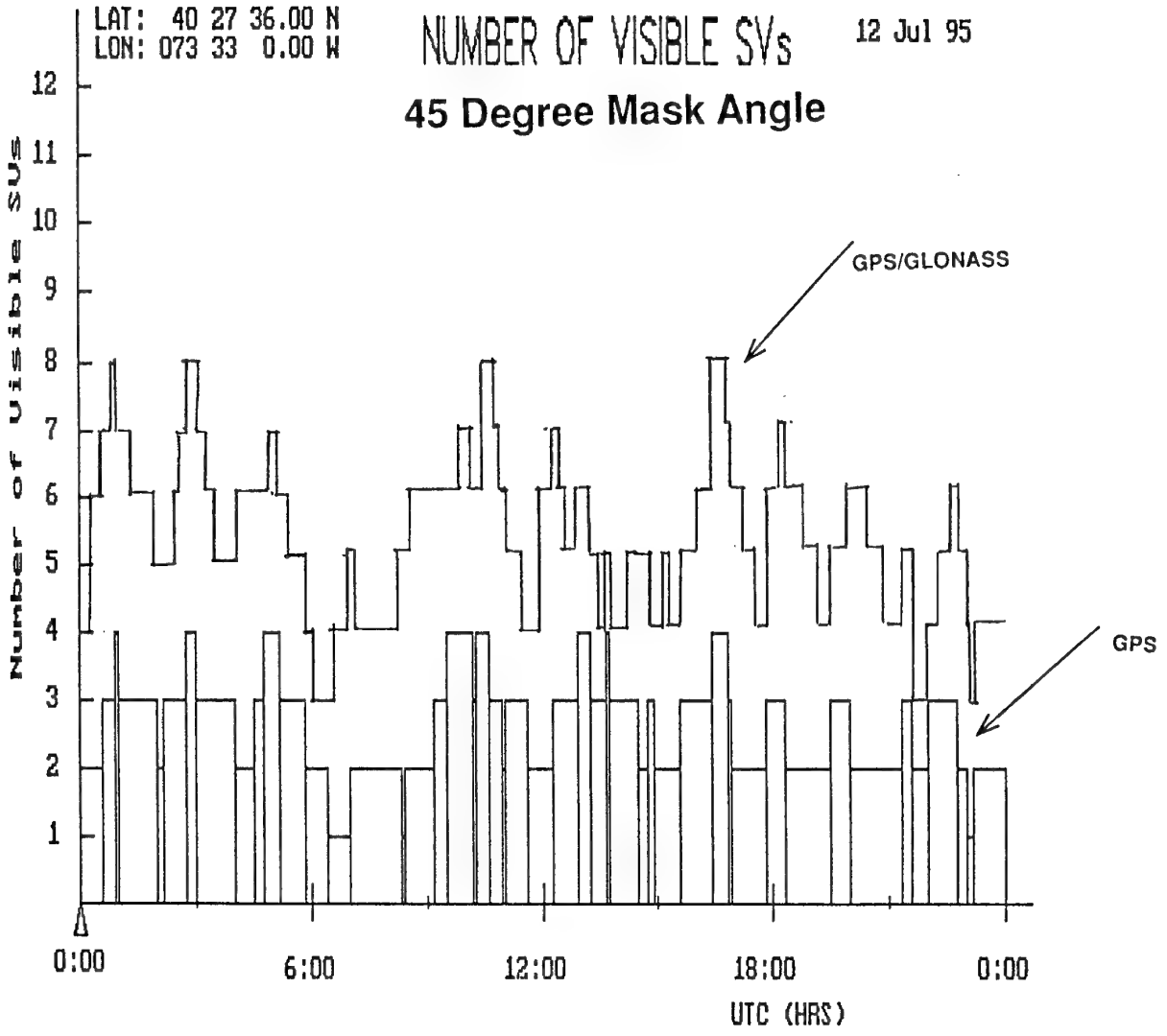

FIGURE 3-1 NUMBER OF VISIBLE SATELLITES. GPS VS GPS/GLONASS. NEW-YORK CITY. 45 DEGREE MASK ANGLE

A GLONASS pseudorange measurement can be represented as:

$$PR_{GLN} = R + c(\delta tR_{GLN} - \delta t_{SVGLN}) + \delta atmos + noise$$

with similar definitions for its components.

Any solution based on a combination of GPS and GLONASS measurements would require the determination of two receiver clock offsets, namely δtR_{GPS} and δtR_{GLN}, instead of only one. Filter state vectors could be increased to include this additional unknown, requiring five measurements instead of four. Alternatively, if the GPS-to-GLONASS time difference relationship could be determined ahead of time, GLONASS (or GPS) measurements could be software corrected to the GPS (or GLONASS) time base, thereby negating the problem, as shown by the following:

$PR_{GLN} \rightarrow PR_{GLN} + c(t_{GLN} - t_{GPS})$

$= R + c(\delta tR_{GLN} - \delta t_{SVGLN}) + \delta atmos + noise$

$+ c(t_{GLN} - t_{GPS})$

$= R + c(\delta tR_{GLN} + t_{GLN} - t_{GPS} - \delta t_{SVGLN}) + \delta atmos + noise$

$= R + c(t_R - t_{GPS} - \delta t_{SVGLN}) + \delta atmos + noise$

$= R + c(\delta tR_{GPS} - \delta t_{SVGLN}) + \delta atmos + noise$

Either way, this issue can be handled with limited effort.

GPS time is related to UTC(USNO), while GLONASS time is related to Moscow time or UTC(SU). As was shown in the work performed by Daly (Ref.9), the difference can reach several μsecs and is therefore extremely significant to overall dual mode accuracy. This work also showed that the relation between the two references can be measured and communicated to users in a timely manner to allow dual operation. However, the dependence on the broadcast time difference would subject the user to potentially large errors. Given the doubling of the number of satellites, it is recommended to solve for both time offsets and not rely on a broadcast value.

Another issue in the dual mode operation is the different ellipsoids used by the two systems, the World Geodetic Survey 1984 (WGS-84) ellipsoid for GPS and the Soviet Geocentric Coordinate System 1990 (SGS-90 aka PZ-90) for GLONASS. Since satellite data broadcast by GLONASS are in PZ-90 ECEF coordinates, whereas GPS ephemeris data and satellite position algorithms are based on WGS-84, the relationship between these two ellipsoids has to be clearly defined. The only published transformation is provided in Ref 8 by the MIT Lincoln Laboratories.

3.3.3 Overall Accuracy

The overall positioning accuracy can be obtained, in a statistical sense, by multiplying the measurement accuracy with the Position Dilution Of Precision (PDOP). In the previous section, it was shown that GLONASS measurement accuracy of 8.75 meters was achievable, whereas GPS accuracy with SA implemented would yield 25 meters accuracy.

Assuming a PDOP of 3.0, this leads to 26 meters (1σ) accuracy for GLONASS and 75 meters (1σ) for GPS.

The accuracy of the dual operation would depend on the combined effect of improved PDOP over either system alone, coupled with the reduced accuracy of GPS measurements versus GLONASS measurements, as well as the residual error in the estimate of the difference between time references.

3.3.4 System Integrity

Integrity is a major obstacle for widespread acceptance of GPS (or GLONASS). In the case of operation with a single system, it can be tested by comparing an overdetermined solution using the various possible combinations to arrive at a solution. For example, in the case of five satellites, there are five combinations of four satellites. If one satellite is providing "bad" measurements, one of the five solutions will be good, whereas the other four will be poor, thereby pointing to the bad satellite. But this approach requires calculating many solutions, thereby putting an increased computational burden on the receiver processor.

An alternate approach would be to process all-in-view. This, with a combination of residual tests, would rapidly point to a bad satellite, without requiring the calculation of multiple solutions. This requires at least five and preferably more satellites in view at any given time. Either system alone cannot provide this under all but very optimal visibility conditions. The dual GPS/GLONASS implementation, with its doubled constellation, would provide a much better integrity capability.

3.4 Tradeoff Issues

Advantages and disadvantages of the dual GPS/GLONASS implementation versus GPS only are summarized in Table 3-1.

4.0 INTEGRATED GPS/GLONASS RECEIVER DESCRIPTION

The only commercially-available GPS/GLONASS receivers are manufactured by 3S Navigation in Laguna Hills, California. The overall architecture of the R-100 series of receivers is described below to illustrate the design issues.

Combined processing of GPS and GLONASS signals is tightly integrated in the R-100 receiver architecture. Individual satellite tracking channels can be arbitrarily assigned to any GPS or GLONASS satellite. As shown schematically on Figure 4-1, the R-100 receiver includes a broadband antenna, an RF/IF subsystem, and a GPS/GLONASS Digital Signal Processor, which is implemented on an IBM PC XT/AT-compatible expansion board. The user operates the receiver through the PC host computer utilizing either NMEA 0183-formatted commands or an interactive menu-style user interface. The host computer can either be a standard-sized PC or a portable. The R-100 can be configured to include up to 16 GLONASS P code channels(user-selectable L1 or L2 for each channel), and up to 12 L1, C/A GPS or GLONASS channels.

TABLE 3-1. GPS/GLONASS VS GPS ONLY

ADVANTAGES	DISADVANTAGES
* Better accuracy due to:	* Slightly more complex receiver
* Better geometry	
* GLONASS unaffected by SA	* GLONASS future not secure
* Complementary coverage at all latitudes	
* Better availability due to more satellites in view	* US users. GLONASS not under US control
* Better integrity with all-in-view implementation	* Unproven GLONASS reliability
* Non-US users. GLONASS not under US control.	

The Antenna/Preamp assembly includes a circularly polarized L1, broadband antenna, preselection filter, and low noise preamplifier. The assembly is bolt mountable and constructed for all-weather use. A single coaxial cable connects the assembly to the RF/IF Unit. Sufficient gain is provided to permit cable lengths of up to 100 feet using RG-223 coaxial cable.

The RF/IF unit amplifies and filters the RF signal from the antenna, down converts to various intermediate frequencies (IF), selectively amplifies the desired spectra, down converts to near baseband, and digitizes in-phase and quadrature-phase samples at 17.5 MHz. The L1 RF/IF Unit synthesizes its own 10 MHz reference frequency or optionally accepts an external 10 MHz input. A coupling unit at the input provides DC power to the Antenna/PreAmp Assembly. A cable connects the RF/IF Unit to the GPS/GLONASS Digital Signal Processor.

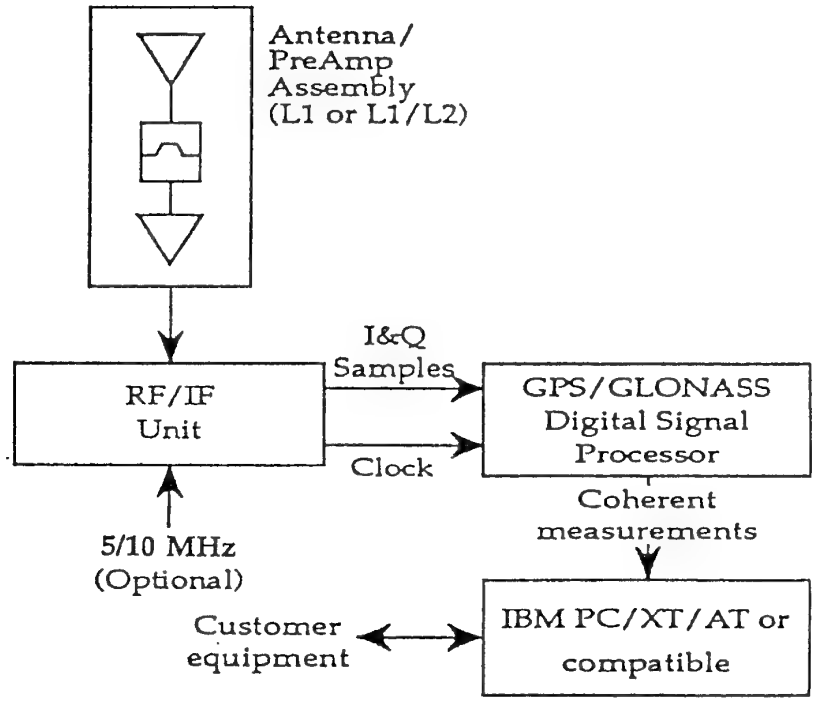

FIGURE 4-1. R-100 INTEGRATED GPS/GLONASS RECEIVER ARCHITECTURE.

The GPS/GLONASS Digital Signal Processor receives digital samples from the RF/IF Unit and continuously tracks multiple GPS and/or GLONASS satellites. It tracks phase and frequency errors due to clock drifts, satellite Doppler, receiving platform motion and thermal noise. It also provides fast-sequencing all-in-view tracking. It extracts ephemeris and almanac data from satellite data messages and transfers separate channels of satellite data to the PC host. Each P code channel occupies a standard PC expansion card which plugs into a PC 8-bit bus expansion slot. The 12-channel GPS/GLONASS L1, C/A expansion occupies a single PC expansion card.

The PC Host Computer provides an easy-to-operate user interface. It controls receiver operation and selects healthy satellites that provide best solution geometry. It calculates and displays filtered two or three-dimensional position and velocity as well as time and status information. Solutions as well as error estimates and satellite status are displayed to the user, logged to the PC hard disk, and transferred to an RS-232C output port. NMEA 0183 and RTCM SC-104 formats are supported. The tracker software is downloaded from the PC to the Digital Signal Processor boards, along with the Doppler frequency and search strategy to be used by the tracker.

An IEEE-488 interface between the host computer and a customer-supplied computer is also available.

For accurate time transfer applications, a 1 PPS output as well as synchronization with a 1 PPS input are available.

4.1 RF/IF Description

As shown in Figure 4-2, the R100/40 receiver utilizes dual down conversion for both its L1 and L2 bands. The RF signal path for L1 and L2 is kept common from the antenna down through the cable and through the first preamp of the RF/IF unit. It is then split into separate L1 and L2 paths. Each path has a first down conversion LO selected to center the GLONASS IF spectrum at or near 70 MHz. L1 uses an LO frequency of 1540 MHz and L2 uses an LO frequency of 1182.5 MHz. The down converted IF signals are amplified and then filtered by special flat group delay filters. The filtered IF signals are then passed through Automatic Gain Control (AGC) amplifiers and applied to complex I/Q down converters. This second stage of down conversion is accomplished with 70 MHz LO signals. The resulting complex baseband spectrums are centered around 0 Hz. The I and Q paths for each band (L1 and L2) are digitized with 3 bit Analog-to-Digital Converters (ADC) using a 17.5 MHz sample clock. The 3 bit data samples for L1-I, L1-Q, L2-I and L2-Q are then sent to the digital processing boards via differential ECL drivers.

L1 GPS is obtained from the L1 signal path after the first down conversion. The 1575.42 MHz RF signal results in a 35.42 MHz IF signal after this down converter. This IF signal is amplified and filtered in a separate GPS signal path. It is down converted to baseband using a 35 MHz LO and digitized with a single 2 bit ADC. The ADC operates at the same 17.5 MHz clock rate as the GLONASS path and the data bits are also sent to the digital processor using differential ECL drivers.

All LOs and digitizing clocks are phase locked to a single 5 or 10 MHz reference oscillator. This reference oscillator can either be the internal stable ovenized oscillator or any external 5 or 10 MHz source plugged into the rear panel input jack. One-Pulse-Per-Second (1PPS) timing signals applied to the rear panel of the RF/IF unit along with a corresponding 5 or 10 MHz reference signal serve to synchronize any digital divider ambiguities in the LO phase lock loops. The 1PPS signal is also buffered and sent to the digital processor boards where it is compared against 1PPS timing information from the received satellite signals.

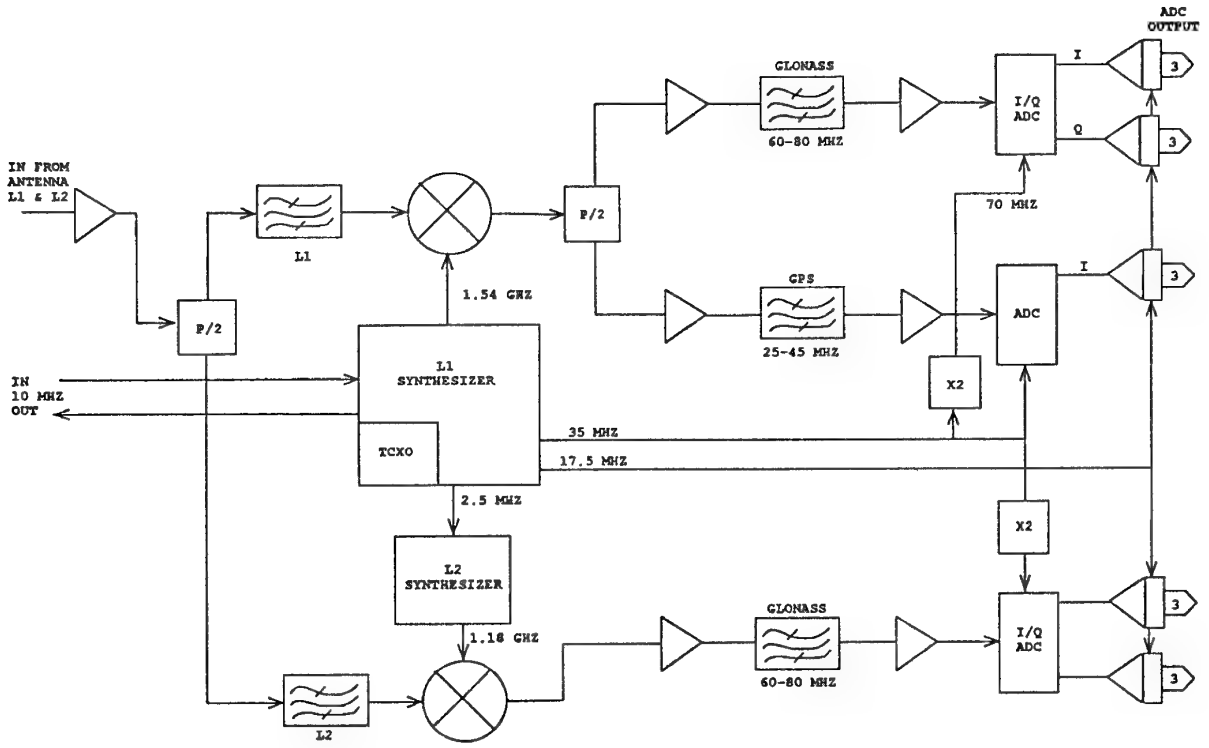

FIGURE 4-2 R100 L1/L2 RF/IF UNIT

4.2 Measurements

A satellite can be tracked by the receiver by utilizing carrier and code tracking loops. A carrier loop is usually second or third order to be able to track the satellite while the receiver is undergoing dynamic maneuvers. The designer needs to pick the loop gains so as to be capable of tracking the required dynamics levels while minimizing the added noise which is introduced by opening the loop bandwidths.

With the carrier loop tracking the dynamics, the code loop can be first order as it can benefit from a code doppler value obtained from a scaled carrier doppler measure. The code loop then only needs to track the error in this frequency, which is of much smaller dynamics.

For each tracked satellite, several measurements are formed in order to calculate the navigation solution. Position is determined using the pseudorange, while velocity and acceleration are determined using either the integrated carrier phase or the pseudorange rate (or doppler).

A pseudorange is defined as:

$$PR = R+c(\delta t_{ue}-\delta t_{sv})+iono+tropo+SA+n$$

where:

PR is the pseudorange
R is the geometric user-to-satellite range
c is the speed of light
δt_{ue} is the receiver clock bias
δt_{sv} is the satellite clock bias
iono is the ionospheric delay
tropo is the tropospheric delay
SA is the selective availability degradation
n is noise

A pseudorange is obtained by correlating a locally generated replica of the code with the received code. The required shift in the local code to achieve correlation provides a measure of the transit time. As indicated in the pseudorange expression, this transit time includes several terms besides the range. The user clock error is common to all measurements of the same constellation and is solved as part of the navigation process. The satellite clock error is largely compensated by data provided via the satellite navigation message. The ionospheric delay can be partially compensated using the Klobuchar model, again with the help of parameters broadcast by the satellites. Or, if dual frequency measurements are available, the ionospheric delay can be measured by combining the L1 and L2 measurements. The SA effects can be offset by authorized, suitably equipped users only.

The integrated carrier phase is obtained by summing the whole and partial carrier cycles detected by the receiver as it is tracking the satellite. Obviously, any loss of lock would introduce a new whole cycle ambiguity once tracking is reestablished. The change of integrated carrier phase from one measurement epoch to the next is an indication of the line of sight velocity between the receiver and the satellite.

An integrated carrier phase can be represented as:

$$\Phi=R+c(\delta t_{ue}-\delta t_{sv})-iono+tropo+N\Gamma+SA+n$$

where:

Φ is the integrated carrier phase
R is the range
c is the speed of light
δt_{ue} is the receiver clock error
δt_{sv} is the satellite clock error
$N\Gamma$ is the whole cycle ambiguity
SA is the selective availability degradation
n is the noise

The change in carrier phase over successive epochs (δT) is:

$$\delta\Phi=V\delta T+c(d_{ue}-d_{sv})\delta T-\delta iono+\delta tropo+\delta SA+\delta n$$

where:
V is the average line of sight velocity over the interval δT
d_{ue} is the receiver clock drift
d_{sv} is the satellite clock drift

The iono and tropo terms are very small and are usually neglected. The user clock drift is solved as part of the navigation process. The satellite clock drift is provided in the navigation message. SA effects can be compensated by authorized, suitably equipped users only.

A direct doppler measurement due to the receiver motion can also be performed by comparing the tracked frequency with that expected given the satellite location relative to the user. This value will typically be more noisy than the integrated carrier phase as it is an instantaneous measure.

4.2.1 Measurement Calibration

Since GLONASS satellites broadcast on different frequencies, one important consideration in the overall accuracy is the calibration of frequency-dependent errors. For example, given the larger bandwidths to be dealt with, it is likely that hardware-induced delays will not be constant across the frequency band and that interchannel delays will be introduced. This is of course also true for L1 vs L2 measurements.

4.3 Navigation Process

Once the measurements are available, it is a simple matter to compute the navigation solution. Position and velocity processing can be handled separately to avoid carrying large matrices.

The overall process is as follows:

For combined GPS/GLONASS operations there are five unknowns for the position process (three components of position plus receiver clock biases with respect to GPS and GLONASS times) and five for the velocity process (three components of velocity plus receiver clock drifts with respect to GPS and GLONASS times).

A minimum of five satellites is therefore needed for a combined solution.

For each process, the measurements-to-navigation solution relationship is:

$$\delta Z = H \, \delta X$$

where:

δZ is the matrix of measurements residuals, i.e. the difference between the measured quantity and the estimate of that quantity based on the current navigation solution,

H is the measurement matrix, i.e. consisting of a set of rows, each of which is a unit vector from the receiver to the satellite, a one for the applicable clock term and a zero for the other clock term.

δX is the navigation correction vector, i.e. a correction to the position (or velocity) vector and a correction to the applicable clock bias (or drift).

These corrections can be determined by using a Kalman filter implementation, or, more simply a weighted least squares implementation. A weighting scheme is necessary to differentiate between the relative quality of the measurements, specifically, SA-free GLONASS measurements vs GPS measurements.

The navigation solution at the next epoch is determined a priori by using the last velocity, acceleration and clock drift values to propagate to the current epoch. These values are then updated by the results of the least squares (or Kalman filter) processing of the measurements.

5.0 CURRENT GPS/GLONASS RECEIVERS

In addition to the R-100 series of receivers, 3S Navigation, in cooperation with MAN Technologie of Munich, Germany, has developed the 12 channel GNSS-200. This receiver, shown on Figure 5-1, consists of:

1. a patch antenna/preamp unit,
2. an RF/IF/Digital unit, consisting of:
    a. an internal PC/AT host computer with I/O for a keyboard, monitor ,two serial ports and one parallel port

b. twelve channel GPS/GLONASS digital processor card

c. L1 RF/IF processor card

d. AC/DC converter

This unit is quite smaller and less expensive than the R-100 series receivers. It has been tested in ground, air and sea applications in both stand-alone and differential configurations. Results are shown in the next section.

The GNSS-200 architecture is presented in Figure 5-2.

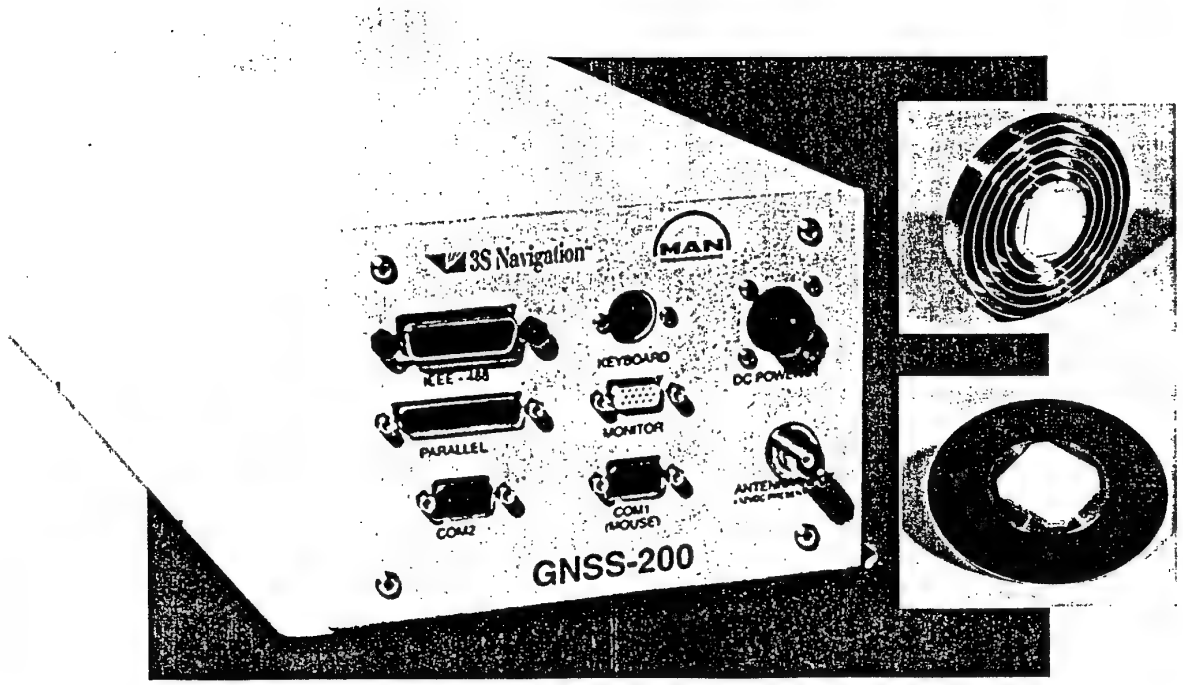

FIGURE 5-1. GNSS-200 GPS/GLONASS RECEIVER

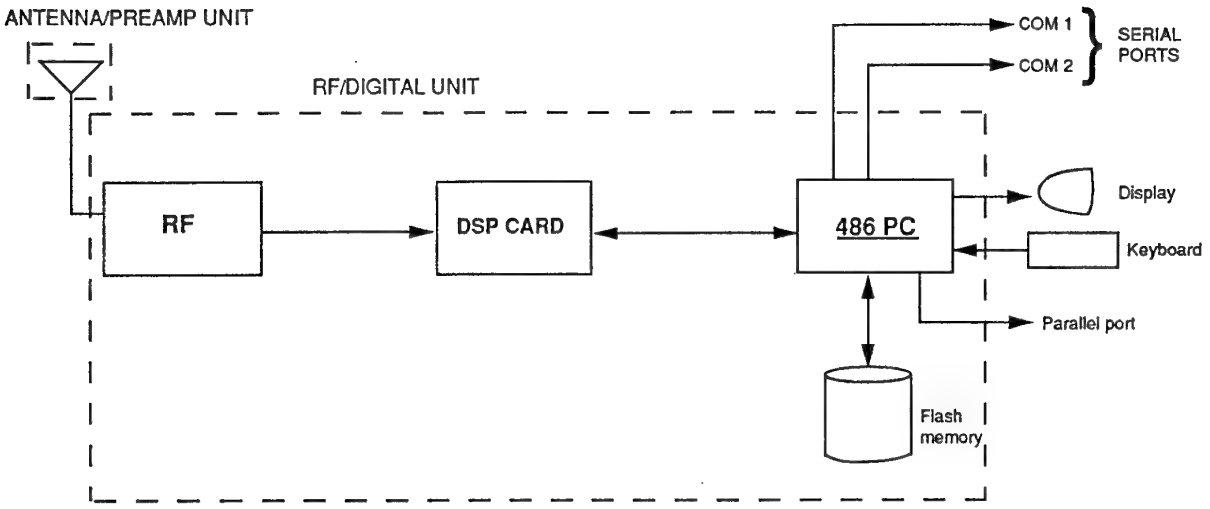

FIGURE 5-2. GNSS-200 ARCHITECTURE

6.0 PERFORMANCE DATA

6.1 R-100 Results

In this section, GPS and GLONASS stationary R-100 performance results are presented.

The antenna location was in Laguna Hills, California:

Latitude: 33.6263°N
Longitude: 117.7299°W
Altitude: 60.29 m above WGS84 Ellipsoid.

6.1.1 GLONASS-only results

GLONASS-only navigation results were obtained with an 8-channel, dual frequency R-100/40 GLONASS receiver from 14 October to 16 October 1995. During the run, slot 1, frequency channel 23 malfunctioned for a period of one hour or so, resulting in errors in excess of 10 Km. These data were removed from the data set. No other data were edited out. Statistical analysis was performed on the resulting data set (which had to be divided in four sets due to the limitations of the statistics package). The results are provided in Table 6-1.

The antenna was placed at a surveyed location whose accuracy is on the order of a few cm. The resulting mean error on the order of 1 m in each axis is a good indication of the GLONASS

performance and of the accuracy of the PZ-90 to WGS-84 transformation used by 3S Navigation. However, this assumption regarding the transformation is only valid at our location and may not be true at other locations. An organized measurement campaign at several locations is necessary to determine a global transformation.

The North vs East as well as Vertical vs East position errors are provided in Figures 6-1 and 6-2. In Figures 6-3 and 6-4, the errors have been normalized by their corresponding DOP (i.e East and North errors are divided by HDOP, while vertical errors are divided by VDOP).

TABLE 6-1. R-100/40 , 8 CHANNELS, 14-16 OCTOBER 1996 AT 3S NAVIGATION, LAGUNA HILLS, CALIFORNIA

	Test Set	E_ERR		N_ERR		U_ERR		E_ERR/HDOP		N_ERR/HDOP		U_ERR/VDOP	
(# pts)		m	SD	m	SD	m	SD	m	SD	m	SD	m	SD
(4998)	1.1	0.79	7.78	1.34	6.44	0.17	12.93	0.45	4.47	1.15	4.22	0.28	5.06
(5000)	1.2	-1.31	5.81	2.79	3.72	-0.48	13.27	-1.08	3.87	2.03	2.74	-0.41	5.37
(4996)	2.1	-0.24	5.52	1.03	6.18	-0.48	17.77	-0.18	3.77	0.91	4.31	-0.30	6.79
(5341)	2.2	-2.47	6.52	1.39	4.25	2.31	14.83	-1.92	5.05	1.01	3.26	0.94	6.54
Cum Statistics		-0.84	6.47	1.63	5.27	0.41	14.82	-0.70	4.33	1.27	3.68	0.14	6.00

Mean error is: − 0.84m E, + 1.63m N, + 0.41m U

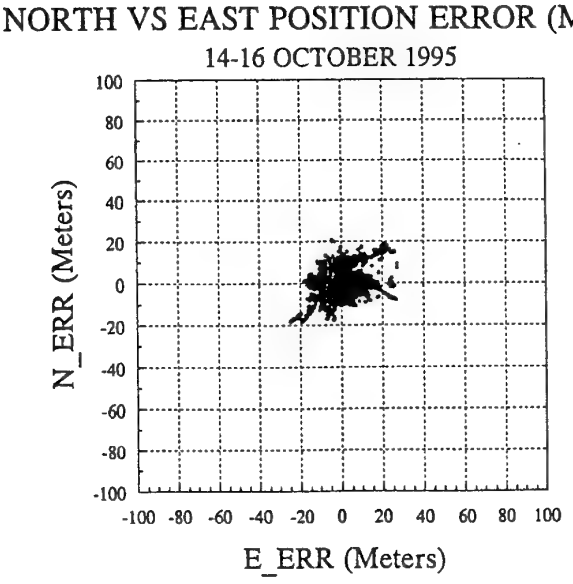

FIGURE 6-1 NORTH VS EAST POSITION ERROR DUAL FREQUENCY GLONASS R-100/40 RECEIVER

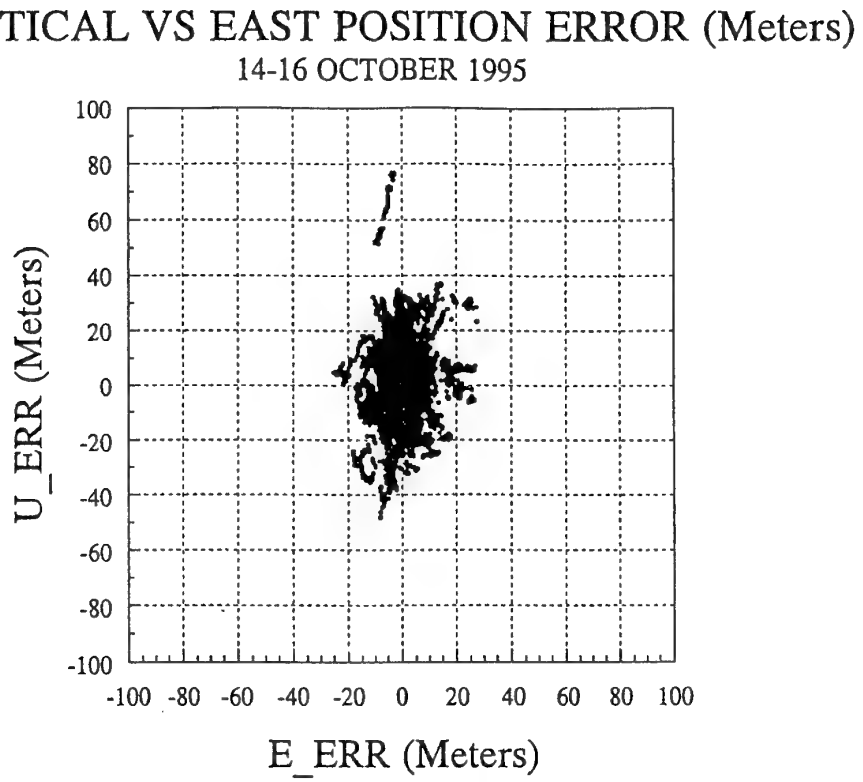

FIGURE 6-2 VERTICAL VS EAST POSITION ERROR
DUAL FREQUENCY GLONASS
R-100/40 RECEIVER

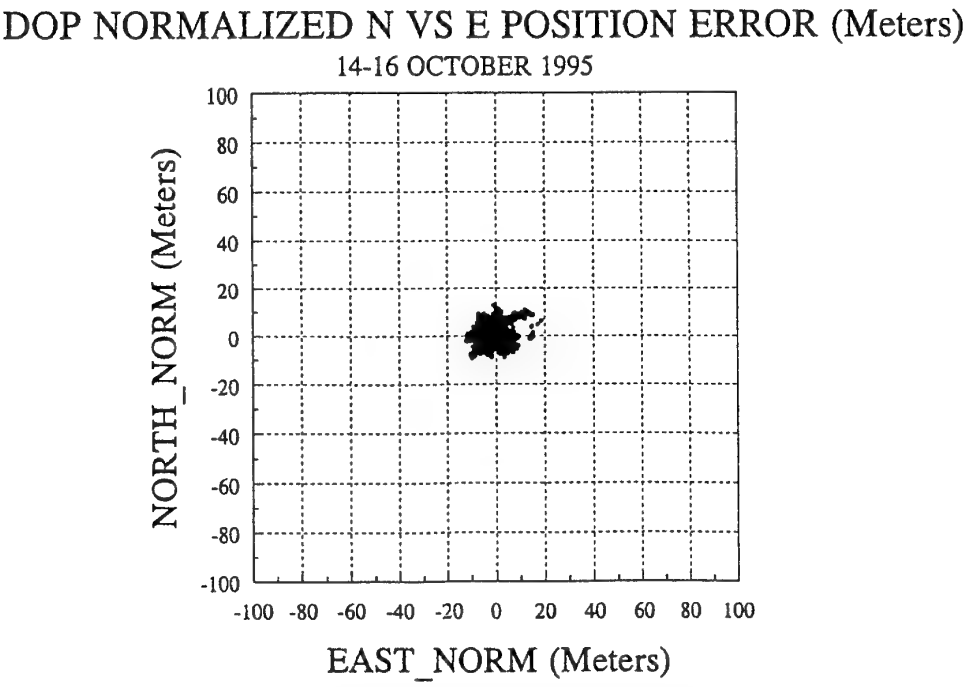

FIGURE 6-3 DOP NORMALIZED NORTH VS EAST POSITION ERROR
DUAL FREQUENCY GLONASS
R-100/40 RECEIVER

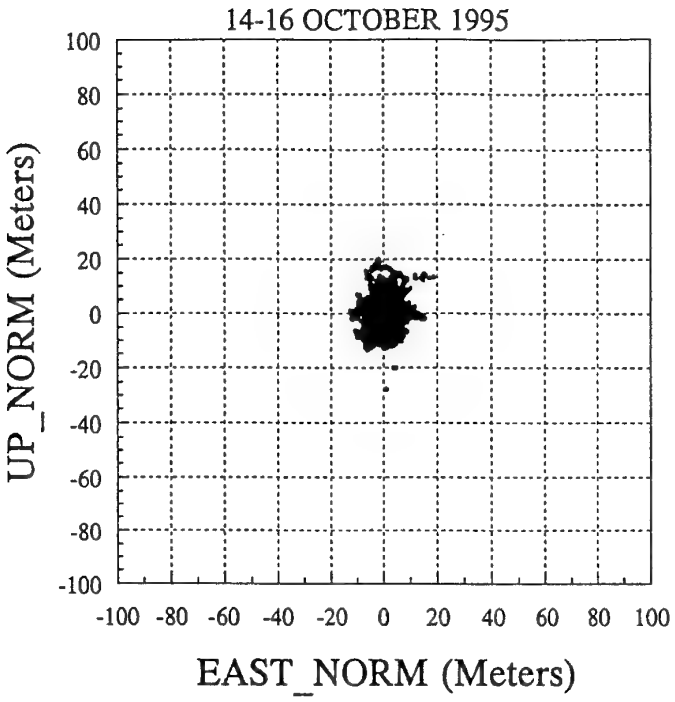

FIGURE 6-4. DOP NORMALIZED VERTICAL VS EAST POSITION ERROR DUAL FREQUENCY GLONASS R-100/40 RECEIVER

6.1.2 GPS/GLONASS Results

With additional software, the R-100 can be used as a differential reference station for both GPS and GLONASS. Both code and carrier corrections are generated in the RTCM-SC-104 format (Ref.10). Zero baseline tests were conducted at 3S navigation offices in Laguna Hills, California utilizing two separate receivers connected to the same antenna. Data were collected on 9 September 1994 from 21:32 to 21:55 UTC. Four GLONASS satellites (slots 5, 6, 16, and 21) and five GPS satellites (PRN 1, 17, 21, and 28) were tracked. During post-processing, pseudoranges and carrier phase measurements from one of the receivers were processed to generate GPS and GLONASS differential corrections at a one Hz rate. These corrections were applied to the measurements of the other receiver, after proper extrapolation. The corrections for GPS measurements are shown in Figure 6-5 and the corrections for GLONASS measurements ar shown in Figure 6-6. The SA effects are clearly visible except for satellite PRN 28 which is not SA-capable. Integrated GLONASS/GPS navigation solutions were generated for the second receiver using first the uncorrected measurements, then the differentially corrected measurements. Figures 6-7 and 6-8 present the East-North position and velocity errors, respectively, for both the baseline and differentially corrected solutions. HDOP ranged from 1.2 to 1.5 during the test.

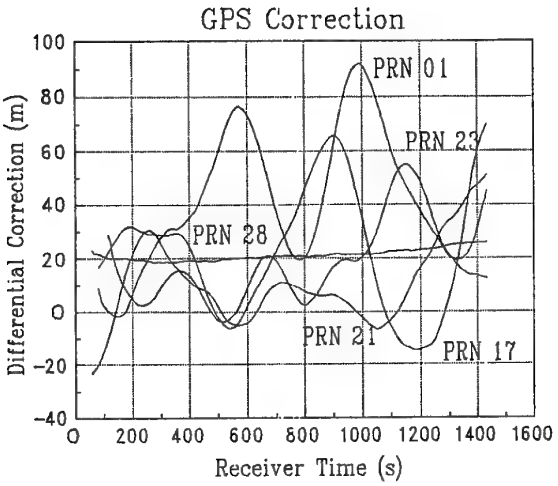

Differential Correction for GPS SVs.
09 September 1994 at 3S Navigation.

FIGURE 6-5. GPS DIFFERENTIAL CORRECTIONS

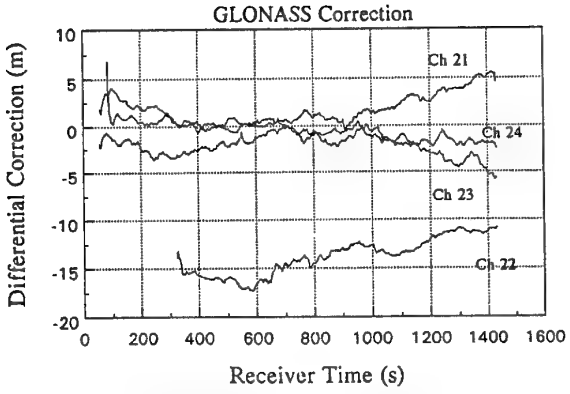

Differential Correction for GLONASS SVs.
09 September 1994 at 3S Navigation.

FIGURE 6-6. GLONASS DIFFERENTIAL CORRECTIONS

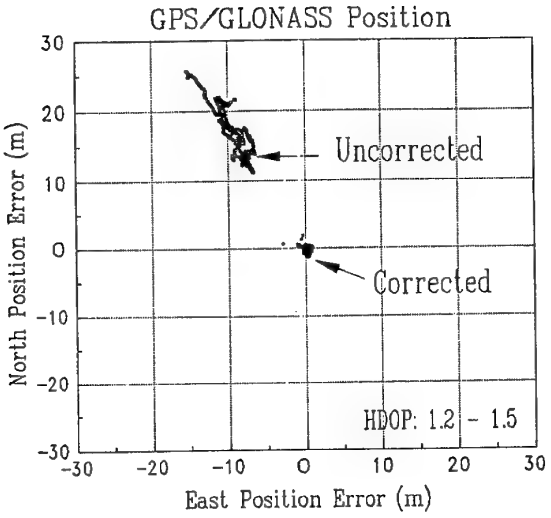

Horizontal Position Error using Uncorrected
& Differentially Corrected Measurements. 09 Sept. 1994.

FIGURE 6-7. HORIZONTAL POSITION ERRORS

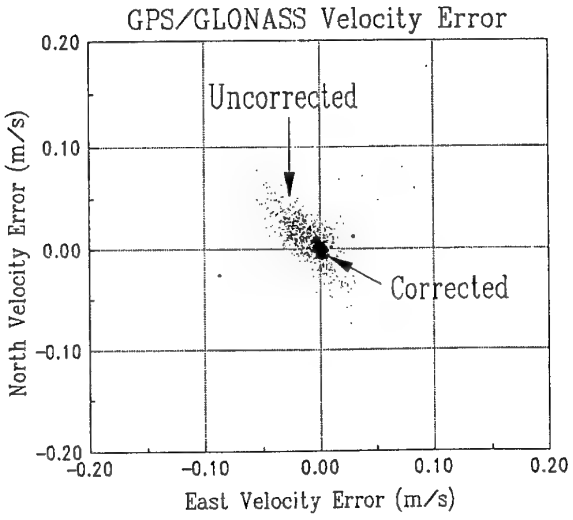

Horizontal Velocity Error using Uncorrected
& Differentially Corrected Measurements. 09 Sept. 1994.

FIGURE 6-8. HORIZONTAL VELOCITY ERRORS

6.2 GNSS-200 TESTS

Field tests were performed using the GNSS-200 receiver. This included ground, air and sea tests, as shown in Figure 6-9.

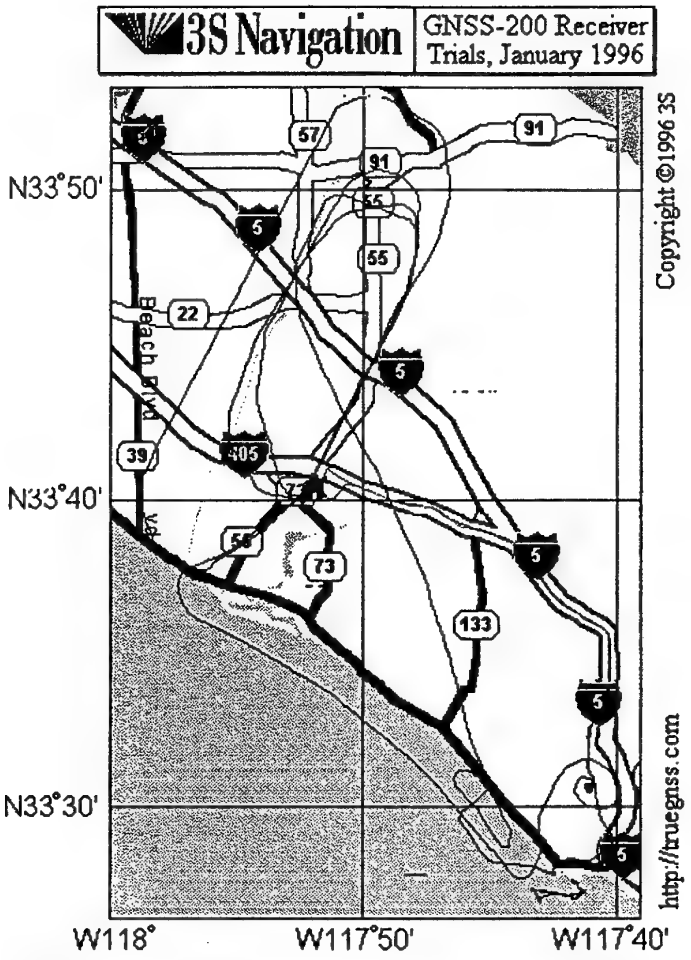

FIGURE 6-9. GROUND, SEA AND AIR TESTS SUMMARY

For the ground tests, the receiver was placed in a Sport Utility Vehicle(Isuzu Trooper), with the antenna on the roof. We left 3S navigation offices in Laguna Hills, California and headed South on the San Diego Freeway, as can be seen in Figure 6-10. We exited the freeway and proceeded to a hilly (read high mask angles!) residential area, where we drove around several streets, as can be seen on Figure 6-11. The significance of this figure is that continuous navigation is achieved with an accuracy sufficient to identify specific streets, a feat not achievable with GPS alone, when operating in non-differential mode.

The sea tests were performed using a 30 foot cabin-cruiser. We left the Dana Point harbor dock, as can be seen on Figure 6-12 and proceeded to the harbor entrance, after which we headed to the buoy outside the Dana Point bluffs. What looks like errors in the navigation solution is actually our attempts to get closer to whales which

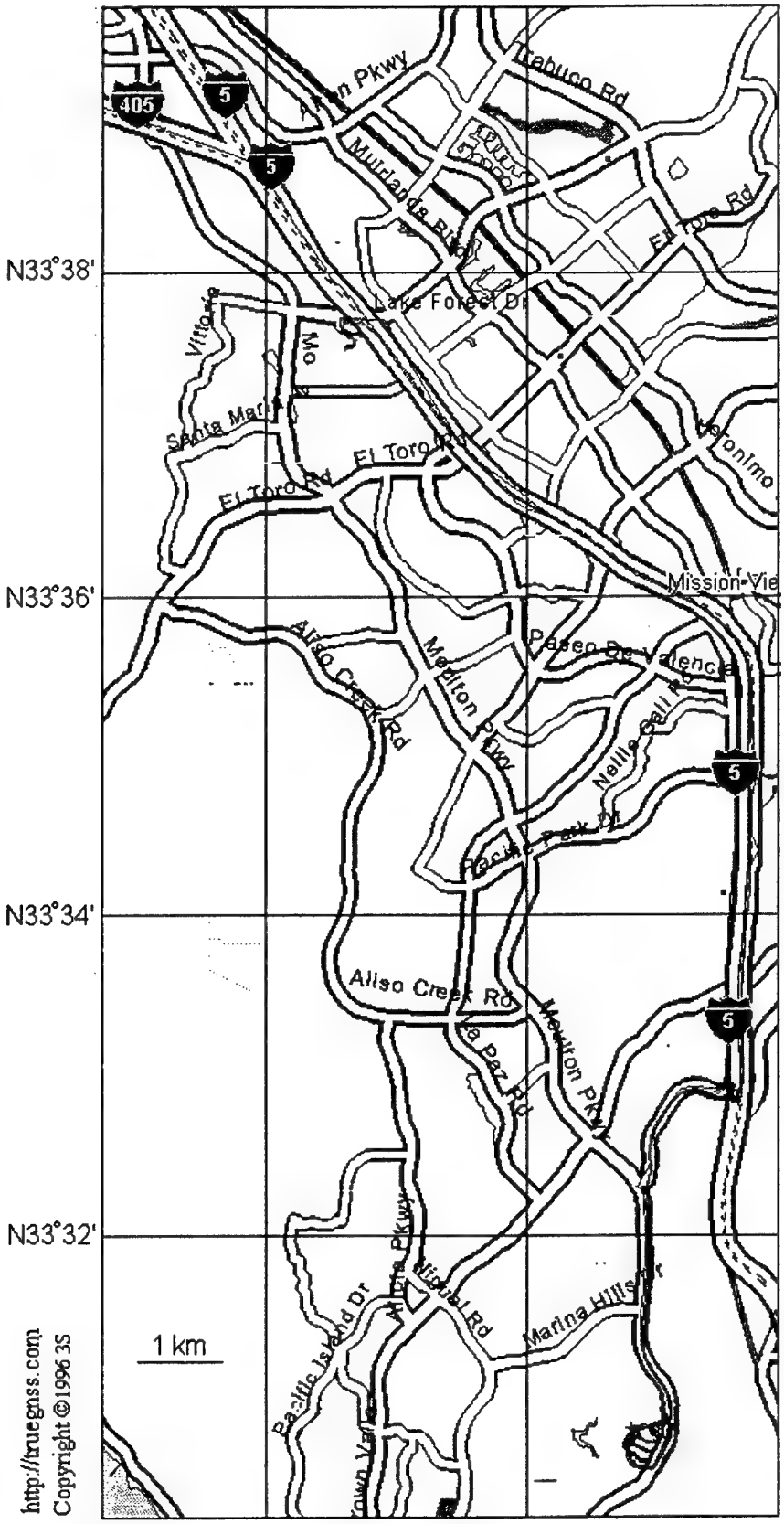

FIGURE 6-10. GNSS-200 GROUND TEST

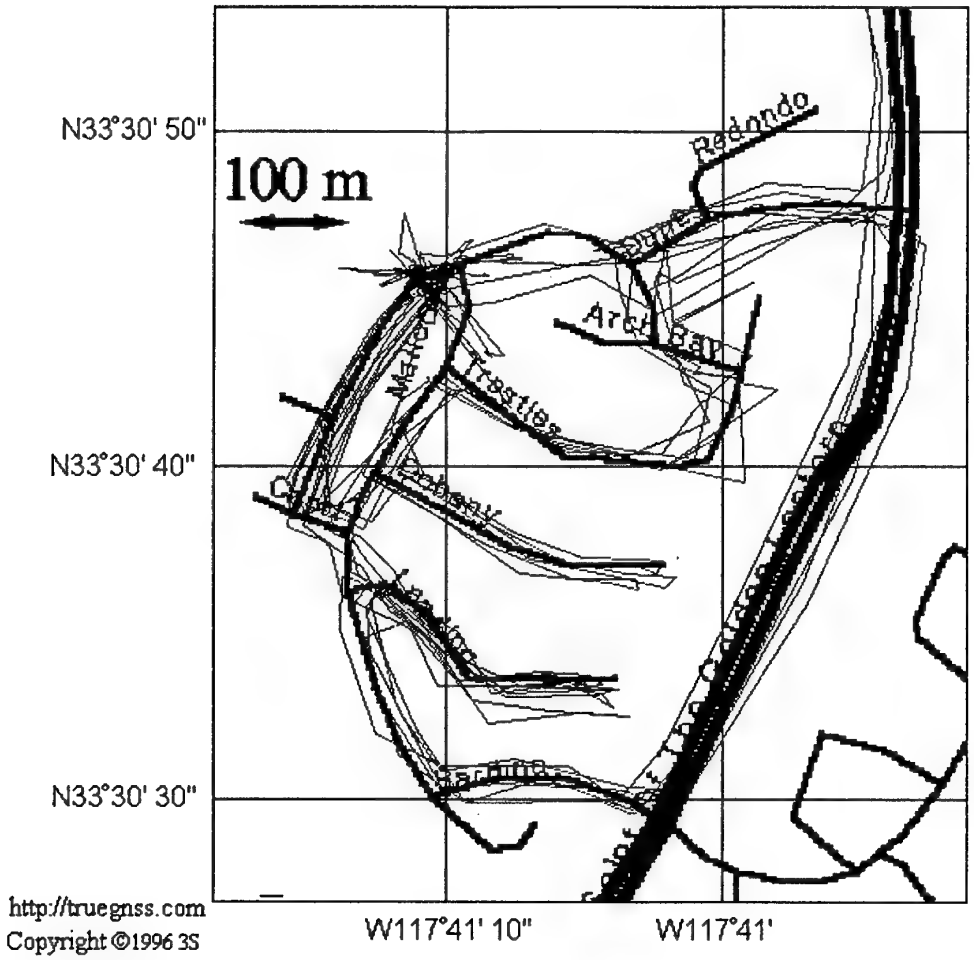

FIGURE 6-11. GNSS-200 GROUND TEST. DETAIL

were observed in January 1996 during their winter migration.

The most spectacular tests were our aircraft tests. We installed our receiver in a Cessna 172 with the antenna taped to the back window! As can be seen on Figure 6-13, we taxied to the runway threshold at the John Wayne airport, took off, and followed the vectoring provided by the control tower. We "shot" several approaches which can be seen on the figure, performed a few touch and go and also flew to Dana Point. Once again, the accuracy of the solution was excellent, with the receiver tracking an average of 5 satellites from each constellation at all times.

7.0 ACKNOWLEDGMENTS

The author acknowledges the support of the technical and clerical staffs at 3S Navigation whose dedicated efforts towards the design and development of the R-100 and GNSS-200 receivers allowed this paper to be written.

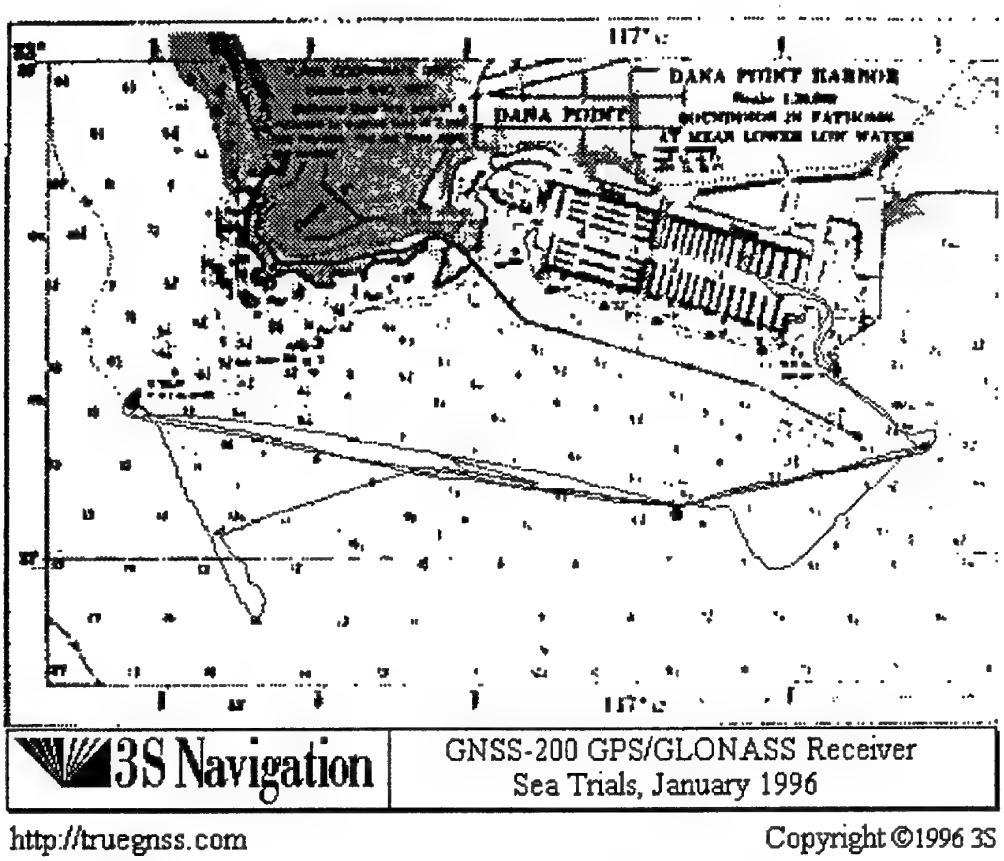

FIGURE 6-12. GNSS-200 SEA TEST

8.0 REFERENCES

1. Spilker, J.J.,"GPS Signal Structure and Performance Characteristics", Navigation GPS Issue Vol I.

2. GLONASS Interface Control Document, (Second Wording), Research and Production Association of Applied Mechanics, January 1992.

3. Daly, P., Review of GLONASS System Characteristics, Proceedings, ION-GPS-90, September 1990.

4. Beser, J. and Danaher, J., The 3S Navigation R-100 Family of Integrated GPS/GLONASS Receivers: Description and Performance Results, Proceedings, ION 1993 National Technical Meeting, San Francisco, CA January 1993.

5. Beser, J. and Balendra, A., Integrated GPS/GLONASS Navigation Results, Proceedings, ION GPS 93, Salt Lake City, UT, September 1993.

6. Balendra, A., Kim, S. and Beser, J., Fully Integrated GLONASS Dual Frequency P Code and GPS/GLONASS Single Frequency C/A Code Receiver. Features and Performance, ION GPS 94, Salt Lake City, UT, September 1994.

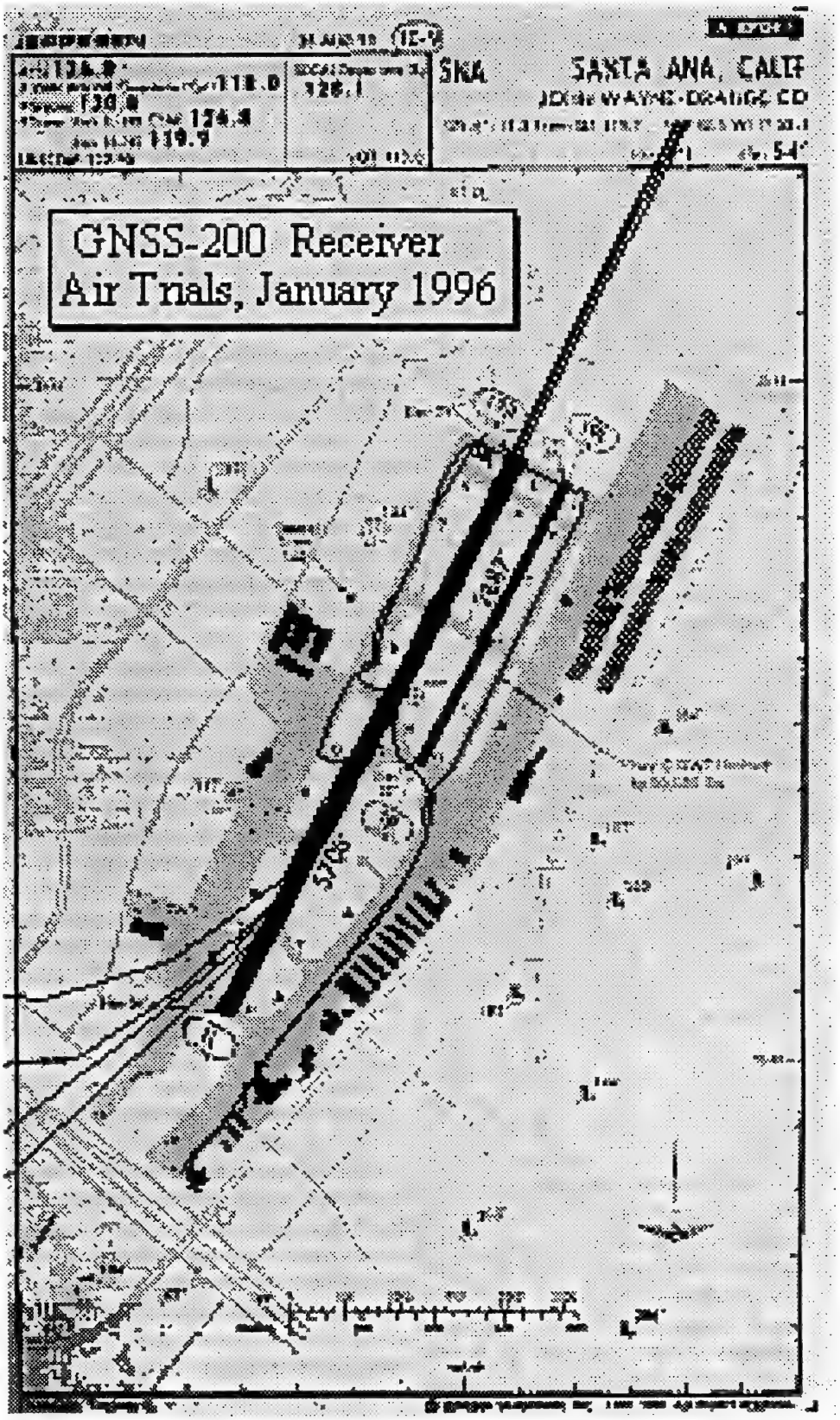

FIGURE 6-13. GNSS-200 AIR TEST

7. Beser, J., GPS and GLONASS Visibility Characteristics and Performance Data of the 3S Navigation R-100 Integrated GPS/GLONASS Receiver, Proceedings ION-GPS-92, September 1992.

8. P. Misra & All, Integrated Use of GPS and GLONASS in Civil Aviation Navigation II: Experience with GLONASS, Proceedings ION GPS-91, Albuquerque, NM, September 1991

9. P. Daly & All, Satellite Time Transfer between UTC(USNO) and UTC(SU) Using Navstar GPS and GLONASS, Proceedings ION GPS-91, Albuquerque, NM, September 1991

10. Anon., RTCM Recommended Standards for Differential NAVSTAR GPS Service, Version 2.1, January 3, 1994

NAVIGATION ACCURACY FOR ABSOLUTE POSITIONING

Dr. Gérard Lachapelle
Department of Geomatics Engineering
The University of Calgary
2500 University Drive, N.W.
Calgary, Alberta, T2N 1N4, Canada
Tel: 403 220 7104; fax: 403 284 1980
e-mail: lachapel@ensu.ucalgary.ca

ABSTRACT

The real-time absolute (i.e., single point, stand-alone) accuracy achievable with the Global Positioning System (GPS) is a function of the User Equivalent Range Error (UERE) and the Dilution Of Precision (DOP). The latter parameter is a function of satellite geometry. The various error components affecting the magnitude of the UERE are quantified. They include satellite, atmospheric, and receiver dependent errors. The DOP's expected under ideal operational conditions are a function of space and time. The absolute accuracies currently specified for the Standard Positioning Service (SPS) and the Precise Positioning Service (PPS) are described. Various experiments conducted in recent years show that the actual PPS accuracy performance usually exceed the specified level. Potential PPS accuracy enhancements which comprise satellite clock and Ephemeris error reduction, tropospheric error reduction and receiver noise and multipath reduction are described. Recent test results by the 50th Space Wing of the U.S. Air Force to reduce satellite clock and ephemeris errors show an improvement of nearly 50% in absolute positioning accuracy using current Y-code receiver technology. As a military application example, a comparison of the NATO STANAG 2373 artillery survey requirements with PPS accuracies shows that the artillery positioning requirement can be met under ideal satellite geometry with the currently specified PPS accuracy. Future PPS accuracy enhancements show that the artillery positioning requirements could be met under severely degraded satellite geometry, which is a more realistic scenario, given the concealment requirements for artillery. Selected recommendations of an independent study mandated by the U.S. Congress and conducted by the National Academy of Public Administration and the National Research Council pertaining to both PPS and SPS enhancements are presented. Finally, the impact of the worldwide civilian GPS tracking network deployed by the International GPS Service for Geodynamics on post-mission absolute accuracy is discussed. The use of post-mission precise orbits and 30-second satellite clock corrections are resulting in absolute kinematic accuracies at the 1-3 m accuracy level using civilian receivers. The potential for this post-mission information to become available in real-time is mentioned.

1. INTRODUCTION

The characteristics of GPS and its error sources are described in detail in the literature [e.g., NATO 1991]. The most important characteristics for this lecture are summarized in Table 1. Absolute positioning is based primarily on code measurements; carrier phase measurements are of secondary importance from an accuracy performance aspect although their role might be important for velocity determination and aiding purpose. The SPS was intended to be based on the L_1 C/A code and the PPS either on the L_1 C/A, L_2 P or L_1/L_2 P code. Civilian receivers which employs the semicodeless method can access the L_1 and L_2 P code which can be used for estimating the ionospheric propagation delay.

Table 1
Relevant GPS Characteristics For Artillery Survey

- 21 satellites + 3 active spares, for a total of 24
- Fully operational in early 1995
- 24-hour availability
- 20,000 km above the earth's surface
- Line-of-sight (Upper UHF)
- Carriers: L_1 = 1575.42 MHz , L_2 = 1227.6 MHz
- PRN 1.023 MHz C/A (L1) and 10.23 MHz P (L1 & L2) codes
- Standard Positioning Service (SPS) - non-authorized (civilian) users
- Precise Positioning Service (PPS) - authorized, i.e., U.S. military and NATO

The U.S. DoD plan for GPS satellite replacement is shown in Figure 1. The constellation currently consists of Block II and IIA satellites. Around 1997, the launching of Block IIR satellites will begin. The launching of Block IIF would begin in the

Paper presented at the AGARD MSP Lecture Series on "System Implications and Innovative Applications of Satellite Navigation", held in Paris, France from 1-2 July 1996; Rome, Italy from 4-5 July 1996; Madrid, Spain from 8-9 July 1996 and St. Petersburg, Russia from 11-12 July 1996, and published in LS-207.

middle of the first decade of the next century. The launching schedule is shown here because it is needed to understand at which time certain absolute positioning accuracy enhancements might become available, as discussed later.

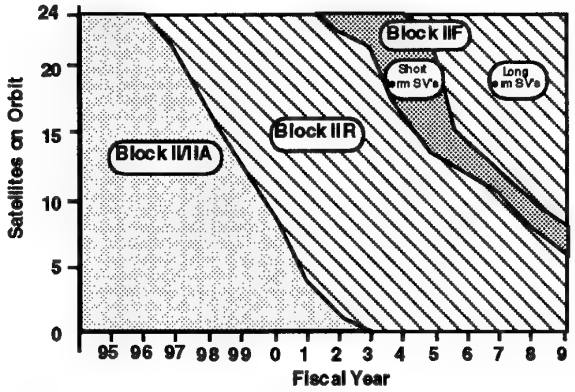

Figure 1: Current Plan for GPS Satellite Replacement [NRC 1995]

2. DOP AND UERE

2.1 DOP - Dilution Of Precision

A minimum of four satellites is required to resolve the three coordinates and the time bias of the receiver, unless constraints are used. Since the satellites are moving with a speed of 4 km s^{-1} and they may appear and disappear frequently due to signal masking, the DOP is changing continuously.

In order to understand the DOP concept and accuracy measures, the covariance matrix of the estimated parameters is needed. The covariance matrix for the tridimensional (3D) case with a range bias cdT is given, in least-squares estimation, by the expression

$$C_x = [A^T P_\ell A]^{-1} = \begin{vmatrix} \sigma_\phi^2 & \sigma_{\phi\lambda} & \sigma_{\phi h} & \sigma_{\phi cdT} \\ \sigma_{\lambda\phi} & \sigma_\lambda^2 & \sigma_{\lambda h} & \sigma_{\lambda cdT} \\ \sigma_{h\phi} & \sigma_{h\lambda} & \sigma_h^2 & \sigma_{hcdT} \\ \sigma_{cdT\phi} & \sigma_{cdT\lambda} & \sigma_{cdTh} & \sigma_{cdT}^2 \end{vmatrix}$$

where the estimated variances of the latitude, longitude, height and range bias components are on the diagonal. **A** is the design matrix whose elements consist of the partial derivatives of the pseudorange observation equations with respect to the relevant unknown parameters and P_ℓ is the weight matrix of the observables. If P_ℓ is replaced by the identity matrix **I**, an unscaled covariance matrix C_x' which is used to define the DOPs is obtained:

$$C_x' = [A^T A]^{-1} = \begin{vmatrix} \sigma'_\phi{}^2 & \sigma'_{\phi\lambda} & \sigma'_{\phi h} & \sigma'_{\phi cdT} \\ \sigma'_{\lambda\phi} & \sigma'_\lambda{}^2 & \sigma'_{\lambda h} & \sigma'_{\lambda cdT} \\ \sigma'_{h\phi} & \sigma'_{h\lambda}{}^2 & \sigma'_h{}^2 & \sigma'_{hcdT} \\ \sigma'_{cdT\phi} & \sigma'_{cdT\lambda} & \sigma'_{cdTh} & \sigma'_{cdT}{}^2 \end{vmatrix}$$

The instantaneous 3D PDOP (Position DOP) , 2D HDOP (Horizontal DOP) , and 1D VDOP (Vertical DOP) are defined as:

$$\begin{aligned} \text{PDOP} &= [\sigma'_\phi{}^2 + \sigma'_\lambda{}^2 + \sigma'_h{}^2]^{1/2} \\ \text{HDOP} &= [\sigma'_\phi{}^2 + \sigma'_\lambda{}^2]^{1/2} \\ \text{VDOP} &= \sigma'_h \end{aligned}$$

For a given satellite configuration, HDOP < PDOP, VDOP < PDOP, and

$$\text{PDOP} = [\text{HDOP} + \text{VDOP}]^{1/2}.$$

There are several types of HDOPs, namely

(i) HDOP with unconstrained height and time,
(ii) HDOP with a constrained height,
(iii) HDOP with a constrained time, and
(iv) HDOP with constrained height and time.

The HDOP implied by (iv) is smaller than that implied by (i), (ii) or (iii), which means that a geometrically stronger solution can be obtained using height and/or time constraints. If the height is constrained within known error bounds due to the use of a barometer for instance, i.e., it can be effectively held within these bounds while strengthening the horizontal coordinate solution using a least-squares inequality constraint method. The use of a precise clock also enables one to constrain time. A rubidium clock is sometimes used to constrain time over significant periods of time, i.e., up to 30 minutes. Such a constraint can be useful under poor geometry, e.g., when losses of signal are frequent due to masking effects such as foliage.

DOP values are used to predict the absolute accuracy using the following equation:

$$\text{Positioning Accuracy} = \text{DOP} \times \text{UERE}$$

where UERE is the User Equivalent Range Error. This value includes all effects which contribute to the range error. The smaller the DOP value, the better the positioning geometry. Assuming no line-of-sight limitation, the GPS PDOP for a 21-satellite constellation typically varies from 1.5 to 8

with a median of 2.7 [Parkinson et al 1995]. The corresponding HDOP is often assumed to be 2.0 when the best four satellites are used, although it has been shown that the value will be ≤ 1.5, 95% of the time, if an all-in-view receiver and a masking angle of 5° is used [NAPA/NRC 1995]. The corresponding VPOP is typically of the order of 2.1 to 2.4.

Although the HDOP takes only the variances of the latitude and longitude components into account, its value will decrease if the height and the range/time bias components are constrained to fixed values or within known error bounds. If fixed values are used, the dimension of C_x' is reduced and this affects σ'^2_ϕ and σ'^2_λ. If error bounds are used, a relative weight matrix (P_ℓ) of the observables is introduced in the calculation of C_x' and σ'^2_ϕ and σ'^2_λ are also affected. The PDOP decreases if the range bias is constrained to a known value or within known error bounds.

2.2 UERE - User Equivalent Range Error

The UERE consists of the quadratic root sum square of the contributing errors of the space segment, the control segment, the propagation medium and the user. The error breakdown utilized by NATO [1991] to obtain a PPS P(Y) code UERE of 6.5 m (1σ) is shown in Table 2. The value of 6.5 m is slightly higher than the 6.0 m value specified in other documents [e.g., Parkinson et al 1995]. This may be due to the use of a very conservative value of 4.5 m for the ionospheric error. In 1995, yet lower values were estimated by NRC [1995] for the PPS and SPS UERE as shown in Table 3. A PPS UERE of 4.1 m (1σ) was obtained. The SV clock and ephemeris error now clearly dominates the PPS UERE budget. In the case of the SPS, the UERE is dominated by the effect of SA (Selective Availability).

2.3 Selective Availability (SA) and Anti-Spoofing (A-S)

Selective Availability is used to deny non-authorized users certain levels of accuracy otherwise possible with unclassified C/A-code receivers. It is implemented through the injection of two error types in the broadcast navigation message, namely the orbit or ε-type SA, and the satellite clock dithering, or δ-type SA. The latter adversely affects the velocity accuracy. The ε-type is implemented through the injection of errors in the broadcast ephemerides while the δ-type is implemented through clock dithering in which case the Δt_{sv} satellite clock term transmitted as part of the navigation message no longer represents the actual clock behavior. The dominant SA effect has been, until now, that of satellite clock dithering (δ-type). The magnitude of SA errors recently agreed

Table 2

PPS P(Y) Code UERE Budget [NATO 1991]

Segment	Error Source	UERE (95%) Contribution
Space	Frequency stand. stability	6.5 m
	Delay variation	1.0
	Space vehicle acc. uncertainty	2.0
	Other	1.0
Control	Ephem.pred. and model implement.	8.2
	Other	1.8
User	Ionospheric delay compensation	4.5
	Tropospheric delay compensation	3.9
	Receiver noise and resolution	2.9
	Multipath	2.4
	Other	1.0
Total (UERE)	95% (2σ)	13.0
	68% (1σ)	6.5 m

Table 3

SPS and PPS UERE Budget [NRC 1995]

	Typical UERE[1] (1σ)	
	SPS	**PPS**
Selective Availability	24.0 m	0.0 m
Ionospheric Error	7.0	0.01
Tropospheric Error	0.7	0.7
Clock and Ephemeris Error	3.6	3.6
Receiver Noise	1.5	0.6
Multipath	1.2	1.8[2]
Total UERE	25.3 m 8.1 (no SA)	4.1m
Horiz. Acc. (2 DRMS)[1]	101.2 m	16.4 m

1 Assuming a *typical* 4-channel receiver and an HDOP of 2.0
2 Multipath is higher than for the SPS case due to the error amplification caused by the L1/L2 linear combination

upon by the DOD/DOT Signal Specification Issues Technical Group are [NRC 1995]:

- range rate bound - not to exceed 2 m s^{-1}
- range acceleration bound - not to exceed 19 mm s^{-2}
- range acceleration 2σ - 8mm s^{-2}.

The typical behavior of satellite atomic clocks with and without SA is shown in Figure 2. PRN#12 is a Block I satellite on which clock dithering can not be implemented. The drift, which is nearly linear as expected, is predicted by the Ground Control Segment and transmitted to the user via the three clock drift parameters. PRN#5 and 7 are Block II satellites and were clearly under the effect of SA during the period shown, with variations of up to 30 cm s^{-1}. These variations will be a limiting factor in obtaining accurate SPS absolute positions using post-mission precise orbits.

A-S was turned on in February 1994. The encrypted Y-code is obtained by some modification of the P-code. PPS P-code receivers can be fitted with an Auxiliary Output Chip (AOC) to recover the Y-code. Codeless and semicodeless civilian technologies have been gradually developed during the past 15 years to overcome A-S from a civilian aspect and perform measurements on Y L_1 and L_2 in the presence of A-S.

3.0 REAL-TIME ABSOLUTE ACCURACY PERFORMANCE

3.1 Current Performance

The currently specified and derived absolute real-time instantaneous GPS positioning accuracies are given in Table 4. The position accuracy is obtained by multiplying the DOP required by the UERE. The MRSE, DRMS and vertical errors are therefore

MRSE = PDOP x UERE
DRMS = HDOP x UERE
Vertical Error = VDOP x UERE

The HDOP and VDOP implied by the accuracies given in Table 4 are 1.6, and 2.2, respectively.

The PPS UERE of 4.1 m recently estimated by NRC [1995] is 4.1 m. The use of an HDOP of 2.0 results in a 2DRMS error of 16.4 m as compared to 21 m for the specified accuracy given in Table 4. Measured PPS UERE's of the order of 2.5 m and corresponding CEP of 4.6 m and SEP of 8.3 m have been reported using all-in-view dual-frequency PPS receivers [Parkinson et al 1995]. These values are nearly twice as good as those given in Table 4.

3.2 Future PPS Enhancements

Two possible PPS enhancements are currently being investigated, namely receiver enhancements and reduction of satellite clock and ephemeris errors.

NRC [1995] analysed the impact of emerging PPS receiver technologies and SV clock and ephemeris error reductions on absolute GPS accuracies. The findings are summarized in Table 5. The "advanced receiver" which was assumed would track six to eight satellites simultaneously, would have lower noise and a better multipath rejection capability than current PPS receivers. In addition, the use of a better tropospheric model than that curently used in PPS receivers is assumed.

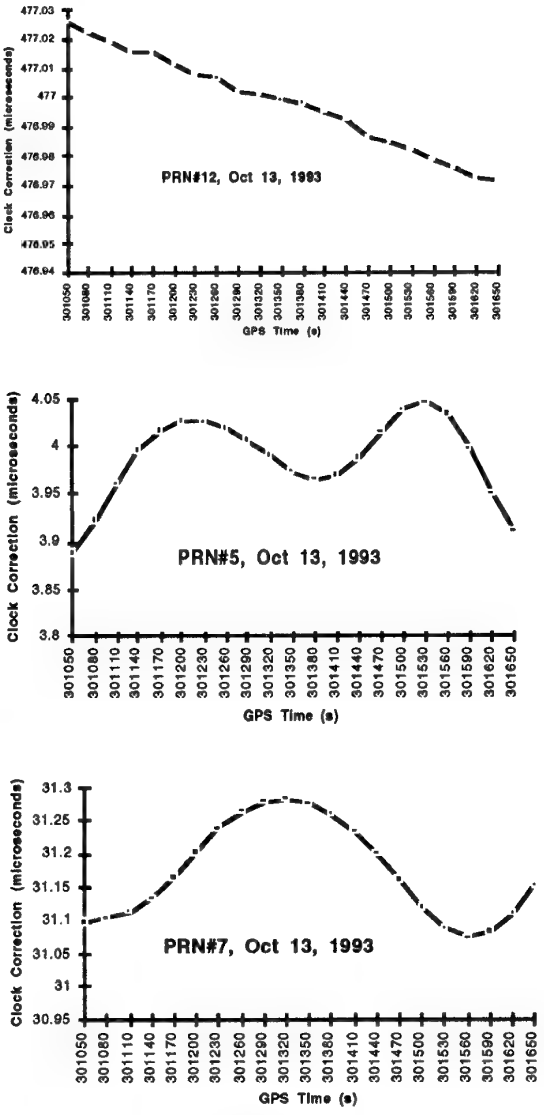

Figure 2: Typical Behavior of Satellite Atomic Clocks with and without SA

Table 4
Currently Specified and Derived GPS Instantaneous Real-Time Absolute Positioning Accuracies

	50th Percentile[2]		DRMS (65 - 68%)		2DRMS (95%)	
	PPS	SPS	PPS	SPS	PPS	SPS
POSITION						
• **Horizontal**	8 m	40 m	10.5 m	50 m	21 m	**100 m**
• **Vertical**	9 m	47 m	14 m	70 m	28 m	140 m
• **Spherical**	**16 m**[1]	76 m	18 m	86 m	36 m	172 m
VELOCITY						
• **Any axis**	0.07 m s^{-1}		**0.1 m s^{-1}**		0.2 m s^{-1}	
TIME						
• **GPS**	17 ns	95 ns	26 ns	140 ns	52 ns	280 ns
• **UTC**	68 ns	115 ns	**100 ns**	170 ns	200 ns	340 ns

1 Formal accuracies are in bold
2 50th Percentile is equivalent to P.E. (1D), CEP (2D), or SEP (3D)

The effect of receiver enhancements alone would be to reduce the UERE (1σ) from 4.1 m to 3.7 m. Several methods were proposed to reduce the satellite clock and ephemeris error. The effect of these improvements would be to further reduce the UERE from 3.7 m to 1.4 m. Since more than four satellites would be tracked, the HDOP would be reduced from 2.0 to 1.5, assuming a masking angle of 5°. A 2DRMS accuracy of 4.2 m, as compared to the currently stated accuracy of 21 m, would result.

Independent testing of the satellite clock and ephemeris error reduction using more frequent correction uploads to the satellites was recently carried out by the U.S. Air Force [Shank et al 1995]. The trials were conducted with the PPS version of the 12-channel Ashtech Z-12 dual-frequency receiver. CEP and SEP values of 2.5 m and 3.2 m, respectively, were obtained. These corresponds to DRMS and MRSE values of 3.0 m and 3.7 m, respectively. The PPS user equipment modifications required to accommodate the broadcast message modifications tested by the U.S. Air Force are minor. These PPS enhancements may be implemented in the near future.

Table 5

Impact of Reduced Clock and Ephemeris Errors on PPS Accuracy Using an Advanced Receiver [NRC 1995]

Error Source	Typical UERE (1σ)	
	Current PPS - Typical Rx	Improved PPS - Advanced Rx
Ionospheric Error	0.01m	0.01 m
Tropospheric Error	0.7	0.2
Clock and Ephemeris Errors	3.6	1.2
Receiver Noise	0.6	0.3
Multipath	1.8	0.6
Total UERE	4.1	1.4
Typical HDOP	2.0	1.5
Horizontal Accuracy (2 DRMS)	16.4 m	4.2 m

3.3 Future SPS Enhancements

Several recommendations have also been made by NAPA [1995] to enhance the SPS. Major recommendations include immediate reduction of Selective Availability to 0 and removal within a few years, the addition of a second frequency (L_4) for civilian use, and the satellite clock and ephemeris improvements discussed previously. The resulting SPS 2DRMS accuracies are shown in Figure 3.

Removal of SA would result in a UERE of 8 m. A key to reduce further the SPS UERE would be to correct the observations for the effect of the ionosphere. Although this is possible through the use of codeless and semicodeless technologies, the L_4 frequency recommended above would accomplish and other purposes without any loss of signal strength. Such an addition could not however be implemented on the current satellites but would have to wait for future launches, likely Block IIF launches. In such a case, the full benefits would not be felt until after 2010, as can be deducted by inspecting the launch schedule shown in Figure 1. Given the rapid improvements in civilan receiver technologies, a 2DRMS accuracy better than 6 m would more than likely result from the addition of L_4.

4.0 USER EQUIPMENT FOR ABSOLUTE POSITIONING

Two general classes of GPS receivers are available, namely SPS and PPS. Several types exists within each class, as summarized in Table 6.

The single-frequency type 2 PPS receiver includes the PLGR. Type 3 includes the military version of the 12-channel dual-frequency Ashtech Z-12 unit available from E-Systems Inc. Type 4 may be available in future if the recommendation of the NRC committee in this respect is taken into account. The major limitation of type 1, 2 and 4 receivers for absolute positioning is the effect of the ionosphere. Likewise, L1 SPS receivers suffer from this limitation. Types 6 and 7 SPS receivers were partially developed to estimate the effect of the ionosphere. Several multipath reduction techniques are now used in civilian receivers, e.g., Narror Correlator™ [Van Dierendonck et al 1992] and MET and MEDLL [Townsend et al 1995]. These techniques are important for post-mission absolute positioning as it shall be seen later and would become important for real-time applications.

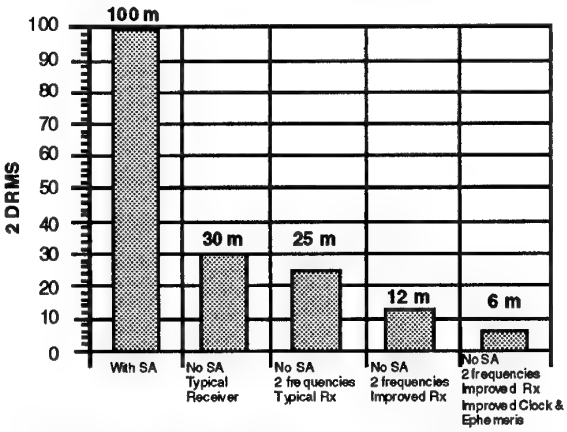

Figure 3: Absolute 2DRMS SPS Accuracy Resulting from NAPA Recommended Improvements and Enhancements [NAPA 1995]

Table 6: Receiver Types

No.	Type	Characteristic
		PPS CLASS
1	C/A code L1	C/A code on L1
2	P code L1	P code on L1
3	P code L1/L2	P code on L1 and L2
4	P code L2	Direct P code L2 acquisition
		SPS CLASS
5	C/A code L1	C/A code on L1
6	C/A code L1 + cross-correlation on L2	C/A code on L1 and ionospheric correction through inter-frequency Y-code measurements
7	C/A code L1 + Y code on L1 & L2	C/A code on L1 and Y code on L2 or on L1/L2

Table 7
NATO STANAG 2373 Specified and Derived Positioning Accuracy Requirements for Artillery Survey

Dimension	Accuracy measure and Probability	Value
1D (N or E or A)	Probable Error (P.E.), 50%	10 m
1D (N or E or A)	Standard deviation (1σ), 68%	15 m
1D (A)	2σ, 95%	30 m
2D (N, E)	DRMS (65-68%)	21 m
2D (N, E)	2DRMS (95%)	42 m
2D (N, E)	CEP (50%)	18 m
3D (N, E, A)	MRSE (61%)	26 m
3D (N, E, A)	SEP (50%)	23 m

5.0 CASE STUDY: CAN ABSOLUTE GPS MEET NATO ARTILLERY REQUIREMENTS?

This case study is discussed by Cannon et al [1996]. The NATO STANAG 2373 requirements for artillery survey include positioning and orientation requirements. The stated and derived horizontal and vertical positioning requirements are given in Table 7. The question is whether absolute PPS can meet these requirements. A comparison of Tables 4 and 7 shows that the positioning requirements listed in Table 7 can be met with the currently specified GPS accuracies, provided that a HDOP of 1.6 and a VDOP of 2.2 can be achieved, an optimistic assumption for artillery positioning due to concealment requirements which will invariably result in poorer DOPs. A more interesting question is the DOP degradation which can be tolerated until the artillery positioning requirements cannot be met. These are given in Table 8 for three different UERE values. The effect of a lower UERE is dramatic as it allows a HDOP degradation from 3.5 to 15.0. A HDOP of 15.0 is a much more realistic assumption than a corresponding value of 3.5 in many types of terrrain and foliage conditions.

Table 8
GPS PPS UERE and DOP Required to Meet Artillery Survey Accuracies in Instantaneous Absolute Mode[1]

	DOPs Required	
UERE Assumed	**HDOP**	**VDOP**
6 m (current specification)[2]	3.5	2.5
2.5 m (currently measured)[2]	8.4	6.1
1.4 m (satellite & clock corr improvements)[3]	15.0	11.0

1 An all-in-view dual-frequency PPS receiver is assumed
2 After Parkinson [1995]
3 Table 5 [After NRC 1995].

6.0 POST-MISSION CIVILIAN ABSOLUTE POSITIONING

Assuming that a civilian dual-frequency receiver is used, the errors limiting the absolute SPS accuracy are the satellite ephemerides and the effect of SA on satellite clocks. If these errors can be recovered in post-mission through data collected continuously by a network of permanent tracking stations, the absolute accuracy can be improved. Precise GPS satellite post-mission ephemerides have been available from various government agencies for nearly a decade. The reference frame used for the generation of these precise ephemerides is the International Earth Rotation Service (IERS) Terrestrial Reference Frame (ITRF) referred to a specific epoch to account for crustal motion [e.g., Boucher & Altamimi 1992, Beutler & Brockmann 1993, IGS 1995]. The earth-fixed ITRF is realized by the IERS through coordinates of adopted geocentric stations derived from various space techniques, namely GPS, Very Long Baseline Interferometry, Satellite Laser Ranging, and Lunar Laser Ranging.

WGS84(G730), which is used by the GPS Ground Control Segment to predict the ephemerides broadcast to users, is now consistent with ITRF to within 20 cm [Malys & Slater 1994]. The IERS, which is jointly operated by the International Union of Geodesy and Geophysics (IUGG) and the International Astronomical Union (IAU), is realized by the permanent GPS tracking network of the International GPS Service for Geodynamics (IGS) of the IUGG International Association of Geodesy [e.g., Mueller 1993]. The permanent IGS stations at the end of 1994 are shown in Figure 3 [IGS 1995]. The IGS produces precise GPS orbits and associated parameters which are used by the IERS.

GPS TRACKING NETWORK OF THE INTERNATIONAL GPS SERVICE FOR GEODYNAMICS
OPERATIONAL STATIONS

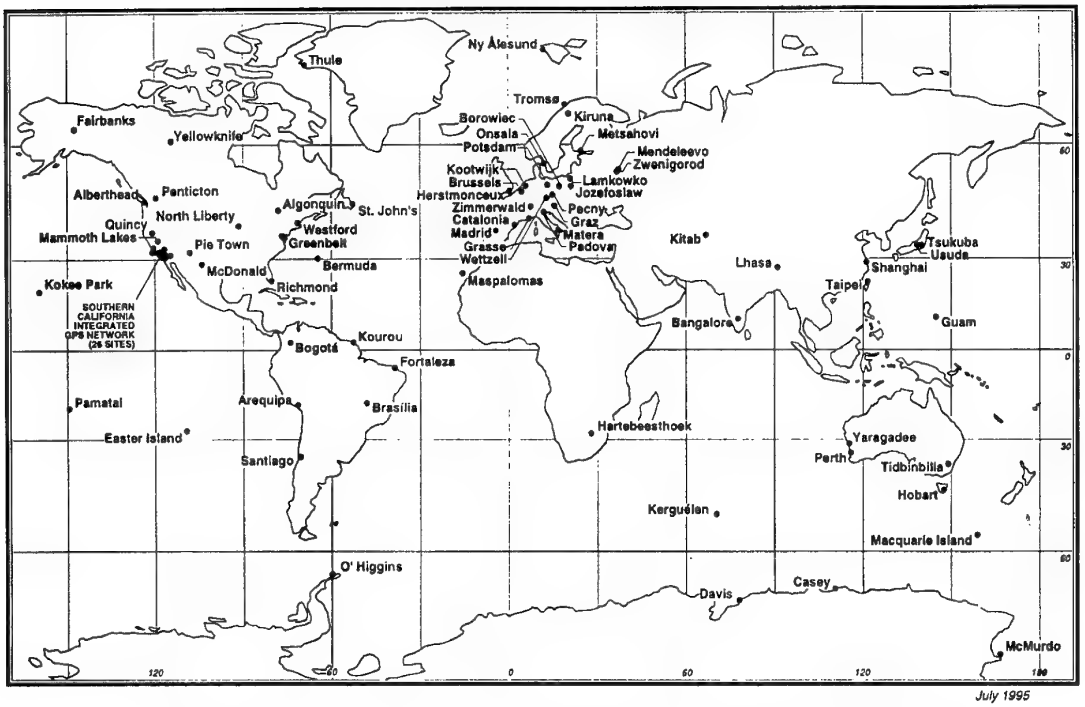

Figure 3: Operational Stations of IGS GPS Tracking Network (End of 1994)

Static absolute positioning performance with post-mission ephemerides and satellite clock corrections using smoothed dual-frequency P code data was investigated by Héroux et al [1993] and Lachapelle et al [1994]. Short and long term rms agreements at the sub-metre level in each of the three components were obtained. Of more general interest from an operational aspect is the accuracy level which can be obtained in kinematic mode under normal operating field conditions. The results of a case study which shows that rms accuracies at the 1-3 m level in each coordinate component can be obtained are summarized below.

7.0 CASE STUDY: ABSOLUTE SHIPBORNE POSITIONING WITH POST-MISSION EPHEMERIDES AND SATELLITE CLOCK CORRECTIONS

This trial was conducted in Autumn 1993 off the coast of Vancouver Island, Canada, using a 1,600 tonnes, 75-m vessel of the Canadian Department of National Defence (DND) [Lachapelle et al 1994a]. A Narrow Correlator™ spacing L1 C/A code receiver, namely a NovAtel GPSCard™ was used. The trial was conducted over a period of several days and the ship trajectories are shown in Figure 4. Throughout the trial, a shore reference station located near Victoria, B.C., was used to collect data to derive ship DGPS positions at the 1-m accuracy level. These positions were used to assess the accuracy of the absolute ship positions obtained using post-mission ephemerides and satellite clock corrections.

Post-mission precise ephemerides and 30-s interval satellite clock corrections were provided by the Geodetic Survey Division of Natural Resources Canada (NRCan). The ephemerides are computed from data collected by the Canadian Active Control System (CACS) and augmented by up to 16 globally distributed core stations of the IGS [e.g., Kouba et al 1993]. CACS stations form a subset of the IGS network. Ephemeris data are computed in the ITRF. Based on IGS orbit comparisons, the CACS precise ephemerides are determined to better than 0.2 m (1 σ) in each coordinate [Kouba & Popelar 1994]. The precise satellite clock corrections, which consist of offsets between the individual satellite clocks and the CACS reference clock, account for the long term drift of the satellite clocks and for the dithering effect introduced by Selective Availability. They are estimated with an accuracy $\leq$ 1 ns. Experience has shown that calculating satellite clock corrections at intervals of 30 seconds is sufficient for sub-metre interpolation. (Since 1995, NRCan can calculate

precise orbits and satellite clock corrections for any user location in the world).

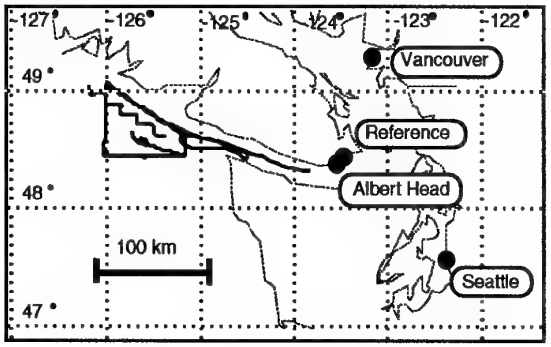

Figure 4: Ship Trajectories

Absolute positions based on pseudorange measurements and post-mission orbits and satellite clock corrections were calculated at every epoch. Satellite antenna and relativistic clock corrections were applied to improve the consistency of the results. The effect of the troposphere was calculated using a standard model. In order to quantify the effect of the ionosphere on the single frequency (L1) results, the ionospheric corrections derived using a dual-frequency receiver on shore were applied to all L1 measurements on the ship to determine the accuracy of ionospherically versus non-ionospherically corrected absolute positions. All absolute positions were generated with The University of Calgary software C^{3}NAV^{TM}.

Figures 5 and 6 summarize the mean and RMS differences obtained for five 20-hour periods for the L1 and ionospherically corrected positions. The results in ech coordinate are very consistent from one period to the next. The larger differences in the height component obtained with the L1 solutoin are due to the effect of the ionosphere. Once ionospheric corrections are applied, the rms differences in each coordinates are generally at or slightly above the 1 metre accuracy level.

These results demonstrate that post-mission absolute kinematic positioning at the 1 m (1 σ) accuracy level in latitude and longitude is possible with the use of a high performance dual-frequency civilian receiver, when using precise ephemerides and satellite clock corrections. NRCan has plans to experiment with the possibility of providing precise ephemerides and satellite clock corrections information in real-time in mid-96.

The post-mission absolute accuracies reported herein with SPS receivers have recently be achieved using PPS [Hermann & Malys 1995].

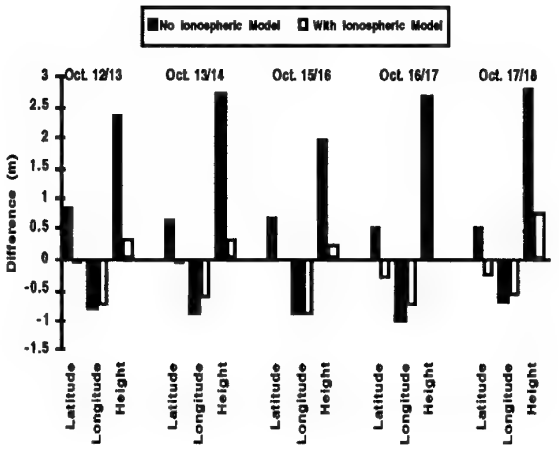

FIGURE 5: Mean Differences Between Absolute and DGPS Solutions

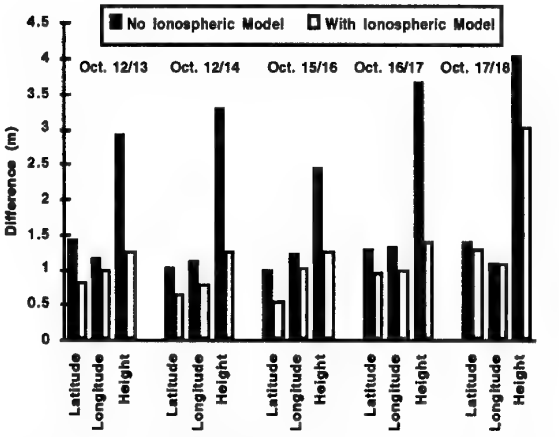

FIGURE 6: RMS Differences Between Absolute and DGPS Solutions

REFERENCES

BEUTLER, G., and E. BROCKMANN, Eds. [1993] Proceedings of the 1993 IGS Workshop. Published by the Astronomical Institute, University of Berne.

BOUCHER, C., and Z. ALTAMIMI [1992] The IERS Terrestrial Reference System. Proceedings of 6th International Geodetic Symposium on Satellite Positioning, Defense Mapping Agency/Ohio State University, pp. 47-55.

CANNON, M.E., G. LACHAPELLE, and J. BIRD [1996] Evaluation of GPS-Aided Artillery Positioning and Orientation Methods. 1996 Canadian Navigation Society Symposium, 43rd Annual Conference, Canadian Aeronautics and Space Institute, Ottawa, April 29 - May 1.

HERMANN, B., and S. MALYS [1995] Precise Absolute Navigation: An Evaluation of PPS Position Improvement. Proceedings of GPS-95, The Institute of Navigation, Alexandria, VA, pp. 431-436.

HÉROUX, P., M. CAISSY, and J. GALLACE [1993] Canadian Active Control System Data Acquisition And Validation. Proceedings of the 1993 IGS Workshop, Astronomical Institute, University of Berne, 49-58

IGS [1995] 1994 Annual Report of the International GPS Service for Geodynamics, IGS Central Bureau, Jet Propulsion Laboratory, Pasadena, CA.

KOUBA, J., and J. POPELAR [1994] Modern Reference Frames in Precise Positioning and Navigation. Proceedings of International Symposium on Kinematic Systems in Geodesy, Geomatics and Navigation - KIS94 (Banff, August 30 - September 2], Dept of Geomatics Engineering, The University of Calgary, pp. 79-85.

KOUBA, J., P. TÉTREAULT, R. FERLAND, and F. LAHAYE [1993] IGS Data Processing at the EMR Master Active Control System Centre. Proceedings of the 1993 IGS Workshop, Astron. Institute, University of Berne, 123-132.

LACHAPELLE, G., M.E. CANNON, W. QIU, and C. VARNER (1995) An Analysis of Differential and Absolute GPS Aircraft Positioning. Proceedings of ION National Technical Meeting (Anaheim, January 18-20), pp. 701-710.

LACHAPELLE, G., R. KLUKAS, D. ROBERTS, W. QIU, and C. McMILLAN (1994a) One-Meter Level Kinematic Point Positioning Using Precise Orbit and Tming Information. Proceedings of GPS-94 (Salt Lake City, September 21-23), The Institute of Navigation, Alexandria, VA, pp. 1435-1443.

LACHAPELLE, G., R. KLUKAS, W. QIU, and T. MELGARD (1994) Single Point Satellite Navigation Accuracy - What the Future May Bring. Proceedings of PLANS'94, IEEE, New York, pp. 16-22.

MALYS, S., and J. SLATER [1994] Maintenance and Enhancement of the World Geodetic System 1984. Proceedings of GPS-94 (Salt Lake City, September 20-23), The Institute of Navigation, pp. 17-24.

NAPA/NRC [1995] The Global Positioning System - Charting the Future. National Academy of Public Administration, Washington, D.C., 1995.

NATO [1991] Technical Characteristics of the Navstar GPS, June 1991. NATO Navstar GPS Project Steering Committee. Reprinted by Navtech Seminars, Alexandria, VA, October 1993.

NRC [1995] The Global Positioning System - A Shared National Asset: Recommendations for Technical Improvements and Enhancements. Committee on the Future of GPS, U.S. National Research Council, Washington, D.C., 1995

PARKINSON, B., et al [1995] A History of Satellite Navigation. Navigation, ION, 42, 1, pp. 109-164.

SHANK, C., B. BROTTLUND, and C. HARRIS [1995] Navigation Message Correction Tables: On-Orbit Results. Presented at 51st Annual Meeting of The Institute of Navigation, Colorado Springs, June 5-7.

TOWNSEND, B., R. van Nee, P. Fenton and K. Van Dierendonck [1995] Performance Evaluation of the Multipath Estimating Delay Lock Loop. Proc. ION NTM (Anaheim, Jan 18-20), pp. 277-283)

VAN DIERENDONCK, A.J., P. FENTON, and T. FORD [1992] Theory and Performance of Narrow Correlator Spacing in a GPS Receiver, Navigation, The Institute of Navigation, Alexandria, VA., 39, 3, 265-283.

RELATIVE AND DIFFERENTIAL GPS

Richard E. Phillips
George T. Schmidt
The Charles Stark Draper Laboratory
Cambridge, MA 02139

ABSTRACT

Many aerospace vehicles will have an avionics suite that includes an integrated INS/GPS (Inertial Navigation System/Global Positioning System) set. This means of navigation motivates examination of whether high accuracy (≈ 10 ft Circle of Equal Probability (CEP)) may be obtainable using only this set of weapon avionics operating in a ***relative or differential*** GPS mode, rather than in an ***absolute*** GPS mode where CEP's of 30 to 40 ft would be expected. [Ref. 1] This paper will explain how 10 ft accuracy may be achieved and it will present several different concepts that exploit such a capability.

Fundamentally, two problems must be solved to achieve an accuracy of 10 ft: (1) destination or "target" location must be determined to better than 10 ft, and (2), the GPS/INS "user vehicle" must be guided accurately to better than 10 ft. This paper will explain how the use of ***relative*** GPS can solve the guidance problem and how the use of ***relative*** targeting in a GPS based coordinate system can solve the target location problem. The use of ***differential*** GPS will also be discussed.

The paper begins with a discussion of relative GPS and reports the results of ***actual experiments*** to determine accuracy degradation of relative GPS guidance systems as a function of baseline length and targeting latency. Various baseline lengths and latencies are considered showing that relative (or differential) GPS guidance may achieve high accuracy over baselines and latencies useful for various applications. Appendix A shows that to first-order, relative and differential GPS systems give the same accuracy.

Next, the target location part of the problem is addressed. There must be an accurate sensor that locates the target relative to the GPS reference receiver. The sensor may be on either the vehicle carrying the receiver or at a remote location. The reference receiver could either be on the surveillance aircraft or the ground. If on the ground, both it and the target could have been located prior to the mission.

Real-time target location concepts that will be explained include the use of aircraft equipped with an INS/GPS/Synthetic Aperture Radar (SAR) avionics suite to perform a ***real-time relative*** targeting function. The importance of reasonable aircraft maneuvers to enhance observability and speed up the three-dimensional (3-D) target determination solution will also be addressed.

Simulation results for several realistic scenarios will be presented. An example of an INS/GPS equipped guided parafoil for supply delivery will be discussed as one of the relative (or differential) GPS applications.

Next, several concepts will be discussed that all make use of highly accurate ***premission relative*** target positioning, i.e., the ability to specify the 3-D location of two points, or localized areas, on the earth relative to each other in a suitable reference frame such as WGS-84. It is of interest to speculate how such a capability could be exploited. Scenarios involving several existing or planned systems will be described. A detailed design example of an INS/GPS guidance system for a munition fired from a gun will then be presented. A final section will then discuss some of the practical issues in using relative (or differential) GPS.

1.0 INTRODUCTION

The nomenclature of navigation techniques that measure one position in relation to another is not consistent in the literature or in common usage, so we begin by defining "relative GPS" as it is used here. By "relative GPS" we mean techniques that provide high relative position accuracy between two GPS receivers even though the absolute locations of each receiver are not known precisely. We refer to position estimation by a single receiver as "absolute GPS". "Differential GPS" refers to the situation where corrections to absolute GPS are generated by a single receiver (or base station) and transmitted to other user receivers.

Relative GPS techniques can be used to remove the large, highly correlated common GPS errors between two receivers at a particular time and achieve relative accuracies of a few feet. The key to achieving high accuracy is to require that both receivers use a common set of GPS satellites for navigation. In this way, correlated errors cancel out of the relative navigation solution. Table 1 lists the typical absolute GPS error budget. [Ref. 1]

Relative GPS (RGPS) using two receivers attempts to cancel out the "bias-like" GPS errors common to the two receivers. Not all error sources are perfectly correlated, however, and the degree of correlation tends to decrease as the distance between the two receivers - the baseline

Paper presented at the AGARD MSP Lecture Series on "System Implications and Innovative Applications of Satellite Navigation", held in Paris, France from 1-2 July 1996; Rome, Italy from 4-5 July 1996; Madrid, Spain from 8-9 July 1996 and St. Petersburg, Russia from 11-12 July 1996, and published in LS-207.

GPS Noise-like Range Errors	1σ Values
Multipath	5.9 ft
Receiver noise	2.0 ft
Total noise-like error	6.3 ft
GPS Bias-like Range Errors	**1σ Values**
Satellite ephemeris	4.6 ft
Satellite clock	11.2 ft
Atmospheric residual	2.3 ft
Total bias-like error	12.3 ft
Total absolute horizontal GPS rms error: $(6.3^2+12.3^2)^{1/2}$(HDOP) = 20.7 ft for HDOP = 1.5 or 17.2 ft CEP	

Table 1. "Typical" Absolute GPS Error Budget

length- increases. Also, the correlated errors themselves change slowly with time, so that if corrections are to be used at some time after they are computed, an additional position error will be introduced. The effects of these error sources need to be quantified before relative GPS techniques can be applied to guidance problems. It is the effects of these errors-the spatial and temporal decorrelations- that the experiment reported in Section 2 measures.

Whereas relative navigation solutions implement differences between two navigation solutions, differential GPS implementations (DGPS) explicitly calculate the bias-like ranging errors to each satellite by placing the reference receiver at a precisely-known, surveyed location ("A" in Figure 1) and by comparing the receiver measurements with calculations based on the survey. The differences between the measured and calculated ranges are the pseudorange corrections that are transmitted to other user-receivers. The accuracy with which the bias-like errors are removed from the position solution depends on the temporal and spatial error variations between the reference receiver and the user receivers. Again it is important to note that DGPS implementations require knowledge of receiver absolute location while RGPS only requires knowledge of relative vectors between receivers.

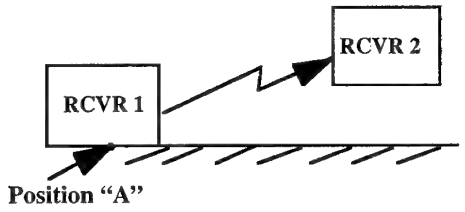

Figure 1. Differential GPS Concept

The cartoon sequence of Figures 2 through 4b develops the ideas of relative GPS. In Figure 2, two identical receivers are located at true position "B" and they are made to track the ***same*** 4 or more satellites. Although both identical receivers are in error from the true position "B" by an uncertain amount (say 12.3 ft) due to major error sources such as satellite clock drift, ephemeris errors, and propagation delays, they both read the ***same*** position with the exception of much smaller errors expected to be random and on the order of a few feet. These smaller remaining errors may include receiver noise, multipath, and other noise-like errors shown in Table 1.

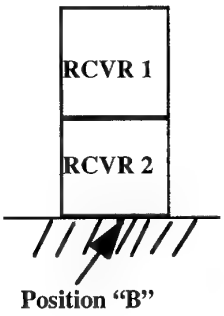

Figure 2. The Relative GPS Concept - Reference and Active Receivers on Target

In Figure 3, RCVR "2" is now on a vehicle whose guidance system receives the broadcast position of RCVR "1". "1" is located at the target. As long as RCVR "2" tracks the same satellites as RCVR "1" and the vehicle guidance system follows its commands with small errors, then the vehicle will guide to impact at RCVR "1" within receiver noise. Even though the absolute position coordinates of RCVR "1" and RCVR "2" may be incorrect, the "target" position B would be reached essentially perfectly. Clearly, RCVR "1" position would need to be broadcast continuously if both receivers use C/A code only and selective availability (S/A) is turned on. However, the use of GLONASS receivers or P(Y) code receivers may allow targeting to be done with one data transmission of target position and the identity of satellites being tracked by the "targeting" receiver. Thus a central question is: "Can one transmission of RCVR "1" position and the satellites it is using, be sufficient for RCVR "2" to guide the vehicle to RCVR "1"?" Alternately stated, the question is: "How far in time prior to arriving at "B" can the transmission be performed and still achieve better than 10 ft (relative) accuracy at the target?" Experimental results described in Section 2 will answer this question.

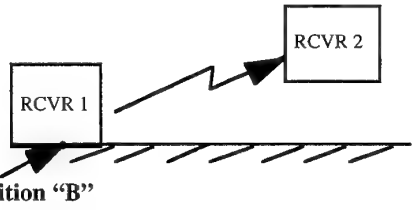

Figure 3. The Relative GPS Concept - Active Receiver Moved Away from Target

In addition, the target location problem needs to be addressed because it may not be practical to put a broadcasting GPS receiver on the target. The next step in the cartoon sequence is thus to move RCVR "1" some distance away from the target while still maintaining its accurate location relative to that target. Fig. 4a shows the target and receiver locations and the relative location vector between receiver "1" and the target - $\overline{RTL}$.

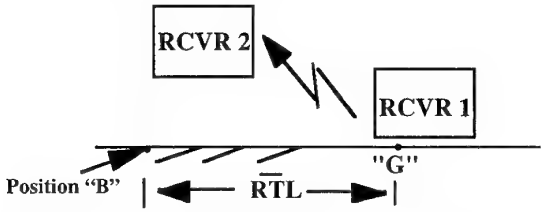

Figure 4a. The Relative GPS Concept - Reference Receiver Moved Away from Target

Note that now two additional sources of error have been added to the errors associated with Figure 3. First, an error in the GPS coordinates of the target because the reference receiver "1" is not located exactly at the target. The GPS bias-like errors at "G" are slightly different from those at "B" and the lines-of-sight to the satellites are also slightly different. The central question is: "How far can receiver "1" be from the target and still predict with better than 10 ft relative accuracy what receiver "2" should read at the target?" Experimental results described in Section 2 will answer this question.

The second additional source of error is in the scheme used to measure the *relative* location between the reference receiver "1" and the target. There are various means to determine the *relative* location vector, $\overline{RTL}$, to the target. In one of the schemes described in Section 3, a high resolution SAR radar is used to locate the target relative to an aircraft in coordinates established by the aircraft INS/GPS system (RCVR "1"). The target coordinates are used by the GPS/INS guided vehicle (RCVR "2") to reach the target. These approaches are summarized in Figure 4b.

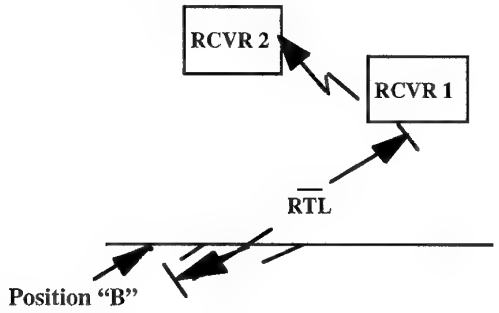

Figure 4b. The Relative GPS Concept - Reference Receiver on Surveillance Aircraft

In contrast, for the systems to be described in Sec. 4, the reference receiver "1" is located on the ground, as in Figure 4a, and the relative location vector $\overline{RTL}$ is determined prior to the mission and not in real-time. Section 5 will give an example of a GPS/INS guided munition using this concept variation.

All of the approaches to be described require the two receivers being able to receive signals from a common set of GPS satellites while possibly separated by ground distances of several hundred miles. Section 6 will show this to be true for separations greater than 540 nmi. Section 6 also discusses practical implementation issues.

Section 7 gives some concluding remarks. Finally, Appendix A develops a mathematical comparison between RGPS and DGPS showing comparable first-order accuracies.

2.0 EXPERIMENTAL RESULTS CONFIRMING RELATIVE GPS ACCURACY WITH SEPARATIONS IN TIME AND HORIZONTAL DISTANCE

The experiment was implemented by placing GPS receivers at eleven sites across the continental United States. [Ref. 2] Data was collected in two phases: one on the East Coast conducted in December 1993, and one on the West Coast conducted in March 1994. Figure 5 is a map showing the locations of the receiver sites and baselines used. Table 2 lists baseline endpoints and baseline lengths. Over thirty hours of receiver data was collected for each of the eight East Coast baselines, approximately half of that at a 1 Hz sampling rate, the other half at a 1/30 Hz rate.

Figure 5. East and West Coast Baselines

Between twelve and sixteen hours of receiver data was collected for each of the West Coast baselines, all of it at a 1/30 Hz rate. The "true" positions were established by an independent survey accurate to better than a foot at each location. The experiment consists of reading the GPS receiver at one location, adding to its position the "true" relative location vector to a second receiver, and then predicting what the second receiver reads given that it is commanded to use the same satellites as the first receiver. The difference between predicted and actual position will be statistically analyzed to obtain a model for the error behavior.

A third set of data was collected in Nov. 1995. Two

East Coast Baselines		
Endpoint	**Endpoint**	**Baseline Length (nmi)**
Cambridge, MA	Portsmouth, NH	45
Eglin AFB, FL	Ft. Stewart, GA	263
Langley AFB, VA	Cambridge, MA	400
Langley AFB, VA	Ft. Stewart, GA	405
Langley AFB, VA	Portsmouth, NH	442
Langley AFB, VA	Willow Run, MI	452
Willow Run, MI	Cambridge, MA	552
Willow Run, MI	Portsmouth, NH	558

West Coast Baselines		
Endpoint	**Endpoint**	**Baseline Length (nmi)**
San Diego, CA	Long Beach, CA	80
Stockton, CA	Fallon, NV	152
Ft. Irwin, CA	Fallon, NV	268
San Diego, CA	Fallon, NV	409

Table 2. Baseline Endpoints and Baseline Lengths

receivers were driven by a single antenna placed on the rooftop at Draper. This "zero baseline" data was used to characterize receiver noise, estimate the effect of multipath, and provide the primary source of time delay data. For all the data a single value for the position error was defined for each baseline and time delay. This value was the square root of the sum of the squares of the root mean square (RMS) of each of the three position error components. Hereafter this quantity will be referred to as the "RSS position error".

Figures 6a and 6b show the position error for the East Coast and West Coast data respectively. This raw data contains both receiver noise and the effects of multipath as well as the long term behavior we expect from differences in pseudo-range biases between the two sites. It thus indicates the level that can be expected for the total error in implementing relative (or differential) navigation techniques.

To observe the behavior of the position error with time delay such delays were introduced into the data by shifting the data in 30 second increments and comparing it with the unshifted data. For each time shift, a single difference was defined as before and will again be referred to as "RSS position error". The results of this temporal decorrelation analysis are shown for all four West Coast baselines in Figure 7.

The uniform increase in error with increasing time delay and baseline distance suggests representing the error as a linear function of the two variables. A least squares fit to the data yields coefficients, E_0, A, and B for the deterministic definition of the resulting plane:

$$E = E_0 + A\Delta l + B\Delta t$$

where E is the position error, Δl is the baseline length and Δt is the time delay
The coefficients are:

$E_0 = 7.6$ ft.
$A = 2.7 \times 10^{-3}$ ft/nmi
$B = 4.4 \times 10^{-3}$ ft/s

These results show slow growth in the composite total error between the two receivers for baseline lengths on the order of 540 nmi and times of flight after data transfer (time delay) of up to 15 minutes.

This indicates that relative (or differential) techniques will give acceptable navigation accuracy. The raw data was subjected to further analysis [Ref. 3] to separate the effects of receiver noise, multipath and pseudo-range bias. Four operations were performed on the data before the time and distance decorrelation of the biases was determined. Those operations were: 1) breaking the data into sets for which there were no satellite switches, 2) measuring and removing receiver noise, 3) normalizing the position errors by the PDOP at the collection time, and 4) removal from consideration of the data taken with C/A code receivers.

Data sets used in the time decorrelation analysis should be restricted to the same satellite set throughout. This results in breaking several of the long data sets into smaller pieces. This analysis method determines the decorrelation due to time shift only, and excludes the decorrelation due to satellite switch. This is appropriate to the "normal" mode of operation for relative GPS. The decorrelation due to satellite switch can be analyzed separately and added to the relative error if appropriate. (This is not done herein.)

For zero timeshift, the zero baseline rooftop experiment is a measure of receiver noise. This rooftop data revealed a value of about 0.5 ft for this noise (RSS of the RMS values of the three components of position error) for each receiver. Thus, to remove receiver noise, a value of 2×0.5^2 ft^2 was subtracted from the mean square differences for both time and distance decorrelation data.

Each of these data sets has an associated value for PDOP which effects the general level of the error in a way that is not indicative of the decorrelation with baseline distance and time delay. Imagine the unlucky event of having all the data with the San Diego - Fallon baseline be taken when the PDOP was 3.5 and the data with the Stockton - Fallon baseline with a PDOP of 2.1. Then the raw position error at 152 nmi separation might be bigger than the raw position error at 80 nmi. To avoid this confusion each data set was normalized by its PDOP. The resulting numbers are essentially average pseudo-range errors rather than position errors. To recover the effect on position error it will be necessary to multiply the pseudo-range error by the appropriate PDOP. It is thought that the pseudo-range results are of more general interest because they can be applied to any specific situation by using the appropriate PDOP.

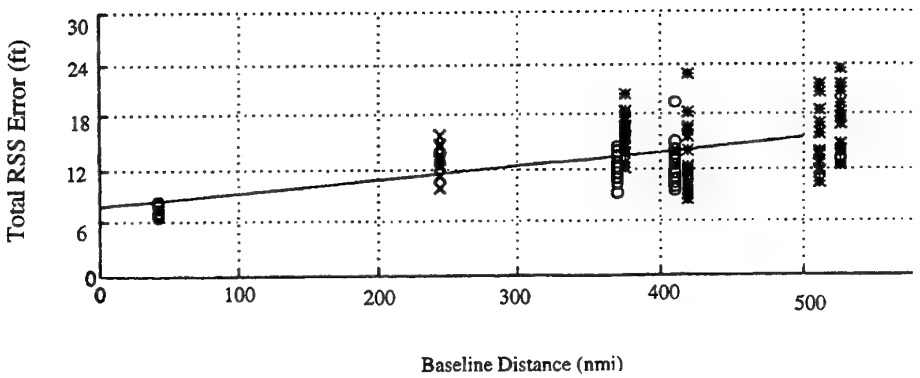

Figure 6a. Total RSS Error, East Coast Data

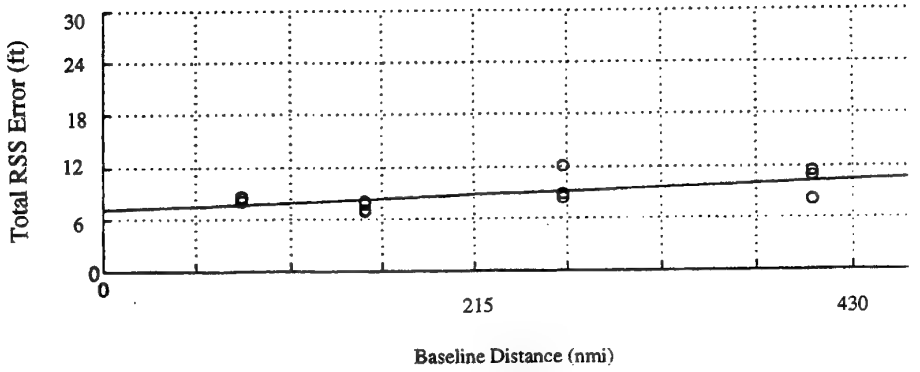

Figure 6b. Total RSS Error, West Coast Data

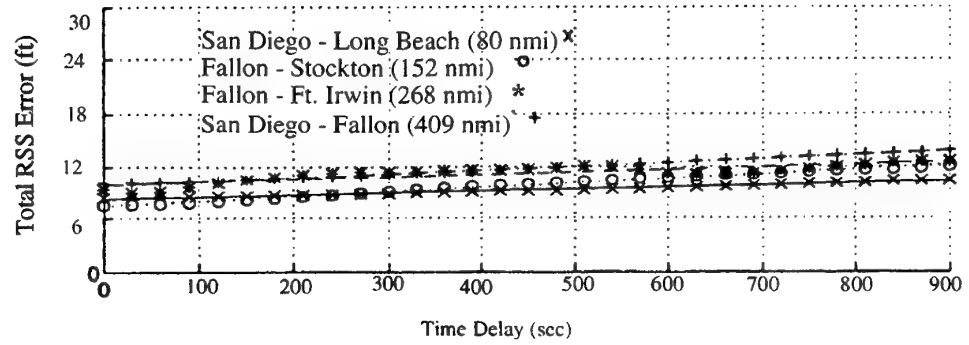

Figure 7. Total RSS Error vs Time Delay, West Coast Data

As it happened, position differences for three of the baselines, (those associated with Willow Run) used "C/A only" receivers. Although the effects of SA were supposedly removed during post processing it was felt that this data was still suspect, so it was removed from the data sets being analyzed.

Having taken these steps we were left with data which we believe reflected only the time and distance decorrelation of GPS pseudo-range biases and the effects of multipath. Three steps in the analysis still remained: 1) estimating the time decorrelation and removing the error due to multipath, 2) estimating the distance decorrelation parameters, and 3) proposing a "unified" time and distance decorrelation model. The following paragraphs describe these analysis steps.

Close examination of the time shifted position errors revealed a short term oscillatory behavior attributable to multipath. For the Draper rooftop experiments the frequency of the oscillations was consistent with reflections from nearby buildings and a metal roof edge . No note of reflecting surfaces was made for either the East and West Coast experiments and the oscillatory

component in that data was significantly smaller, perhaps indicating an effort to avoid multipath by careful antenna placement. The removal of multipath and the estimation of pseudo-range biases were accomplished in a single step by fitting the data to a dual single order Markov model [Ref. 3]. This model was suggested by the appearance of the ensemble averages of the data sets. There was an initial rise from zero error which "looked exponential". However, rather than approaching a limit as expected, the differences approached a "ramp" which we took to be the slower rising exponential associated with the pseudo-range decorrelation. (The first exponential being due to the ensemble average of the oscillatory behavior associated with the multipath.)

Having thus prepared the raw data and developed a model for the remaining error, we were now ready to begin evaluating for time and distance decorrelation constants. As an example, Fig. 8 shows the behavior of the mean squared range difference vs. time delay due to both multipath and pseudo-range biases for an ensemble of data collected over a 24 hour period on the Draper rooftop. The oscillatory behavior is masked for this ensemble average, but with a little imagination the existence of two decorrelation processes can be seen.

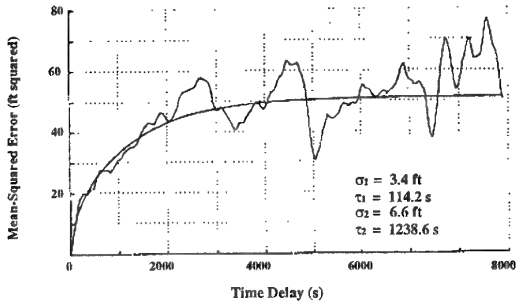

Figure 8. Mean Squared Error vs. Time Delay

More importantly the fitting program computed the values shown in the figure for the two Markov processes. As previously stated the process with short time constant was attributed to multipath; the process with the long time constant was attributed to pseudo-range biases. For this particular set of data, the error attributed to multipath was 3.4 ft (RMS). Root mean square values ranging from 3 ft to essentially zero were observed for the East and West Coast data sets.

Having removed the mean square differences due to multipath we are ready to use the East and West Coast data to derive a model for the decorrelation of errors with separation distance. The mean square error at the different baseline distances and a first order Markov fit to the data are shown in Fig. 9. The magnitude of the resulting Markov error is 5.2 ft and the distance constant is 66.4 nmi.

Fitting the time decorrelation and distance decorrelation separately ignores the fact that common phenomena is giving rise to both behaviors, namely the several sources of error for pseudo-range bias. Thus for sufficiently long distances and long time delays, DGPS errors will rise to the same final common value. That is to say there is only one value of σ_0. This suggests the use of the following unified model for the behavior of the pseudo-range biases:

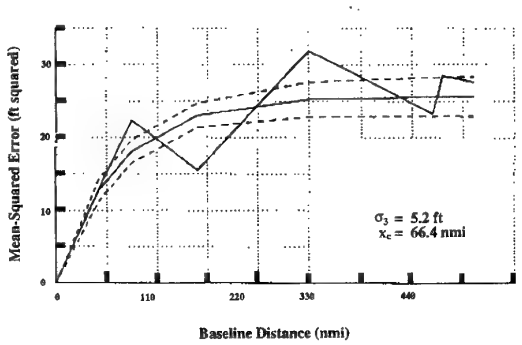

Figure 9. Mean Squared Error vs. Baseline Distance

$$\sigma_{RGPS} = \sigma_0\left(1 - e^{-t/T - x/x_c}\right)$$

A fit to this model yielded the following values for the magnitude, and time and distance constants:

$\sigma_0 = 12.2$ ft
$T = 3847$ s
$x_c = 66.4$ nmi

Note the factor of three difference in time constants for this unified model, 3847s, compared with the determination of time delay decorrelation alone, 1238s. Bierman [Ref. 3] shows that the accurate determination of time constants generally requires data sets which extend over several time constants. We do not have any data like this since the data sets are limited by the desire to stay with the same satellites throughout the data set.

Additional time delay data (not shown herein) has caused the increase in magnitude from the neighborhood of 5.2 to 6.6 ft to 12.2 ft. At this point we see no reason to exclude the data that causes the increase to 12.2 ft nor would we feel uncomfortable using a value of 5 to 6 ft. We would note that there was a large variation in the data collected at different times and places. In any case, the values are not inconsistent with the goals of relative GPS accuracy.

The next part of the problem, relative location of the target will now be discussed.

3.0 REAL TIME RELATIVE TARGET LOCATION TECHNIQUES

In Section 2 it was shown that a GPS/INS guided vehicle, using the same set of satellites as a reference receiver, will be able to maintain precision accuracies over long flight distances and flight times. The next part of the problem is to determine the target location relative to the

reference receiver. This target location, when used by the vehicle GPS/INS navigation system, will result in precision accuracy even though it can be substantially in error in an "absolute" sense. The target is then determined by adding this relative location to the reference GPS receiver location.

Figure 10 shows one concept in which the relative targeting is done by a foot soldier with a reference GPS receiver and a target location device. The target location device might consist of a laser range finder combined with an attitude determination device. The target location (relative to the soldier) would be added to the GPS location to determine the target location in GPS coordinates. The target location and the satellite set used by the reference receiver would be transmitted to the vehicle. The receiver on the vehicle would use this set of satellites and the guidance would use the computed target location to achieve precision accuracy.

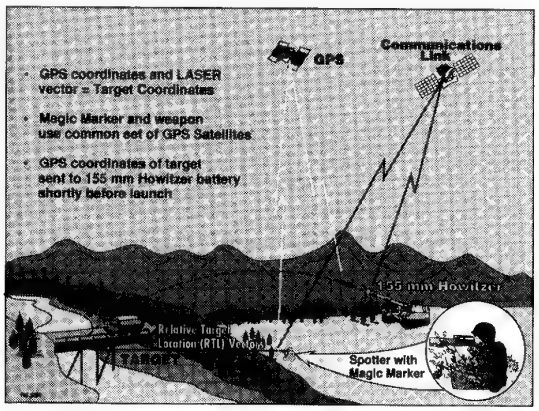

Figure 10. Determining Relative Location

Other implementations might involve the use of a high resolution synthetic aperture radar (SAR) onboard the aircraft in order to accurately determine the relative target location vector in the aircraft GPS/INS coordinate system. The remainder of this section provides an extensive analysis of this case.

To achieve high 3-D position resolution of ground targets using SAR range and range-rate (Doppler) measurements, SAR uses the velocity vector of the aircraft to create, in effect, an antenna length (or aperture) that is proportional to the velocity of the aircraft times the integration time used in the radar processing. Errors in knowledge of the actual velocity vector directly translate into cross-range errors in the slant plane defined by the velocity vector and the line of sight (LOS) to the target location. GPS provides accurate navigation information that helps the aircraft's Kalman filter sort out the GPS errors, the inertial system errors, the radar errors, and importantly, to relate the SAR Doppler measurement to cross-range position in the slant plane.

As an example, Fig. 11 shows an aircraft trajectory during which a sequence of simulated SAR maps were made. The radar range resolution was set to 3 ft. The aperture length/integration time was adjusted so that each measurement in the sequence also resulted in a radar cross-range resolution of 3 ft. It was assumed that the ARPA GPS Guidance Package (GGP) was the inertial/GPS system on the aircraft. It is approximately a 1 nmi/hr inertial system if the inertial system is calibrated but unaided by GPS. [Ref. 4] An error covariance analysis of a system which used these measurements in combination with GPS/INS navigation to determine target location was performed. The relative GPS errors were modeled as discussed in Section 2. Several results of this analysis are of interest. Figure 12 contrasts the results in target location determination with and without the use of GPS. For this figure, the initial target location error was 500 ft (1σ) in each of three axes. In the graph on the left, "Without GPS", the first radar measurement (at $t = 0$) immediately results in relative target accuracy in the range direction of less than 3 ft. However many more measurements are required to resolve cross-range accuracy. Even at 1000s, the cross-range coordinate is not known to better than about 60 feet (1σ). This error is primarily due to velocity errors in the inertial system corrupting the relationship between the SAR Doppler measurement and cross-range position. The component of error out of the slant plane is not resolved at all until the slant plane is rotated shortly after 1000s. In the graph on the right, the accuracy provided by GPS velocity measurements greatly aids in translating the SAR Doppler measurement into cross-range position. By about 10 minutes, both in-plane components of target location are accurately measured. Again the third component is not resolved at all until the slant plane is rotated at about 1000s. The GPS aided resolution of this third component is better but still not to the desired level.

The observability of this third component must be further enhanced by slant plane rotations. The idea is to align the measurement directions, either in range or cross-range, along the unresolved direction. There are two approaches to this, one to change the aircraft position, the other is to change the aircraft velocity. It takes much less time to change the aircraft velocity, so this was the approach used here. A series of dive and climb maneuvers, (porpoising) were incorporated into the flight plan. These maneuvers rotate the slant plane by rotating the velocity vector. Figure 13 shows the resulting target determination accuracy. Again the graph on the left shows errors when GPS measurements have been forgone. The graph on the right shows errors when GPS measurements are included. In this later case, accurate measurements are achieved relatively quickly. After about 20 minutes the RSS errors are 7.6 ft. Although perfectly feasible in terms of SAR processing (and some aircraft capability), there seems to be a desire in the SAR community to fly straight and level. Practically speaking this undoubtedly simplifies processing algorithms which even so require extensive computing resources. Perhaps a more practical scenario for target location and subsequent weapon delivery is shown in Figure 14. On its way to the target, the aircraft executes a dogleg and altitude change, thus dividing the trajectory into three segments with different slant planes. SAR measurements are made along the dogleg with the SAR beam squinted quite far forward, first + 20 deg, then at - 20 deg. For this study both the range and cross-range resolution was 8 ft.

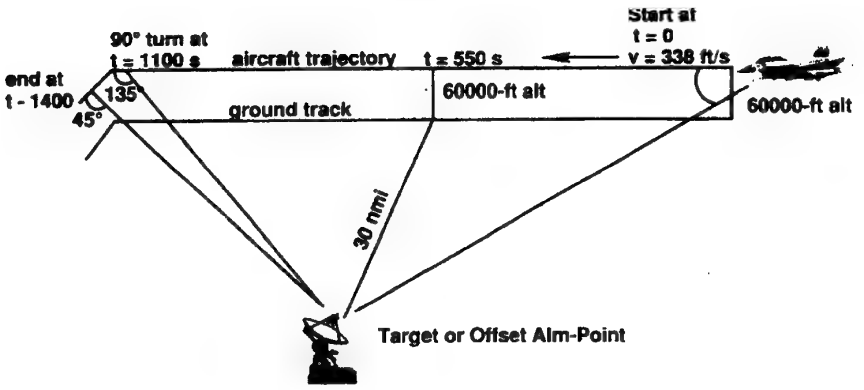

Figure 11. Trajectory 1 Geometry

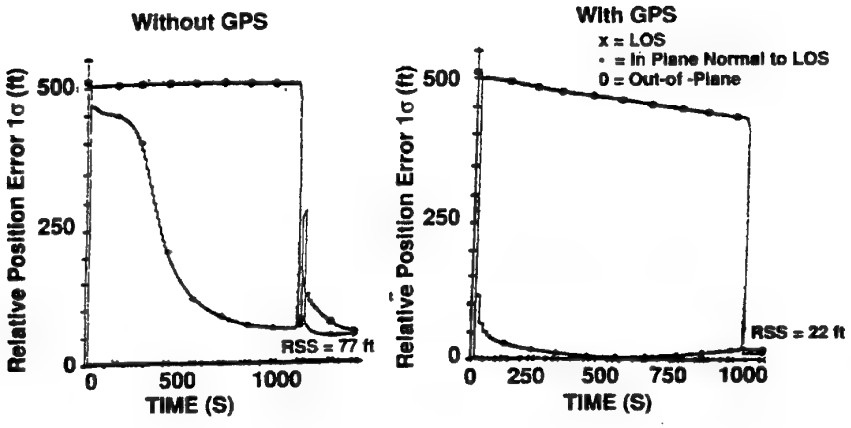

Figure 12. GPS Measurements Greatly improve SAR Performance

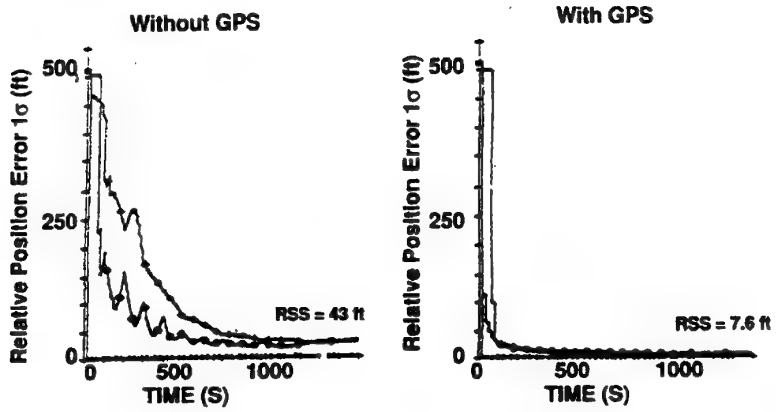

Figure 13. GPS Measurements and slant plane changes greatly improve SAR Performance

Table 3 shows resulting target location accuracy for two variations. In the first, Case 1, six SAR maps were made, two for each segment of the trajectory. For Case 2, a sequence of several measurements was made along each segment with the aperture time adjusted to yield an 8 ft. cross-range error for each measurement. The last measurement was made at t = 143s. At t = 376s, a guided bomb was launched. The bomb GN&C system included a GPS/INS reference receiver locked to the same satellites as the receiver on the aircraft and used the target coordinates determined by the GPS/INS/SAR system. The resulting bomb impact errors shown in Table 3 demonstrate the efficiency of relative GPS/INS navigation and target determination by this system at weapon delivery time.

Another example of relative techniques using real-time targeting is illustrated in Figure 15. In this example an actively guided and controlled parafoil is launched from an aircraft and guides to a destination where supplies are needed. [Ref. 5]

The details of an experimental design to demonstrate this mission are shown in Figure 16. The uplink receiver can be used to initialize the relative targeting function from the aircraft or it could be receiving initialize functions from a receiver at the target landing site. Alternately, it could be receiving differential GPS corrections. accuracies would be expected to be dominated by parafoil control system errors not the relative (or differential) navigation errors.

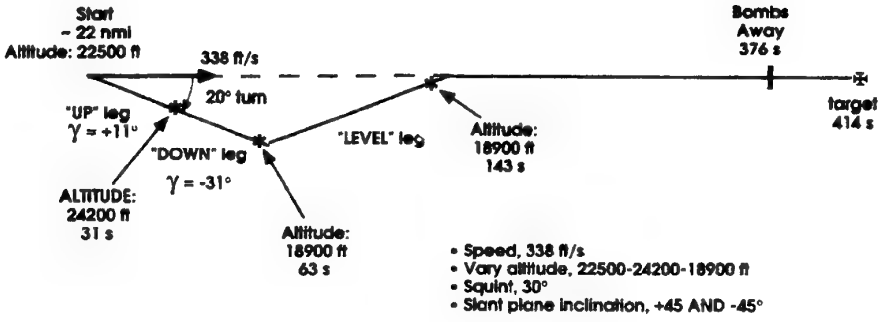

Figure 14. Trajectory 3

		1 σ Relative errors, ft LOS = Along the line-of-sight to target CR = Perpendicular to LOS in the slant plane Norm = Perpendicular to the slant plane FWD = Forward CRR = Cross range at impact										
Case	SAR Measurement Conditions	"Up" Leg Y = + 11° Plane Inclination +45° Altitude: 24,200 ft			"Down" Leg Y = - 30° Plane Inclination -45° Altitude: 18,900 ft			"Level" Leg Y = - 0° Plane Inclination -45° Altitude: 18,900 ft			Bomb Impact	
		LOS	CR	Norm	LOS	CR	Norm	LOS	CR	Norm	FWD	CRR
1	2 at end of each leg	8.0	49.1	500	5.7	31	32	No measurement			9	21
2	Continuous	4.0	51	500	2.7	32	33	1.9	15	21	5	15

Table 3. Trajectory 3 Results

The next section analyzes scenarios for which the relative target vector has been determined premission.

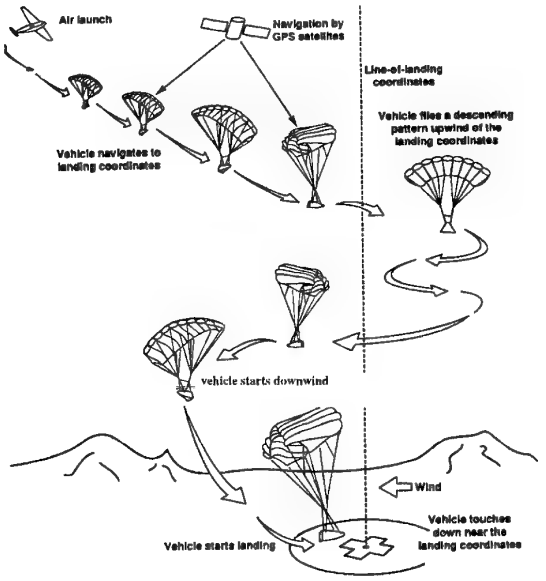

Figure 15. Autonomous Parafoil

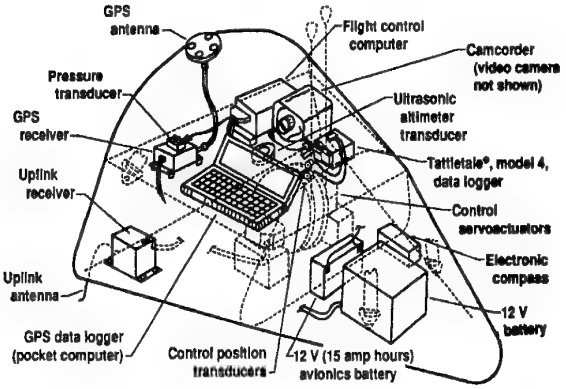

Figure 16. Experimental Demonstration Impact Avionics

4.0 RELATIVE TECHNIQUES EMPLOYING GROUND-BASED RECEIVERS

In this section, we shall consider how various existing or planned GPS-guided vehicles could exploit an hypothetical capability that accurately determines 3-D relative target location vectors prior to the mission. We shall make the explicit assumption that someday we may have the capability to accurately determine these vectors to an accuracy of better than 10 ft (1σ per axis) over distances up to, say, 540 nmi.

Such a capability would allow one to provide relative (or absolute if a surveyed point is used) targeting information on many locations over reasonably large areas. For example, Figure 17 shows how a cooperative receiver located in Sicily provides extensive coverage of that region. Of course, we might expect increasingly better accuracy as the distance between the cooperative ground-based receiver and target is shortened. We shall now illustrate how several, somewhat different, existing or planned systems could exploit such a capability.

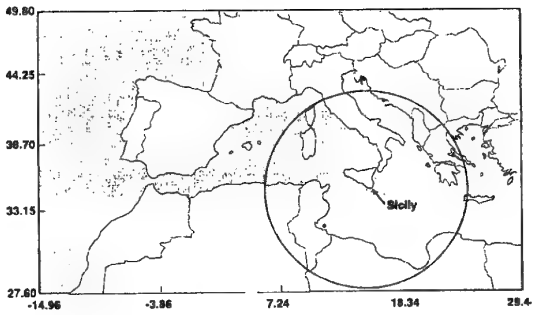

Figure 17. 540 nmi "Coverage" for One Cooperative GPS Receiver/transmitter.

First, consider the cruise missile scenario shown in Fig. 18. Here, a ground-based receiver has been located with respect to a target. It will be necessary for the ground-based receiver to update the cruise missile shortly before its arrival at the target. It is not certain how "short" this time must be to be consistent with our accuracy goals. However, the results of Section 2 indicate that several minutes are permissible.

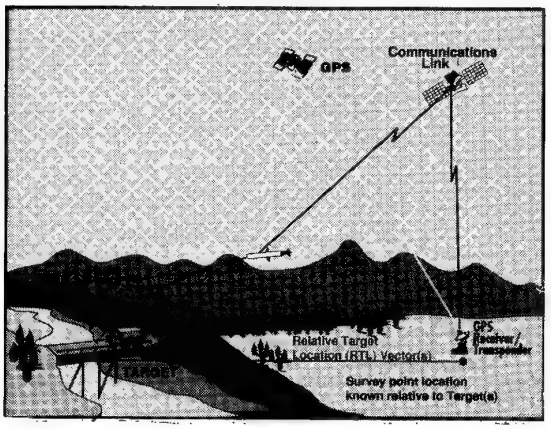

Figure 18. Cruise Missile Concept Employing Relative GPS

So, a few minutes before impact, we transmit from the cooperative receiver to the missile the receiver's indicated position and the set of satellites it is using to form its navigation solution. A communications relay (satellite or aircraft) might be used if there were line-of-sight constraints.

It is also assumed that prior to launch we store the relative vector from the cooperative receiver to the target in the cruise missile's flight computer. Then, on receipt of the short data message from the cooperative receiver, the cruise missile ensures it is tracking the correct set of

satellites and then adds the indicated position of the cooperative receiver to the $\overline{RTL}$ vector—thereby making an estimate of the indicated GPS position of the target. The cruise missile then steers itself to that location.

An equally simple scenario can be mechanized for a standoff weapon. Fig. 19 illustrates this concept. The slight difference in this scenario from that of the cruise missile is that the communication would probably go from the cooperative receiver to the aircraft carrying the weapons. This is feasible due to the relatively short time of flight of the weapon. Thus, just before launch of the weapons, the A/C receives the targeting data, computes the indicated GPS coordinates of the target(s) and downloads these new coordinates and the set of satellites to be tracked into the weapon computer.

The ship-based Navy can also take advantage of this relative targeting technique just as well for precision shore bombardment. Fig. 20 illustrates this scenario.

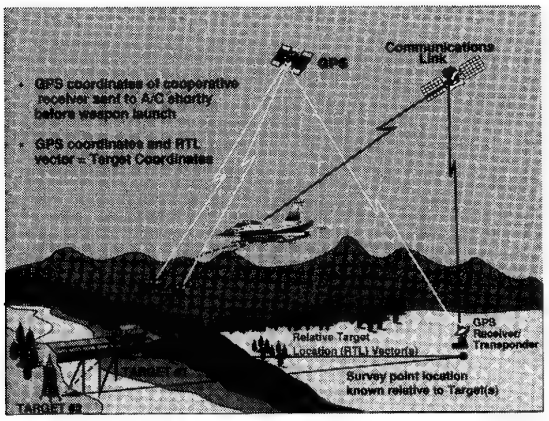

Figure 19. Stand-off weapon employing relative GPS

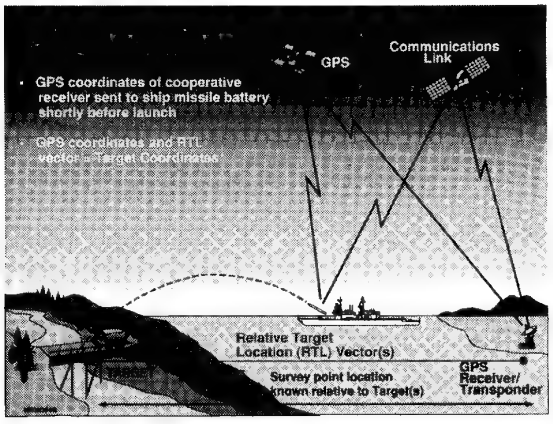

Figure 20. Relative GPS for Ship-based Munition

Possibly the simplest scenario might involve a land-to-land rocket launch. A missile battery could be set up at one end of a predetermined $\overline{RTL}$ vector. Then the GPS receiver in the weapon itself could act as the "reference" receiver. The target location would be obtained by adding the $\overline{RTL}$ vector to its own indicated position just before launch . The same satellites would be tracked during the mission.

This scenario is shown in Fig. 21. If it is not possible to locate the missile battery on a surveyed site (at the end of a $\overline{RTL}$ vector), a separate reference receiver can be used as in the other scenarios. Now, however, a communications link is required between the cooperative receiver and the battery.

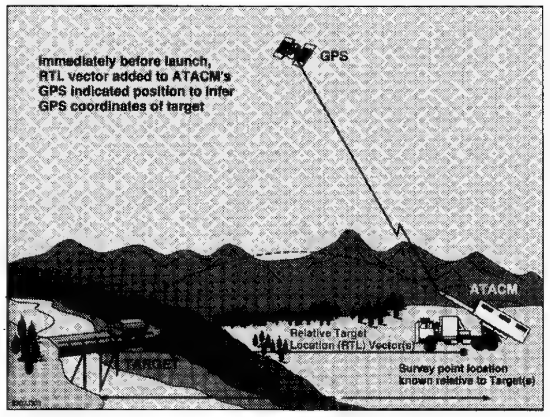

Figure 21. Rocket launch using Relative GPS

Variations on these scenarios can be applied to many other existing or contemplated GPS-guided systems. For example, the SAR equipped aircraft of Section 3 could be used to image off-set aimpoints (rather than the target). The points could be in friendly territory and have been mapped relative to the target prior to the mission. (See Figure 22.) In some tactical situations it might even be conceivable to include the reference station and the target in the same SAR image.

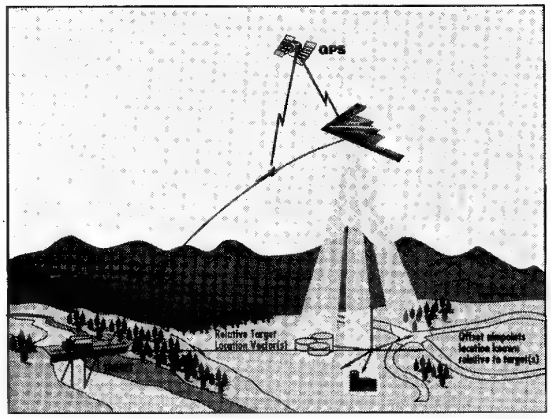

Figure 22. Relative GPS/Bomber Scenario

The next section will present a detailed design application using relative techniques to guide a munition.

5.0 A INS/GPS SYSTEM FOR GUIDED PROJECTILES

Recent advances in silicon microfabrication technology have led to the development of low-cost, tactical performance grade, micro-mechanical inertial sensors. The inherent small size, low weight, and low cost of these sensors permit onboard insertion of gyroscopes and accelerometers for inertial instrument applications previously impractical because of size and cost considerations.

Among the emerging opportunities for micromechanical inertial sensor insertion is the application to guided projectiles. [Refs. 6,7] This application is distinguished by the extremely high-acceleration (high-g) sensor measurement environment experienced during projectile launch; peak accelerations on the order of 100,000 g are possible during firing.

Draper Laboratory has developed a range of micro accelerometers to measure muzzle velocity and projectile flight acceleration, and a micro gyroscope to measure projectile attitude. [Refs. 8,9] Only the high-g accelerometer is operational in the barrel; the other sensors operate outside the barrel, but must be able to survive the launch environment. The total sensor system furnishes eight orders-of-magnitude acceleration dynamic range capability. A description of the sensors will be given later in this section.

Performance simulations for a high-dynamic-range micromechanical inertial sensor assembly (MMISA) coupled with a GPS receiver, will also be given. GPS supplies position information at low frequencies, and the micromechanical instruments supply high-frequency information. The data are combined with a Kalman filter and navigator to generate high-frequency position, velocity, and attitude information. The high-frequency information is then used in the guidance and control of the projectile.

Demonstration System Concept

A typical guided projectile is shown in Figure 23 and comprises a spinning aft section and a despun, actively controlled fore section. The micromechanical INS/GPS implementation uses GPS pseudo and delta-range measurements in conjunction with MMISA measurements to estimate both the vehicle state (position , velocity, and attitude) as well as the MMISA calibration errors. This provides an improved navigation solution, especially when jamming is present near the target and/or tracking some of the satellites is "lost", since the inertial system performance is improved via in-flight calibration. Inertial information is used to aid the receiver tracking loops. Most of the integrated GN&C system will reside entirely within the fuze area. In addition to the size, power, and weight benefits associated with such a system, having all sensors in the despun section provides clear performance advantages.

Figure 23. Guided Projectile

A concept for flight testing the projectile is shown in Figure 24. An external power source will be used to initialize the system outside of the gun barrel prior to gun loading, thereby minimizing battery requirements. An auxiliary L1/L2 GPS receiver will be interfaced to the projectile through a ground control computer to provide an accurate estimate of GPS time, the projectile's position, and the satellites that will be tracked during flight. This is conceptually the same as would be done in a fielded system, and is necessary to minimize the time to reacquire GPS following launch. In addition to the GPS receiver initialization, the navigation algorithm will be loaded with the MMISA calibration parameters, and the GN&C system will be initialized with the coordinates of the target aimpoint. The projectile navigates to the target using a relative GPS navigation approach in which the target's position relative to the shell is provided to the guidance system prior to launch. Since the ionospheric effects do not change substantially over the test scenario, this requires the receiver to track only the GPS L1 signal.

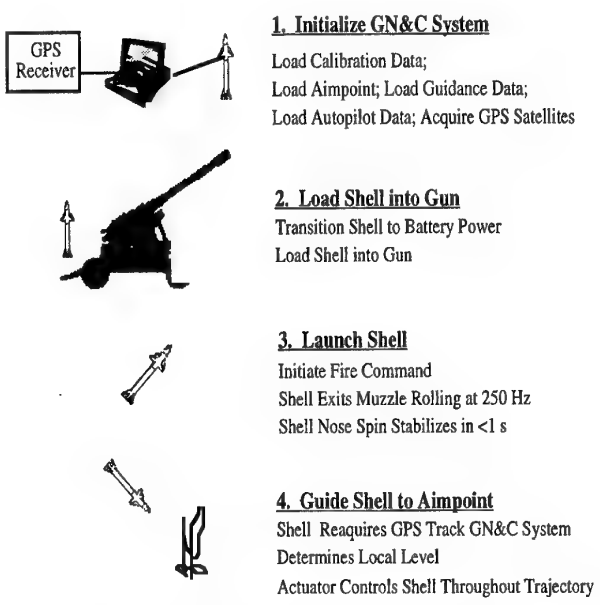

Figure 24. Projectile Flight Test Scenario

Following initialization, the projectile will be inserted into the barrel for launch. A battery will be required to power the flight processor and memory prior to launch to maintain the GPS estimates of time, position, and velocity. During launch, a high-g accelerometer will be used to measure the longitudinal forces on the shell. This information will be combined with a priori knowledge of the barrel orientation to estimate vehicle position and velocity during the first several milliseconds of flight. This approach reduces the position and velocity uncertainty following barrel exit and speeds reacquisition of the GPS. In addition to the position and velocity uncertainty associated with the shell, the estimate of GPS time will also degrade during launch due to the effects of the high-g environment on the GPS frequency reference. A reference oscillator that exhibits low sensitivity to high-g shock (currently anticipated at 1.5 to 2 ppm) and requiring fast reacquisition algorithms in the GPS receiver is required.

At the time of barrel exit, the projectile will be rolling at up to 250 Hz. The roll rate of the forward section will stabilize to somewhere between 0 Hz and a few Hz in less than 1 second after launch. During this transient period of high dynamics, GPS tracking will be lost. Reacquisition of GPS track will therefore be required following roll stabilization of the forward section of the projectile. The current concept for reacquisition assumes the same satellites tracked prior to projectile loading by the initializing GPS receiver will be reacquired. Reacquisition will be accomplished by first establishing C/A code and carrier track for a single satellite, from which GPS time can be accurately determined, followed by reacquisition of the P(Y) code and carrier for all remaining satellites.

A fundamental problem that must be resolved in the implementation of the GN&C system is the determination of local vertical. The algorithm and hardware requirements for "down" determination rely upon processing GPS velocity estimates to extract an estimate of projectile pitch and yaw angles (assuming that angle of attack and sideslip are small) and using the gyroscope measurements to estimate the roll orientation.

The guidance system will be based upon a simple gravity-compensated Proportional Navigation (Pro-Nav) guidance law. The system will begin nulling cross-range errors as soon as GPS track has been reestablished, and the altitude profile will be shaped during the course of the scenario. In the end game, a gravity-compensated Pro-Nav guidance law will be used to null downrange errors.

The GPS receiver will be integrated with Draper's MMISA in the configuration shown in Figure 25. The integration filter will accept pseudo-range and delta-range measurements from the GPS receiver hardware and uncorrected acceleration and rate measurements from the MMISA and process them to estimate the position, velocity, and attitude of the shell, as well as the calibration parameters for the MMISA. Additionally, the integration filter will output an estimate of vehicle velocity to aid the GPS receiver's tracking loops. The pertinent features of this approach are (1) the MMISA calibration improves as the scenario evolves, so that an inertial-only navigation solution would improve during the scenario, and (2) all GPS measurements are processed to navigate. The advantage of this approach is that for tactical scenarios, in which jamming is present near the target, the inertial-only navigation solution will provide a lower CEP than a system that does not use in-flight calibration when GPS track of all satellites is lost. Additionally, if track is maintained for some of the GPS satellites, processing of that information continues, providing a lower CEP than would otherwise be possible. The baseline concept assumes that all of the software is integrated into a single microprocessor.

A GPS L-band antenna and an S-band telemetry antenna will be required. The L-band antenna can be either a patch or band antenna that resides on the actuator. The telemetry antenna will be placed on the rear of the projectile near the telemetry electronics.

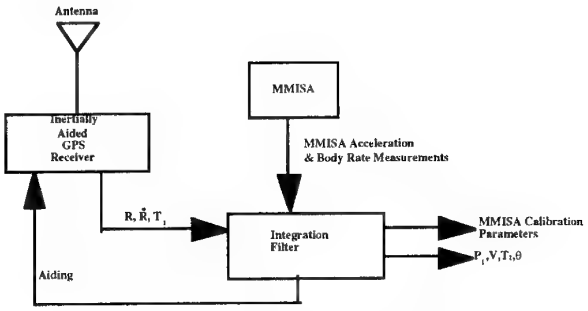

Figure 25. GPS/MMISA Integration

Subsystem Interfaces

The principal components and subsystems are the GPS receiver and the antenna, the MMISA, the telemetry (TM) antenna and transceiver, the actuator, interface electronics (including the flight processor), and the projectile itself. Figure 26 depicts the functional interfaces required to integrate these components into a system.

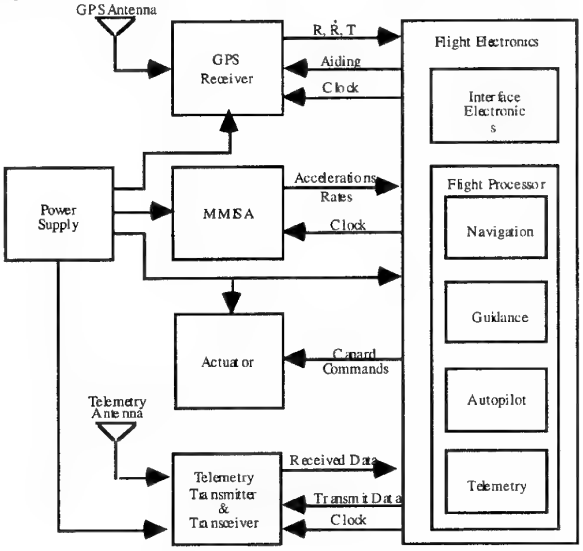

Figure 26. Subsystem Integration

As shown in Figure 26, the GPS receiver will accept as inputs the clock (i.e., reference frequency) and inertial (velocity) aiding. It will provide pseudo-range, delta-range, and time estimates as outputs that will be passed to the navigation algorithms in the flight processor. The MMISA will use the same frequency reference as input, and will provide accumulated accelerations and angular rates as output. These measurements will be passed to the flight processor's navigation code, supporting both the navigation function and the autopilot.

The guidance algorithm will accept estimates of the projectile's position and velocity from the navigation algorithm and will develop a normal acceleration command and a roll command that are passed to the autopilot. The autopilot will then produce canard deflection commands to the actuator.

Finally, the projectile will be equipped with a telemetry antenna and transceiver, which will interface with the flight processor to downlink data to a ground station.

Micromechanical ISA

Draper Laboratory has been developing miniature inertial instruments the past 8 years using the rapidly maturing silicon micro-fabrication technology. Draper is currently integrating a high-dynamic-range micro-accelerometer array, which satisfies the environmental and performance requirements of a guided projectile system, and a micro-mechanical tuning-fork gyroscope, which meets guided projectile performance requirements, and has demonstrated high-g survivability in air gun testing at Picatinny Arsenal. [Ref. 10]

The following table lists typical function and performance requirements for the microsensors:

Sensor	Function	Performance
Accelerometers	Muzzle Velocity Augmented Position	0.1 - 1 mg 500 ppm
Gyroscopes	Shell Attitude	10-100 deg/h 1,000-10,000 ppm

Table 4. Function and Performance Requirements

Figure 27 shows the launch acceleration profile seen by a typical munition shell during firing. The acceleration load on the projectile reaches a maximum in approximately 0.2 ms, after which the loading decreases rapidly to approximately 100 g at projectile exit. The projectile is within the barrel for approximately 4 ms.

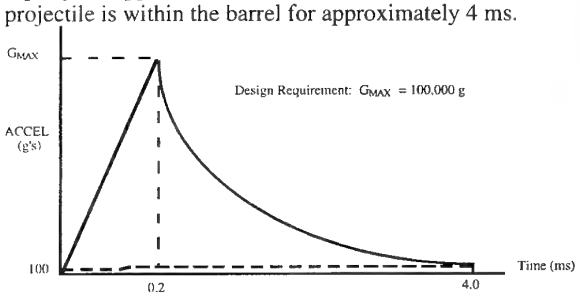

Figure 27. Launch Acceleration Profile

The accelerometer system must function while the projectile is within the barrel to determine muzzle velocity. The gyroscopes must survive the launch but do not begin measuring the projectile attitude until it has exited the barrel.

Micromechanical Accelerometer Array

Measurement of projectile muzzle velocity and subsequent downrange measurement of projectile flight acceleration places a large dynamic range burden on the accelerometer. During launch, acceleration levels can reach peaks of 100,000 g whereas the downrange position requirements dictate milli-g resolution. Consequently the total dynamic range burden for this application is 10^5 to 10^{-3}, or 10^8 total.

An array implementation was developed to satisfy the dynamic range requirements, and is shown in Figure 28. The total dynamic range burden is partitioned among a series of accelerometers. For example: the first accelerometer has a peak capability of 100,000 g and a noise floor below 100 g; the second accelerometer in the array has a peak capability of 100 g and a noise floor below 1 g, etc. The array is filled out with increasingly more sensitive accelerometers until a sub-milli-g noise floor is achieved.

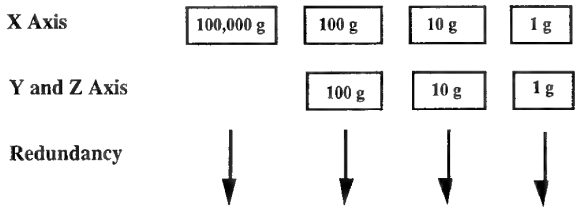

Figure 28. High-Dynamic-Range Accelerometer Array

It is apparent that the 100,000 g accelerometer will be functioning during the launch portion only, and that the 100 g accelerometer will take over immediately after the projectile has exited the cannon. Consequently, the "mission" of the high-g accelerometer is to furnish muzzle velocity of the projectile, and the "mission" of the other accelerometers is to measure the downrange shell acceleration with sub-milli-g accuracy.

The output signals of the accelerometer array can be combined and filtered to furnish acceleration information throughout flight. The microscale of the accelerometers permits the addition of redundant rows to improve reliability, and to improve the array signal-to-noise (S/N) ratio. If the noise sources in the individual accelerometers are uncorrelated, the net S/N ratio improves by the square root of the number of redundant rows employed.

High-g Accelerometer

Table 5 gives performance specifications for the high-g (100,000-g) accelerometer.

The principal performance specification listed is the 3 ft/s velocity error requirement. Typical munition muzzle velocities are in the 3000 ft/s range, so the high-g accelerometer must furnish velocity information accurate to 0.1 percent. The bias, scale factor, and scale-factor linearity requirements are ancillary requirements that are simply a partitioning of the 3 ft/s velocity error budget into conventional accelerometer performance parameters.

Parameter	Value
Maximum Acceleration	100,000 g
Mission Time	4 ms
Bias Stability (4 ms)	10 g
SF Stability (4 ms)	500 ppm
Velocity Error (@ 4 ms)	3 ft/s
SF Nonlinearity @ gmax)	1%

Table 5. Performance Specifications

Figure 29 shows a Scanning Electron Microscope (SEM) photo of the high-g accelerometer. The proof mass and flexures are a single-thickness piece of silicon that is formed using the dissolved wafer microfabrication process. Anchor pads, integral with the proof mass and flexures, are also formed and used as anodic bonding sites to attach the acceleration-sensitive elements to the substrate. The substrate is Pyrex glass, which is electroplated with the signal generator (SG) electrodes, leads, and wire bond pads.

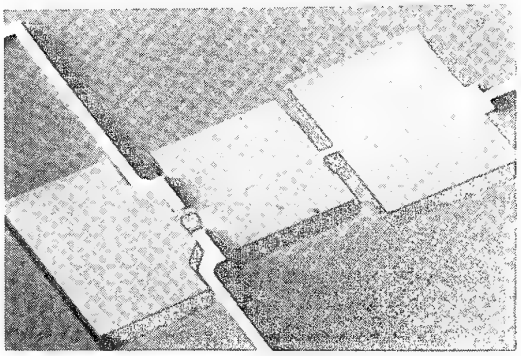

Figure 29. High-g Accelerometer

The high-g accelerometer design has been verified through bench testing and centrifuge testing. Flight performance was simulated using the 2-in air gun at Picatinny Arsenal, Picatinny NJ. In this test, the high-g accelerometer and its electronics were mounted in an aluminum cylinder dummy "shell." The cylinder was attached to a fixed flange through a thin circumferential rim. The cylinder was "fired" by pressurizing the breach until the thin circumferential rim broke free, releasing the cylinder with the high-g accelerometer and its electronics.

Figure 30 shows air gun test results with the high-g accelerometer measuring a peak acceleration level of 63,000 g. The 100-g device is functional once the shell leaves the gun barrel where it must measure shell acceleration to 1-mg accuracy. The flight accelerometers are not operational in the barrel, but must survive the high-g launch portion of the flight.

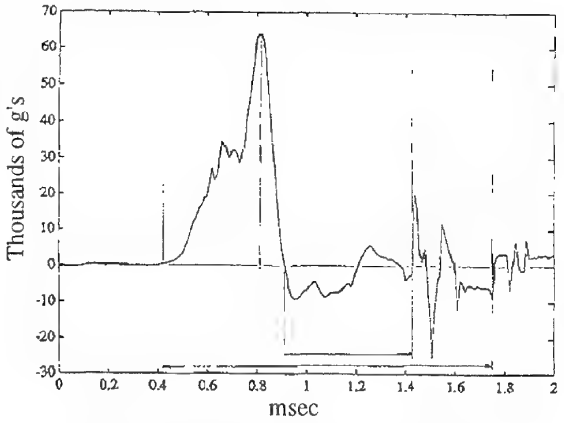

Figure 30. Measurement of Launch Acceleration Flight Accelerometers

The performance specifications established for the flight accelerometers are listed in Table 6.

Parameter	100-g Accel	10-g Accel
Max Acceleration (Survival)	100,000 g	100,000 g
Max Acceleration (Operational)	100 g	10 g
Mission Time	100 s	100 s
Bias Stability	1 mg	0.1 mg
Resolution (0-60 Hz)	1 mg	0.1 mg
SF Stability	500 ppm	500 ppm
SF Nonlinearity (@ gmax)	1%	1%

Table 6. Accelerometer Performance Specifications

The 100-g accelerometer is shown in Figure 31. It has a pendulous proof mass that is supported on a pair of torsional flexures. A pair of SG electrodes detect the rotation of the proof mass under input acceleration. The 10-g device is similar.

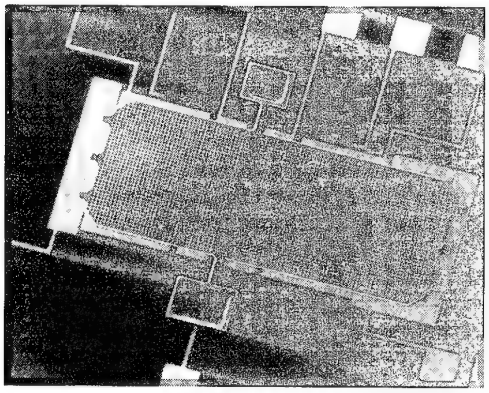

Figure 31. 100-g Accelerometer

The fundamental difference between the flight and high-g accelerometers is that the flight devices have an additional pair of electrodes for force rebalancing the proof mass, i.e., for closed-loop operation. The performance requirements for the 100-g device dictate an acceleration dynamic range of 10^2 to 10^{-3} for a total of 10^5, an operational dynamic range best achieved through a closed-loop design configuration.

Figure 32 shows a three-axis hybrid of 100-g accelerometers used in air gun testing.

The micromechanical Tuning-Fork Gyroscope (TFG) is shown in Figure 33. [Ref. 11] The TFG has construction similar to the micromechanical accelerometers. Its dynamic, rate-sensing elements are fabricated from a single-thickness piece of silicon using the dissolved wafer process. The silicon portion is anodically bonded to a Pyrex substrate.

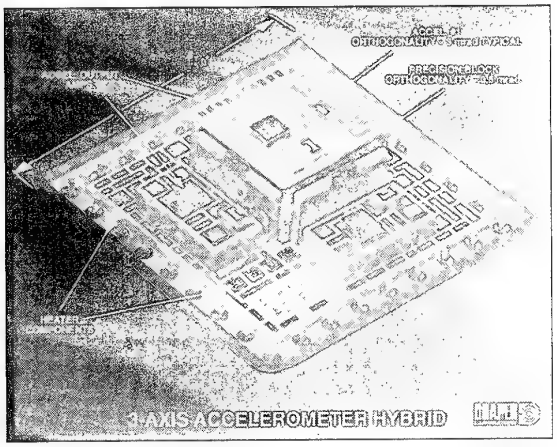

Figure 32. 3-Axis 100-g Accelerometer Hybrid Micromechanical Gyroscope

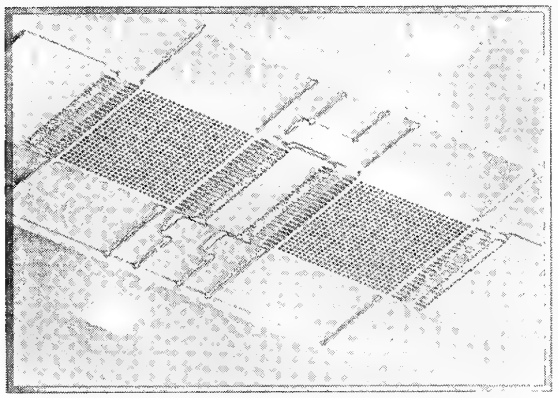

Figure 33. Micromechanical Tuning-Fork Gyroscope (TFG)

The TFG consists of a pair of proof masses that are supported by a set of beams anchored to the substrate at four points. Finger-like extensions on the proof mass engage motor drive fingers that are fixed to the glass substrate. AC excitation is applied to this comb drive to sustain lateral oscillation of the gyro structure "tuning-fork" mode. The ac excitation is applied at the resonant frequency of the TF mode (approximately 25 kHz) to ensure large amplitude displacement, and hence, high-gyro gain (sensitivity).

An angular rate directed along the in-plane axis will interact with the velocity of the oscillating proof masses and produce a Coriolis acceleration directed normal to the plane of the substrate. Since the proof masses are driven in tuning-fork mode, their velocities are 180 deg out of phase (i.e., opposed). Consequently, the subsequent Coriolis acceleration developed by the applied rate drives the proof masses out of plane in opposing directions. The amplitude of this displacement is proportional to the applied rate.

Currently, the TFG has demonstrated bias stability of 100 deg/h (1 sigma over 24 hours) and resolution of 450 deg/h over a 60-Hz bandwidth. In addition, air gun testing at Picatinny Arsenal has verified high-g operation pre- and post-65,000 g along all axes.

Performance Simulations

Two generic munition applications were simulated to determine the shell position and attitude error estimates using onboard micromechanical accelerometers and gyros. One case is a 18 nmi flight, typical of a gun-launched shell. The second is a shorter 1.8 nmi flight typical of a tank-launched shell. The MMISA in the 18 nmi flight is assumed to be despun to 2-Hz, and in the 1.8 nmi flight, to exit the tank barrel at 0 Hz.

The simulations use a Kalman filter blending of inertial instrument data and relative GPS updates to determine rms position and attitude errors throughout the flight. The 18 nmi flight takes 75 s to complete, and the 1.8 nmi flight takes only 8 s. GPS is acquired after 10 s in the 18 nmi flight and after 4 s in the 1.8 nmi case.

Figure 34 shows position and attitude errors for both flights when accelerometers with 1 milli-g bias errors and gyros with 500 deg/h bias errors are used in the onboard inertial system.

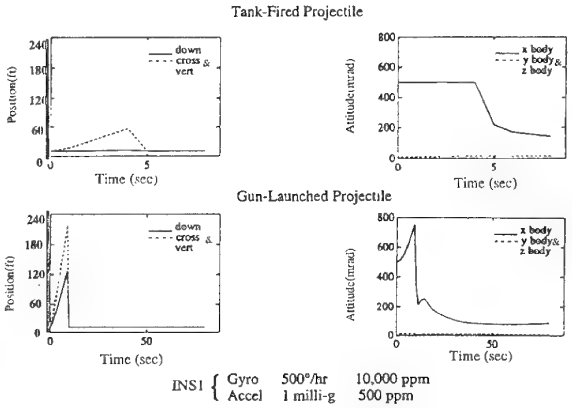

Figure 34. Position and Attitude RMS Errors - INS1

In the 18 nmi flight, the position error peaks at approximately 240 ft at 10 s when updating begins, then falls below 12 ft. In the shorter 1.8 nmi flight, the position error falls well below 12 ft after updating begins at 4 s.

An initial 500-mrad error was assumed for the roll attitude simulations. With 500 deg/h gyros, the worst-case roll attitude error grows to approximately 750 mrad just prior to GPS acquisition, due primarily to gyro scale-factor error (10,000 ppm). Approximately 10 s after GPS is acquired, the roll attitude error, which is the most significant contributor to guidance error, falls to less than 150 mrad. The azimuth and pitch angle errors remain less than 20 mrad after GPS acquisition. The roll angle is also the worst axis for the shorter 1.8 nmi flight, with a maximum error of less than 12 deg for the last 3 s of the flight. The azimuth and pitch angles errors are less than 20 mrad at the end of the flight.

Figure 35 shows the same simulations with gyro and accelerometer performance upgraded to 50 deg/h and 0.1-mg bias stability's, respectively. As expected, the improved gyro performance has little impact on the

position or attitude estimates, except that roll attitude errors are reduced by 50 percent.

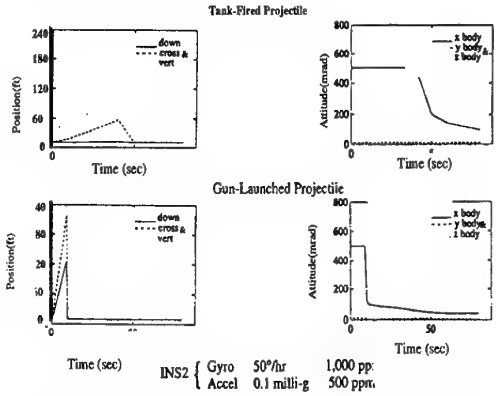

Figure 35. Position and Attitude rms Errors-INS2

Figure 36 shows the tank shell position and attitude errors assuming GPS is jammed. The navigation errors are dominated by fire control launch errors. INS-induced errors have little time to grow; therefore, there is little difference between the two INSs. For the GPS-jammed 18 nmi flight, the INS-induced errors would grow significantly and can exceed the trajectory deviations of an unguided round.

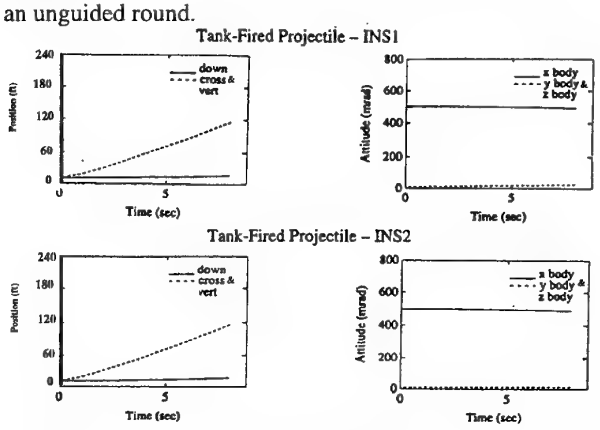

Figure 36. Position and Attitude rms Errors- GPS-Jammed

GPS Technology Requirements

In order for guided projectiles to be effective weapons, there are a variety of requirements that must be satisfied beyond those of a technology demonstration system. Of particular importance is the ability of the system to rapidly acquire GPS following barrel exit, potentially in a jamming environment. Jammers represent a realistic current threat to integrated GPS/inertial guidance systems, and must be seriously considered in the design of guided weapons particularly those with short-range missions.

Short-range missions are the most challenging since there is little time available to acquire GPS between barrel exit and the onset of intense jamming, and there is also little time available for in-flight calibration of the MMISA by the tightly coupled navigation system. In contrast to the C/A acquisition approaches that are presently prevalent, future systems will feature fast direct P-code acquisition to satisfy mission requirements. This will be facilitated by massively parallelized P-code correlators on a chip with associated software to control the search process. Additional anti-jam (AJ) capability during acquisition will be provided by advanced antennas that null the effects of both broadband and continuous-wave (CW) jammers and by front-end filters and adaptive A/Ds that combat CW jammers.

Once acquisition is complete, a tightly integrated navigation filter will be used to process pseudo- and delta range measurements and recalibrate the MMISA during flight. It is expected that jammers will be placed near high- value assets, so that in the terminal portion of the mission jamming will be most severe. Here the benefits of adaptive antennas and front end filters provide AJ enhancements and delay loss of GPS code and carrier lock. However, additional signal processing techniques, such as extended range correlation and adaptive tracking can provide significant additional ECCM. [Ref.13] When loss-of-lock does occur, the guidance system will use an inertial-only navigation solution to lead the projectile to the target aimpoint. Hence, it is imperative that the GPS receiver has adequate ECCM to provide time for in-flight calibration of the inertial system.

6.0 PRACTICAL ISSUES

This section addresses the important issue of GPS satellite availability as a function of (1) target-to-receiver separation, and (2) the time interval between when the target location is estimated and when the weapon actually arrives at the target. In other words, is it reasonable to expect that as the weapon approaches the target that both it and the cooperative GPS receiver located "far" from the target will have a sufficient number of common satellites in view to enable a relative GPS mechanization? A study was undertaken to address this important issue.

The study assumes the full constellation of 24 GPS satellites. A simulation was written to model the orbital motion with respect to the earth. In the simulation, pairs of receivers were located at various latitudes (0 to 90 deg) and at various orientations (i.e., N/S or E/W, etc.) with respect to each other. Time was advanced in increments so as to let the geometry evolve for a long enough period so that all the behavior patterns could be observed. Both distance and "time delay" between receivers were varied, the process is illustrated for one location in Figure 37. Table 7 summarizes the results of the study. If, for example, we update the cruise missile aimpoint coordinates 5 minutes before impact using data computed from a receiver located 945 nmi away from the target at 60 deg latitude, the table indicates that there will never be a condition with fewer than 4 satellites in view common to both receivers. One might also note that using a tightly-coupled GPS/INS navigation system allows continued navigation using less than four satellites.

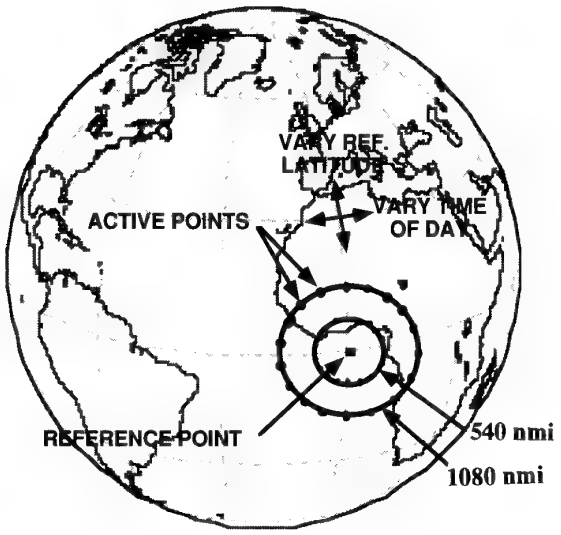

Figure 37. Reference and Active Receiver Locations

High accuracy, however, is not guaranteed solely by having a set of four or more common satellites in view. Satellite constellation geometry (PDOP) is also important. On rare occasions, the geometry may be such that a change in the attack time by +/- a few minutes may result in a substantial improvement in accuracy (as when a new satellite appears over the horizon and has a dramatic effect on the available constellation geometry). This rare condition can be predicted weeks ahead of time if the approximate target location and time of attack are specified, thus allowing the mission planners to either select times with extremely favorable GPS geometry or to avoid the very rare instances of poor geometry. Draper has developed a prototype software/simulation tool for analyses and fire control applications involving these issues. Again, it should be emphasized that instances of poor geometry are, indeed, the rare exception. Additional practical considerations can be found in Ref. 12.

7.0 CONCLUDING REMARKS

This lecture has addressed several potential methods for achieving high accuracy (≈ 10 ft CEP) using GPS/INS. The approaches were all variants of relative (or differential) GPS guidance schemes. Simulated accuracies were shown to have promise for achieving the high accuracy goals. Actual experimental results were presented confirming the theory of relative navigation between receivers separated by long baselines and also separated in time.

Reference Latitude, Degrees - North	Time Delay (Minutes)	Minutes Number in View for Zero Separation	Max. Separation with four satellites in View (nmi)
0	0	6	1458
	5	6	1296
	15	6	1377
	30	6	1080
30	0	5	1350
	5	5	1188
	15	4	918
	30	4	324
60	0	4	918
	5	4	945
	15	4	702
	30	4	432
90	0	7	1836
	5	7	1944
	15	6	1836
	30	6	1458

Two specific examples:

Lati-tude	Time Delay (min)	Sep. Distance (nmi)	Min. # of Common Satellites	Ave-rage #	Ave-rage GDOP
30	15	540	4	6.2	4
60	15	540	4	6.5	3.9

Table 7. Summary of Results

APPENDIX A

THE RELATION OF RELATIVE TO DIFFERENTIAL GPS AND AN ERROR ANALYSIS OF RELATIVE AND DIFFERENTIAL GPS

INTRODUCTION

This appendix distinguishes between RGPS and DGPS. For both of these modes of operation it is necessary to transfer information from a reference receiver to an active receiver. This appendix also evaluates the errors associated with three different data "formats" for this transfer. It is stated that for DGPS the reference receiver must be placed at a known location. It is a major effort to accurately survey such a location, but it is never perfectly known and location errors play a role in the resulting DGPS performance. This is in contrast to the RGPS strategy which admits that surveying errors exist but insures that they are correlated between reference receiver and target.

The two major sources of error are the difference in GPS bias errors between reference receiver and active receiver and the difference in mapping or surveying error between reference receiver and target. Although the relative GPS information can be transferred by one of three methods, it will be shown that there are first order differences which depend on receiver separation and which suggests which method is appropriate as a function of the relative magnitude of these two error sources.

ANALYSIS

Figure A-1 shows the location of the reference receiver and the target. The reference receiver is on the right; the active receiver and the target are on the left. The reference receiver is at the true location. It "thinks" it is at the surveyed location, and GPS indicates that is at the GPS location. The RTL_{survey} vector is obtained by either a survey or real time sensor as explained in the main part of this paper.

The diagram shows examples of errors in the GPS solution at the reference receiver and at the active receiver. At the reference receiver the error is all in a northerly direction. On the left, at the active receiver, there is also a westerly component in the GPS solution error. Similarly on the right, where the reference receiver is located, the survey error is all in the northerly direction; but on the left, at the target, the survey error has a slight easterly component. Thus the diagram shows GPS errors and survey errors - and the differences between those errors when measured at the reference receiver and at the active receiver/target.

The difference between the active receiver position and the target position is the error-on-target, ε. It is a nearly horizontal vector with a circle located about 1/5 of the way from left to right. To the left of the circle is the part of the error-on-target which can be attributed to the relative survey error. To the right of the circle is the part of the error-on-target which can be attributed to GPS error. An expression can be derived for the error-on-target based on three "formats" for transferring information from the reference receiver to the active receiver. The transfer format can either be target coordinates, an offset to the target coordinates, or an offset to the pseudo-range biases. It will be seen that there are only two forms for the error-on-target, one for transfers in position space, the other for transfers in pseudo-range space. It will also be seen that there are first order terms in the errors which depend on receiver separation. The relative magnitude of surveying error vs. pseudo-range errors determines which transfer format will have the smaller errors.

Offset Target Transfer

In what is probably the most straightforward data transfer format, an "offset" target is computed at the reference receiver by simply adding the surveyed RTL vector to the GPS coordinates currently being read from the reference receiver. The active receiver is guided such that its GPS solution is equal to this "offset" target. The error-on-target using this method can be computed by simply adding up the vectors in the diagram.

$$\varepsilon = r_{A,true} - r_{T,true}$$

From the diagram it is seen that the vector $r_{T,true}$ is equal to $r_{R,true}$ plus the true relative target location vector, RTL_{true}. The vectors which lead from the reference receiver to the active receiver are the GPS error at the reference receiver plus the surveyed RTL vector minus the GPS error at the active receiver. In equation form this is:

$$\begin{aligned} r_{T,true} &= r_{R,true} + RTL_{true} \\ r_{A,true} &= r_{R,true} + \delta r_{R,GPS} \\ &+ RTL_{survey} - \delta r_{A,GPS} \end{aligned}$$

and the difference, ε, is:

$$\begin{aligned} \varepsilon &= \delta r_{R,GPS} + RTL_{survey} \\ &- \delta r_{A,GPS} - RTL_{true} \end{aligned}$$

A regrouping of terms yields:

$$\begin{aligned} \varepsilon &= \delta r_{R,GPS} - \delta r_{A,GPS} \\ &+ RTL_{survey} - RTL_{true} \end{aligned} \qquad \text{(A-1)}$$

The first two terms are the results of the GPS pseudo-range biases at the reference and active receivers. (Other error contributors exist, noise and multipath for example, but they are not included in this analysis). The two terms on the second line are the relative survey error.

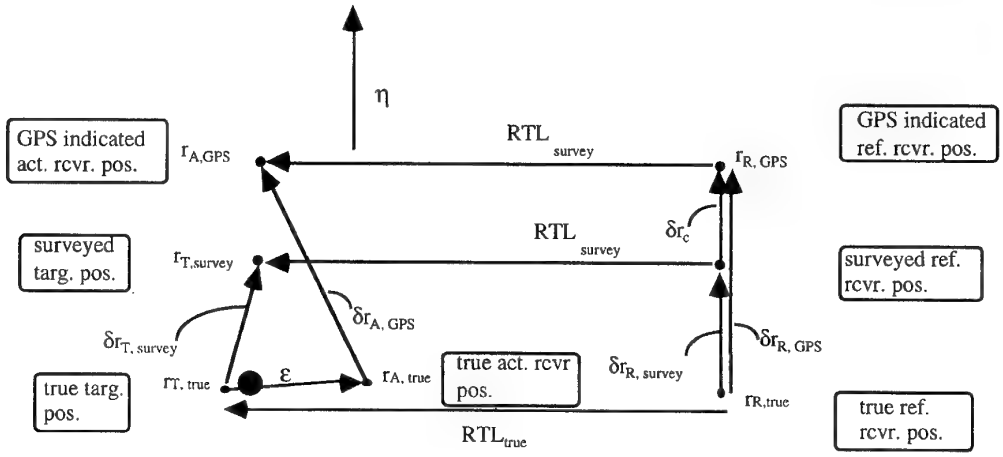

Figure A-1. The Effect of GPS Errors and Survey Errors on the Error on Target

To be consistent with the remaining analysis, this expression will be rewritten. The GPS position differences will be expressed as functions of the pseudo-range biases, the actual "source" of the error. The survey error will be expressed in terms of surveying errors at the target and reference receiver locations.

The first term on the right in the next equation simply indicates that the GPS position solution at the reference receiver is a function of the true pseudoranges and the biases in the pseudoranges at the reference receiver, $\delta\rho_{R,GPS}$.

$$\begin{aligned}\delta r_{R,GPS} &= r_{R,GPS}(\rho_{true}+\delta\rho_{R,GPS}) \\ &- r_{true}\end{aligned}$$

Expanding the function relationship to first order yields:

$$\begin{aligned}\delta r_{R,GPS} &= r_{true}+[\partial r/\partial\rho]_R\,\delta\rho_{R,GPS} \\ &- r_{true} \\ \delta r_{R,GPS} &= [\partial r/\partial\rho]_R\,\delta\rho_{R,GPS}\end{aligned}$$

The term in brackets is the Jacobean or total derivative of the position vector, r, with respect to pseudo-ranges, ρ, that is, it is a matrix of partial derivatives relating deviations in pseudo-range to deviations in position. (Note that the vector "r" includes the user clock component bias.) The subscript on the matrix indicates where the derivative was taken, at the reference receiver in this case.

Similarly, the expression for the GPS error at the active receiver can be written:

$$\delta r_{A,GPS} = [\partial r/\partial\rho]_A\,\delta\rho_{A,GPS}$$

Now the expression for the surveyed RTL vector can be written in terms of survey error at each location:

$$\begin{aligned}RTL_{survey} &= r_{T,survey} - r_{R,survey} \\ RTL_{survey} &= r_{T,true}+\delta r_{T,survey} \\ &\quad -r_{T,true}-\delta r_{R,survey}\end{aligned}$$

The first and third terms comprise the true RTL vector and the second and fourth comprise the relative survey error

$$\begin{aligned}RTL_{survey} &= RTL_{true} \\ &+ \delta r_{T,survey}-\delta r_{R,survey}\end{aligned}$$

Using these expressions for GPS and survey errors the expression for error-on-target can be rewritten. For convenience, define matrices $H_R=[\partial\rho/\partial r]_R$ and $H_A=[\partial\rho/\partial r]_A$. Further define the inverses (or pseudo-inverses if more than four satellites are being tracked) as $H_R^{\#}=[\partial r/\partial\rho]_R$ and $H_A^{\#}=[\partial r/\partial\rho]_A$.

$$\begin{aligned}\varepsilon &= H_R^{\#}\delta\rho_{R,GPS}-H_A^{\#}\delta\rho_{A,GPS} \\ &+ RTL_{true}+\delta r_{T,survey}-\delta r_{R,survey} \\ &- RTL_{true} \\ \varepsilon &= H_R^{\#}\delta\rho_{R,GPS}-H_A^{\#}\delta\rho_{A,GPS} \\ &+ \delta r_{T,survey}-\delta r_{R,survey} \qquad (A-2)\end{aligned}$$

Position Offset Transfer

The second format for transmitting compensation for surveying and GPS errors is to send a position correction from the reference receiver to the active receiver.

The position corrections are simply the difference between the GPS solution at the reference receiver and the surveyed location of the reference receiver. (We must always use surveyed locations since the true locations can never be known.) We emphasize that these survey errors do not have to be small. They can be on the order of hundreds of feet. This opens up many possibilities for quick surveys; there is no need to average GPS positions for two days or to call in the astronomical survey team.

The correction, δr_c, using the terminology in Fig. A-1, is:

$$\delta r_c = r_{R,GPS} - r_{R,survey}$$

Alternatively the two terms in this expression can be expanded in terms of the true reference receiver position and the survey and GPS errors. One can anticipate this result by simply looking at the error vectors for the reference receiver in Fig. A-1.

$$\delta r_c = \delta r_{R,GPS} - \delta r_{R,survey}$$

The position deviation can be expressed in terms of pseudo-range biases using the Jacobean, $H_R^{\#}$.

$$\delta r_c = H_R^{\#}\delta\rho_{R,GPS} - \delta r_{R,survey} \qquad (A-3)$$

This bias will be subtracted from the position solution of the active receiver.

In the third alternative, pseudo-range biases will be transmitted from the reference receiver to the active receiver. In anticipation of this an expression for these biases will be given now. The pseudo-range biases are also based on the difference between the GPS position solution and the surveyed receiver location. To first order they are:

$$\begin{aligned}\delta\rho_c &= H_R\delta r_c \\ \delta\rho_c &= H_R H_R^{\#}\delta\rho_{R,GPS} - H_R\delta r_{R,survey} \\ \delta\rho_c &= \delta\rho_{R,GPS} - H_R\delta r_{R,survey} \qquad (A-4)\end{aligned}$$

This bias will be subtracted from the pseudo-ranges at the active receiver before the position solution is computed.

Regardless of the correction method the active receiver is guided such that its corrected solution is driven to the surveyed target coordinates. The error-on-target is defined, as before, to be the difference between the true active receiver location and the true target location.

$$\varepsilon = r_{A,true} - r_{T,true}$$

This expression will be evaluated first for transfer of position corrections, δr_c, then for the transfer of pseudo-range biases, $\delta\rho_c$.

We will now proceed with the use of position corrections. The guidance constraint, that the corrected solution is driven to the surveyed target coordinates, is expressed below.

$$r_{A,c} = r_{T,survey}$$

$$r(\rho_A) - \delta r_c = r_{T,survey}$$

The pseudo-ranges at the active receiver, ρ_A, and the survey target position may both be expanded into true values plus errors.

$$\rho_A = \rho_{A,true} + \delta\rho_{A,GPS}$$

$$r_{T,survey} = r_{T,true} + \delta r_{T,survey}$$

Substituting for these expressions for ρ_A and $r_{T,survey}$ yields:

$$r(\rho_{A,true} + \delta\rho_{A,GPS}) - \delta r_c = r_{T,true} + \delta r_{T,survey}$$

A first-order expansion of the function on the left side of the equation yields:

$$r_{A,true} + H_A^{\#}\delta\rho_{A,GPS} - \delta r_c = r_{T,true} + \delta r_{T,survey}$$

Rearranging terms yields:

$$r_{A,true} - r_{T,true} = \delta r_{T,survey} - H_A^{\#}\delta\rho_{A,GPS} + \delta r_c$$

The two terms on the left side of the equation are recognized as the error-on-target and the expression for δr_c, Eq. A-3, can be substituted on the right side of this equation. The result is:

$$\varepsilon = \delta r_{T,survey} - H_A^{\#}\delta\rho_{A,GPS} + H_R^{\#}\delta\rho_{R,GPS} - \delta r_{R,survey}$$

Simply reordering terms yields the expression for error-on-target when using position corrections.

$$\varepsilon = H_R^{\#}\delta\rho_{R,GPS} - H_A^{\#}\delta\rho_{A,GPS} + \delta r_{T,survey} - \delta r_{R,survey} \qquad \text{(A-5)}$$

Pseudo-Range Bias Transfer

Finally, a similar analysis for the use of pseudo-range biases will be given. Starting from the same point, the guidance constraint is:

$$r_{A,c} = r_{T,survey}$$

$$r(\rho_A - \delta\rho_c) = r_{T,survey}$$

where the function $r(\rho_A - \delta\rho_c)$ represents the corrected solution at the active receiver.

The pseudo-ranges at the active receiver, ρ_A, and the survey target position may both be expanded into true values plus errors.

$$\rho_A = \rho_{A,true} + \delta\rho_{A,GPS}$$

$$r_{T,survey} = r_{T,true} + \delta r_{T,survey}$$

Again substituting these expressions for ρ_A and $r_{T,survey}$ yields:

$$r(\rho_{A,true} + \delta\rho_{A,GPS} - \delta\rho_c) = r_{T,true} + \delta r_{T,survey}$$

A first order expansion of the function on the left side of the equation yields:

$$r_{A,true} + H_A^{\#}(\delta\rho_{A,GPS} - \delta\rho_c) = r_{T,true} + \delta r_{T,survey}$$

Rearranging terms yields:

$$r_{A,true} - r_{T,true} = \delta r_{T,survey} - H_A^{\#}(\delta\rho_{A,GPS} - \delta\rho_c)$$

The two terms on the left side of the equation are recognized as the error-on-target and the expression for $\delta\rho_c$, Eq A-4, can be substituted on the right side of this equation. The result is:

$$\varepsilon = \delta r_{T,survey} - H_A^{\#}(\delta\rho_{A,GPS} - \delta\rho_{R,GPS} + H_R^{\#}\delta r_{R,survey})$$

Multiplying through and rearranging terms yields:

$$\varepsilon = \delta r_{T,survey} - H_A^{\#}H_R\delta r_{R,survey} + H_A^{\#}(\delta\rho_{R,GPS} - \delta\rho_{A,GPS}) \qquad \text{(A-6)}$$

So the error is seen to consist of a relative surveying error and a difference in GPS bias errors.

Transfer Format Comparison

For convenience, the expressions for error-on-target for the three data transfer formats: transfer of target coordinates, transfer of target position corrections and transfer of pseudo-range corrections, are listed together.

$$\varepsilon = H_R^{\#}\delta\rho_{R,GPS} - H_A^{\#}\delta\rho_{A,GPS} + \delta r_{T,survey} - \delta r_{R,survey} \quad \text{(A-2)}$$

$$\varepsilon = H_R^{\#}\delta\rho_{R,GPS} - H_A^{\#}\delta\rho_{A,GPS} + \delta r_{T,survey} - \delta r_{R,survey} \quad \text{(A-5)}$$

$$\varepsilon = \delta r_{T,survey} - H_A^{\#}H_R\delta r_{R,survey} + H_R^{\#}(\delta\rho_{R,GPS} - \delta\rho_{A,GPS}) \quad \text{(A-6)}$$

The errors in transfer of target coordinates and transfer of target position corrections are identical as would be expected. Note that for the transfer of pseudo-range corrections, Eq. A-6, the relative survey error is sensitive to the separation between the reference receiver and the target/active receiver. The sensitive term is:

$$\delta r_{T,survey} - H_A^{\#}H_R\delta r_{R,survey} \quad \text{(A-7)}$$

The product $H_A^{\#}H_R$ would be identity if the reference receiver were collocated with the active receiver. It is non-identical for receiver separation and if a different set of satellites is used at the two receivers. For the transfer of position corrections, Eq. A-5, the term that is sensitive to receiver separation is the differential (GPS) bias term. That term is:

$$H_R^{\#}\ \delta\rho_{R,GPS} - H_A^{\#}\ \delta\rho_{A,GPS}$$

This deviation in position space can be mapped into pseudo-range space by pre-multiplying by H_R.

$$\delta\rho_{R,GPS} - H_R H_A^{\#}\delta\rho_{A,GPS} \quad \text{(A-8)}$$

Comparison of Eq's A-7 and A-8 emphasizes the symmetry between the two error types. These results might suggest that if the survey error is expected to be dominant, then position corrections should be transferred. If the pseudo-range biases are expected to be dominant, then pseudo-range biases should be transferred. The importance of these effects is assessed by Fikes in Ref. 13.

Summary

In summary we have 1) distinguished between DGPS and RGPS, stating that RGPS recognizes and controls the relative surveying error between reference receiver and target, whereas DGPS simply assumes that the reference receiver is at a known location, and 2) shown that there are first order errors in both types of transfer which depend on receiver separation and satellite selection.

ACKNOWLEDGMENTS

The authors wish to thank Ms. Dianne Bennett for preparing this paper for publication.

REFERENCES

[1] National Research Council, "The Global Positioning System, A Shared National Asset," *National Academy Press,* Washington, D.C., 1995.

[2] Mullen, F., Fink, B., and Setterlund, R., "Verification of Relative GPS Targeting Concept," *Proceedings of the 22nd Joint Services Data Exchange,* Scottsdale, AZ, October 1994, Section 5A.

[3] Bierman, G., "Error Modeling for Differential GPS," Draper Laboratory Report, T-1241, Cambridge, MA, May 1995.

[4] Ebner, R. and Rickords, T., "The Status of the Global Positioning System Guidance Package," *Proceedings of the 22nd Joint Services Data Exchange,* Scottsdale, AZ, October 1994.

[5] Hattis, P., and Benney, R., "Demonstration of Precision Guided Ram-Air Parafoil Airdrop Using GPS/INS Navigation," *Proceedings of the Institute of Navigation 52nd Annual Meeting,* Cambridge, MA, June 1996.

[6] Gustafson, D., et.al., "A Micromechanical INS/GPS System for Guided Projectiles," *Proceedings of the Institute of Navigation 52nd Annual Meeting,* Cambridge, MA, June 1996.

[7] Dowdle, J., et.al., "An Integrated GPS/Micro-Mechanical IMU for 5" Navy Shells," *Proceedings of the Institute of Navigation 52nd Annual Meeting,* Cambridge, MA, June 1996.

[8] Weinberg, M., et.al., "A Micromachined Comb Drive Tuning Fork Rate Gyroscope," Draper Laboratory, *Proceedings of the Institute Of Navigation 49th Annual Meeting,* June 1993.

[9] Sitomer, J., and Connelly, J., "High Dynamic-Range Microdynamic Accelerometer Technology," Draper Laboratory, *Proceedings of the Institute of Navigation 49th Annual Meeting,* June 1993.

[10] Hopkins, R., et.al., "Micromechanical Sensors for Kinetic Energy Projectile Test and Evaluation," *U. S. Army TECOM Test Technology Symposium VII,* March 29-31, 1994.

[11] Weinberg, M., et.al., "A Micromechanical Comb Drive Tuning Fork Gyroscope for Commercial Applications," Draper Laboratory, *Sensors Expo,* September 20-22, 1994.

[12] Youhanaie, M., et.al., "Robust Implementation of Relative GPS Guidance," *Proceedings of the ION/GPS 95,* Palm Springs, CA, Sept. 1995.

[13] Dowdle, J., et.al., "GPS Anti-Jam Enhancement Techniques," *Proceedings of the Institute of Navigation 49th Annual Meeting,* June 1993.

[14] Fikes, M., "Relative Targeting with Differential GPS and Associated Error Mechanisms," to be published in the Journal of the Institute of Navigation, *Navigation.*

Requirements on GNSS For Civil Navigation

F. van Graas
Avionics Engineering Center
School of Electrical Engineering and Computer Science
361 Stocker Center
Ohio University
Athens, Ohio 45701
USA

1. SUMMARY

The Civil Aviation Community has had decades of experience in regulating the quality of land-based navigation aids and developing the procedures for their use that guarantee safe operation. The drafting of these principles and procedures into standards for satellite-based navigation aids has now been underway for more than a decade. This lecture will trace the evolution towards internationally-accepted definitions of "required navigation performance", including accuracy, integrity, continuity, and availability considerations. Inasmuch as this is an on-going activity, the lecture will include a road map for the completion of actions that are underway.

2. BACKGROUND

The most common method to indicate required navigation capability for a specific route is to specify carriage of certain equipment (Ref 1). With the development of integrated navigation aids and the introduction of new navigation aids, it is difficult to specify particular equipment required for a certain route without constraining the effective application of new technology. To address this problem, the International Civil Aviation Organization (ICAO) established the Special Committee on Future Air Navigation Systems (FANS), in 1983. The FANS committee developed the concept of required navigation performance capability (RNPC). RNPC was defined as "a parameter describing lateral deviations from assigned or selected track as well as along track position fixing accuracy on the basis of an appropriate containment level" (Ref 1).

ICAO approved the RNPC concept and assigned the concept to the Review of the General Concept of Separation Panel (RGCSP) for further development. The RGCSP modified RNPC to required navigation performance (RNP) noting that capability and performance are two different parameters. The RGCSP also noted that airspace planning is dependent on measured performance, rather than a designed capability. Therefore, the RNP must be a statement of the navigation performance accuracy within a defined airspace. This led to the following definition of RNP (Ref 2).

> RNP (as defined in the ICAO Manual on Required Navigation Performance): A statement of the navigation performance accuracy necessary for operation within a defined airspace.

A specific type of RNP is intended to define the navigation performance of users within the airspace commensurate with the navigation capability of the airspace. As such, RNP types are identified by a single accuracy value. Although the RGCSP definition of RNP only includes accuracy, (Ref 2) also states the following with respect to other requirements:

> While the navigation performance accuracy is the basis for defining an RNP type, the other navigation performance parameters of availability, coverage, reliability, fix rate, fix dimension, capacity, time to recover and integrity determine the utilization and limitations of the individual navigation systems, both ground and airborne, and characterize the means by which a user derives navigation information within an RNP type airspace, as described in Appendix C. Numerical values for these parameters will be quantified by the appropriate technical bodies.

These additional parameters were taken into account by RTCA Special Committee 181 and EUROCAE Working Group 13 in the development of Minimum Aviation System Performance Standards (MASPS): RNP for Area Navigation (Ref 3).

To include approach, landing and departure phases of flight, an extension of the RNP was required. In 1993, the Air Navigation Commission (ANC) of ICAO tasked the All Weather Operations Panel (AWOP) to consider such an extension. AWOP extended the RNP concept by including integrity, continuity and availability in addition to lateral and vertical deviation containments and defined RNP as follows.

> RNP (as defined by AWOP): A statement of the navigation performance accuracy, integrity, continuity and availability necessary for operation within a defined airspace.

This AWOP RNP concept was accepted by the Special Communications/ Operations Divisional Meeting (1995), and AWOP was tasked to further develop the concept and to determine the feasibility of RNP for approach, landing and departure operations (Ref 4).

RNP defines the airspace system and not the carriage of specified equipment for air navigation. This allows an aircraft flexibility in the carriage of equipment to satisfy the airspace requirements (Ref 5). RNP, however, is only one of the factors required to arrive at an acceptable target level of safety (TLS). Other factors include air traffic density, surveillance, communications, and air traffic control. In general, RNP represents the requirements at the highest level. Lower-level

Paper presented at the AGARD MSP Lecture Series on "System Implications and Innovative Applications of Satellite Navigation", held in Paris, France from 1-2 July 1996; Rome, Italy from 4-5 July 1996; Madrid, Spain from 8-9 July 1996 and St. Petersburg, Russia from 11-12 July 1996, and published in LS-207.

implementation and certification requirements are also needed, including Standards and Recommended Practices (SARPS) and aircraft system specifications. SARPS specify the signals-in-space for all radiating systems to ensure a consistent interpretation of these signals for the use in navigation transmitters and receivers.

The next section presents the application of the RNP concept to en-route airspace, followed by a section on approach, landing and departure operations using the RNP concept.

3. RNP FOR EN-ROUTE APPLICATIONS

3.1 ICAO RNP

The RGCSP of ICAO specified RNP airspace types by a single parameter, which is the 95% containment value in the horizontal plane. The containment value is the distance from the intended position within which flights would be found for at least 95% of the time. Currently, four RNP types are defined by the 95% containment value in nautical miles: RNP 1; RNP 4; RNP 12.6; RNP 20.

It is emphasized that RNP is only one of the factors required to arrive at an acceptable target level of safety (TLS). Other factors include air traffic density, surveillance, communications, and air traffic control. To implement the RNP concept, many other parameters must be specified as well. The next section shows an example of this process for Area Navigation within a RNP environment.

3.2 RTCA SC-181/EUROCAE WG-13 RNP

A joint committee was created in 1994 by RTCA Inc. and EUROCAE to develop Minimum Aviation System Performance Standards (MASPS) for airborne navigation systems operating in a RNP environment. The MASPS are intended to provide tools to the service providers, vendors and users of the airspace to develop the airspace and operational procedures needed to implement CNS/ATM. ICAO developed the Communications Navigation Surveillance/Air Traffic Management (CNS/ATM) concept to increase airspace efficiency while maintaining or improving current levels of safety. The joint committee consisting of RTCA Special Committee 181 and EUROCAE Working Group 13, started with the ICAO RNP definition from the Manual on Required Navigation Performance (Ref 2) and modified this definition to accommodate additional requirements (Ref 3).

> RNP RNAV (MASPS): A statement of the navigation performance accuracy necessary for operation within a defined airspace. Note that there are additional requirements, beyond accuracy, applied to a particular RNP type.

The term RNAV was added to indicate Area Navigation functional and performance requirements. Also, one RNP type was added to specify accuracies better than 1 nmi, the so-called RNP < 1 RNAV. Several assumptions are listed in the RTCA RNP RNAV document for the purpose of defining the airborne equipment, including (Ref 3)

1. Path Definition;
2. Path Steering (position and time);
3. Lateral Steering;
4. User Interface (controls, displays, alerts, reporting, navigation systems controls and features).

Most of these assumptions are specifically to address Area Navigation, such that all aircraft will have *predictable and repeatable ground tracks*. Furthermore, these assumptions will allow for the integration of RNP with Area Navigation.

In addition to the Area Navigation requirements, the committee also expanded the definition of the term containment to include containment integrity, containment continuity, and containment region. Figure 1 shows the cross-track containment parameters.

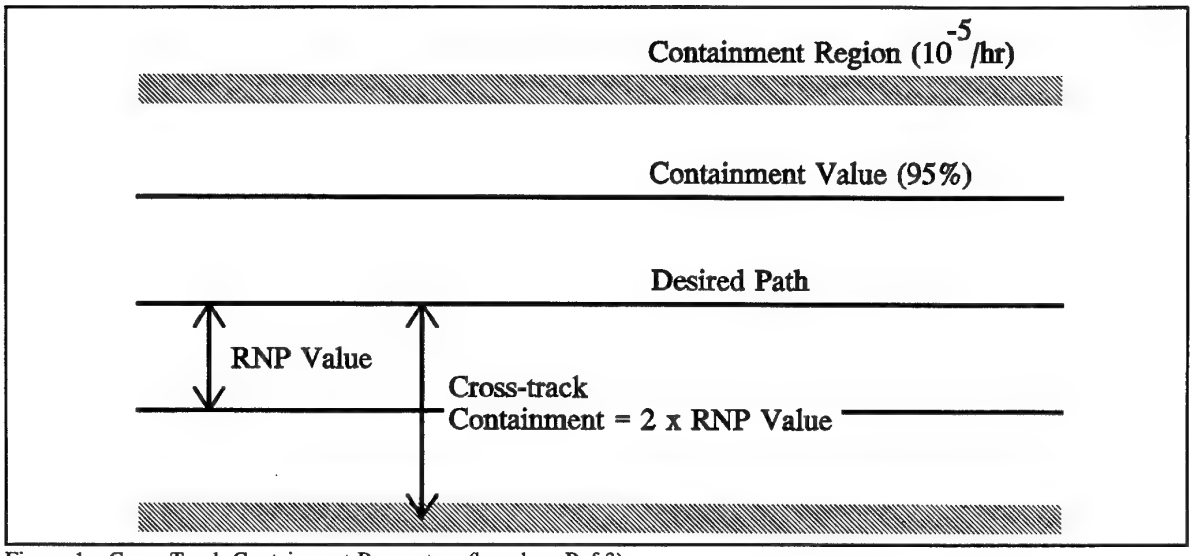

Figure 1. Cross-Track Containment Parameters (based on Ref 3)

Containment Integrity. A measure of confidence in the estimated position. This is expressed as the probability that the system will detect and enunciate the condition where the total system error (TSE) is greater than the cross track containment limit. The containment integrity risk represents the case where TSE is greater than the containment limit and no alert is provided to the pilot. Containment integrity risk shall be less than 10^{-5} per flight hour.

Containment Continuity. A measure of the expected uninterrupted operation time for the navigation system. This is expressed as the probability of maintaining the required containment integrity without interruption. Interruption in operation can be caused by a false alert or by true system failures. The containment continuity risk represents the case where an interruption exists, which shall be less than 10^{-4} per hour.

Containment Region. A region, centered on the desired path, to which the containment integrity and containment continuity are referenced. Currently, the cross-track containment is specified as twice the RNP 95% containment value.

Operational benefits from the RNAV RNP can be derived in several areas, including (Ref 3)

1. Reduced Separation Minima. The combination of path definition, position estimation and containment requirements will assist in the design of airspace that will allow for the most effective use of aircraft and ground-based equipment.

2. Advanced Monitoring and Surveillance Techniques. The containment requirements in combination with a downlink of aircraft position data will allow for the use of automatic dependent surveillance in areas where no ground-based surveillance is available. This will allow for reductions in air traffic separation and a resulting increase in airspace capacity.

3. User-Preferred Trajectories. The path definition and steering concepts defined in the MASPS may be used to predict aircraft ground tracks in support of conflict probing and detection, which is an important element for the implementation of user-preferred trajectories.

4. RNP FOR APPROACH, LANDING AND DEPARTURE

4.1 AWOP Provisional RNP Definitions

The All-Weather Operations Panel (AWOP) of ICAO is in the process of applying the RNP concept to approach, landing and departure operations. To facilitate this process, AWOP developed provisional definitions of the four RNP parameters:

Accuracy is the ability of the total system to maintain the aircraft position within a total system error (TSE) limit, with a 95% probability at each point along the specified procedure, and to keep it within an outer performance boundary with a probability of no less than $1 - 10^{-7}$ per approach.

The TSE is based on a combination of navigation system error (NSE) and flight technical error (FTE). The NSE includes source signal-in-space, airborne processing and airborne computation error components. The components of TSE are shown in Figure 2.

Integrity relates to the trust which can be placed in the correctness of the information supplied by the total system. Integrity includes the ability of a system to provide timely and valid warnings to the user then the system must not be used for the intended operation. Integrity risk is the probability of an undetected failure which will result in a loss of the specified accuracy.

Continuity is the ability of the total system to perform its function without interruption during the intended operation.

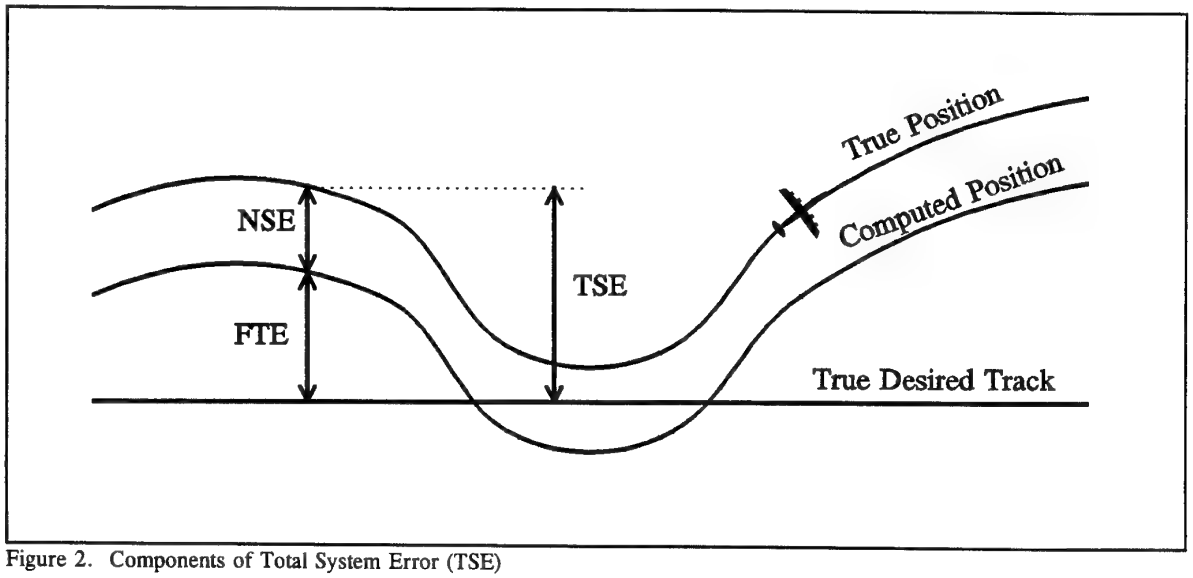

Figure 2. Components of Total System Error (TSE)

Continuity risk is the probability that the system will be interrupted and not provide guidance information for the intended operation.

Availability is the ability of the total system to perform its function at the initiation of the intended operation. Availability risk is the probability that the required guidance will not be present at the initiation of the intended operation.

Again, it is noted that the RNP concept does not specify all parameters required for a successful landing operation. For example, an aircraft must be stabilized on the final approach prior to the decision height or runway threshold crossing, which characteristic is not addressed by the RNP parameters.

4.2 Target Level of Safety and Containment Surfaces

To allocate a risk budget for the RNP, AWOP used a Target Level of Safety (TLS). Figure 3 shows the RNP risk allocation (Ref 6). In the risk tree, parallel boxes represent an addition of risks and serial boxes represent a multiplication of risks. The TLS is based on an analysis of historical loss-of-aircraft records. A TLS of 10^{-8} per approach was proposed for the approach and landing phases of flight. This TLS is a factor of 25 better than that reflected by the historical data. This improvement was deemed necessary if the total number of accidents per year are not to be increased under conditions of increasing air transportation.

Each approach and landing has an associated flight path and containment surfaces to assure a successful landing. Two containment surfaces are used: the inner containment surface and the outer containment surface. The inner containment surface specifies the 95 percent aircraft lateral and vertical deviations about the desired flight path, while the outer containment surface should contain the aircraft flight path with a high probability consistent with the TLS. Figure 4 illustrates the inner and outer containment surfaces (Ref 6).

Following Figure 3, not every containment surface incident will result in a loss-of-aircraft. Therefore, for the approach phase of flight, the accident/incident ratio is 1 in 10. For the landing phase of flight, however, the accident/incident ratio is taken to be 1 in 1. Next, the RNP risks are assigned to the aircraft and the non-aircraft sub-systems to ensure that the system design will satisfy the TLS and the containment surface incident probability.

4.3 Category I RNP

The allocation of the RNP risk parameters to aircraft and non-aircraft sub-systems allows for the design of the approach and landing system. Once the sub-system risk allocations are known, these requirements translate into specifications for error budgets, monitor alarm thresholds, equipment redundancy, and many other design elements.

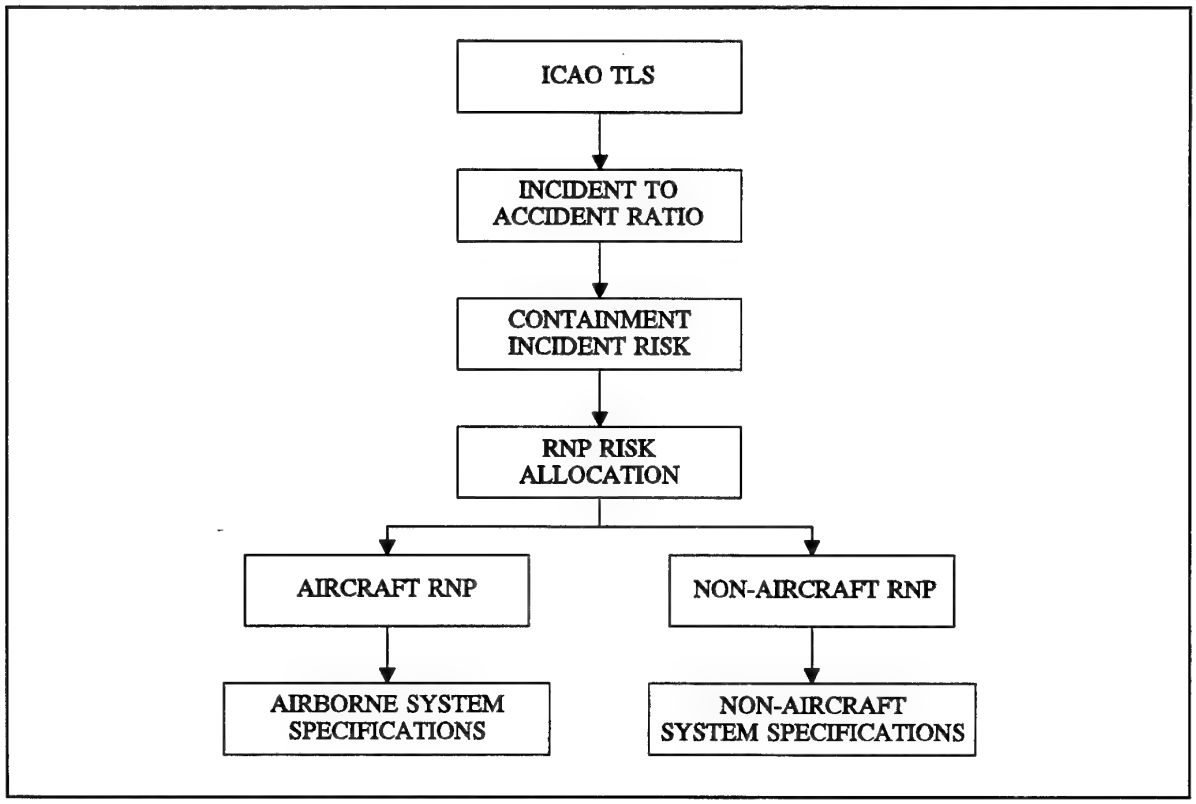

Figure 3. RNP Risk Allocation (based on Ref 6)

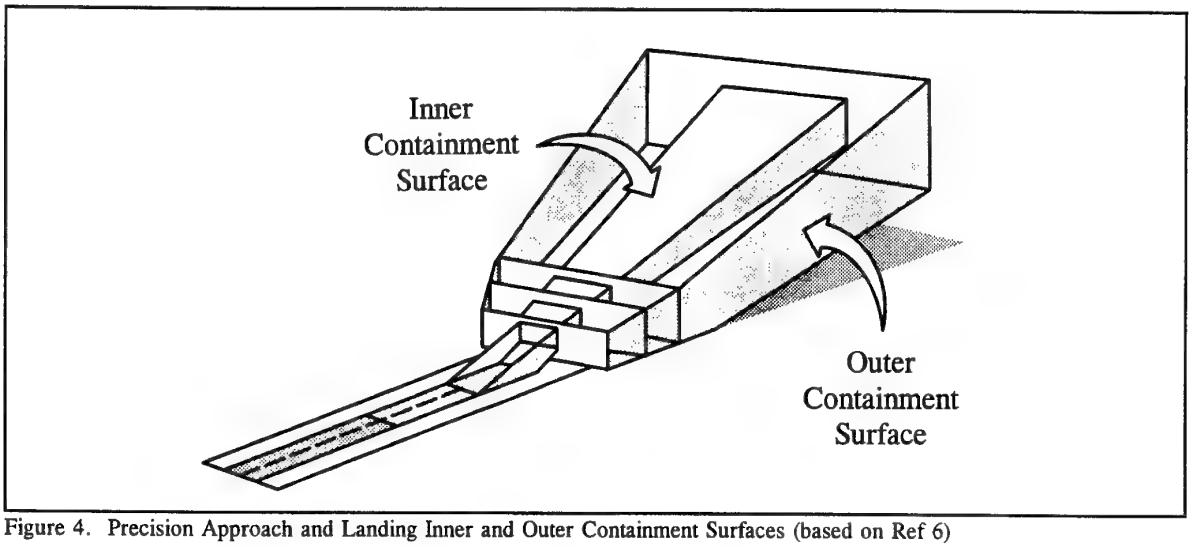

Figure 4. Precision Approach and Landing Inner and Outer Containment Surfaces (based on Ref 6)

Figure 5 shows the RNP risk allocation for a Category I (CAT I) approach (Ref 6). The CAT I RNP defines operations from the final approach fix (FAF) to a 200 ft decision height (DH). The CAT I RNP is intended for manual flown approaches with improved cockpit displays. Containment surface incidences are calculated on a per approach basis, where the exposure time for each approach is assumed to be 150 seconds. The containment surface incident risk is equally divided among continuity, accuracy, and integrity incident risks. Pilot missed detection could result from a hardware

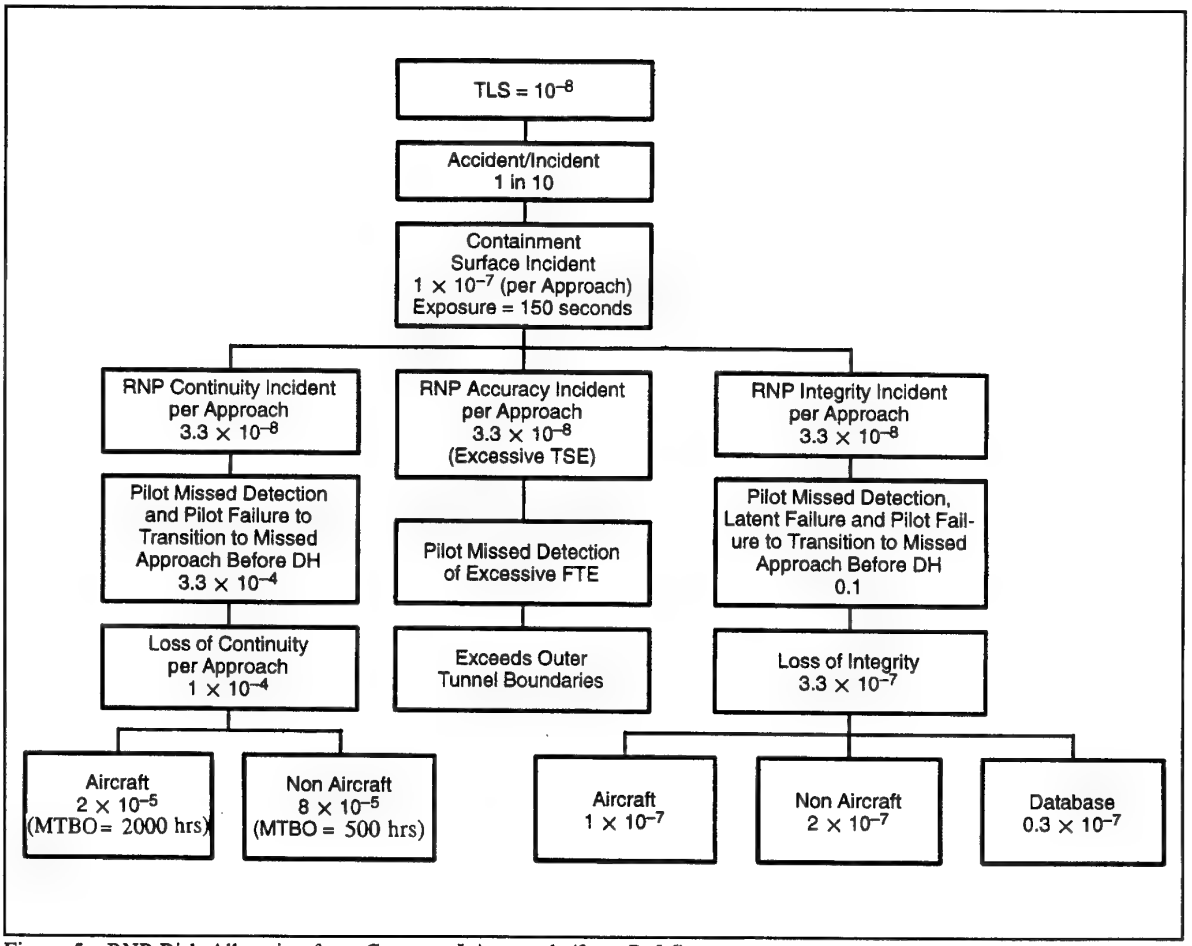

Figure 5. RNP Risk Allocation for a Category I Approach (from Ref 6)

monitor failure or from a piloting failure, where piloting failures can be attributed to inadequate training, fatigue or excessive workload.

Figure 6 shows the CAT I RNP inner and outer containment surfaces as well as provisional numbers for continuity, integrity and availability. In the tables, GPIP refers to the glide path intercept point with the runway; HAT is the height above threshold; and FAF is the final approach fix. The inner containment surface is derived from the ICAO collision risk model TSE standard deviation. The outer containment surface dimensions are equal to three times the inner containment surface dimensions.

4.4 Category III RNP

For comparison with the CAT I approach, Figure 7 shows the CAT III RNP risk allocation and Figure 8 shows the CAT II/III inner and outer containment surfaces. The CAT III RNP is intended for flight director aided manual approaches to 100 ft DH and autopilot flight to touchdown. The CAT II landing also includes a roll-out portion, which is defined to be the period of time from TD to where the aircraft has decelerated to a velocity of 60 kt or less. Note that the accident to incident ratio is 1 in 1: pilot intervention can not be used in the risk allocation because the aircraft is close to the touchdown point such all the risk must reside in the landing guidance equipment.

It is also noted that the provisional containment requirements are based on the performance of current approach and landing systems (i.e. ILS and MLS). Due to the angular nature of these systems, the requirements are also specified in angular terms. The main effect of angular specifications is that the requirements are most stringent at the decision height (DH). It is not clear at this time if linear requirements can be used which are less stringent than angular requirements at the DH.

5. RNP CONSIDERATIONS AND DEVELOPMENTS

The MASPS for RNP RNAV are scheduled to be approved by RTCA in mid-1996. RTCA Special Committee 181 in conjunction with EUROCAE WG-13 will then continue to expand the MASPS to also include vertical (3D) and longitudinal requirements, including time (4D).

In 1993, the Air Navigation Commission of ICAO established the GNSS Panel (GNSSP) to develop the technical and performance requirements for GNSS and its interoperability with other systems. The GNSSP work programme includes Operational Issues (Working Group A), GNSS SARPs (WG-B), Long Term GNSS (WG-C), and Data Broadcast (WG-D). WG-A is specifically tasked to address system performance requirements for GNSS and to develop proposals on operational approval, certification and other aspects of GNSS introduction. System performance requirements are to be developed in consolidation with AWOP, RTCA SC-181 and EUROCAE WG-13. The development of GNSS SARPs by WG-B is required to maintain interoperability and safety.

The AWOP work programme, to be completed in 1996, includes the assessment and development of appropriate

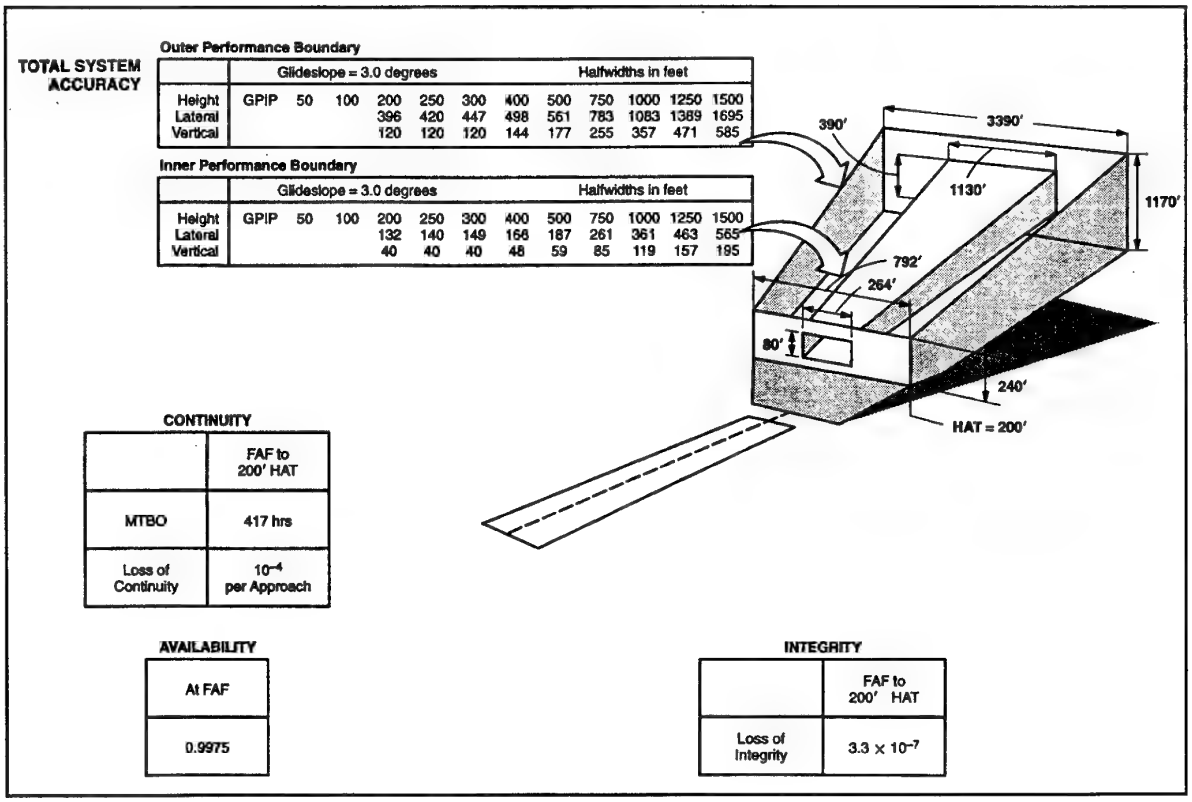

Figure 6. RNP CAT I for Precision Approach and Landing (from Ref 6)

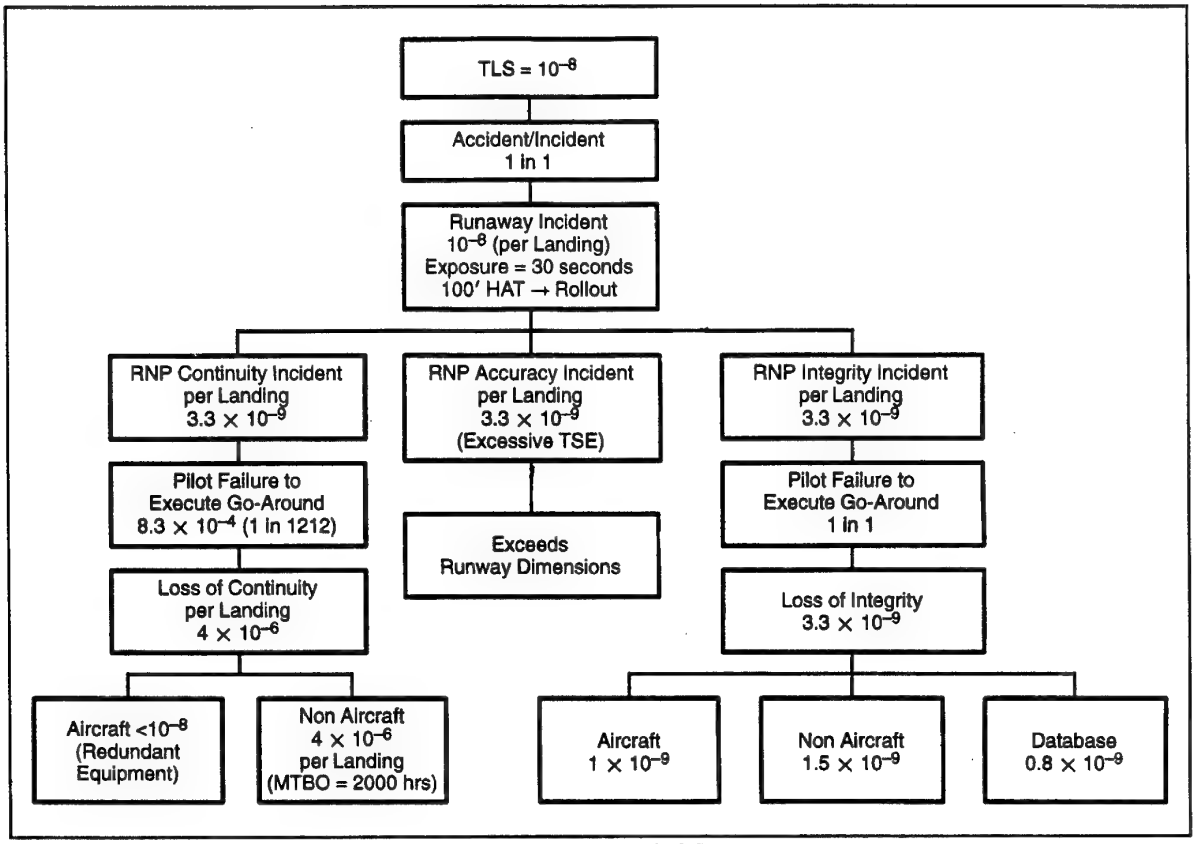

Figure 7. RNP Risk Allocation for a Category III Approach (from Ref 6)

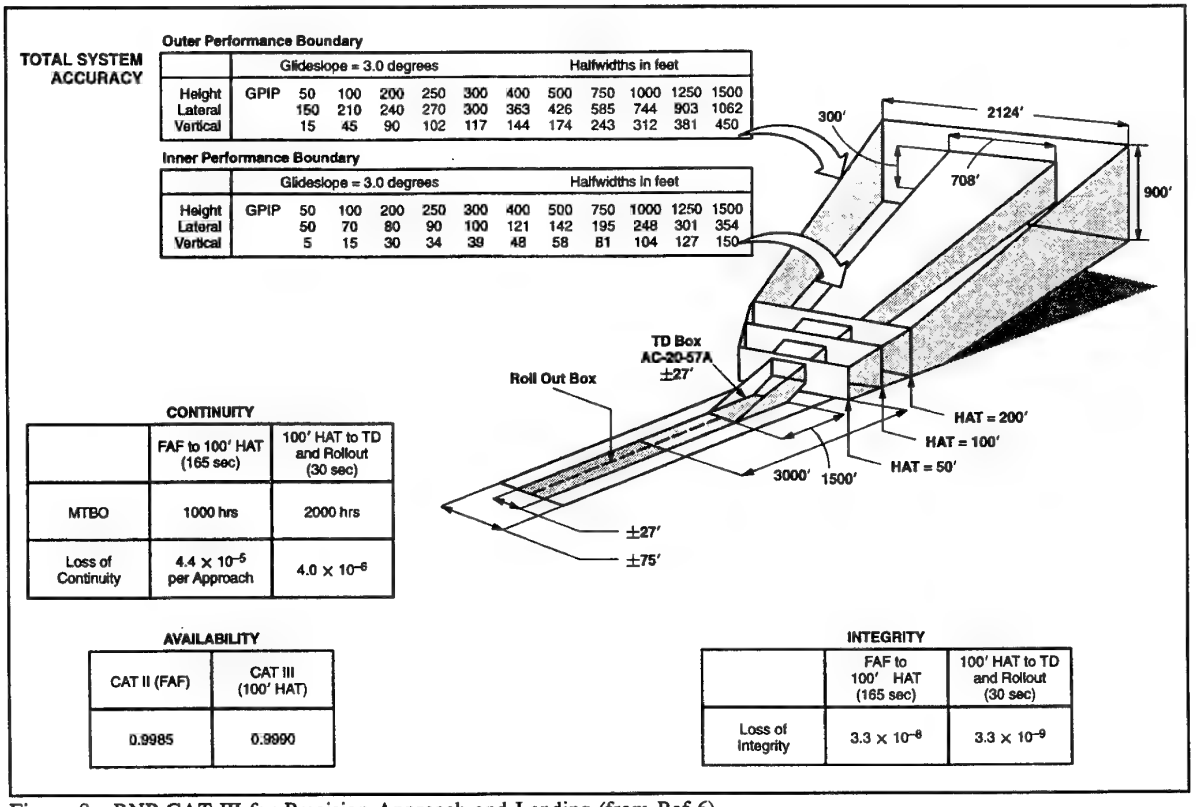

Figure 8. RNP CAT III for Precision Approach and Landing (from Ref 6)

recommendations on extension of the RNP concept to include approach, landing and departure operations (Ref 7). AWOP is currently considering several proposed changes to the RNP concept, including

- Incorporate accuracy risk in integrity and continuity risk, since there are only two scenarios in which an aircraft would violate the containment region:
  - In the presence of a detected failure, which is a loss of continuity;
  - In the presence of an undetected failure, which is a loss of integrity.
- Require system monitors and warnings to ensure compliance with the outer containment boundary.
- Allow for the use of linear RNPs in addition to the angular RNP.

With respect to RNP for precision approach, landing and departure operations, it is emphasized that the RNP alone does not guarantee a safe and acceptable landing. Many other factors must be taken into consideration, including pilot acceptance factors, air traffic density, surveillance, communications, air traffic control, aircraft stabilization, non-navigation system failures (such as hydraulic or engine failures). RNP could, however, be the main high-level requirement to determine aircraft and obstacle separation standards in the absence of failures.

6. REFERENCES

1. Summary of The Proposed Required Navigation Performance (RNP) Concept for Approach, Landing and Departure Operations, ICAO Secretariat, Special Communications/Operations Divisional Meeting (1995), Working Paper 10, Montreal, Canada, 27 March - 7 April 1995.

2. Manual on Required Navigation Performance, ICAO Document 9613-AN/937, Montreal, Canada.

3. Minimum Aviation System Performance Standards: Required Navigation Performance for Area Navigation, Final Draft, RTCA, Inc., Paper No. 097-96/SC181-060, Washington, D.C., 4 March 1996.

4. Report of the Special Communications/Operations Divisional Meeting (1995), ICAO Document 9650, Montreal, Canada, March 1995.

5. Kelly, R.J. and Davis, J.M., "Required Navigation Performance (RNP) for Precision Approach and Landing with GNSS Application," NAVIGATION, the Journal of The Institute of Navigation, Vol. 41, No. 1, Spring 1994.

6. Report on Proposed Required Navigation Performance (RNP) Concept for Approach, Landing and Departure Operations, ICAO Secretariat, Special Communications/Operations Divisional Meeting (1995), Working Paper 11, Montreal, Canada, 27 March - 7 April 1995.

7. Report on Agenda Item 7, All Weather Operations Panel (AWOP) Fifteenth Meeting, Montreal, Canada, 26 September - 12 October 1994.

Signals Integrity

F. van Graas
Avionics Engineering Center
School of Electrical Engineering and Computer Science
361 Stocker Center
Ohio University
Athens, Ohio 45701
USA

1. SUMMARY

Providers of a GNSS service will be required to demonstrate that users of their service will be informed within a limited time (now set at ten seconds for terminal area navigation and nonprecision aproach) of any satellite that fails to operate within its range of acceptable signal quality. The lecture will describe approaches to provide this "integrity" feature including Receiver Autonomous Integrity Monitoring (RAIM) as well as systematic approaches that involve augmentations of the navigation satellite constellation. Prominent among these is the Wide Area Augmentation System for GPS.

2. INTRODUCTION

Integrity is the ability of a system to provide timely warnings to the pilot when the system should not be used for navigation. Integrity is required to ensure that an aircraft will not deviate from its intended course beyond the airspace route width requirements for a particular phase of flight without a warning being generated to the pilot. Course deviations unknown to the pilot could result in a collision, or in a large navigation error which would make it difficult to re-establish the intended course.

Traditionally, the signals-in-space of a navigation systems are verified by a ground-based monitor. In the case of GNSS, the satellites are also monitored, however, the probability of a satellite integrity failure is not consistent with aviation integrity requirements. For example, the probability of a GPS integrity failure has been estimated at 10^{-4} per hour, while the aviation integrity requirement is 10^{-7} per hour (Refs 1, 2). This results in an additional monitoring requirement, which must provide a detection probability of 0.999 for satellite integrity failures. The probability of loss-of-integrity is then given by

$$\text{P(Loss-of-integrity)} = \text{P(GPS Failure)} * \text{P(Missed Alert)}$$
$$10^{-7}/\text{hour} = 10^{-4}/\text{hour} * 10^{-3} \quad (1)$$

Three techniques exist to provide the additional detection capability: 1) Receiver Autonomous; 2) Aircraft Autonomous; and 3) External Methods. Aircraft Autonomous methods rely on additional sensors available in the aircraft to achieve integrity. Examples are inertial navigation or other radionavigation system position outputs, which are used to compare with the GPS position output. If not a simple comparison is performed, but a sensor integration, then the determination of integrity depends on the actual system architecture. Receiver Autonomous and External Methods are discussed in detail in the next two Sections. Receiver Autonomous Methods can also be applied to integrated systems.

3. RECEIVER AUTONOMOUS INTEGRITY

3.1 Introduction and Requirements

Initially, receiver autonomous integrity techniques were referred to as Receiver Autonomous Integrity Monitoring or RAIM. Because additional requirements were added to the original RAIM concept, the terminology was changed to Fault Detection and Exclusion or FDE.

Receiver Autonomous integrity requirements for supplemental use of GPS are summarized in Table 1 (Refs 3, 4). Integrity requirements for primary means use of GPS and for GPS Wide Area Augmentation System (WAAS) receivers differ from those listed in Table 1 in the following major areas (Refs 1, 5):

- The output of a Horizontal Protection Level (HPL) is required;
- The false alert probability is reduced to 10^{-5} per hour;
- Fault exclusion is required in addition to fault detection;
- A step detector is required;
- An availability requirement is added.

The HPL is defined as follows (Ref 1): The HPL is the radius of a circle in the horizontal plane, with its center being the indicated position, which describes the region which is assured to contain the true position. It is the horizontal region for which the missed alert and false alert requirements can be met when autonomous fault detection is used. It is only a function of the satellite and user geometry and the expected error characteristics: it is not affected by actual measurements. Therefore, this value is predictable.

An alert is defined to be an indication that is provided by the equipment that the positioning performance achieved by the equipment does not meet the integrity requirements. A detection is defined to be internal to the FDE algorithm and does not refer to an alert that is issued by the equipment.

Upon fault detection, the fault exclusion process is initiated, which can result in either a correct exclusion, a failed exclusion, or a wrong exclusion. A failed exclusion is defined to occur when a true satellite malfunction is detected and the detection condition is not eliminated within the time-to-alert.

Paper presented at the AGARD MSP Lecture Series on "System Implications and Innovative Applications of Satellite Navigation", held in Paris, France from 1-2 July 1996; Rome, Italy from 4-5 July 1996; Madrid, Spain from 8-9 July 1996 and St. Petersburg, Russia from 11-12 July 1996, and published in LS-207.

Table 1. Integrity Requirements for Supplemental Use of GPS.

Phase of Flight	Performance Item			
	Alert Limit	Maximum Allowable Alert Rate	Time to Alert	Minimum Detection Probability
En Route	2.0 nmi	0.002/Hr	30 seconds	0.999
Terminal	1.0 nmi	0.002/Hr	10 seconds	0.999
Nonprecision Approach	0.3 nmi	0.002/Hr	10 seconds	0.999

A failed exclusion would cause a loss of navigation alert. A wrong exclusion is defined to occur when a positioning failure is detected and the failed satellite remains in the solution after the exclusion operation. Additional, detailed definitions of FDE terms can be found in (Ref 1).

3.2 Autonomous Fault Detection Techniques

Fault detection techniques for GNSS involve consistency checks on pseudorange measurements. Two methods of consistency checking can be used (Ref 6):

1. Consistency checks based on the history of the pseudorange measurements (no redundancy is required);

2. Instantaneous ("snapshot") consistency checks based on a redundant set of pseudorange measurements.

The first method uses the pseudorange measurement history to predict the next pseudorange measurement for each of the satellites. This prediction is accurate to within the limits of measurement noise and unmodeled aircraft dynamics during the time period between measurement updates. A pseudorange (pr) innovation is formed for each of the satellites, where the innovation is the difference between the actual measurement and the predicted measurement based on the measurement history:

$$\text{pr innovation} = |\text{predicted pr} - \text{measured pr}| \quad (2)$$

If the pseudorange innovation exceeds a predetermined threshold, the satellite is removed from the position solution. As such, this method serves as a step detector for each of the satellites. No redundancy is required, and the malfunctioning satellite is immediately excluded from the position solution without the need for additional calculations.

The second method is used in cases where subtle measurement malfunctions are anticipated, such as slow drift errors. This method involves the calculation of a test statistic, which represents the inconsistency, or disparity, in a redundant set of pseudorange measurements with respect to an instantaneous least squares solution based on all measurements (all-in-view). If the test statistic exceeds a predetermined threshold, a detection occurs. Figure 1 illustrates the principle of fault detection. Satellite positioning requires four range measurements to solve for three dimensional position and time. If a fifth measurement is available, it is possible to form five sub-set positions leaving out one satellite at the time. These sub-set positions should be close to one another in the absence of a satellite malfunction. The receiver would output the all-in-view position solution for navigation purposes. If one of the satellites malfunctions, for example satellite 1 (SV 1), then the sub-set positions that contain SV 1 will be scattered. The all-in-view position will be in error as well. A detection test statistic is derived from the amount of scattering of the sub-set positions relative to the all-in-view position. In addition, a Horizontal Protection Level (HPL) can be calculated that guarantees that the all-in-view position will not exceed this level with specified probabilities of false and missed alerts. The position output can be used whenever the HPL is less than the required Horizontal Alert Limit (HAL) for the phase of flight in progress and no unresolved detections are present in the receiver.

If, after detection of an inconsistency, continuity must be assured, the receiver algorithm is required to reconfigure the position solution by selecting a different set of measurements that does not cause a detection. Note that a fault detection only results in an alert to the pilot if the reconfiguration algorithm is not able to find an acceptable set of measurements.

For supplemental use of GPS, only the fault detection function is required for operational applications, including non-precision approaches (Ref 4). For primary oceanic operation and for operation in conjunction with the WAAS, the fault exclusion function and the step detector are required to be implemented in the GPS receiver in addition to the fault detection function (Refs 1, 5).

Figure 2 shows the FDE fault tree for a GPS receiver (Ref 1). The fault tree has two main branches, one for the case of no GPS satellite integrity failures and one for the case of a GPS satellite integrity failure. In the absence of satellite integrity failures, a false detection causes the receiver to attempt the exclusion of a healthy satellite. The receiver will revert back to normal operation, unless the exclusion function was not successful. In that case, the positioning function is no longer available and an alert is issued to the pilot. In the presence of an actual satellite integrity failure, detection must occur with probability greater than 0.999. Otherwise, a missed detection (or missed alert) exists which represents a loss of integrity.

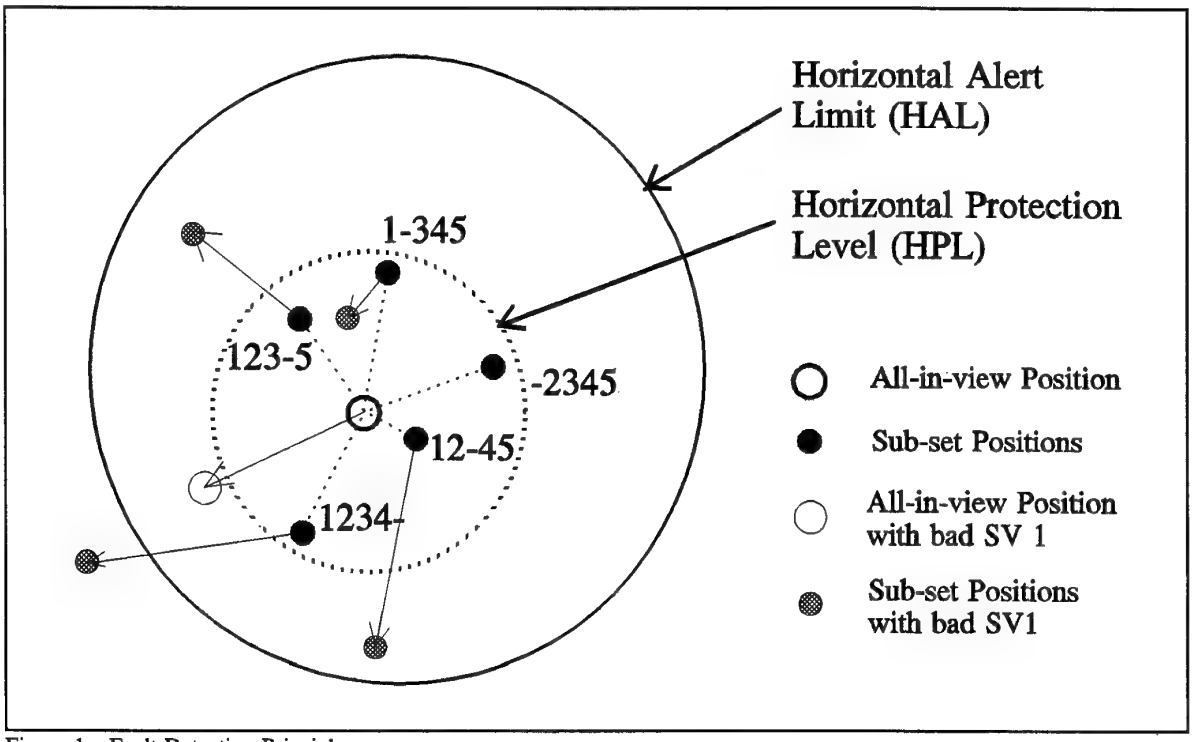

Figure 1. Fault Detection Principles

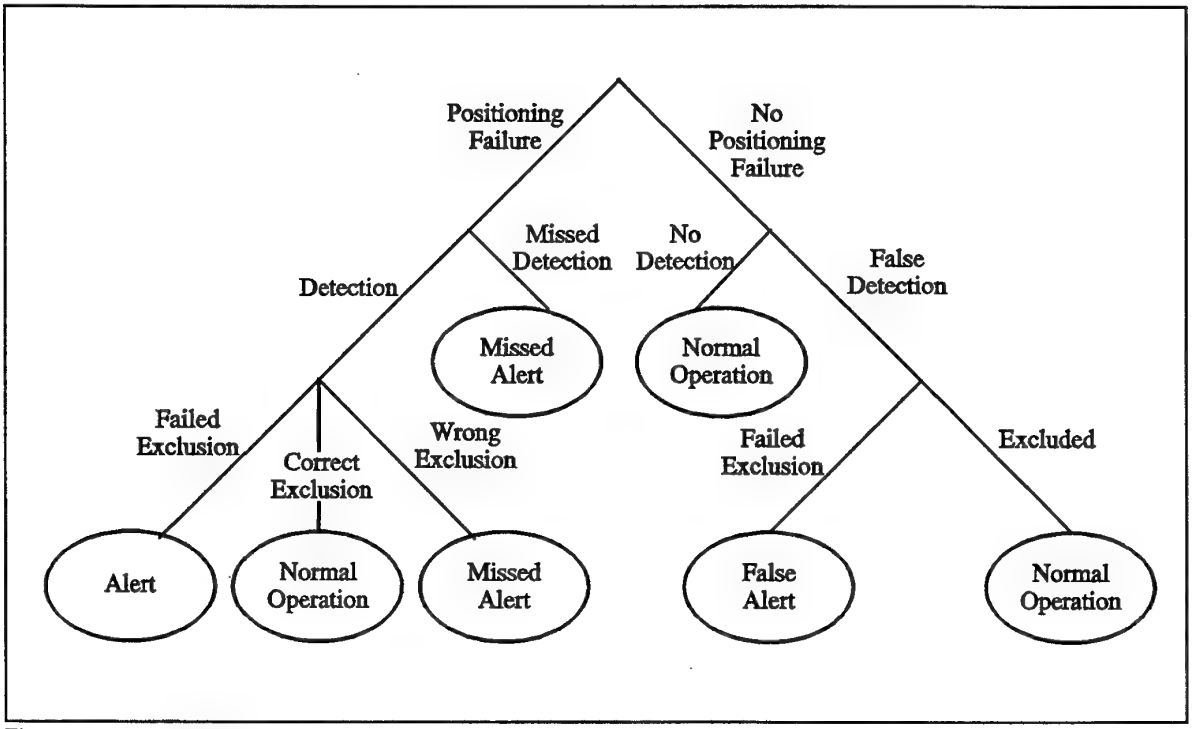

Figure 2. Fault Detection and Exclusion Fault Tree

Upon detection, the FDE algorithm will attempt to exclude the "bad" satellite. Three outcomes are possible: 1) the "bad" satellite is excluded from the position solution and the receiver reverts back to normal operation; 2) the exclusion failed, resulting in an alert to the pilot; or 3) the wrong satellite was excluded from the position solution, which will likely result in a missed alert either immediately upon exclusion or shortly thereafter. The latter case also represents a loss of integrity.

Figure 3 is provided to illustrate the different states of the FDE algorithm (Ref 1). This FDE Markov diagram shows the transitions between the different states which are relevant to the proper functioning of the FDE algorithm.

3.3 Fault Detection Algorithm Overview

Two key parameters must be computed by the fault detection algorithm. First, the threshold T_D for the test statistic, p, is calculated based on the desired false detection probability, P_{FD}. The detection threshold is a function of the measurement noise, the number of measurements, and P_{FD}. This is followed by the calculation of the bias in the test statistic which is needed to satisfy the desired probability of missed detection, P_{MD}. These thresholds are illustrated in Figure 4 for the norm of the test statistic, $|p|$. The left side of the figure shows the probability density function (pdf) of $|p|$ in the absence of a bias error. The detection threshold is set such that the false detection probability is less than 3.3×10^{-7} for this example. This corresponds to a false detection probability of 10^{-5}/hour if 30 independent samples are available per hour. The assumption of 30 independent samples follows from Selective Availability which is the dominant GPS error source (Ref 3). The right side of the figure shows the pdf of $|p|$ in the presence of a bias error. The bias error in the test statistic, μ_M, must be large enough such that the probability of missed detection is less than 10^{-3} for this example. Note that the probability of loss of integrity is conditional upon the presence of a bias error. If the probability of a bias integrity failure is less than 10^{-4}/hour, then the probability of loss of integrity is less than 10^{-7}/hour for this example.

Once the minimum required bias in the test statistic, μ_M, is known, it is translated to the measurement range domain for each of the satellites. This results in a minimum required range bias, b_i, for each of the satellites ($i = 1$ through the number of satellites). The bias in the pseudorange measurement must be greater than b_i for detection with the desired probability of detection. Next, each of the range biases are translated to horizontal position errors. The worst possible horizontal radial position error is termed the Horizontal Protection Level (HPL). If the position solution exceeds the HPL, it will be detected with probability 0.999 for this example. It is further noted that the probability of detection dramatically increases with increasing range error. This effect can be seen in Figure 4 by moving the biased pdf to the right, which results in a decrease in the area under the

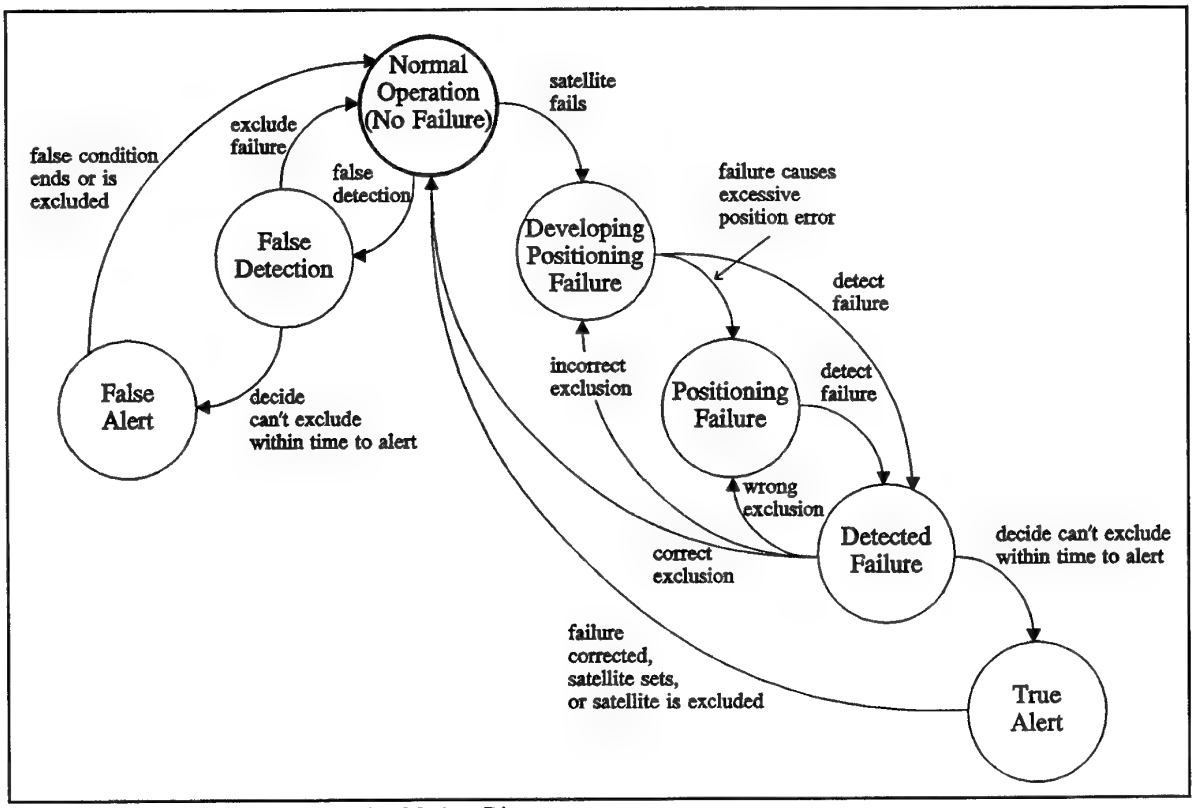

Figure 3. Fault Detection and Exclusion Markov Diagram

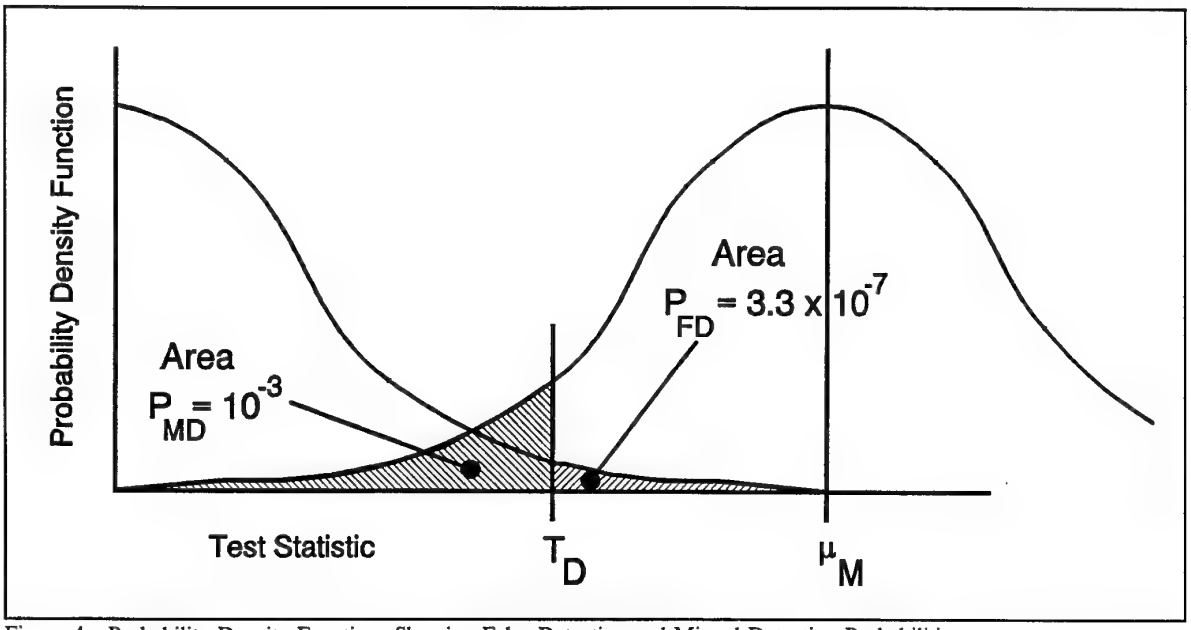

Figure 4. Probability Density Functions Showing False Detection and Missed Detection Probabilities

"tail" of the pdf left of T_D. In other words, a missed detection will quickly turn into a detection if the range error continues to increase.

3.4 Fault Exclusion Algorithm Overview

The basic scheme to perform fault exclusion is to search for satellite sub-sets that do not have a fault detection condition. A sub-set must contain at least 5 satellites such that fault detection can be performed on the sub-set. This requires that before detection, at least 6 satellites are available.

The fault exclusion algorithm first rank-orders all combinations of sub-sets containing (n-1) satellites if the receiver was tracking n satellites before fault detection occurred. Next, the receiver selects the sub-set with the smallest test statistic among those that satisfy the following two conditions:

- The HPL is less than the HAL;
- The test statistic is less than a detection threshold, which is set for a probability of failed exclusion of less than 10^{-3}.

It is noted that the detection threshold upon fault detection is much smaller than the detection threshold before fault detection. As a result, the false alarm probability after detection is much higher (10^{-3}) than the false alarm probability before detection (3.3×10^{-7}). This results in a failed exclusion probability of 10^{-3}. On the other hand, the probability of a wrong exclusion upon detection is much smaller ($< 10^{-6}$) than the probability of missed detection before detection (10^{-3}). The latter effect, a small probability of wrong exclusion, is desirable.

3.5 Step Detector

The step detector must have the following performance characteristic:

The step detector is able to detect and exclude a satellite that has a pseudorange step error of 700 meters (1000 meters for primary oceanic use) or more from one measurement to the next.

It is noted that the step detector should not act on smaller steps to avoid interference with the FDE algorithm. The operation of the step detector is illustrated in figures 5 and 6. Figure 5 shows the case where fault detection is available. After the occurrence of a step, the receiver could lose lock or continue to track the satellite. If loss-of-lock occurred and fault detection is available, then the receiver must perform a screen test (SCREEN A) on the lost satellite before it is re-accepted into the position solution. The screen test must be such that the probability of accepting a satellite with a pseudorange bias of greater than 700 meters is less than 0.001 for acceptable geometries. Following loss-of-lock, the receiver is expected to re-acquire and provide pseudorange measurements within 10 seconds (from the receiver acquisition requirement). Therefore, the screen test is not performed if the loss-of-lock time in the absence of fault detection is greater than 10 seconds, because this would indicate a loss-of-lock due to other conditions such as signal shielding. Loss-of-lock due to aircraft maneuvers is considered more likely than due to the occurrence of a step error.

In general, excluded satellites are monitored for possible future inclusion into the position solution using the screen test. However, after a satellite has been excluded without loss-of-lock, it must remain excluded until positive integrity is available through autonomous fault detection.

Figure 6 show the case where fault detection is not available. In this case, a different screen test (SCREEN B) is used. This screen test uses a larger acceptance threshold to account for aircraft dynamics.

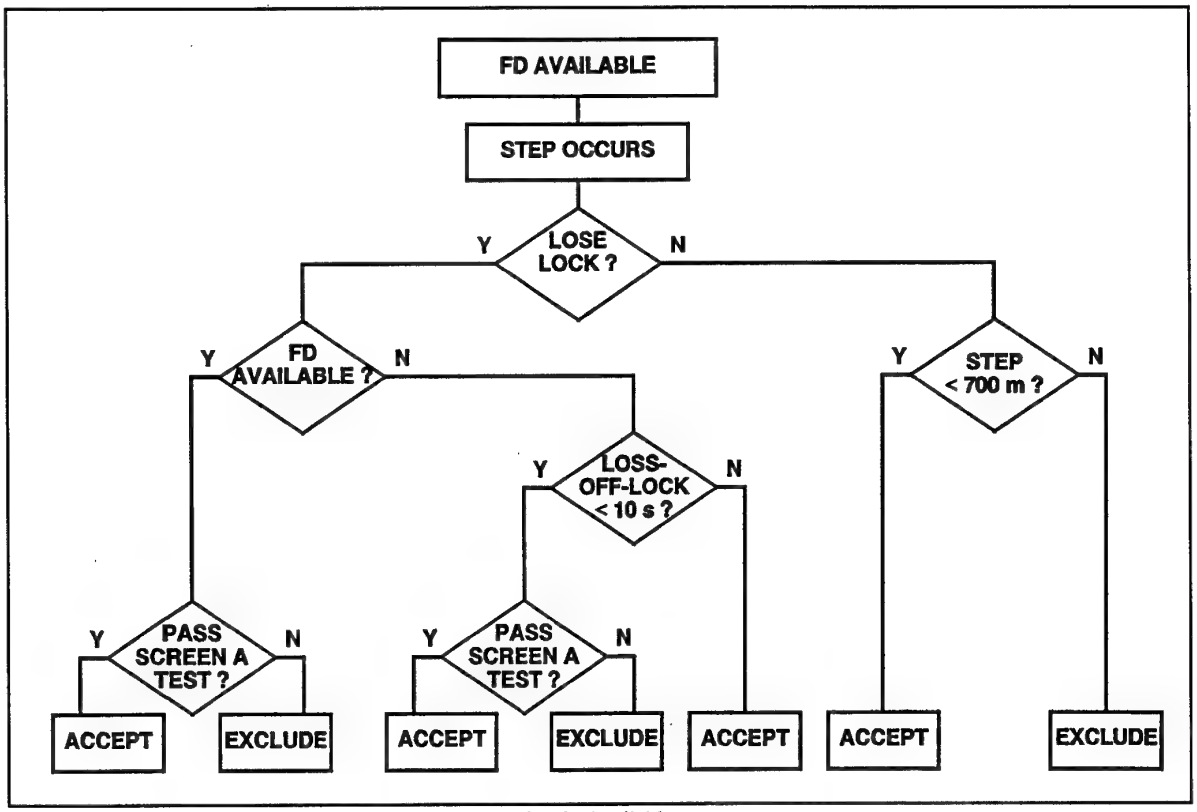

Figure 5. Step Detector Flow Diagram if Fault Detection is Available

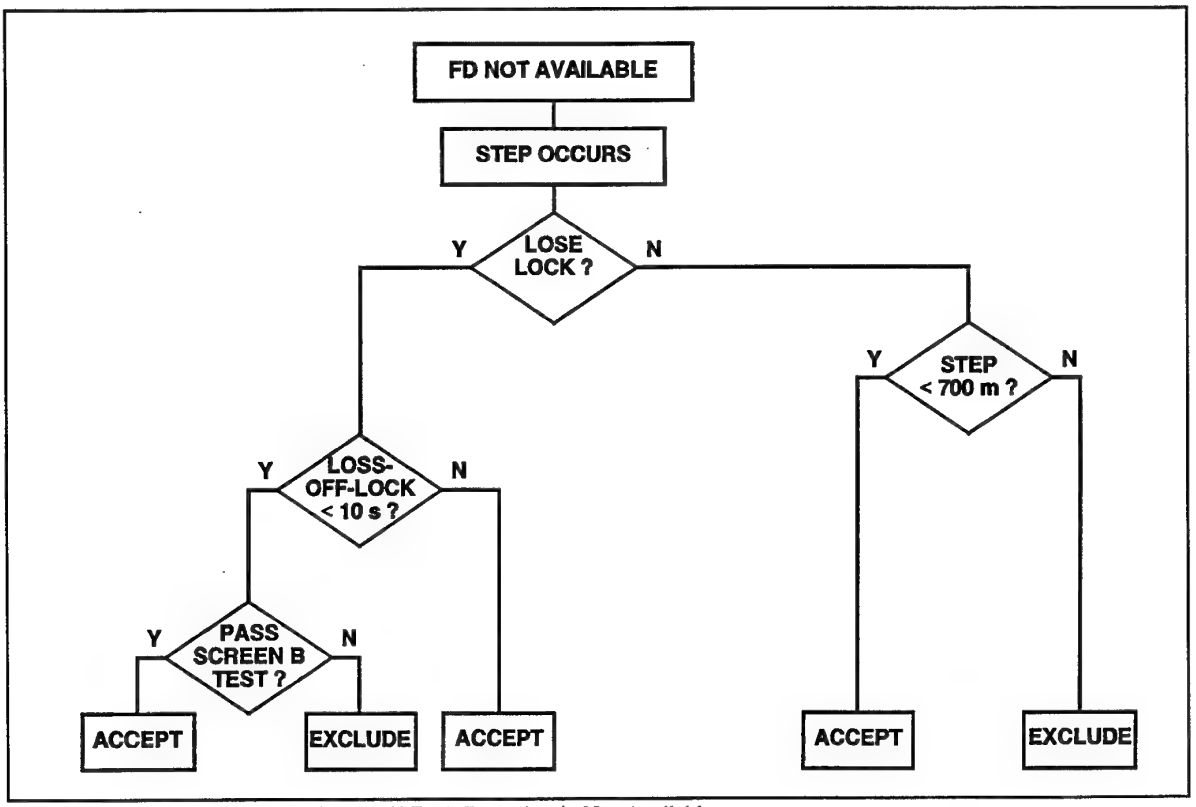

Figure 6. Step Detector Flow Diagram if Fault Detection is Not Available

3.6 FDE Test Considerations

Current systems (e.g. VOR and ILS) burden the ground sub-systems with providing a high-integrity path in space. If the signal exceed monitor limits, the signal is withdrawn and the airborne receiver displays a flag. For integrity, the airborne receiver complexity is minimized and test procedures and equipment needed to prove compliance with the requirements can be relatively simple.

GNSS receivers using FDE shift the responsibility for positioning integrity to the airborne receiver. The GNSS receiver uses complex integrity methods, which require complex test procedures.

To test the FDE algorithm two types of tests are used:

1) Off-line computer simulation tests. Software is used to simulate the GPS receiver, including the FDE algorithm. The software also generates the necessary inputs for the FDE algorithm, including simulated pseudorange errors.

2) On-line or real-time tests. A GNSS simulator provides inputs to the GPS receiver according to a pre-determined simulation scenario.

FDE algorithms are statistical in nature, requiring a large number of test, such that most FDE algorithm tests are performed off-line. The statistical nature of the FDE requirements is illustrated below:

- False alert probability $< 10^{-5}$/hour (or 3.3×10^{-7} per sample)
- Missed alert probability $< 10^{-3}$
- Failed exclusion probability $< 10^{-3}$

These probabilities must be tested with confidence. If the actual probabilities are twice the requirement, then the probability of passing the test must be less than 0.01. At the same time, properly designed equipment should have a probability of 0.99 to pass the test. This is a compromise between opposing goals of ensuring that requirements are met while minimizing the required test time. The confidence requirement results in the following number of tests:

- False alert: 99000000 tests
- Missed alert: 33000 tests
- Failed exclusion: 33000 tests

The expected number of false or missed alerts or failed exclusions is 33 for each of the tests. To ensure that receivers with actual probabilities of twice the required values are rejected with 99% confidence, the maximum number of false or missed alerts or failed exclusions is 47 each.

Noise scaling can be used to reduce the number of test runs, as all three probabilities to be tested are very sensitive to the input noise level. For example, a 10 percent increase in the pseudorange measurement noise increases the false alert probability by a factor of 9 (Ref 7), which would reduce the number of required tests by a factor of 9.

Because most of the FDE algorithm tests are performed off-line, it is required that the FDE algorithm implementation used for testing, and the implementation used in the actual receiver, are *"functionally equivalent"*. To ensure equivalence, on-line verification tests are required during which selected off-line test scenarios are repeated. The results from the off-line and on-line tests must be equivalent within the limitations of the test set-up. It is emphasized that the on-line verification test is crucial for receiver certification.

4. EXTERNAL TECHNIQUES

4.1 Overview

Receiver external integrity methods rely on an independent GNSS monitor network in combination with geostationary satellites or ground-based transmitters for the broadcast of integrity information. Examples are the U.S. Wide Area Augmentation System (WAAS) under development by the FAA, the European Geostationary Navigation Overlay System (EGNOS), and differential GPS networks. This section provides an overview of geostationary satellite augmentation techniques, followed by a section on the WAAS.

Three levels of geostationary satellite transponder augmentation of GNSS services can be identified in order of increasing performance and complexity:

1. Ranging Geostationary Satellite (Ranging GEO);
2. Ranging GEO and Integrity Information (GIC);
3. GIC and Wide Area Differential Correction Data (WAD).

Each of these augmentations is discussed in the following three sections. It is assumed that the GEO will broadcast GPS-like navigation signals.

4.1.1 Ranging Geostationary Satellite (Ranging GEO)

The Ranging GEO service is intended to augment the availability and continuity of GNSS. This service requires a ground segment which operates the geostationary satellite transponder in such a way that the GEO can be used as an additional navigation satellite.

The ground segment determines the GEO satellite position and clock parameters and controls the broadcast of the GPS-like GEO signal. The accuracy of the GEO position and clock parameters should be at least as good as the GPS satellites. Also, the timing of the GEO broadcast should be closely synchronized with GPS time to minimize the magnitude of the clock correction. The ground segment also determines an accuracy exponent (URA) for the GEO, which is modulated onto the GEO transmissions together with the satellite position and clock data.

4.1.2 Ranging GEO and Integrity Information (GIC)

In addition to the Ranging service, the geostationary satellite transponder is also used to broadcast GNSS integrity information. This service increases the level of GNSS integrity and also improves the availability and continuity of GNSS. If the GIC service is available, the GNSS user no longer requires the presence of redundant satellite signals to determine the integrity of the position solution.

In order to broadcast integrity information, the ground segment must estimate the range error to each of the GNSS satellites. This requires the estimation of the GNSS satellite positions and clock offsets. The integrity information is also modulated onto the GEO transmissions.

4.1.3 GIC and Wide Area Differential Correction Data (WAD)

Wide area differential corrections improve GNSS accuracy over a large service area. This increase in accuracy improves the availability and continuity of GNSS, but also enables operations requiring accurate positioning such as aircraft precision approaches.

To determine differential correction data that is valid over a large service area, it is necessary to separate the differential corrections into its major components: satellite position error, satellite clock error, and ionospheric delay error. In addition, a User Differential Range Error (UDRE) is estimated as well. The differential corrections are divided into fast and slow corrections, depending on the dynamics of the individual error components. The differential correction data is also modulated onto the GEO transmissions.

To gain some insight into the generation of the WAD corrections, Figure 7 shows a simplified block diagram of the correction process.

The nominal GNSS ephemeris and clock parameters are perturbed by errors and by propagation delays. These signal arrive both at the Wide Area Reference Stations (WRS) and at the user receivers. At that point, thermal noise, clock offsets and receiver measurement errors are added to the signal in space. The measurement data from the WRS and user receivers contain all the above error sources. The WRS then estimates the ionospheric propagation delays through the use of dual-frequency measurements. Next, tropospheric delays are removed from the data through the use of temperature, pressure and humidity measurements. Finally, the data from several WRS receivers is combined to estimate the ephemeris and clock errors for all GNSS satellites in view. The ionospheric delay information along with the satellite clock and ephemeris error estimates are then broadcast by the GEO satellites.

At the user, the measurement data is corrected for tropospheric propagation delays by applying a tropospheric model. Next, the received WAD corrections are applied to correct for ionospheric delays, and satellite position and clock errors.

4.2 Integrity Provided by the WAAS

The WAAS is an augmentation to GPS, currently under development by the U.S. FAA, which uses a network of ground-based reference stations and integrity monitors to calculate GPS integrity and pseudorange correction data. When fully operational, the WAAS will provide Ranging GEO, GIC, and WAD services.

It should be emphasized that current requirements for GPS/WAAS receivers include the implementation of receiver autonomous FDE techniques (Ref 1). This is to allow for operation outside the WAAS service volume and to allow for continued operation in the absence of WAAS signals in the user receiver.

This section addresses the WAAS-provided integrity monitoring function. The user equipment will be capable of computing a horizontal protection level HPL_{WAAS} that bounds the horizontal position error using the WAAS signal-in-space. The probability that the horizontal position error exceeds the HPL_{WAAS} must be less than or equal to 0.001 (probability of missed alert).

A GPS or WAAS satellite shall be designated as WAAS HEALTHY if the following condition is met:

> WAAS has assigned a WAAS fast correction value other than -256 meters or +255.875 meters, indicating that the WAAS has declared the satellite usable.

Four different HPL_{WAAS} values can be calculated for en route through nonprecision approach phases of flight (Ref 1):

1. For Monitoring Integrity Indication;
2. When Applying Fast Corrections;
3. When Applying Fast and Long-Term Corrections;
4. When Applying Fast, Long-Term, and Ionospheric Corrections.

For monitoring integrity indication, the following equation is used:

$$HPL_{WAAS} = \underset{j}{MAX}\left(HDOP\sqrt{(PRC_j + UDRE_j)^2 + 300^2 + 50^2}\right) \quad (3)$$

where: HDOP is the horizontal dilution of precision for the satellites used in the position solution; PRC_j is the fast WAAS correction for the j^{th} satellite; $UDRE_j$ is the user differential range error for the j^{th} satellite; 300 meters is a bound on the combination of long-term clock and ephemeris errors if corrections are not applied by the user; 50 meters is the extreme value of horizontal ionospheric error after correction with the single-frequency Klobuchar model.

When Fast Corrections are applied by the user, equation (3) reduces the HPL to

$$HPL_{WAAS} = \underset{j}{MAX}\left(HDOP\sqrt{UDRE_j^2 + 300^2 + 50^2}\right) \quad (4)$$

If the user applies both Fast and Long-Term Corrections, equation (4) reduces the HPL further to

$$HPL_{WAAS} = \underset{j}{MAX}\left(HDOP\sqrt{UDRE_j^2 + 50^2}\right) \quad (5)$$

Finally, if the user applies all corrections and does not use a weighted solution, then the HPL_{WAAS} is given by

$$HPL_{WAAS} = \underset{j}{MAX}\left(HDOP\sqrt{UDRE_j^2 + (F_j UIVE_j)^2}\right) \quad (6)$$

where: F_j is the ionospheric obliquity factor for the j^{th} satellite; and $UIVE_j$ is the interpolated user ionospheric vertical error for the j^{th} satellite.

Under typical conditions with UDRE = 2 meters, equation (5) will support the nonprecision approach mode as long as

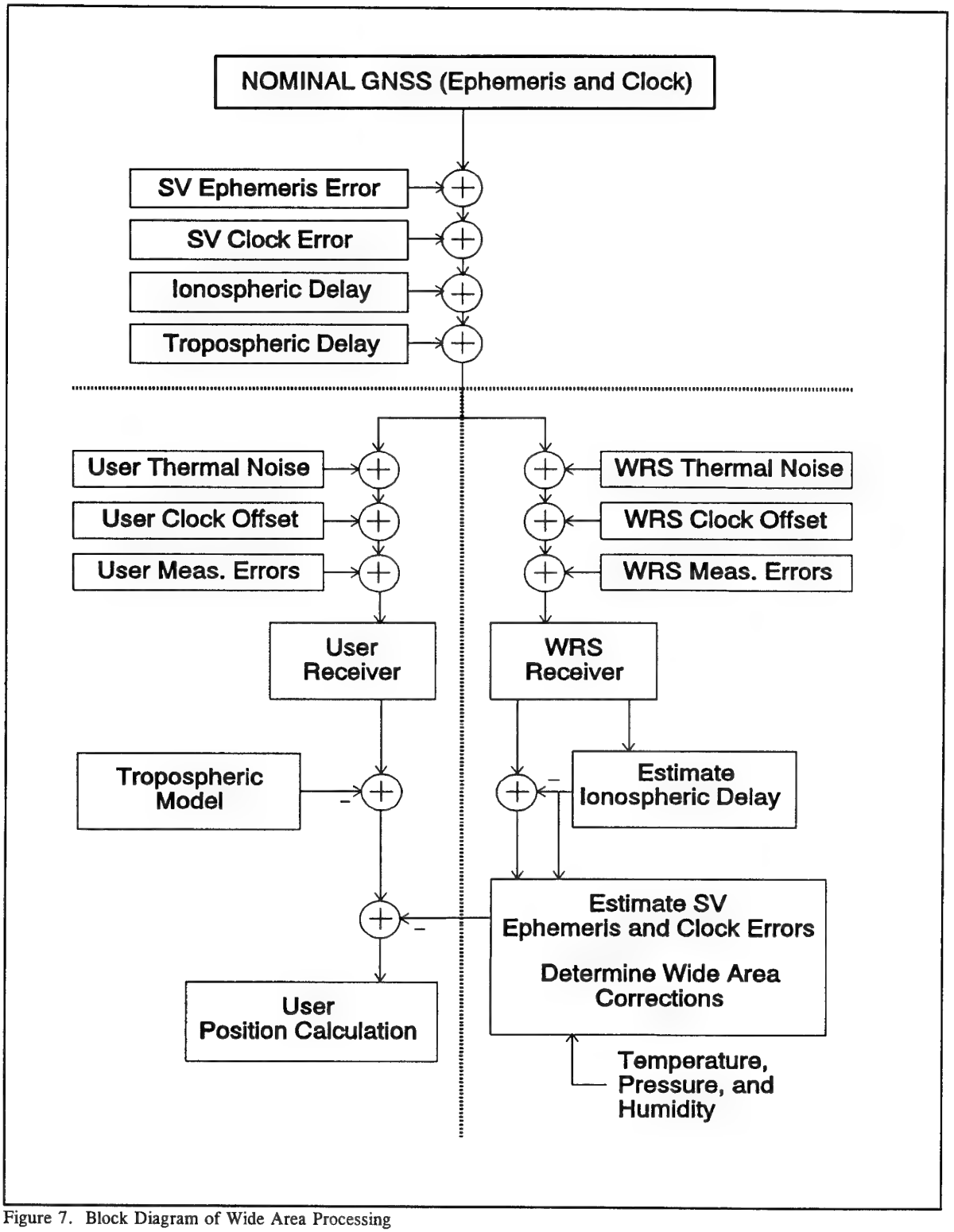

Figure 7. Block Diagram of Wide Area Processing

HDOP is no greater than 11.1, such that a HAL of 556 meters (0.3 nmi) is supported. Note that if no corrections are applied, equation (3) will support the terminal mode (HAL is 1852 meters or 1 nmi) as long as HDOP is no greater than 5.5.

5. REFERENCES

1. Minimum Operational Performance Standards for Global Positioning System/Wide Area Augmentation System Airborne Equipment, RTCA/DO-229, RTCA, Inc., Washington, D.C., 16 January 1996.

2. Lee, Y., et al., "Summary of RTCA SC-159 GPS Integrity Working Group Activities," in Proceedings of the National Technical Meeting of The Institute of Navigation, January 1996.

3. Minimum Operational Performance Standards for Airborne Supplemental Navigation Equipment Using Global Positioning System, RTCA/DO-208, RTCA, Inc., Washington, D.C., July 1991.

4. Technical Standard Order (TSO) C-129, Airborne Supplemental Navigation Equipment Using the Global Positioning System (GPS), FAA Aircraft Certification Service, Washington, D.C., 10 December 1992.

5. GPS As a Primary Means of Navigation for Oceanic/Remote Operations, FAA Notice N8110.60, FAA Aircraft Certification Service, Washington, D.C., 1996.

6. Joyner, G., "RAIM Experiences," ICAO All Weather Operations Panel (AWOP) Fifteenth Meeting, Montreal, Canada, 26 September - 12 October 1994.

7. Van Graas, F. and Farrell, J.L., "Receiver Autonomous Integrity Monitoring (RAIM): Techniques, Performance and Potential," in Proceedings of the 47th Annual Meeting of The Institute of Navigation, Williamsburg, VA, 10-12 June 1991.

APPENDIX

This appendix contains an example Fault Detection algorithm.

The linearized relation between changes in the measurements and the corresponding change in the user state vector is given by

$$\underline{\delta y} = H\,\underline{\delta x} \tag{A-1}$$

where $\underline{\delta y}$ is a m-by-1 vector containing the changes in the measurements to m sources, $\underline{\delta x}$ is the change in the n-by-1 user state vector, and H is a m-by-n data matrix.

The data matrix H can be decomposed into the product of a real orthonormal matrix Q and an upper triangular matrix R using a "QR" factorization,

$$H = Q\,R \tag{A-2}$$

Substituting (A-2) into (A-1) and pre-multiplying both sides by Q^T yields ($Q^TQ = I$)

$$R\,\underline{\delta x} = Q^T\underline{\delta y} \tag{A-3}$$

The rank of R is equal to the rank of H; therefore, if $m > n$, the lower m-n rows of R consist of zeros only, and Equation (A-3) can be divided into two equations

$$U\,\underline{\delta x} = Q_x^T\,\underline{\delta y} \quad \text{or} \quad \underline{\delta x} = U^{-1}\,Q_x^T\,\underline{\delta y} \tag{A-4}$$

$$\underline{0} = Q_p^T\,\underline{\delta y} \tag{A-5}$$

where U consists of the first n rows of R, Q_x^T consists of the first n rows of Q^T, and Q_p^T consists of the last m-n rows of Q^T.

Equation (A-4) relates the change in the measurements to the change in the user state vector, forming the least squares solution. The rows of Q_p^T and $\underline{\delta y}$ are orthogonal; therefore, the columns of Q_p^T span the parity space of H.

If the measurements are corrupted by errors, then $\underline{\delta y}$ is replaced by $\underline{\delta y} + \underline{e} + \underline{b}$, where $\underline{e}$ is a m-by-1 vector representing zero-mean, normally distributed measurement noise, and $\underline{b}$ is a m-by-1 vector containing bias errors. Normally, $\underline{e}$ and $\underline{b}$ are unknown, but their components in parity space are known from equation (A-5):

$$\underline{p} = Q_p^T\,\underline{e} + Q_p^T\,\underline{b} \tag{A-6}$$

The expected value of the parity vector, $\underline{p}$, is

$$E\{\underline{p}\} = Q_p^T\,\underline{b} \tag{A-7}$$

The covariance matrix of $\underline{p}$ is

$$COV\{\underline{p}\} = Q_p^T\,COV\{\underline{e}\}\,Q_p \tag{A-8}$$

If the measurement noise is uncorrelated and normally distributed with equal variances, then the covariance matrix of the measurement noise is

$$COV\{\underline{e}\} = \sigma^2\,I \tag{A-9}$$

where I is a m-by-m identity matrix. It then follows that the covariance matrix of $\underline{p}$ is

$$COV\{\underline{p}\} = \sigma^2\,I \tag{A-10}$$

since $Q_p^TQ_p = I$ (the rows of Q_p^T are orthonormal vectors).

In the absence of bias errors, the parity vector $\underline{p}$ is a function of measurement noise only. In the presence of bias errors, $\underline{p}$ also depends on the bias errors.

One Redundant Measurement

Assume that only one redundant measurement is available, or $m = n + 1$. In this case, the parity space is one-dimensional and Q_p^T is reduced to a row vector (the vector $\underline{q}$ is used to denote the transpose of the first row of Q_p^T), and the parity vector $\underline{p}$ is reduced to a parity scalar p. In the absence of bias errors, p has a zero-mean normal probability density function given by

$$f_p(x) = \frac{1}{\sigma\sqrt{2\pi}}\,e^{-\left(\frac{x}{\sigma\sqrt{2}}\right)^2} \tag{A-11}$$

Assume that the failure detection is based on exceeding a detection threshold T_D, then the probability of a false detection is given by

$$P_{FD} = P\ (|p|>T_D) = \frac{2}{\sigma\sqrt{2\pi}} \int_{T_D}^{\infty} e^{-\left(\frac{x}{\sigma\sqrt{2}}\right)^2} dx \qquad \text{(A-12)}$$

which can also be written as

$$P_{FD} = \text{erfc}\left(\frac{T_D}{\sigma\sqrt{2}}\right) \qquad \text{(A-13)}$$

where erfc is the complementary error function

$$\text{erfc}(z) = \frac{2}{\sqrt{\pi}} \int_{z}^{\infty} e^{-\lambda^2} d\lambda \qquad \text{(A-14)}$$

The false detection probability is set at 3.3 x 10^{-7} on a per sample basis.

In the presence of a bias error in measurement i only, the parity scalar has a normal distribution with a mean value of

$$\mu_i = \underline{q} \cdot \underline{b} = q_i \times b_i \qquad \text{(A-15)}$$

Only the i^{th} elements of $\underline{q}$ and $\underline{b}$ will contribute to the mean. The probability density function of p is then given by

$$f_p(x) = \frac{1}{\sigma\sqrt{2\pi}} e^{-\left(\frac{x-\mu_i}{\sigma\sqrt{2}}\right)^2} \qquad \text{(A-16)}$$

Given the detection threshold T_D, the probability of a missed detection is given by

$$P_{MD} = P\ (|p|\le T_D) = \frac{1}{\sigma\sqrt{2\pi}} \int_{-T_D}^{T_D} e^{-\left(\frac{x-\mu_i}{\sigma\sqrt{2}}\right)^2} dx \qquad \text{(A-17)}$$

When μ_i is positive, an useful upper bound for P_{MD} is given by

$$P_{MD} = P(-T_D < p < T_D) < P(p < T_D)$$

$$P_{MD} < \frac{1}{2}\text{erfc}\left(\frac{\mu_i - T_D}{\sigma\sqrt{2}}\right)$$

when μ_i is negative, a better upper bound is

$$P_{MD} < P(-T_D < p)$$

$$P_{MD} < \frac{1}{2}\text{erfc}\left(\frac{-T_D - \mu_i}{\sigma\sqrt{2}}\right)$$

$$P_{MD} < \frac{1}{2}\text{erfc}\left(\frac{|\mu_i| - T_D}{\sigma\sqrt{2}}\right)$$

Thus regardless of the sign of μ_i, we have

$$P_{MD} < \frac{1}{2}\text{erfc}\left(\frac{|\mu_i| - T_D}{\sigma\sqrt{2}}\right) \qquad \text{(A-18)}$$

Equations (A-13) and (A-18) provide the performance of the fault detection algorithm in terms of probability of a false detection and probability of a missed detection as a function of:

- Detection threshold T_D;
- Measurement noise standard deviation σ;
- Expected value μ_i of the parity scalar p resulting from a measurement bias error in measurement i.

Obviously, the detection algorithm cannot detect a measurement bias error smaller than the level of measurement noise, since the detection threshold T_D must be set high enough to satisfy the requirement for the false detection probability, see equation (A-13).

Given the maximum allowed probability of a detection and the measurement noise standard deviation, an acceptable detection threshold (i.e. one that will be not too likely to cause a detection) is obtained from equation (A-13)

$$T_D = \sigma\sqrt{2}\ \text{erfc}^{-1}(P_{FD}) \qquad \text{(A-19)}$$

A detection occurs when the absolute value of the parity scalar exceeds T_D. Next, given the maximum allowed probability of a missed detection, the measurement noise standard deviation and the detection threshold, we may establish μ_M, the minimum detectable absolute expected value of the parity scalar, from equation (A-18) as follows:

μ_i is detectable with a high enough probability if

$$|\mu_i| > \mu_M = T_D + \sigma\sqrt{2}\ \text{erfc}^{-1}(2P_{MD}) \qquad \text{(A-20)}$$

Since $\mu_i = \underline{q} \cdot \underline{b}$, equation (A-20) implies that the probability of a missed detection is only satisfied if the measurement bias error gives rise to a bias in the parity scalar with absolute value greater than or equal to μ_M. The vector $\underline{q}$ is known from the measurement geometry; therefore, for each measurement i (i = 1 through m), the minimum absolute bias error b_i required to satisfy the probability of a missed detection is calculated from equation (A-15).

$$b_i = \frac{\mu_M}{|q_i|} \qquad \text{(A-21)}$$

Combining equations (A-19), (A-20), and (A-21) gives the simple result

$$b_i = \frac{\left(\text{erfc}^{-1}(P_{FD}) + \text{erfc}^{-1}(2P_{MD})\right)\sigma\sqrt{2}}{|q_i|} \qquad \text{(A-22)}$$

In other words, given the probability of a false detection, the probability of a missed detection, and the measurement noise standard deviation, it follows that the minimum detectable measurement bias error is a function of the measurement geometry.

Horizontal Protection Level

From the probability of a false detection, the probability of a missed detection, the measurement noise standard deviation, and the minimum detectable measurement bias error it is possible to discuss the horizontal radial position error.

Consider the user state error vector resulting from both measurement noise and bias errors. From equation (A-4) the user state error vector is

$$\Delta\underline{x} = U^{-1} Q_x^T (\underline{e}+\underline{b}) \qquad \text{(A-23)}$$

The expected value of the user state error vector is

$$E\{\Delta\underline{x}\} = U^{-1} Q_x^T \underline{b} \qquad \text{(A-24)}$$

and the error covariance matrix of $\underline{\Delta x}$ is

$$\text{COV}\{\underline{\Delta x}\} = \sigma^2 (U^T U)^{-1} \qquad \text{(A-25)}$$

As shown by equations (A-23) through (A-25), the effects of the noise and bias errors can be examined separately.

Assume that the vector $\underline{\Delta x}$ is expressed in a locally-level reference frame, then the horizontal components of the expected value and the variance of the user state error vector are given by

$$E\{\underline{\Delta x}_H\} = \begin{pmatrix} \bar{x} \\ \bar{y} \end{pmatrix} \qquad \text{(A-26)}$$

$$\text{VAR}\{\underline{\Delta x}_H\} = \begin{pmatrix} \sigma^2\ \text{XDOP}^2 \\ \sigma^2\ \text{YDOP}^2 \end{pmatrix} = \begin{pmatrix} \sigma_x^2 \\ \sigma_y^2 \end{pmatrix} \qquad \text{(A-27)}$$

where $\bar{x}$, $\bar{y}$ are the first two components of $E\{\underline{\Delta x}\}$; XDOP^2 and YDOP^2 are the first and second diagonal elements of $(U^T U)^{-1}$, respectively.

First consider the horizontal radial position bias error resulting from measurement bias errors. Each satellite has a minimum bias error necessary for detection with probabilities P_{FD} and P_{MD}, as given by equation (A-21). Each of these measurement bias errors can be converted into a horizontal position error using equation (A-24) with the other bias components zero. Next, the worst case measurement error is the b_i which maximizes the norm of the horizontal radial position error

$$R_{bias} = \max_i \left(\sqrt{\bar{x}_i^2 + \bar{y}_i^2} \right) \qquad \text{(A-28)}$$

The detection algorithm now guarantees that a measurement bias will be detected with the required probabilities P_{FD} and P_{MD} if it contributes to a horizontal radial position error of R_{bias} or greater. Due to the presence of noise, the actual position error will exceed R_{bias} only approximately 50 percent of the time. Therefore, the HPL is conservatively set at R_{bias}.

Two Redundant Measurements

If two redundant measurements are available, or m = n + 2, the parity vector contains two elements. The norm of the parity vector is now used as the detection statistic. The norm of the parity vector squared has two-degrees-of-freedom (2 DOF) chi-square properties.

A similar procedure is used as for the case of one redundant measurement. First, the detection threshold, T_D, is calculated such that the probability of false detection is 3.3×10^{-7}. Next, the minimum detectable bias is calculated which is needed to satisfy the probability of detection of 0.999. This is followed by the calculation of the HPL.

The normalized (σ=1) 2 DOF chi-square density function is given by

$$f_\chi(x) = 0.5 e^{-0.5x} \qquad \text{(A-29)}$$

The area under the tail of the density function is to be P_{FD}. Therefore

$$P_{FD} = \int_{T_D^2}^{\infty} 0.5 e^{-0.5x} dx \qquad \text{(A-30)}$$

$$\text{or } T_D = \sqrt{-2 \cdot \ln(P_{FD})}$$

Using a $P_{FD} = 3.3 \times 10^{-7}$ $T_D = 5.46$. This is the normalized threshold that is used if the magnitude of the parity vector is used as the test statistic. If the threshold is not normalized, then the threshold must be multiplied by the standard deviation of the measurement noise. (e.g. if σ = 33 m and the magnitude of the parity vector is the test statistic, $T_D = 33 \times 5.46 = 180.2$).

The minimum detectable bias is calculated using the normalized 2 DOF noncentral chi-square density function given by

$$f_\chi(x) = 0.5 e^{-0.5(x+\mu_M^2)} \sum_{j=0}^{\infty} \frac{x^j (\mu_M^2)^j}{2^{2j} j! j!} \qquad \text{(A-31)}$$

where μ_M^2 is the noncentrality parameter.

The desired missed detection probability is obtained by integrating equation (A-31) from zero to the detection threshold squared:

$$P_{MD} = \int_0^{T_D^2} f_\chi(x) dx = \int_0^{T_D^2} 0.5 e^{-0.5(x+\mu_M^2)} \sum_{j=0}^{\infty} \frac{x^j (\mu_M^2)^j}{2^{2j} j! j!} dx \qquad \text{(A-32)}$$

Note that μ_M is a function of the number of satellites in view; but, for a given m, it does not vary with the satellite geometry.

Recall that a bias error in measurement i has components along the axes in parity space given by column i of Q_p^T. Each column of Q_p^T defines a measurement axis in parity space: an error in measurement i will lie along the i^{th} measurement axis in parity space. Therefore, a measurement range bias is transformed into a bias in the parity vector by multiplying the range bias by the norm of column i of Q_p^T.

The minimum absolute bias error, b_i, required to satisfy the probability of missed detection is calculated from

$$b_i = \frac{\mu_M}{|\underline{m}_i|} \qquad \text{(A-33)}$$

where $\underline{m}_i$ is the i^{th} column of Q_p^T.

Similar to the case of one redundant measurement, the HPL is calculated from equations (A-24), (A-26), and (A-28).

GNSS Augmentation for High Precision Navigation Services

F. van Graas
Avionics Engineering Center
School of Electrical Engineering and Computer Science
361 Stocker Center
Ohio University
Athens, Ohio 45701
USA

1. SUMMARY

The absolute positioning accuracy of current or planned GNSS services is not good enough to support Category III Precision Approach and Landing requirements, nor is it good enough to support high precision survey applications. The leading solution to this problem is to augment the basic service. The survey community has developed relative positioning techniques based on continuously tracked carrier phase measurements. A static or dynamic user compares accumulated carrier phase measurements to a specific set of satellites with simultaneous measurements taken by a reference receiver at a well-surveyed location. The Civil Aviation Community is also exploring "local area" differential (GPS) concepts in which one or more reference beacons augment the satellite beacons in the vicinity of an airport. The lecture will identify the leading candidates for these augmentations and will characterize predicted performance improvements, and will present results of recent flight tests.

2. INTRODUCTION

High precision GNSS techniques are based on the ability of a receiver to accurately measure the accumulated carrier phase (or integrated Doppler frequency shift) to the satellites. These accumulated carrier phase (ACP) measurements are processed with respect to ACP measurements from a reference receiver. This results in highly precise relative positions between the antennas of the user receiver and the reference receiver. If the reference receiver antenna is in a surveyed location, then (absolute) differential positions are obtained for the user receiver antenna. For the purpose of this paper, user positioning accuracies are expressed relative to the location of the reference receiver.

Two distinct classes of processing methods are currently being evaluated for aircraft precision approach and landing operations:

1. The use of relative ACP measurements to smooth relative code-phase measurements, which results in user positioning accuracies on the order of 1 meter (95%) or better;

2. Ambiguity resolution of the relative ACP measurements to obtain user positioning accuracies on the order of centimeters.

Most ambiguity resolution methods rely on an accurate initial position estimate, which is usually obtained from the relative code-phase position solution.

The next section presents single, double, and triple difference processing, which is commonly used for high-accuracy GNSS position determination. This is followed by two sections on carrier smoothed code phase techniques and ambiguity resolved carrier phase techniques. Next, flight test results are presented for some of the processing techniques that have been demonstrated in real time.

3. SINGLE, DOUBLE, AND TRIPLE DIFFERENCE PROCESSING

A single difference (SD) is the difference between two measurements from the same satellite taken at two different receivers, see Figure 1. Therefore, the SD observable does not contain errors that are common between the two receivers. For small separation distances between the two receivers, these common errors include the satellite clock offset, satellite orbit errors, and atmospheric-propagation delays.

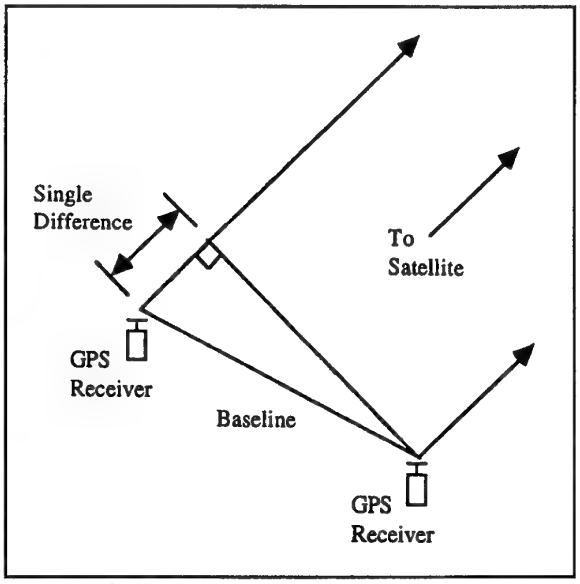

Figure 1. Single Difference Geometry

Single difference observation equations can be written for both the code phase (pseudorange or PR) and the accumulated carrier phase (ACP) measurements, see also (Ref 1)

Paper presented at the AGARD MSP Lecture Series on "System Implications and Innovative Applications of Satellite Navigation", held in Paris, France from 1-2 July 1996; Rome, Italy from 4-5 July 1996; Madrid, Spain from 8-9 July 1996 and St. Petersburg, Russia from 11-12 July 1996, and published in LS-207.

$$SD^{i}_{PR\,12} = \underline{b} \cdot \underline{e}^{i} = PR^{i}_{1} - PR^{i}_{2} + c\,\delta t_{12}$$
$$SD^{i}_{ACP\,12} = \underline{b} \cdot \underline{e}^{i} = \phi^{i}_{1} - \phi^{i}_{2} + N^{i}\lambda + c\,\delta t_{12} \qquad (1)$$

where $\underline{b}$ is the three-dimensional baseline vector in meters pointing from receiver 1 to receiver 2; $\underline{e}^{i}$ is the unit vector in meters pointing from the middle of the baseline vector to satellite i; PR^{i}_{1} and PR^{i}_{2} are the measured pseudoranges in meters for satellite i to receivers 1 and 2, respectively; c is the speed of light in meters per second; and δt_{12} is the clock offset between receivers 1 and 2 in seconds; ϕ^{i}_{1} and ϕ^{i}_{2} are the measured accumulated carrier phases in meters for satellite i to receivers 1 and 2, respectively; N^{i} is the integer ambiguity for satellite i; and λ is the wavelength of the carrier frequency in meters.

The unknown clock offset between receivers 1 and 2 can be eliminated by taking the difference between two independent single differences, also called the double difference (DD)

$$DD^{ij}_{PR\,12} = \underline{b} \cdot (\underline{e}^{i} - \underline{e}^{j}) = PR^{i}_{1} - PR^{i}_{2} - (PR^{j}_{1} - PR^{j}_{2})$$
$$DD^{ij}_{ACP\,12} = \phi^{i}_{1} - \phi^{i}_{2} - (\phi^{j}_{1} - \phi^{j}_{2}) + N^{ij}\lambda \qquad (2)$$

where $N^{ij} = N^{i} - N^{j}$.

The above double difference equations form the basis for all high-precision GNSS processing. The double difference geometry is show in Figure 2.

The unknown ambiguity N^{ij} in the ACP double difference can be eliminated by differencing two DDs at two successive measurement epochs to obtain a triple difference (TD). The TD provides the change of the DD between two successive measurement epochs. As such, it can be used to propagate the DD from one measurement to the next. Moreover, TDs can also be used to precisely propagate the user position from one time to the next with centimeter accuracy. The calculation of the TD, however, must be corrected for the known change in geometry during the interval of time between the two measurement epochs. A very accurate geometry correction is

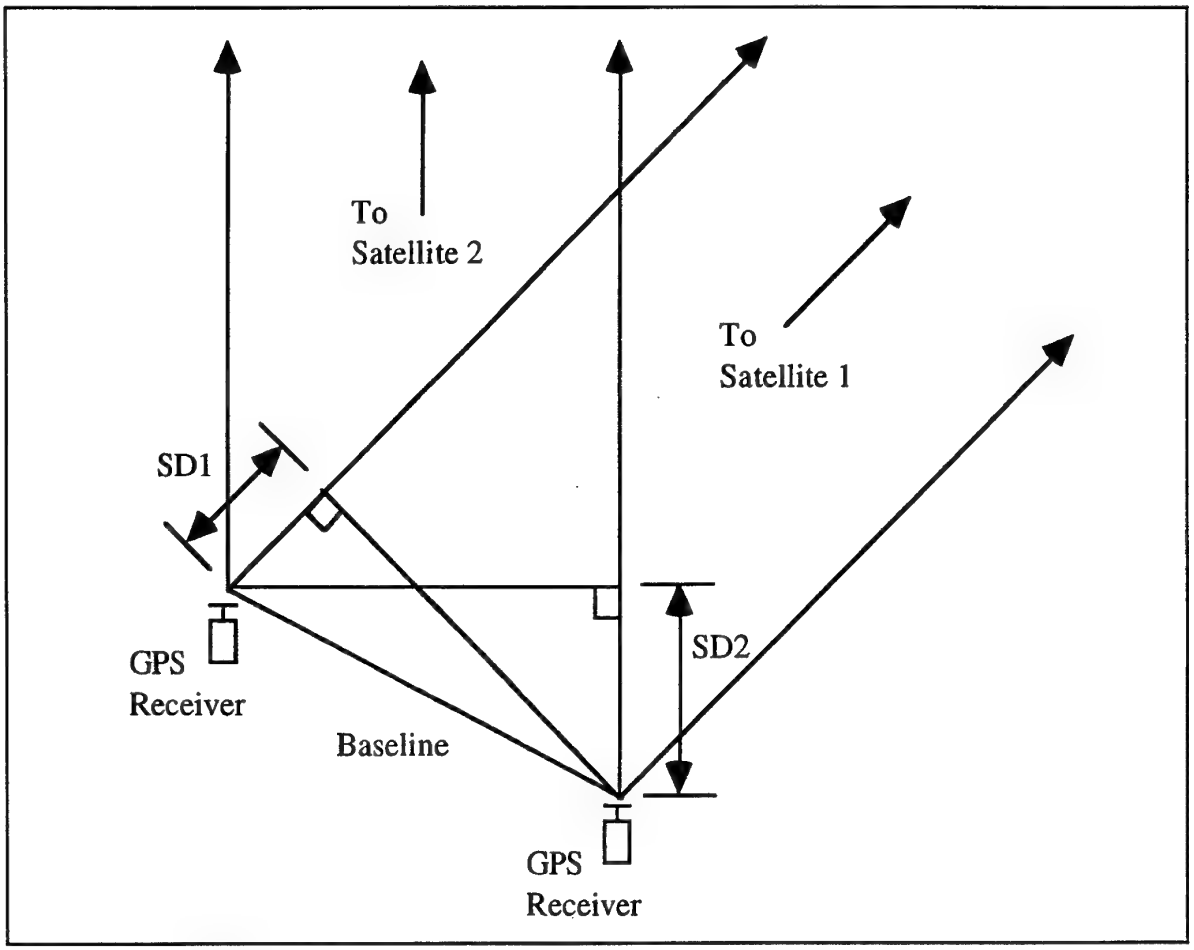

Figure 2. Double Difference Geometry

required to avoid build-up of systematic errors.

To obtain the geometry correction, a set of three double difference equations for four satellites is first rewritten in matrix form using simplified subscripts (Ref 2)

$$\begin{pmatrix} DD_1 \\ DD_2 \\ DD_3 \end{pmatrix} = \begin{pmatrix} (\underline{e}_1 - \underline{e}_r)^T & 1 & 0 & 0 \\ (\underline{e}_2 - \underline{e}_r)^T & 0 & 1 & 0 \\ (\underline{e}_3 - \underline{e}_r)^T & 0 & 0 & 1 \end{pmatrix} \begin{pmatrix} x \\ y \\ z \\ N_1 \\ N_2 \\ N_3 \end{pmatrix} \quad (3)$$

where: the variable DD_i now represents the i^{th} linear combination of four accumulated carrier phase measurements; $\underline{e}_i$ is the unit vector to the i^{th} satellite; $\underline{e}_r$ is the unit vector to the reference satellite; N_i is the integer ambiguity for the i^{th} DD; and x, y, and z are the three-dimensional components of the baseline vector, $\underline{b}$. Equation (3) can be written as

$$\underline{DD} = H\beta \quad (4)$$

Next, consider the DD vectors at time 1 and time 2

$$\begin{aligned} &\text{Time 1: } \underline{DD}_1 = H_1\beta_1 \\ &\text{Time 2: } \underline{DD}_2 = H_2\beta_2 \end{aligned} \quad (5)$$

The difference of the DD vectors at time 1 and time 2 is given by the triple difference vector, $\underline{TD}$

$$\underline{TD} = \underline{DD}_2 - \underline{DD}_1 = H_2\beta_2 - H_1\beta_1 \quad (6)$$

which can also be written as

$$\underline{TD} = H_2^*\underline{b}_2 - H_1^*\underline{b}_1 \quad (7)$$

where H^* is the sub-matrix of H which contains the unit vectors only; and $\underline{b}$ contains the x, y, and z coordinates of the baseline vector.

Equation (7) can be written as

$$\underline{TD} = H_2^*(\underline{b}_1 + \underline{\Delta b}) - H_1^*\underline{b}_1 \quad (8)$$

Finally, the accurate three-dimensional change in the user position from time 1 to time 2 is obtained using the generalized inverse of the H_2^* matrix

$$\underline{\Delta b} = (H_2^{*T}H_2^*)^{-1}H_2^{*T}(\underline{TD} - (H_2^* - H_1^*)\underline{b}_1) \quad (9)$$

Equation (9) can be used to propagate the baseline vector from one measurement time to the next. It is noted that all "usual" GPS corrections must be applied as well, including those to account for the different times of transmission of the signals for receivers 1 and 2; and tropospheric delay corrections. These corrections can be found in detail in (Ref 1).

If the user receiver starts at a known position, then equation (9) can be used to successively propagate the user position with centimeter-level accuracy using accumulated carrier phase measurements only. Figure 3 shows a performance example where equation (9) is applied to actual GPS flight data from a Boeing 757 at Atlantic City International Airport. For a description of the flight test scenario, see section 6. Propagated position results from single-frequency GPS receivers are compared with a post-processed dual-frequency kinematic reference trajectory obtained from Ashtech Z-12 GPS receivers. The Z-12 data was post-processed using the Ashtech PNAV software package. Differences between the two solutions are within 0.1 meters in all three coordinate axes.

4. CARRIER SMOOTHED CODE PHASE TECHNIQUES

4.1 Introduction

Thermal measurement noise and multipath error are the two main error sources for high-precision GNSS techniques. In Section 4.2, it is shown that the code phase errors are much larger than the accumulated carrier phase errors. However, the code phase measurements provide an absolute position reference, while the accumulated carrier phase only provide information about change in the position. The two types of measurements can be combined using a variety of techniques to produce a smoothed-code estimate. For example, a complementary Kalman filter can be used based on the following equations (Ref 3)

$$\begin{aligned} &DD_{k_{EST}}^- = DD_{k-1_{EST}}^+ + (DD_{k_{ACP}} - DD_{k-1_{ACP}}) \\ &p_k^- = p_{k-1}^+ + q \\ &k_k = p_k^-(p_k^- + r)^{-1} \\ &DD_{k_{EST}}^+ = DD_{k_{EST}}^- + k_k(DD_{k_{PR}} - DD_{k_{EST}}^-) \\ &p_k^+ = (1 - k_k)p_k^- \end{aligned} \quad (10)$$

where the superscript '-' indicates that the parameter is predicted, and the superscript '+' indicates that the parameter is estimated; q is the variance of the code phase (PR) double difference; r is the variance of the code phase double difference measurement; p is the variance of the estimation error; and k is the Kalman gain. The first two lines of equation (10) propagate the estimated code phase double difference and the estimation error variance from time (k-1) to time k, followed by the calculation of the Kalman gain (line 3), and the update of the estimated code phase double difference and the estimation error variance (lines 4 and 5). Typical smoothing time constants are on the order of 50 to 100 seconds. Longer time constants can be used, but that would increase the initialization time of the high-accuracy solution.

In some applications, the code and carrier measurements are first converted to the position domain before the smoothing is applied (Ref 4). In this case, equation (9) is used to propagate the position estimate forward in time using the changes in the accumulated carrier phase measurements. Next, the position

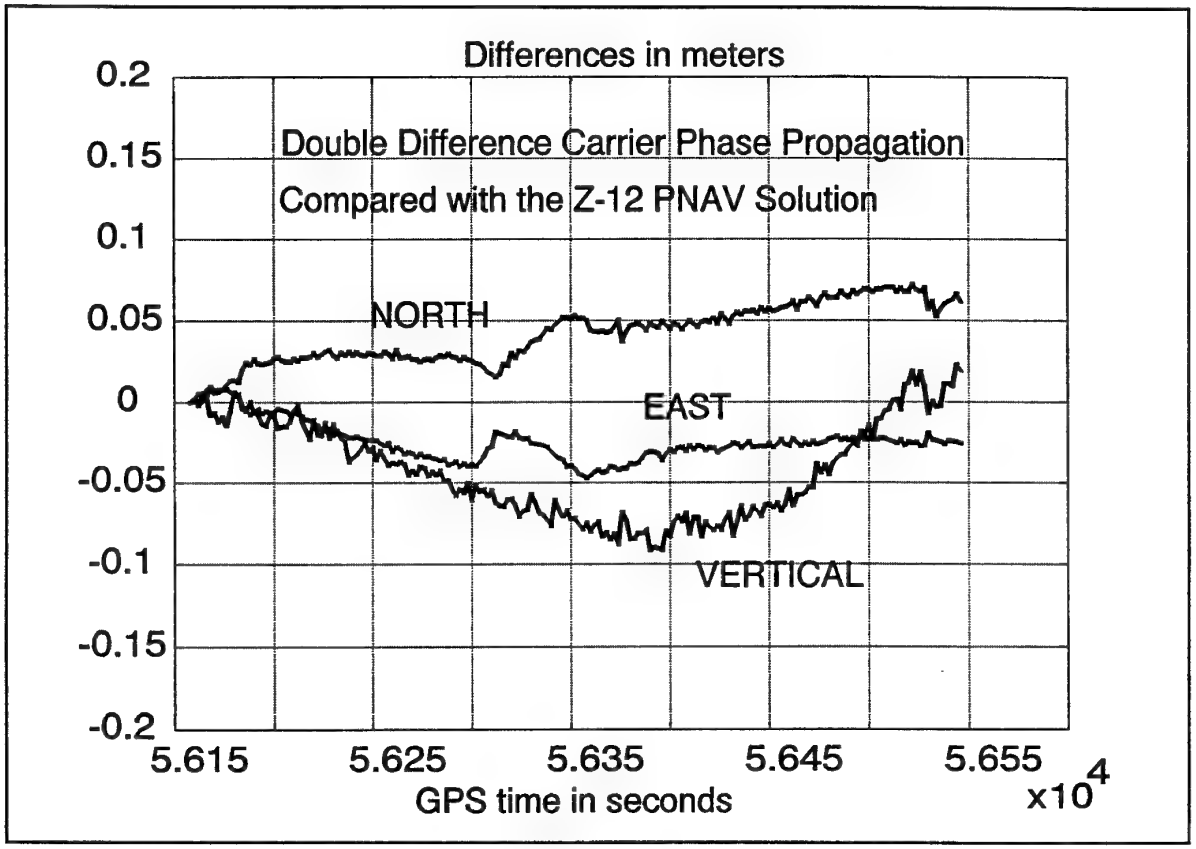

Figure 3. Propagation of Aircraft Position Using Accumulated Carrier Phase Measurements

estimate is updated based on the code phase measurements using a small gain. This method has the advantage that position solution discontinuities to not occur when satellites are switched in and out of the solution. Also, the carrier phase update is very accurate (centimeter-level accuracy), which allows for fault detection with a small threshold on the order of 5-10 cm.

4.2 Thermal Noise and Multipath Error

Code phase measurement noise is typically on the order of 0.5 to 4 meters depending on the receiver architecture and the satellite signal strength (Ref 5). The rms tracking error for a second-order phase coherent delay-lock loop for bi-phase modulation is given by (Ref 6)

$$\sigma = \Delta \sqrt{\frac{B_n N_0}{2S}} \quad \text{(m)} \qquad (11)$$

where B_n is the equivalent noise bandwidth of the loop, Δ is the chip period in meters (293 m for the GPS C/A Code), S is the average received signal power in Watts, and N_0 is the receiver input noise power density, one-sided in W/Hz. As shown in (Ref 7), the rms tracking error for an intermediate frequency (IF) bandwidth of 100 Hz is essentially the same as the rms tracking error given in equation (11) for C/N_0 greater than 40 dB-Hz. Using the carrier-to-noise ratio with $C/N_0 = S/N_0$, equation (11) is written as

$$\sigma = \Delta \sqrt{\frac{B_n}{2C/N_0}} \quad \text{(m)} \qquad (12)$$

Figure 4 shows the rms tracking error as a function of C/N_0 for 0.5 and 4 Hz tracking loop bandwidths. For example, if $B_n = 4$ Hz and $C/N_0 = 40$ dB-Hz, then the rms tracking error for the GPS C/A-Code is 4.24 meters. The tracking loop

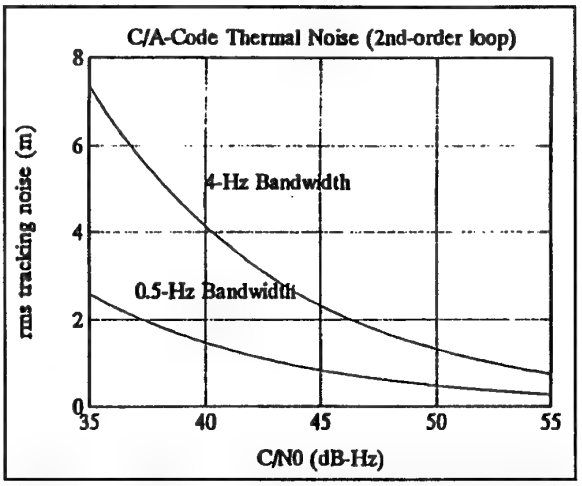

Figure 4. GPS Receiver Code Tracking Measurement Noise

bandwidth is directly related to the data renewal rate. A tracking loop bandwidth of 4 Hz allows for a data renewal rate of 8 samples per second for continuous-wave signals.

The rms tracking error for a coherent carrier tracking loop with a small IF bandwidth is given by (Ref 7)

$$\sigma_\lambda = \frac{\lambda}{2\pi}\sqrt{\frac{B_n}{C/N_0}} \quad \text{(m)} \qquad (13)$$

where λ is the wavelength of the carrier frequency in meters (GPS L1: λ = 0.19 m). Figure 5 shows the rms tracking error as a function of C/N_0 for three different tracking loop bandwidths. For example, if B_n = 16 Hz and C/N_0 = 50 dB-Hz, then σ_λ = 0.4 mm. Note that if the accumulated carrier phase is obtained from the receiver at a rate of once per second, the equivalent B_n is 0.5 Hz, reducing σ_λ to below 0.1 m.

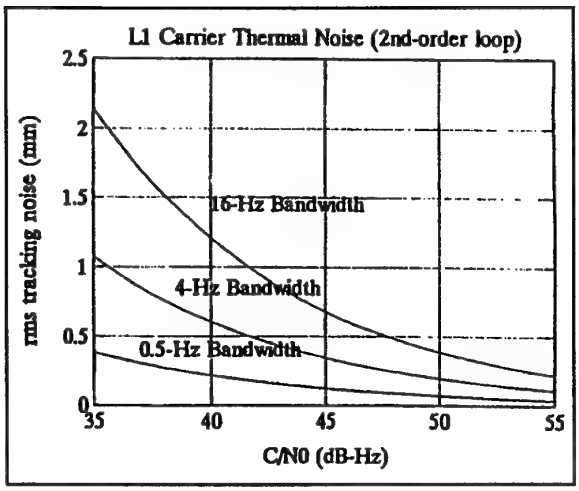

Figure 5. GPS Receiver Carrier Tracking Measurement Noise

Code phase multipath errors for precision landing applications are typically on the order of 1-2 meters, while carrier phase multipath errors are on the order of 1 centimeter (Ref 8). Furthermore, carrier phase multipath errors are limited to a quarter wavelength (approximately 4.8 cm for GPS L1) if the multipath signal is weaker than the direct satellite signal.

5. AMBIGUITY RESOLVED CARRIER PHASE TECHNIQUES

5.1 Ambiguity Resolution Methods

In 1981, the first relative GPS Doppler positioning experiment was reported, which resulted in sub-decimeter accuracies for antenna displacements of 2 to 3 meters (Ref 9). GPS surveying was also performed using only the fractional portion of the GPS carrier phase in combination with satellite orbit information (Refs 10 and 11). During the 1980's, these basic techniques were further developed by many researchers (Refs 12-15).

The basic idea behind all ambiguity resolution methods is to find values for the integer number of unknown wavelengths or ambiguities, N^{ij}, as expressed in equation (2). If only one set of measurements from four satellites is available, then the true ambiguities can only be found if the code phase solution is sufficiently accurate to predict the accumulated carrier phase double differences to within one halve of a wavelength. In the case of a GPS L1-only system, the wavelength is approximately 19 cm. Therefore, a code phase positioning accuracy of better than 9.5 cm would be necessary. If two GPS frequencies are available, then the difference frequency (L1-L2, where L2 = 1227.6 MHz) has a wavelength of approximately 86 cm, which would require a code phase positioning accuracy of better than 43 cm. In some cases, the latter accuracy of 43 cm can be obtained, but an accuracy of 9.5 cm for a L1 code-phase position is not reliably attainable. It is further noted that an uncertainty of one wavelength in each direction corresponds to three possible ambiguities for each double difference, which results in a total number of potential ambiguity sets of $3^3 = 27$. If the uncertainty grows to five wavelengths (approximately 1 meter for GPS L1), then the number of potential ambiguity sets grows to $3^{11} = 177147$.

Therefore, to determine the correct ambiguity set, additional information is required. Two sources of additional information can be identified:

1. Redundant Measurements
2. Time

Redundant measurements can be used to cross-check potential ambiguity sets. This reduces the number of potential sets. Unfortunately, many redundant measurements are required to reduce the number of potential sets to one.

Time can be used in two different ways. First, time can be used to smooth the code phase solution to improve its accuracy, which in turn reduces the position uncertainty and the number of potential ambiguity sets. Similarly, time also provides additional carrier measurements, which can be averaged to improve the consistency of the correct set of ambiguities. Second, as time passes, the geometry changes, which, in essence, results in redundant measurements. Geometry changes can either result from satellite movement or from user movement.

Most current ambiguity resolution methods use a combination of time and redundant measurements. The concept behind these methods is illustrated in Figure 6 for a two-dimensional example. Shown in Figure 6 a) are wavefronts from two different satellites. The separation between the wavefronts is equal to one wavelength. Each intersection point between the two wavefronts represents a potential position solution. Adding a third satellite produces another wavefront, which reduces the number of potential position solutions as shown in Figure 6 b). Potential position solutions are those for which the three wavefronts closely intersect. A changing geometry causes the wavefronts to rotate around the correct position solution as shown in Figure 6 c). Given a sufficient amount of geometry change, the incorrect positions no longer have closely intersecting wavefronts.

In the next sections, four distinct ambiguity resolution methods are summarized.

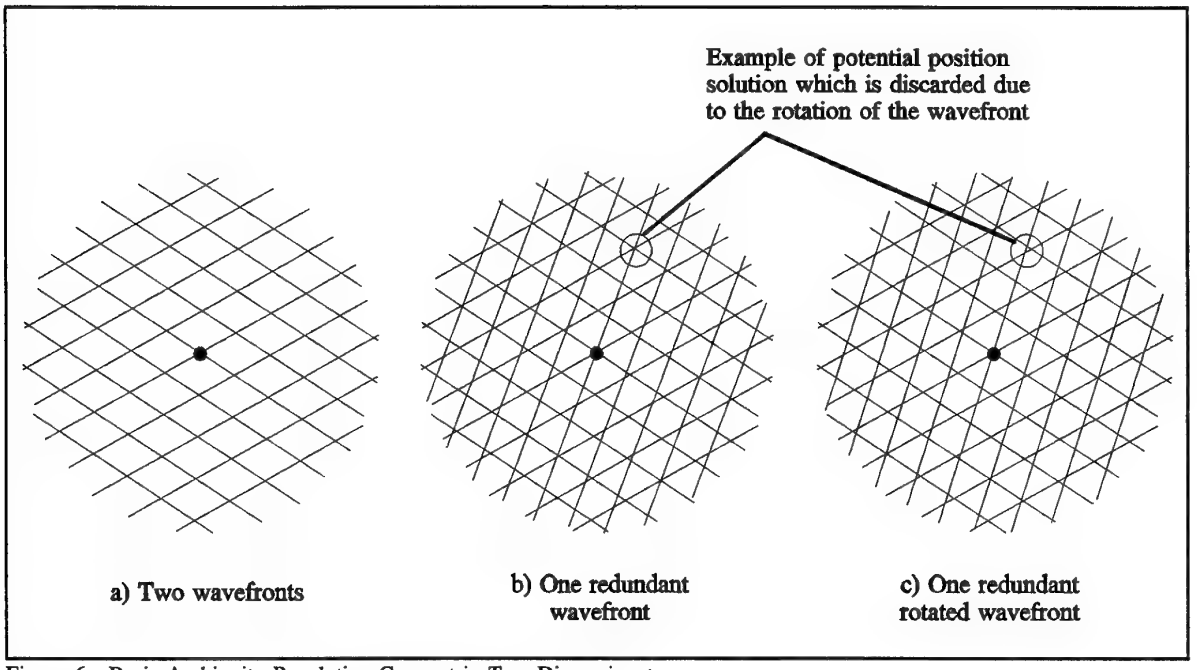

Figure 6. Basic Ambiguity Resolution Concept in Two Dimensions

5.1.1 Ambiguity Function Method

The first method published for ambiguity resolution is the Ambiguity Function Method (AFM) (Ref 10). Rather than evaluating potential ambiguity sets, this technique evaluates trial positions. This is mathematically equivalent to evaluating potential ambiguity sets. The AFM searches for the position where the measured carrier phase double differences minus the predicted double differences based on the trial position are closest to integer values for all double difference measurements. The ambiguity function is given by

$$AF_{TRIAL} = \frac{\sum_{n=1}^{N}\sum_{p=1}^{M} \cos(DD_{ACP}^{np} - DD_{TRIAL}^{np})}{NM} \qquad (14)$$

where N is the number of measurement sets, M is the number of double differences, and DD_{TRIAL} is the predicted double difference based on the trial position.

At the correct location, the ambiguity function is a maximum. Since the initial introduction of the AFM, several methods have been published to improve the processing time, see for instance (Ref 16). Also, methods have been developed to apply the AFM to dynamic applications (Ref 17).

5.1.2 Least Squares Ambiguity Search

The Least Squares Ambiguity Search Method (LSASM) was developed for dynamic positioning at the centimeter level (Ref 18). It uses redundant measurements as well as a good code-phase position solution to constrain the ambiguity search. LSASM uses the following measurement equation:

$$y + e = A\beta \qquad (15)$$

where: y is the observation vector; e is the error vector; A is the design matrix and β is the state vector (position and clock). Also

$$\text{rank}(A) = n,\ E(e) = 0,\ \text{cov}(e) = \text{cov}(y) = \sigma^2 P^{-1} \qquad (16)$$

Next, the projection matrix S is used to map the changes in the ambiguities into changes in the residuals

$$S = (I - A(A^T P A)^{-1} A^T P) \qquad (17)$$

The correct solution will have small residuals. The residual calculation process can be simplified by using other types of transformations, such as those used in the parity space algorithm (Ref 3).

5.1.3 Integrated Doppler Double Difference Method (IDM)

This method relies on both redundant measurements and on changing geometry to estimate the ambiguities. Once the estimate has converged, a small search is performed to find the correct ambiguity set. An interesting feature of this method is that it also works in the absence of code phase measurements (Refs 2, 19). Similar to the previous two methods, a minimum of two redundant satellites is required for a rapid (on the order of minutes) convergence of the position solution. The term Integrated Doppler is used instead of accumulated carrier phase to describe the actual measurement made by the receiver.

Following is a summary of the iterative calculations of the IDM processing.

1. Approximate the current position using the previous position, the previous geometry matrix, and the accumulated carrier phase triple difference (TD) measurements, see equation (9)

$$\underline{b}_2' = \underline{b}_1 + (H_1^{*T} H_1^*)^{-1} H_1^{*T} \underline{TD} \qquad (18)$$

Note that this approximation is accurate to within a few centimeters.

2. Use the approximate current position to construct the current geometry matrix, H_2^*, equation (7).

3. Propagate the user position to the current time, where the accurate change in the user position is obtained from equation (9)

$$\underline{b}_2^- = \underline{b}_1 + \Delta \underline{b} \qquad (19)$$

4. Construct the propagated state vector by replacing the first three (position) elements by the elements of $\underline{b}_2^-$; and construct the current H_2 matrix using $\underline{b}_2^-$ (see also equation (3)).

5. Calculate the Kalman Gain matrix

$$K = P^- H_2 (H_2 P^- H_2^T + R)^{-1} \qquad (20)$$

where P is the error covariance matrix, and R is the measurement covariance matrix.

6. Update the state vector

$$\underline{\beta}^+ = \underline{\beta}^- + K(\underline{DD} - H_2 \underline{\beta}^-) \qquad (21)$$

Note that the carrier phase double differences are used in equation (21).

7. Update the error covariance matrix

$$P^+ = (I - KH_2)P^- + Q \qquad (22)$$

where Q is the process noise covariance matrix, and I is the identity matrix.

8. Replace the state vector, the error covariance matrix, the H matrix, and the user position for the next iteration

$$P^- = P^+; \quad \underline{\beta}^- = \underline{\beta}^+; \quad H_1 = H_2$$
$$\underline{b}_1 = (\beta^-(1) \ \beta^-(2) \ \beta^-(3))^T \qquad (23)$$

Typically, the measurement covariance matrix is initialized as a diagonal matrix, with variances of 2 millimeters squared. The process noise covariance matrix is initialized as a diagonal matrix also, with position coordinate variances of 1-10 centimeters squared and ambiguity variances on the order of 10 micrometers squared. The state vector can be initialized using the reference station position coordinates. A GPS-derived stand-alone or differential position solution could be used also, but this is not required.

5.1.4 Integrity Beacon Method

The Integrity Beacon ambiguity resolution method relies on a large change in geometry obtained by flying over a beacon, which transmits GPS-like signals. A GNSS satellite requires 6-8 hours to complete one pass over the user. The same amount of geometry information can be obtained in approximately 20 seconds by flying over a ground-based satellite. Figure 7 shows the integrity beacon concept (from Ref 20).

If two integrity beacons are used, then the linearized measurement equation for one set of measurements is given by

$$\begin{pmatrix} \delta\varphi_{1k} \\ \vdots \\ \delta\varphi_{mk} \\ \delta\phi_{1k} \\ \delta\phi_{2k} \end{pmatrix} = \begin{pmatrix} -\hat{s}_{1k}^T & 1 & 0 & 0 & \cdots & 0 \\ \vdots & \vdots & 1 & 0 & \cdots & 0 \\ -\hat{s}_{mk}^T & 1 & 0 & 1 & \cdots & 0 \\ -\hat{e}_{1k}^T & 1 & \vdots & \vdots & \ddots & \vdots \\ -\hat{e}_{2k}^T & 1 & 0 & 0 & \cdots & 1 \end{pmatrix} \begin{pmatrix} \delta x_k \\ \delta y_k \\ \delta z_k \\ \tau_k \\ N_2^s \\ \vdots \\ N_m^s \\ N_1^p \\ N_2^p \end{pmatrix} \qquad (24)$$

where $\delta\varphi_{1k}$ through $\delta\varphi_{mk}$ are the single differences for the satellite ACP measurements at time k; $\delta\phi_{1k}$ and $\delta\phi_{2k}$ are the single differences for the beacon ACP measurements; $\hat{s}$ and $\hat{e}$ are the unit vectors to the satellites and the beacons, respectively; τ_k is the clock bias which is common for all measurements at time k; N_2^s through N_m^s are the ambiguities for satellites 2 through m (note that the ambiguity for satellite 1 is set to zero); and N_1^p and N_2^p are the ambiguities for the beacons (note that these ambiguities also contain the hardware and installation biases with respect to the GPS measurements).

The position solution is obtained by iterating approximately 20 sets of linearized single difference measurements as given in equation (24) in a batch solution (Ref 20). Because this method resolves the satellite ambiguities, centimeter-level positioning accuracy are achieved.

5.2 Accuracy Considerations

Successful ambiguity resolution requires that the ACP measurement errors are small enough to allow for a reliable determination of the correct ambiguity set. The larger the measurement errors, the more time the ambiguity resolution process requires to obtain a solution with a high level of confidence. Once the correct set of ambiguities has been determined, several error sources remain that affect the user positioning accuracy.

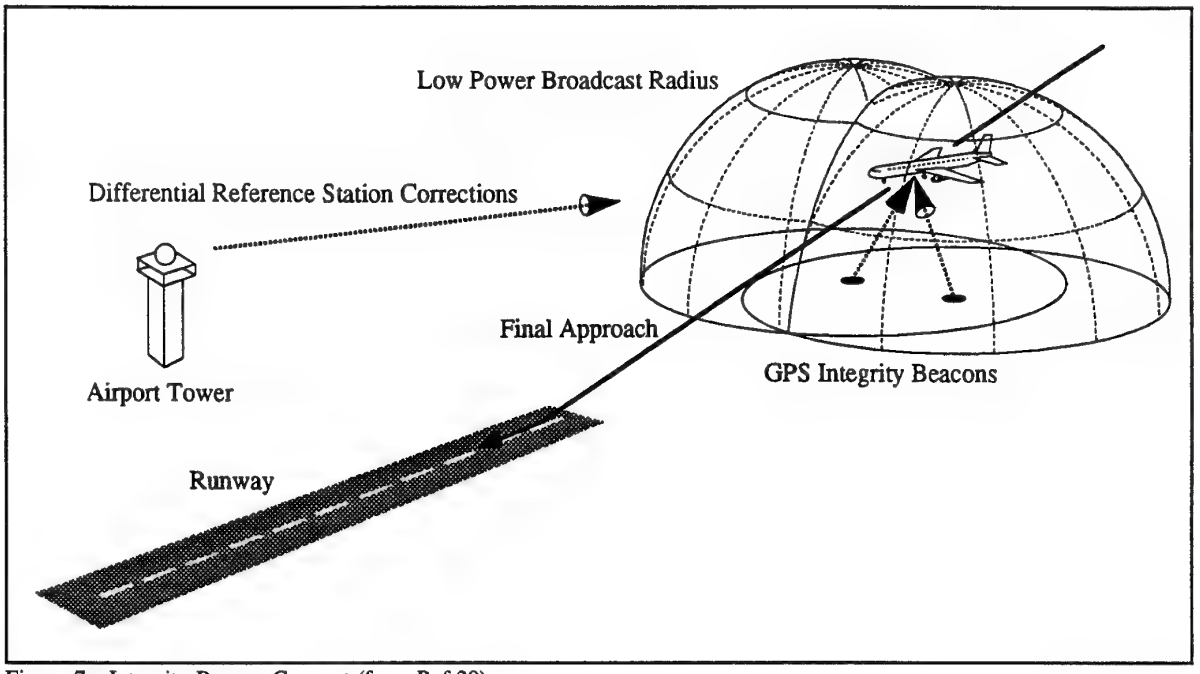

Figure 7. Integrity Beacon Concept (from Ref 20)

For a small baseline between the reference and the user antennas, the main carrier phase error sources are the antenna phase center uncertainty, receiver hardware errors, and multipath. The first two error sources are typically on the order of 3-5 mm, while multipath error is generally less than 1 cm. For longer baselines, satellite orbit errors as well as tropospheric and ionospheric propagation delays decorrelate between the two receivers. Typical values for these errors are listed below as a function of the distance between the reference receiver and the user receiver (Ref 21)

tropospheric delay	0.2 - 0.4 mm/km
ionospheric delay	0.25 - 2.0 mm/km
satellite orbit	3 - 5 mm/km

Note that satellite orbit errors can cause ACP errors on the order of 5 cm at a distance of 10 km. ACP errors of 5 cm would translate into positioning errors on the order of 10 cm. This would clearly cause a problem for single frequency (GPS L1) ambiguity resolution. It is not possible to distinguish between two adjacent carrier phase zero-crossings, which are separated by 19 cm. Furthermore, most of the above listed error sources can change both as a function of location and as a function of time (e.g. multipath). This further complicates the ambiguity resolution process, as most geodetic processing methods strongly rely on the stability of the carrier phase residuals. For this reason, high-precision static surveying techniques do not rely on the broadcast orbits from the satellites. Instead, precision orbits from other sources are used to post-process the measurement data. In summary, carrier-phase ambiguity resolution techniques for aircraft over distances greater than a few km are only practical if dual-frequency techniques are used or if ground-based beacons are used to augment the satellites.

6. FLIGHT TESTS RESULTS

Many of the high-accuracy GNSS techniques described in this paper were recently flight tested as part of a Category III feasibility program conducted by the U.S. Federal Aviation Administration (FAA) (Ref 22). The FAA is pursuing the development of differential GPS (DGPS) in a local area configuration: the Local Area Augmentation System (LAAS). A LAAS at a particular airport is intended to support precision approach and landings (including automatic landings) and airport surface navigation. FAA's LAAS feasibility program was established in 1992 with the plan to show feasibility of accuracy and integrity through research and flight testing by mid-1995. Three high-precision system architectures were evaluated: 1) Carrier-smoothed code-phase DGPS; 2) Kinematic dual-frequency carrier-phase GPS; and 3) Kinematic single-frequency carrier-phase with ground-based integrity beacons.

Evaluation of accuracy for the feasibility program was performed in two different ways (Ref 22):

Navigation Sensor Error (NSE). NSE is defined as the difference between the aircraft position as derived by the navigation system and the laser tracker truth system. Since real-time carrier phase methods have accuracies on the order of 0.1 m, these systems were evaluated with respect to NSE.

Total System Error (TSE). TSE is the offset of the aircraft position from the desired flight path as determined by the laser tracker. TSE is the sum of the NSE and the Flight Technical Error (FTE). FTE is the flight control system's error, when used in the operating environment, in correcting the offset from the desired flight path as indicated by the navigation system.

Code-based systems were mostly evaluated with respect to the TSE due to a larger NSE compared to carrier phase systems.

Details of the accuracy results are available from a number of papers presented by the system developers (Refs 2, 4, 23-27). The CAT III feasibility program flight tests are summarized in Table 1 (Ref 22).

Figure 8 summarizes the accuracy results in terms of NSE and TSE. Results are provided at approximately 50 feet Height Above the runway Threshold (HAT) in terms of the mean + twice the standard deviation ($|\mu| + 2\sigma$). Data for all parameters were collected during all of the flight tests, except for the E-Systems configuration, which did not have an autoland capability.

Table 1. CAT III Feasibility Program Flight Tests (from Ref 22)

Developer	Location of Test/ Host Aircraft	Date of Test	No. of Approaches	Evaluation Criteria
Wilcox	FAA Technical Center/ Boeing 727-200 FEDEX	4/95	100	TSE (Code)
E-Systems	NASA Crows Landing/ Westwind II	6/95	100	NSE (Carrier)
Ohio University	FAA Technical Center/ Boeing 757-200 UPS	10/94,2/95	100	TSE (Code)
Stanford University	NASA Crows Landing/ Boeing 737-300 UA	10/94	100	NSE (Carrier)

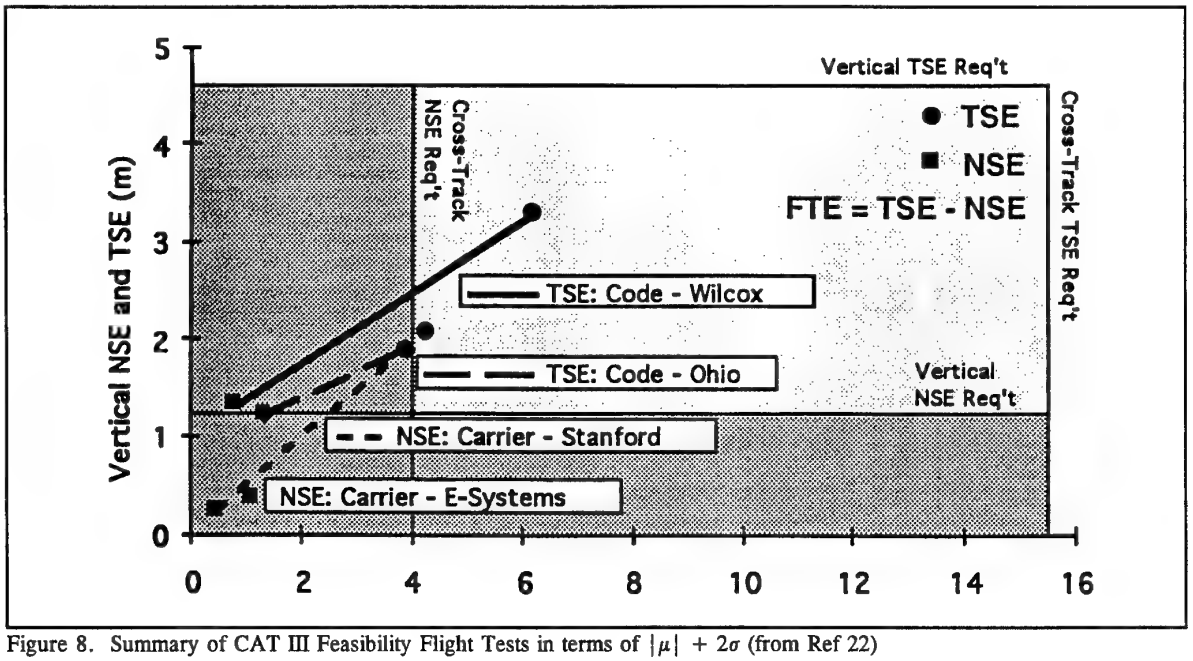

Figure 8. Summary of CAT III Feasibility Flight Tests in terms of $|\mu| + 2\sigma$ (from Ref 22)

Figure 9 show an overview of the Ohio University carrier-smoothed code-phase DGPS system. A similar architecture was also used by the Wilcox-Electric Company. Comparing the two carrier-smoothed code phase systems (Wilcox and Ohio University) shows that the NSEs are comparable, but the Ohio University TSE is significantly smaller than that of Wilcox. This is due to the superior autopilot performance of the newer B-757 as compared to the B-727. Figures 10 and 11 provide additional detail on the Ohio University TSE performance referenced to the proposed Required Navigation Performance 95% accuracy containment. From these figures, it can be observed that the DGPS error is essentially constant throughout the final approach segment of the flights.

The ambiguity resolved carrier phase systems have comparable NSEs, which are smaller than the laser tracker truth reference system specification of approximately 0.3 m (95%).

In addition to the FAA feasibility program results, Figure 12 shows results from a flight test for the Integrated Doppler Double Difference Method (IDM) described in Section 5.1.3. The aircraft flight path for this test is shown in Figure 13. Vertical position accuracy results are shown for initial position uncertainties of 2 and 800 meters. For both cases, the position converges to within 1 meter after 200 seconds. It is noted, however, that this method requires seven or more satellites for a rapid convergence of the position solution.

7. REFERENCES

1. Diggle, D.W. , "An investigation Into The Use Of Satellite-Based Positioning Systems For Flight Reference/Autoland Operations," Ph.D. Dissertation, Department of Electrical and Computer Engineering, Ohio University, Athens, Ohio, 1994.

2. Van Graas, F. and Lee, S-W, "High-Accuracy Differential Positioning For Satellite-Based Systems Without Using Code-Phase Measurements," NAVIGATION: The Journal of The Institute of Navigation, Vol. 42, No. 4, Winter 1995-1996.

3. Van Graas, F. and Braasch, M.S., "GPS Interferometric Attitude and Heading Determination: Initial Flight Test Results," Journal of The Institute of Navigation, Vol. 38, No. 4, Winter 1991-92.

4. Van Graas, F., et al., "FAA/Ohio University/United Parcel Service DGPS Autoland Flight Test Demonstration," in Proceedings of The Institute of Navigation GPS-95 Meeting, 12-15 September 1995.

5. Braasch, M.S. and Van Graas, F., "Guidance Accuracy Considerations for Real Time GPS Interferometry," in Proceedings of the 4th International Meeting of the ION Satellite Division, Albuquerque, NM, 9-13 September 1991.

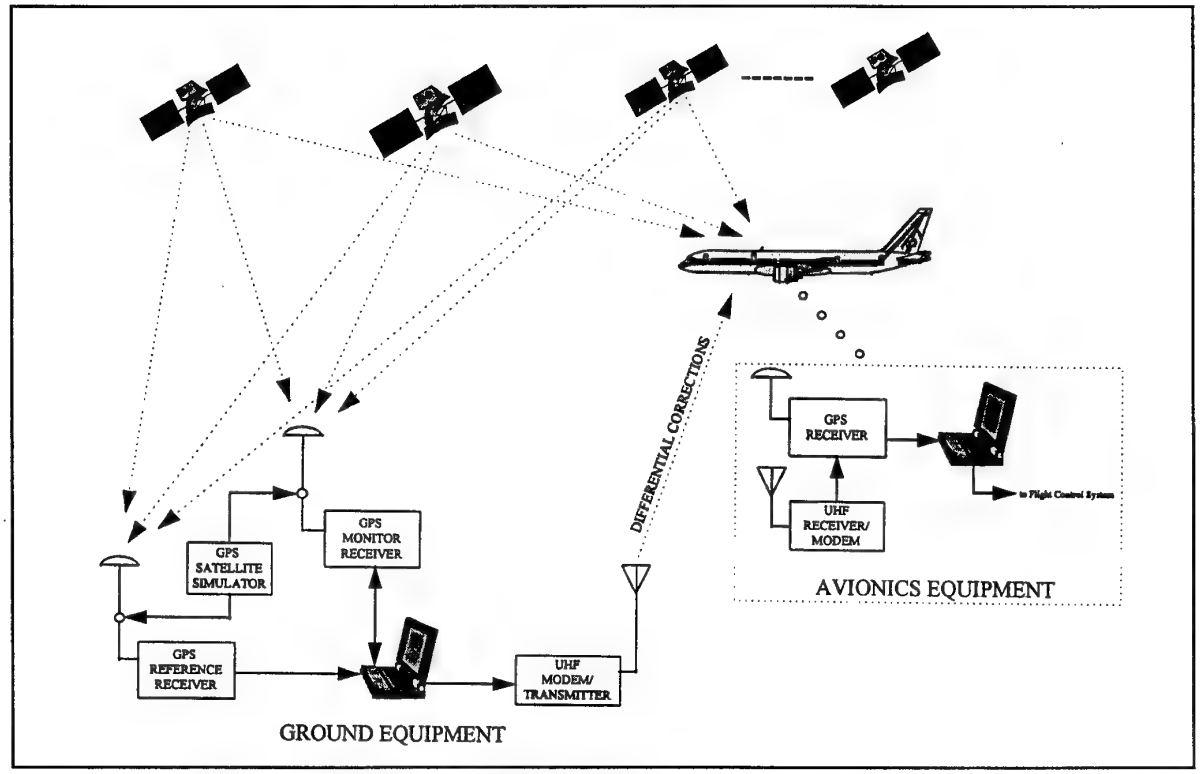

Figure 9. Ohio University Carrier-Smoothed Code-Phase System Overview

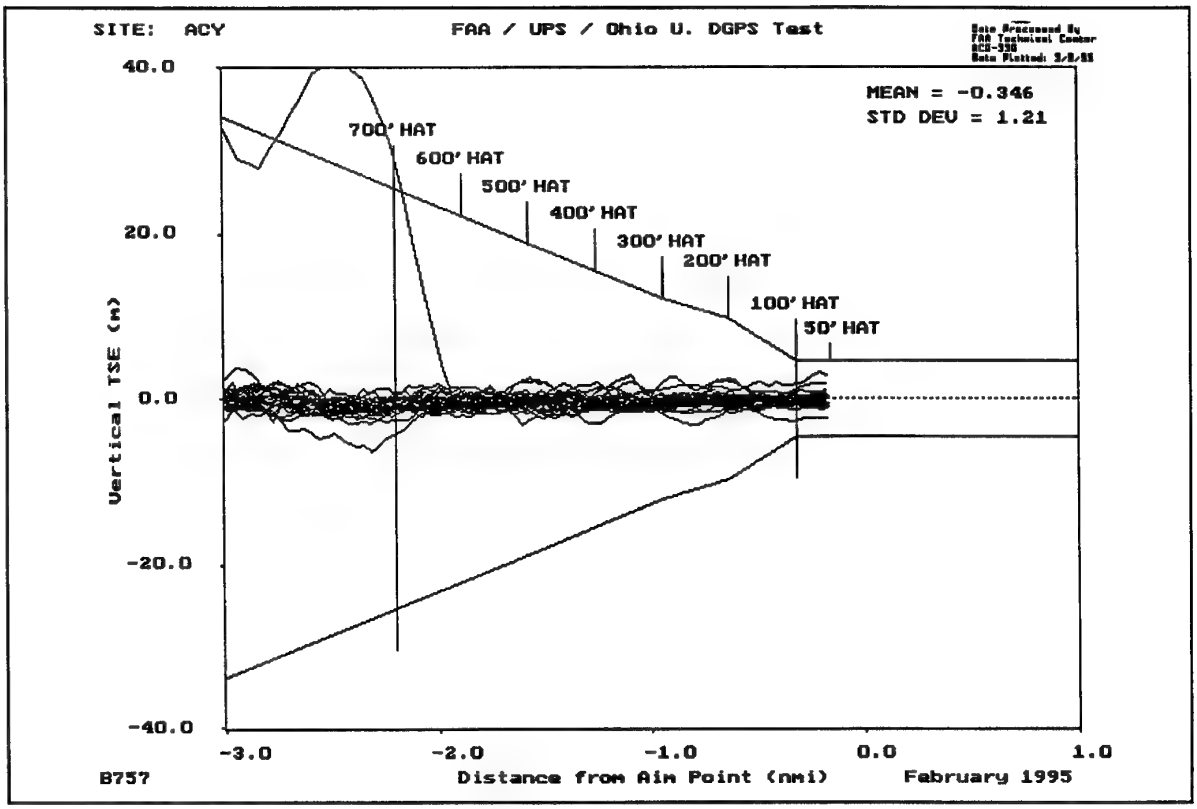

Figure 10. Vertical Total System Error for All DGPS Approaches for the Ohio University System

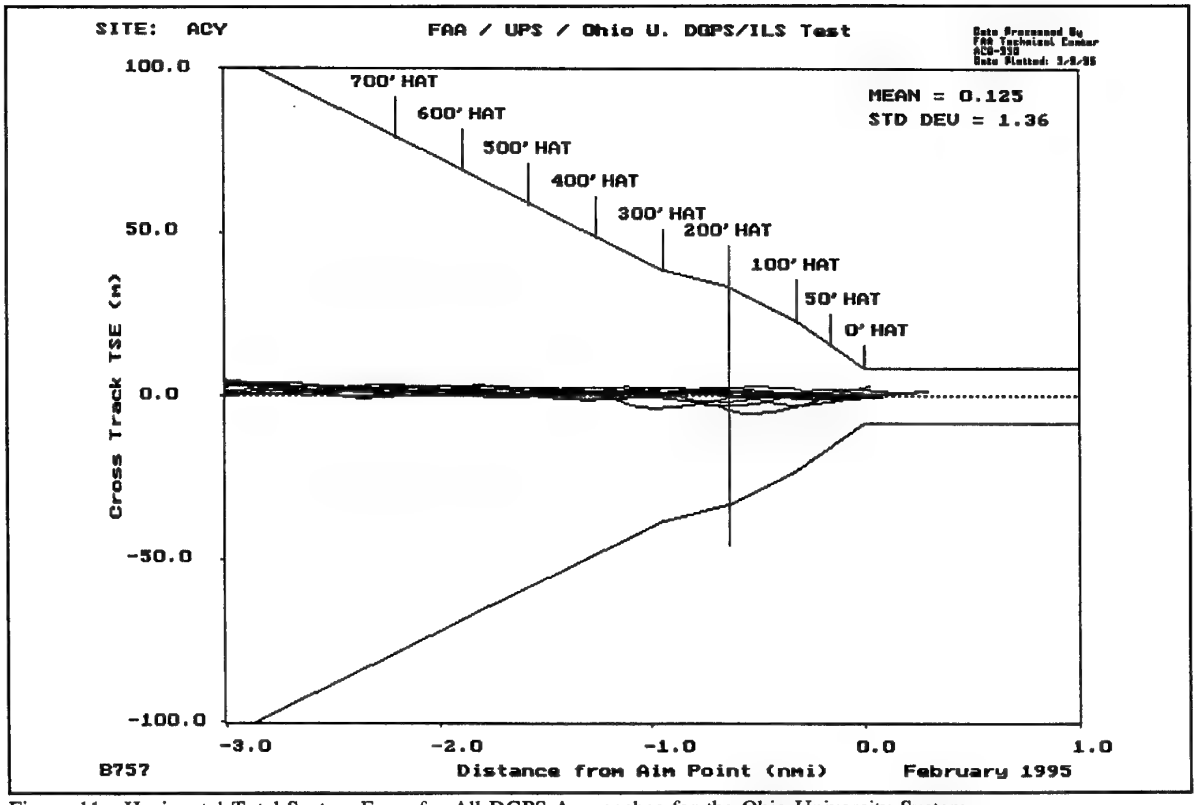

Figure 11. Horizontal Total System Error for All DGPS Approaches for the Ohio University System

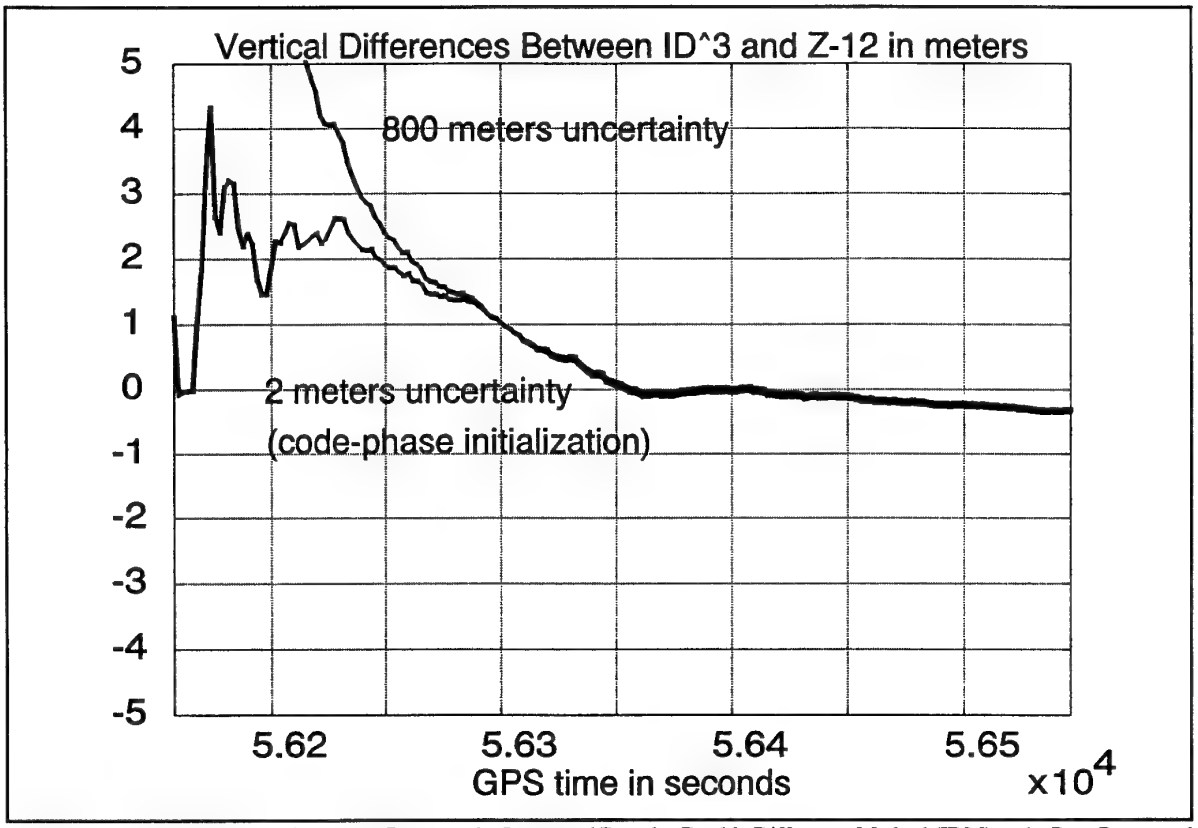

Figure 12. Vertical Position Differences Between the Integrated Doppler Double Difference Method (IDM) and a Post-Processed Dual-Frequency Solution

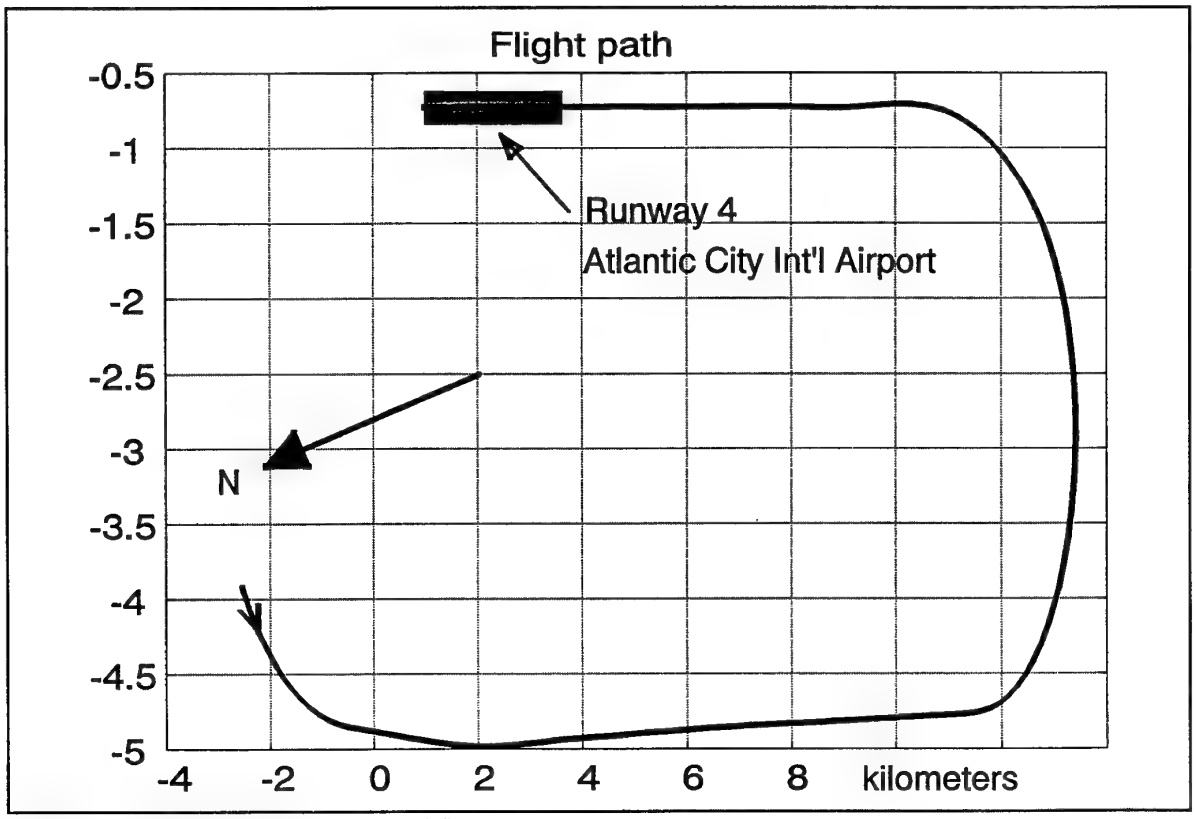

Figure 13. Aircraft Flight Path for the IDM Test

6. Gill, W., "A Comparison of Binary Delay-Lock Tracking-Loop Implementations, IEEE Transactions on Aerospace and Electronic Systems, Vol. AES-2, No. 4, July 1966.

7. Spilker, Jr., J., "Digital Communications by Satellite," Prentice-Hall, Inc., 1977.

8. Braasch, M.S., "On the Characterization of Multipath Errors in Satellite-Based Precision Approach and Landing Systems," Ph.D. Dissertation, Department of Electrical and Computer Engineering, Ohio University, Athens, Ohio, 1992.

9. Evans, A. G., Hermann, B. R., and Fell, P. J., "Global Positioning System Sensitivity Experiment," Navigation, Journal of The Institute of Navigation, Vol. 28, No. 2, Summer, 1981.

10. Counselman, III, C.C. and Gourevitch, S. A., "Miniature Interferometer Terminals for Earth Surveying: Ambiguity and Multipath with Global Positioning System," IEEE Transactions on Geoscience and Remote Sensing, Vol. GE-19, No. 4, October 1981.

11. Greenspan, R. L., A. Y. Ng, J.M. Przyjemski, and J. D. Veale, "Accuracy of Relative Positioning by Interferometry with Reconstructed Carrier GPS: Experimental Results," 3rd International Geodetic Symposium on Satellite Doppler Positioning, Las Cruces, NM, February 8-12, 1982.

12. Remondi, B. W., "Using the Global Positioning System (GPS) Phase Observable for Relative Geodesy: Modeling, Processing, and Results," Ph.D. Dissertation, Center for Space Research, The University of Texas at Austin, Austin, Texas, 1984.

13. Ashjaee, J., "GPS Doppler Processing for Precise Positioning in Dynamic Applications," Navigation, Journal of The Institute of Navigation, Vol. 32, No. 4, Winter 1985-86.

14. Loomis, P. V. W., "A Kinematic GPS Double Differencing Algorithm," Proceedings of the Fifth International Geodetic Symposium on Satellite Positioning, New Mexico State University, Las Cruces, NM, 13-17 March, 1989.

15. Hatch, R., "Instantaneous Ambiguity Resolution," Proceedings of IAG International Symposium 107 on Kinematic Systems in Geodesy, Surveying and Remote Sensing, Springer Verlag, New York, 10-13 September 1990.

16. Frei, E. and Beutler, G., "Rapid Static Positioning Based on the Fast Ambiguity Resolution Approach 'FARA': Theory and First Results," Manuscript Geodaetica, Vol. 15, 1990.

17. Remondi, B., "Pseudo-Kinematic GPS Results Using the Ambiguity Function Method," NOAA Technical Memorandum NOS NGS-52, Rockville, MD, 1990.

18. Hatch, R. "Ambiguity Resolution in the Fast Lane," in Proceedings of The Institute of Navigation GPS-89, Colorado Springs, CO, 27-29 September 1989.

19. Lee, Shane-Woei, "On-The-Fly Carrier Phase Ambiguity Resolution Without Using Pseudorange Measurements for Satellite-Based Positioning," Masters Degree Thesis, Department of Electrical and Computer Engineering, Ohio University, Athens, Ohio, 1994.

20. Cohen, C.E., et al., "Achieving Required Navigation Performance using GNSS for Category III Precision Landing," in Proceedings of The Institute of Navigation GPS-95, 12-15 September 1995.

21. Cannon, M.E., "Airborne GPS/INS with an Application to Aerotriangulation," Ph.D. Thesis, Publication 20040 of the Department of Surveying Engineering, The University of Calgary, Canada, 1991.

22. Braff, R., et al, "FAA's CAT III Feasibility Program: Status and Accomplishments," in Proceedings of The Institute of Navigation GPS-95, 12-15 September 1995.

23. Kaufmann, D., "Flight Test Evaluation of the E-Systems Differential GPS Category III Automatic Landing System," NASA Ames Research Center, Moffett Field, CA.

24. Hundley, W., et al., "FAA-Wilcox Electric Category IIIB Feasibility Demonstration Program - Flight Test Results," in Proceedings of The Institute of Navigation GPS-95, 12-14 September 1995.

25. Van Graas, F., et al., "FAA/Ohio University/UPS Autoland Flight Test Results," in Proceedings of the 1995 National Technical Meeting of The Institute of Navigation, January 1995.

26. Cohen, C., et al., "Autolanding a 737 Using GPS Integrity Beacons," NAVIGATION, The Journal of The Institute of Navigation, Vol. 42, No. 3, Fall 1995.

8. ACKNOWLEDGEMENTS

The author acknowledges the support received from the FAA Satellite Program Office (AGS-100) under Aviation Research Grant 92-G-0023 to conduct the Ohio University Category III feasibility research.

GPS/INS Integration

Richard E. Phillips
George T. Schmidt
The Charles Stark Draper Laboratory
Cambridge, MA 02139

ABSTRACT

An inertial navigation solution exhibits relatively low noise from second to second but tends to drift over time. Typical aircraft inertial navigation errors grow at rates between one and ten nautical miles per hour (1.8 to 18 km/hr) of operation. In contrast Global Navigation Satellite System (GNSS) errors are relatively noisy from second to second but exhibit no long term drift. Using both of these sensors is superior to using either alone. Integrating the information from of each sensor results in a navigation system which operates like a drift free INS. There are further benefits to be gained depending on the level at which the information is combined. This presentation will focus on integration architectures including "loosely coupled" and "tightly coupled" configurations. The advantages and disadvantages of each level of integration will listed. Examples of current and future systems will be cited. A performance comparison of "loosely coupled" and "tightly coupled" systems will be made. Navigation applications for which integration is essential will be given.

1.0 INTRODUCTION

GPS / INS integration is not a new concept [Ref. 1,2]. Measurements of external quantities have long been incorporated into inertial systems to limit error growth. Examples shown in Fig. 1.1 are barometric "altitude" measurements, doppler ground speed measurements, doppler measurements to communications satellites, and range measurements to Omega stations.

Although GPS provides a deterministic solution for both position and velocity it has shortcomings. Among them are: low data rate (typically 1 Hz.), susceptibility to jamming (even unintentional jamming), and lack of attitude information.

GPS and inertial measurements are complementary for two reasons. Their error characteristics are different, and they are measures of different quantities. GPS provides measures of position and velocity. An accelerometer provides a measure of specific force, that is, acceleration exclusive of that due to gravity. (The gyroscopes provide a measure of attitude rate. After initial alignment the they allow the acceleration to be resolved into a known coordinate frame.)

A GPS position measurement is noisy due to a combination of low signal strength, the length of the pseudo-random code, which is about 300 m, and the resolution of the code tracking loop. Multipath, the phenomenon whereby several delayed copies of the signal arrive at the antenna after being reflected from nearby surfaces, is a source of correlated noise especially for a moving vehicle. GPS position measurements also have constant or slowly changing biases. These biases are bounded and are not integrated since they are already at the position level.

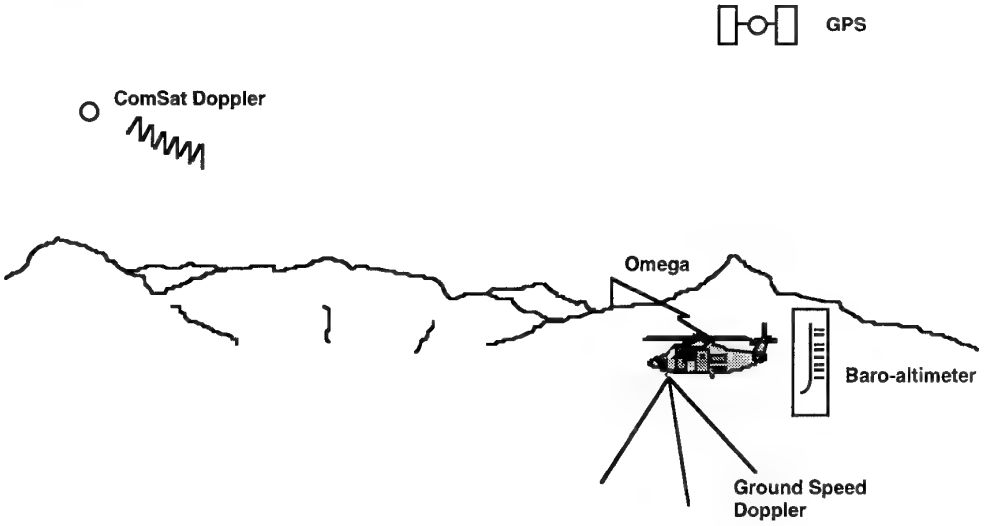

Figure 1.1. Inertial navigation systems can be aided from a variety of sources.

Paper presented at the AGARD MSP Lecture Series on "System Implications and Innovative Applications of Satellite Navigation", held in Paris, France from 1-2 July 1996; Rome, Italy from 4-5 July 1996; Madrid, Spain from 8-9 July 1996 and St. Petersburg, Russia from 11-12 July 1996, and published in LS-207.

GPS velocity (position difference) measurements are also noisy, again due to variations in signal strength, the effects of changing multipath, and user clock instability.

In contrast the accelerometers in an inertial navigation system measure velocity differences (exclusive of that due to gravity) one additional derivative from the position difference measurements made by GPS carrier wave tracking. They have relatively low noise characteristics when compared with GPS measurements. However this noise as well as bias and scale factor errors must be integrated twice before providing position estimates. This fundamental difference in radio navigation measurements and inertial measurements is a clue to the difference in behavior of INS and GPS navigators.

Fig. 1.2 shows accelerometer noise (and its first two integrals). The noise level was specified at 56 micro g's (μg's) per Hz, typical of a 10 nmi/hr inertial system. The accelerometer noise itself is shown in the top graph.

In these graphs the accelerometer is read every 20 ms for 20 s. The integral of acceleration, the middle graph, shows the familiar "random walk" behavior of the integral of random noise. The dotted lines are the 1σ expected errors in the random walk. The second integral, the bottom graph, corresponds to position. (Units are metric: meters, meters/sec and meters/sec/sec.)

GPS receivers typically produce solutions at 1 Hz although it is possible to get data at a higher rate. The data bit rate of 50 Hz sets a "natural" minimum of 20 ms between position and velocity determinations. The middle graph in Fig. 1.3 shows random noise in a set of measurements. The standard deviation of the velocity measurement is 0.01 m/s, typical of a good GPS receiver and strong signals in a benign environment.

Back differencing these measurements to match the 50 Hz accelerometer output results in the noisy measurements as shown in the top graph of the figure. (Again units are metric: meters, meters/sec and meters/sec/sec) The bottom graph of Fig. 1.3 shows the first integral of the velocity over one second intervals as it might be used for "carrier track smoothing" of the GPS position measurement. The circles show the value of the integral after each 1 second interval. They thus indicate the error in the position difference from one GPS measurement (at 1 Hz) to the next. It is considerably smaller than the measurement error in the position measurement itself, thus the impetus for "carrier track smoothing". The position measurement keeps the integral of the carrier track from diverging in the same "random walk" fashion as the integral of accelerometer noise.[1] Users will, quite naturally, want the features of both systems - the high bandwidth and autonomy of inertial systems, and the long term accuracy of GPS.

[1]It is not necessary to break the velocity measurement into 20 ms intervals. As suggested by Cox, et al. [Ref. 1] it is possible to track the carrier phase continuously from satellite rise to satellite set. Another method for extracting a less noisy velocity would be to recognize that the error at the beginning of one interval is the negative of the error at the end of the preceding interval, (if carrier tracking is continuous across the data bit).

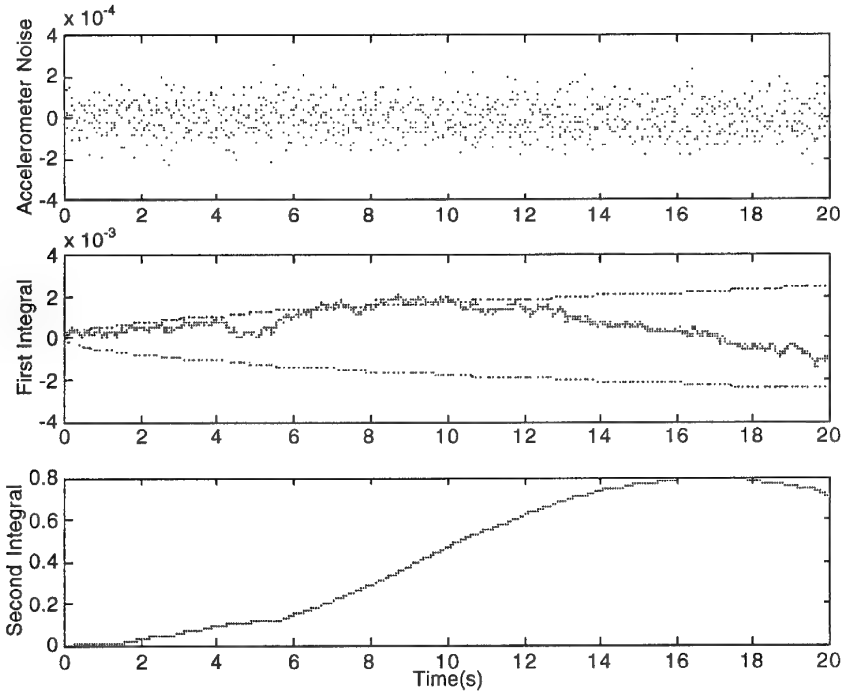

Figure 1.2 Accelerometer noise and its first two integrals.

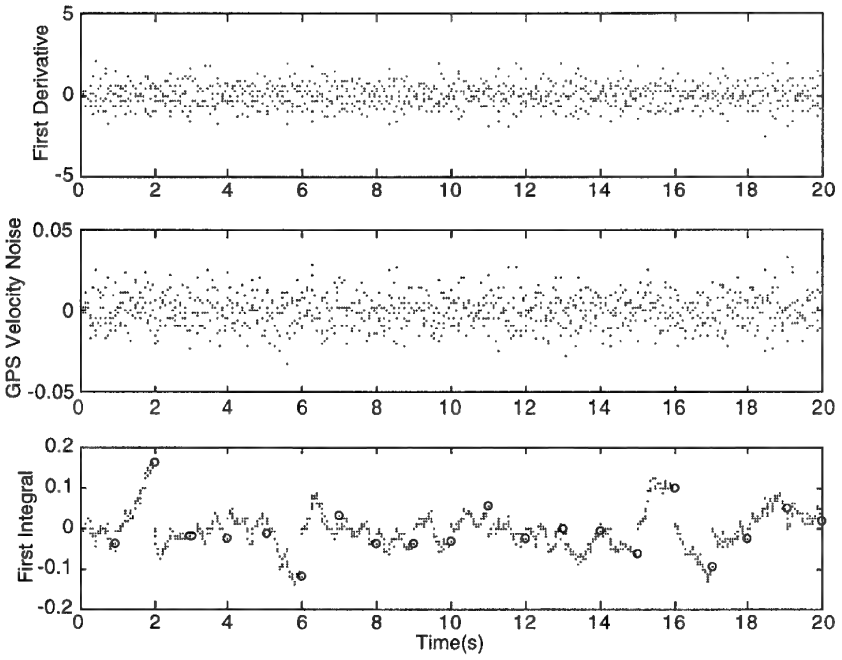

Figure 1.3. GPS velocity measurement noise and its first derivative and first integral.

Table 1.1 summarizes the features and shortcomings of inertial and GPS navigation systems.

Table 1.1. Inertial and GPS attributes and shortcomings.

	Attributes	Shortcomings
GPS	Errors are bounded	Low data rate No attitude information Susceptible to jamming (intentional and unintentional)
INS	High data rate Both translational and rotational information Self-contained (not susceptible to jamming)	Unbounded errors Requires knowledge of gravity

The goal of GPS/INS integration is to get the combined features of both systems. Another obvious benefit is the redundancy inherent with having two systems. But perhaps most importantly there are additional benefits which result from combining the two sensors. These benefits will be discussed in some detail in the following sections.

2.0 Alternate GPS/INS Architectures

Four architectures will be discussed in this paper. Proceeding from the most loosely coupled to the most tightly coupled they are: separate, loosely coupled, tightly coupled[2], and deeply integrated systems. Several variations of loosely coupled and tightly coupled systems will be shown. The deeply integrated architecture uses the same Kalman filter to track the code and carrier as to estimate the position and velocity states of the vehicle [Ref 3, 4, 5].

2.1 Separate Systems

The simplest way to get the features of both systems is to simply have both navigation systems, integrated only in the mind of the user. Only slightly more complex would be to simply add a correction from the GPS to the inertial navigation solution. Figure 2.1 illustrates such a system.

[2]Coupled here refers to combining data from the GPS and INS systems into a single navigation solution. When retrofitting older aircraft with new navigation systems there is often a problem with space and with power and data connections. For these reasons it can be desirable to include GPS in the same box with the inertial navigator. This repackaging will be referred to as embedding.

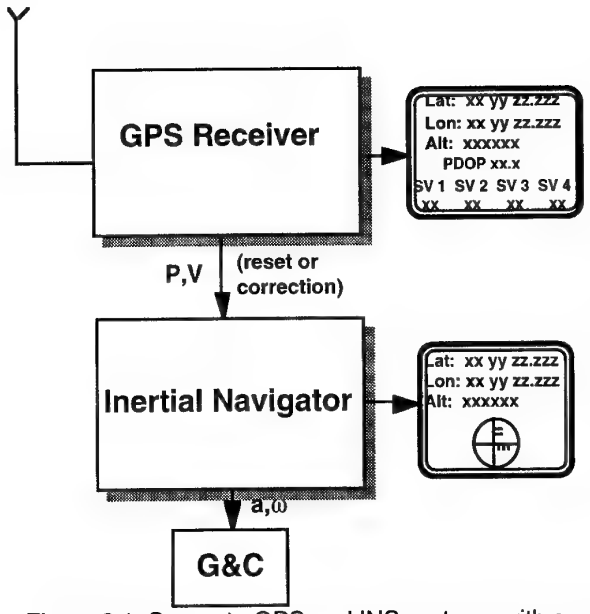

Figure 2.1 Separate GPS and INS systems with a possible INS reset.

This mode of operation or coupling has the advantage of leaving the two systems independent and redundant. But as the IMU drifts the corrections become larger and larger. The inertial solution becomes practically uiseless. Somewhat better would be to have the inertial system "reset" to the GPS solution periodically.

In this situation the inertial system errors are kept bounded, but after the first reset they are no longer independent of the GPS system. Of course the corrections could be monitored for reasonableness to prevent the contamination of the inertial solution with grossly incorrect GPS measurements should they occur. Even if not independent, the systems do remain redundant in the sense that they both still have dedicated displays, power supplies, etc. so that the failure of one does not affect the other or leave the vehicle with no navigator.

Inertial system resets are the proposed mechanization for the U.S. space shuttle GPS integration. The space shuttle has a ground uplink capability in which the position and velocity are simply set to the uplinked quantities. For minimum change to the software the GPS system simply provides a pseudo ground uplink. To make a minimal impact on existing software and hardware is a common rationale for the more loosely coupled systems.

In summary, this architecture offers redundancy, bounded position and velocity estimates, attitude and attitude rate information, high data rates for both translational and rotational information suitable for guidance and control functions, and (for existing systems) minimum impact on hardware and software.

2.2 Loosely Coupled

Most often discussions of GPS/INS integration focus on systems which are more tightly coupled than the system described in the previous section. This will be true of the remaining architectures. Redundancy and solution independence can be maintained, but we will see more benefits from coupling than the simple sum of inertial and GPS navigation features. New software will be required, an integration filter for example.

2.2.1 Loosely Coupled - Conservative Approach

Figure 2.2 shows one version of a loosely coupled system. In this system the functional division could correspond to the physical division with the GPS in a box, the INS in a box, and the computer which combines the navigation solutions in yet another box. Only low rates are required for data links between the boxes. Of course the three functions could be packaged together if desired.

Simplified diagrams for each of the functions are shown. The following paragraphs consist of a high level description of the operation of a receiver and and inertial navigator. It is assumed that the reader has some familiarity with these sensors. The discussion is intended to serve more as a reminder of pertinent features rather than a tutorial. That description which is common to all the architectures will not be repeated.

The receiver diagram shows signals coming into the radio frequency "front end" of the receiver. They are downconverted to baseband and fed into the correlators. Meanwhile a duplicate of the signal is generated internally in the receiver. In fact three (or more) copies are generated. One of these copies is supposedly time synchronized so that it arrives at the "prompt" correlator at exactly the same time as the signal from the antenna. The other copies are intentionally either a little early or a little late compared to what is expected from the satellite. These copies are sent to the early and late correlators. The magnitude of the early and late correlations, indicated by [+,-] in the figure, is given to the code tracking function. The difference in these magnitudes is an indication of the timing error (and thus range error). This error signal is fed back into the code generator which makes a correction to the code phase timing. This process is repeated as long as the signal is present. At some point the phase error will be driven to an acceptable level and the code will be declared "in lock". While "in lock" the time difference between the broadcast of the signal and the receipt of the signal are a measure of the pseudo-range.

Similarly the inphase and quadrature signals are fed into the carrier tracking function. The arctangent of these two signals is a measure of the carrier tracking error. This signal is fed back to the numerically controlled oscillator, and its frequency is adjusted accordingly. It might be noted that the carrier tracking loop is typically of third order, allowing it to "perfectly track" signals with constant range acceleration. Note that the carrier loop (when it is "in lock") "aids" the code loop as indicated by the arrow labeled $\Delta\rho$. In this mode the code tracking loop can be of first order.

For this architecture the only INS data the receiver uses is for the purpose of aiding in acquisition. Knowing the position and velocity of the vehicle enables the code generator and oscillator to make good initial guesses of the frequency and code phase of the incoming signal. The

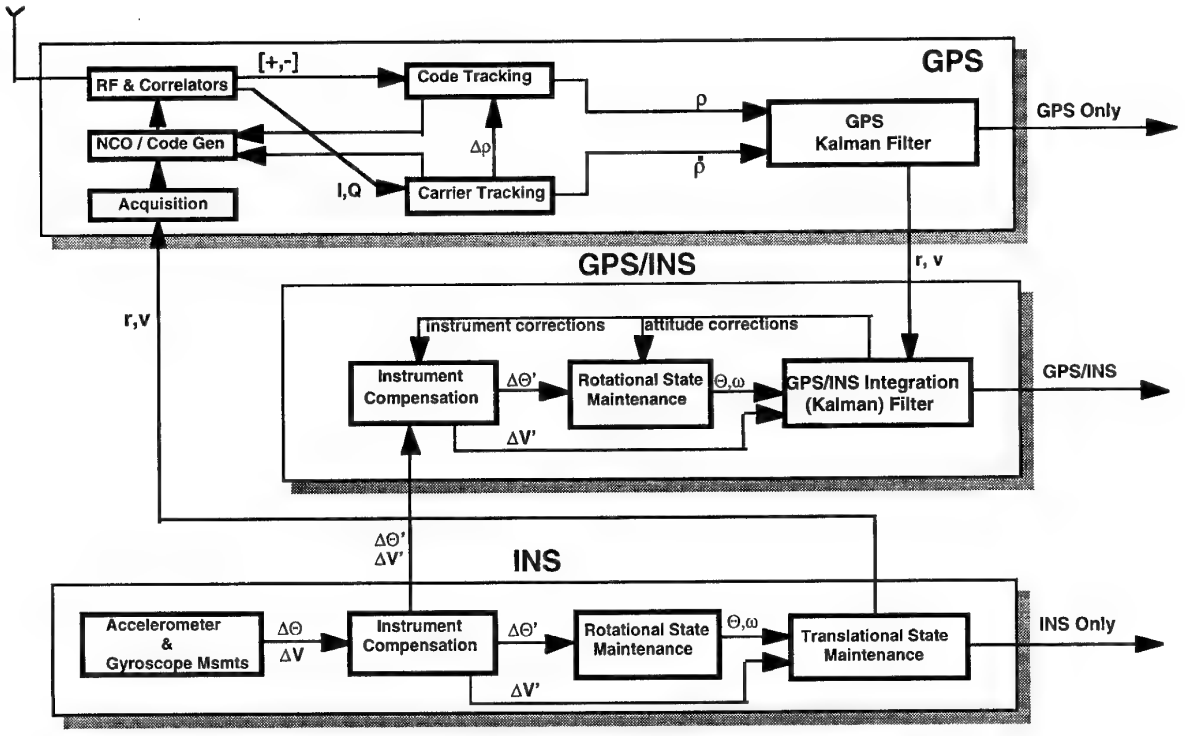

Figure 2.2. A loosely coupled GPS/INS navigation system.

search time during acquisition can be significantly reduced depending on the accuracy of these estimates.

The output of the tracking loops is an estimate of the range and range rate between the vehicle and the satellite. Range and range rate estimates from four satellites are sufficient to resolve the vehicle position, velocity, receiver clock bias and receiver clock drift rate. For some receivers these deterministic quantities determined once per second are the ultimate receiver output. However, receivers which are expected to operate in a dynamic environment use a "polynomial" Kalman filter to estimate position, velocity, and acceleration, and clock bias and clock drift rate.

A (strapdown) INS diagram is shown at the bottom of the figure. Raw measurements from the accelerometers and gyroscopes are compensated using *a priori* values, or values derived from another mode of operation (e.g. a calibration and alignment mode). The gyroscope output is used to maintain the rotational state of the vehicle. Angular rates are integrated into either a quaternion or matrix which relates the vehicle attitude to some reference coordinate system (e.g. local level). Corrected Δv's are rotated into this coodinate system and integrated to maintain the translational state, position and velocity.

The GPS/INS integration function is shown in the middle diagram of the figure. It receives corrected inertial measurements, $\Delta\Theta'$ and $\Delta v'$, from the INS and position and velocity measurements from the GPS receiver. The 1 Hz GPS measurements, coming from a Kalman filter, are highly correlated. The second Kalman filter in this "cascaded" architecture handles this problem by only incorporating these measurements every 10 s. The ten second interval allows each position/velocity measurement to be more or less independent of the previous measurements. A performance comparison between this loosely coupled architecture and a tightly coupled architecture will be given in Section 3. Note that the integration Kalman filter includes calibration and alignment estimates which provide inflight improvement of the INS calibration and alignment. This conservative approach to coupling yielded surprisingly good results in estimating these gyro and accelerometer parameters.

Table 2.1 summarizes the functions of the three components of the system. Table 2.2 lists the attributes of the system.

Table 2.1. Functions of the three components of the loosely coupled system.

Component	Function
GPS	The Kalman filter estimates: position, velocity, acceleration clock bias, clock drift
INS	The INS provides: position, velocity, acceleration attitude, attitude rate
Integration Filter	The integration filter estimates: position, velocity attitude corrections, instrument corrections

Table 2.2. Loosely coupled system attributes.

System Attributes
All the attributes of the previous "uncoupled" architecture including redundant and independent INS and GPS solutions
More rapid acquisition of code and carrier phase
Improved navigation performance
Inflight (and better) calibration and alignment which results in improved navigation during satellite loss/jamming

We distinguish between jamming resistance and mitigation against jamming. By the latter term we simply mean that the inertial bias and scale factor parameters will be better calibrated so that if the GPS signal is lost the GPS/INS solution (receiving only inertial data) will be accurate for longer than otherwise.

2.2.2. Loosely Coupled-Aggressive Approach

Figure 2.3 shows possible variations in what may still be considered a loosely coupled architecture. Inertial aiding of tracking loops has not yet been introduced, and the integration filter still uses position and velocity data rather than pseudo-range and range rate. Additional data transfer beyond that of the previous architecture is indicated by heavy lines. Either one or the other or both data transfers are viable options.

The first of these data transfers is of the corrected velocity increment $\Delta v'$ from the GPS/INS module to be used in the GPS module to propagate the solution between measurements. This provides a vast improvement in dynamic situations [Ref. 6]. Otherwise the propagation must be done using the acceleration estimate from the GPS Kalman filter itself. This acceleration, although a component of the filter state, is derived by back differencing the velocity. Figure 1.3 showed the level of acceleration noise inherent in this operation. It is true that the filter offers some "smoothing". However, it cannot offer much due to the process noise which must be added in the dynamic aircraft environment. There is a requirement by the U.S. GPS Joint Program Office that the receiver be able to maintain track at a jerk level of 10g's/sec for 0.6 sec. Although this requirement is on the tracking loops it most certainly has implications for the process noise which must be added to the acceleration covariance term in the GPS Kalman filter. There is no substitute for using the measured acceleration.

The other optional data transfer is that of the inflight calibration and alignment corrections from the GPS/INS estimator to the INS. This helps keep the INS in closer agreement with the GPS/INS solution. Of course the independence of the two solutions is lost.

In summary we have improved the navigation accuracy of the combined GPS and the INS at the cost of indepence in their solutions. We have maintained redundant systems.

2.2.3. Loosely Coupled-Rockwell's MAGR Approach

This approach might actually be characterized somewhere between loosely and tightly coupled. Fig. 2.4 shows the GPS and INS functions and interfaces between them. The MAGR (military airborne GPS receiver) has an INS mode and a PVA (position, velocity, and acceleration) mode. The latter is a stand alone mode independent of inertial measurements.

In the INS mode inertial measurements are used to aid the code tracking loop when the carrier loop is out of lock and unable provide aiding. The GPS uses the inertial measurements to extrapolate the position and velocity between GPS measurements rather than estimating acceleration in a polynomial filter. The GPS estimates attitude corrections for the IMU. The MAGR (in the INS mode) thus has some of the features of a tightly coupled system. Table 2.3 lists the filter state elements for the PVA and INS mode of operation.

Table 2.3. Filter states for the MAGR.

PVA Mode	INS Mode
position	position
velocity	velocity
acceleration	attitude corrections
clock bias	clock bias
clock drift	clock drift
barometer bias	barometer bias

2.3. Tightly Coupled

Finally the two changes which define a tightly coupled system are introduced. The GPS range and delta range measurements are incorporated directly into the navigation estimate and the position and velocity from the inertial system are used by the GPS receiver to reduce the tracking loop bandwidths even in the presence of high dynamics. First a straightforward system which provides a single combined GPS/INS solution will be presented. Then a system which also maintains independent and redundant GPS and INS solutions will be presented.

2.3.1 Tightly Coupled - Combined GPS/INS Only

Figure 2.5 shows the architecture for a tightly coupled GPS/INS navigation system which offers a single navigation solution. The INS and GPS modules have been truncated. The inertial "system" now simply provides raw measurements. The GPS receiver does not have its own Kalman filter, but it does still have independent tracking loops which provide the values for pseudo-range and range rate. Although it has not been shown in any of the figures it is of course understood that the pseudo-range and range rate to at least four satellites are required for a position and velocity determination. The GPS functions shown in the upper diagram of Fig. 2.5 are duplicated for each satellite either by time sharing or, as is most common today, by having multiple "channels" in a receiver - only one of which is shown in the diagram.

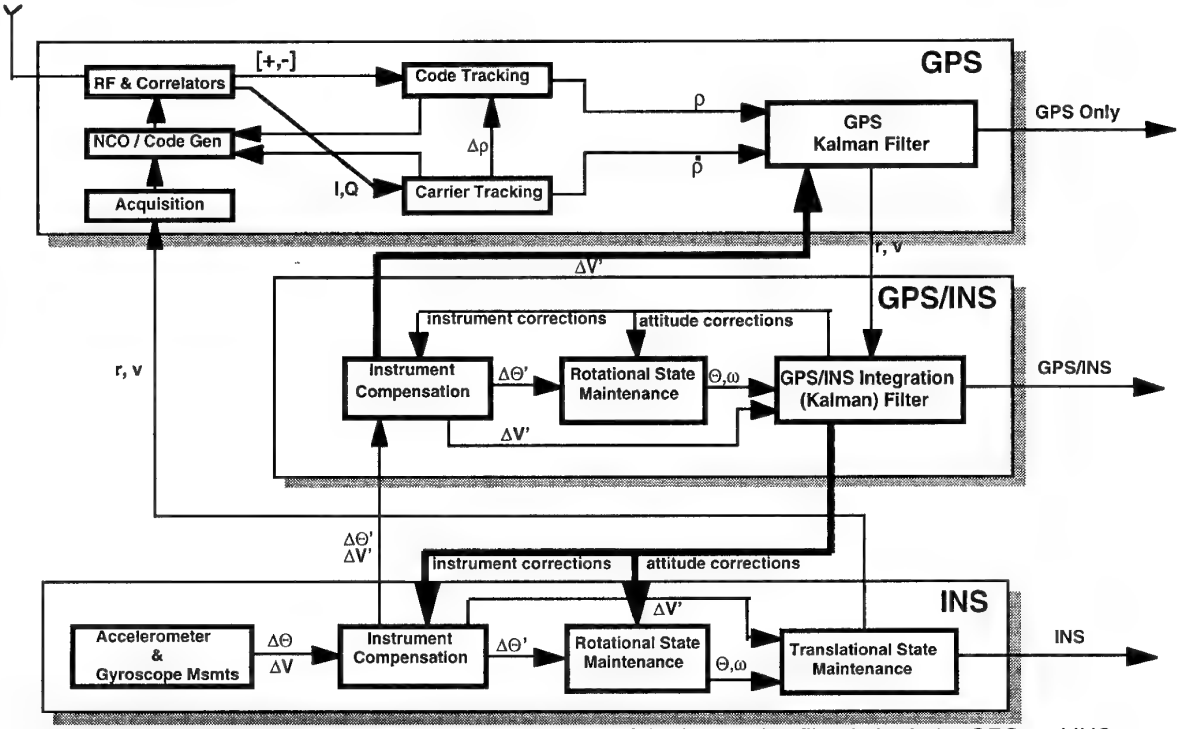

Figure 2.3. Loosely coupled variations use the results of the integration filter in both the GPS and INS solutions

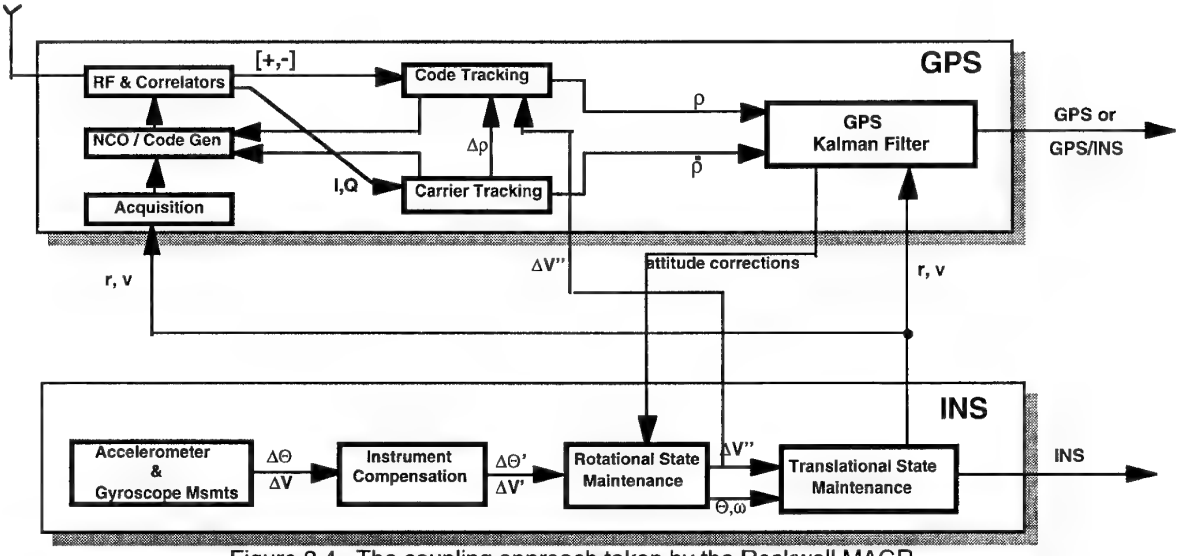

Figure 2.4. The coupling approach taken by the Rockwell MAGR.

The tracking loops in the receiver are aided by data from the GPS/INS state estimator. This data is required at a high rate thus the propagation from one measurement epoch to another is broken into many subintervals for the purpose of tracking loop aiding. The goal is to make these tracking loops "think" the receiver is sitting still. The quantities being estimated by the Kalman filter are position and velocity, whereas the data required by the

tracking loops is code phase (range) and doppler frequency shift (range rate). The estimated position and velocity, and the satellite ephemerides are used to calculate the code phase and frequency shift. The diagrams in this paper will show the transfer of r, v, and delta range and range rate, implying that these calculations are done in the receiver. They could as well be done in the "State Estimator" box. The bandwidth of the tracking loops must only accomodate the errors in the measured acceleration rather than the acceleration. These errors are many orders of magnitude less than the acceleration itself depending on the quality of the inertial system and its calibration.

The tightly coupled navigation systems are more accurate. This will be seen in Section 3, in which tightly and loosely coupled systems are compared. We still have the gains or attributes of the loosely coupled systems except for the loss of redundancy. The bandwidth of the tracking loops can be reduced thus increasing jamming resistance. The integration filter can make optimal use of any and all satellites which are being tracked, even if there are less than four of them. It should be said that GPS only solutions can be maintained with either three or two satellites if one or two or both of the following assumptions are made: 1) the clock bias is constant and 2) the altitude is constant, or is known by some other means (e.g. a baroaltimeter).

Only the redundancy offered by three complete systems is lost for this architecture. A summary of the benefits accrued by coupling will be given at the end of Section 2.3.2.

2.3.2 Tightly Coupled - Redundant Solutions

Figure 2.6 illustrates a tightly coupled architecture which also offers redundant navigation solutions from both the GPS and INS. This figure most closely resembles the figure for the loosely coupled architecture. The additions to that figure are "inertial" aiding of the tracking loops from the GPS/INS solution and pseudo-range and range rate measurements rather than position and velocity from the receiver to the integration filter.

This more elaborate system requires more software. This is the price of the redundancy unless the software is already present in existing INS's and GPS's. This can indeed be the case and is the case in the U.S. GPS joint program office's Embedded GPS Inertial (EGI) program. The concept of the EGI program was to obtain a navigation system with GPS and inertial attributes at minimum cost. Specifications for such a (non-developmental) system were published . Several vendors have produced such embedded systems, among them are Litton's LN-100G [Ref. 7] and Honeywell's H-764G [Ref. 8] combinations of GPS with ring laser gyroscopes.

The U.S. Advanced Research Projects Administration is

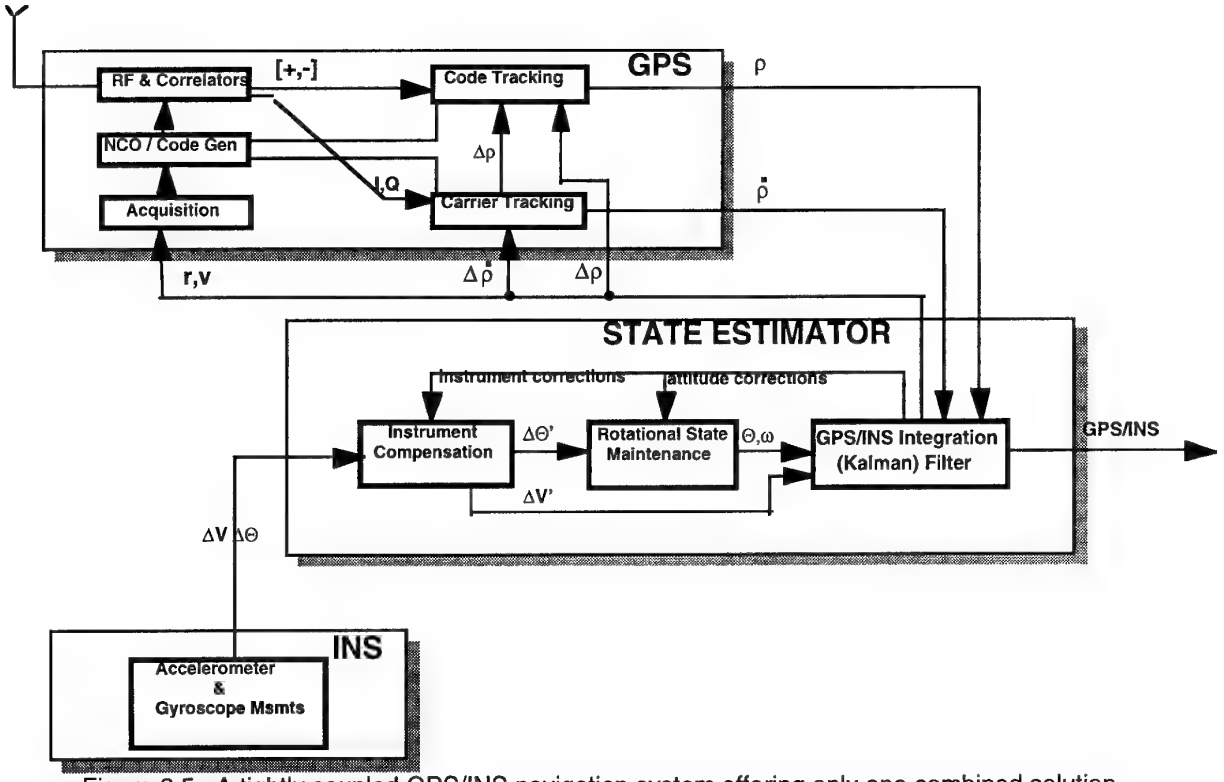

Figure 2.5. A tightly coupled GPS/INS navigation system offering only one combined solution.

sponsoring a tightly coupled and embedded combination, the GPS Guidance Package, using fiber optic gyroscopes.

Embedding the receivers allows the data transfer rates required for tight coupling. EGI specifications state that separate and independent inertial-only and GPS-only solutions are to be maintained. Although they do not specify the two characteristics we have used to define tight coupling, they do state that INS aiding of the tracking loops is allowed [Ref. 9]. This potentially makes the GPS solution dependent on the INS. Mathematical independence is maintained if the tracking loops have adequate signal strength to work with and "maintain lock" such that the error in range rate (for example) is independent of the aiding value. If the error in the tracking loops is independent of the aiding the GPS and GPS/INS solutions will be independent. Logic in the receivers attempts to recognize when lock is lost and not incorporate the resulting "bad" measurements into the GPS solution. This precaution also (arguably) keeps the GPS solution mathematically independent of the other solutions.

The tightly coupled receiver offers elevated jamming resistance. It offers the ability to continue operation when GPS is intermittent, due to wing shadowing, foliage or other natural or man made obstructions. Table 2.4 summarizes the benefits that have been gained by coupling GPS with INS. The benefits are cumulative. That is the benefits for each level also include those for the previous level. (The exception is loss of redundancy and independence for the simpler of the tight coupling architectures.)

There are applications for which the maximum navigation accuracy is required. One such example is the determination of target location using synthetic aperture radar (SAR). The location of the target in some reference coordinate system (e.g. WGS '84) is critically dependent on the most accurate velocity measurements attainable. The accuracy of these measurements determines the accuracy of the cross range component in the SAR slant plane. (This subject is discussed in a subsequent lecture.)

Table 2.4. Cumulative benefits of increasingly tight coupling.

Coupling Level	Benefit
Uncoupled / Reset INS to GPS (Sum of system attributes)	position, velocity, acceleration, attitude and attitude rate information redundant systems - a drift free GPS - a high bandwidth INS
Loosely Coupled	more rapid GPS acquisition inflight calibration and alignment better inertial instrument calibration and alignment - better attitude estimates - longer operation after jamming
Tightly Coupled	better navigation performance better instrument calibration reliable tracking under high dynamics reduced tracking loop bandwidth (jamming resistance) optimum use of however many SV's available

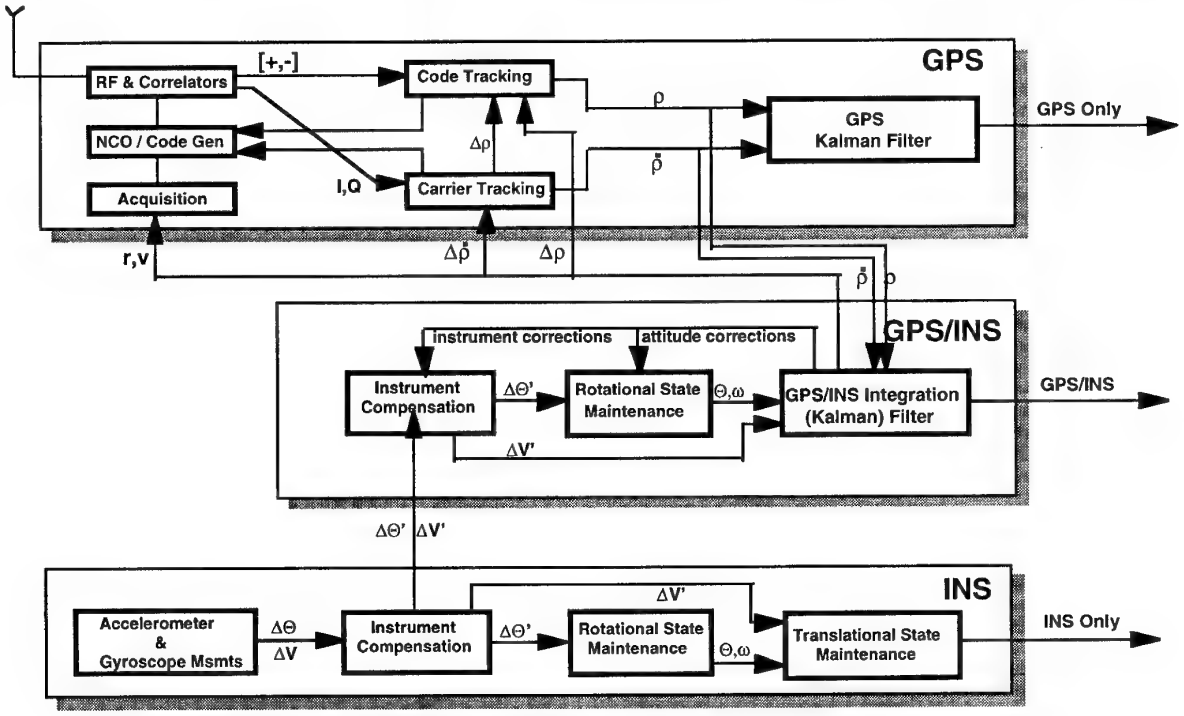

Figure 2.6. Tightly coupled architecture with redundant GPS and INS only solutions

Another application is precision weapon or supply delivery where accuracies of 1 m to 3 m are desired. Still another might be autolanding of aircraft. Each of these will require the precision offered by the tightly coupled architecture. Aircraft landing will probably require redundant systems as well as additional "pseudo satellites" located on the ground for improvement in position dilution of precision (PDOP).

2.4 Deep Integration

Figure 2.7 shows the architecture of a deeply integrated GPS/INS navigation system. This figure compares most closely with the first tightly coupled architecture shown in Fig. 2.4. In the deeply integrated concept independent tracking loops for the code and carrier have been eliminated.

All estimating is done in the Kalman filter, including the estimate of the pseudo-range and range rate. This architecture eliminates the concern with cascaded filters and unstable pseudo-range and range rate estimates. The early and late correlation values and the inphase and quadrature signals (or equivalent information) become measurements for the Kalman filter. The filter state is used to compute estimates of the measured values. The difference between measured and estimated value is weighted depending on the inverse of the variance in the measured and estimated quantities. After measurement incorporation an improved range and range-rate are sent to the code and frequency generators and another measurement is made.

There is certainly some question about the computer throughput required to implement the navigation filter with 20 to 40 states at the rate required to keep up with changes in range and range rate. We would only note that accelerometer data could be used to control the oscillator (NCO). This would allow for long coherent signal integration times, more accurate measurements, and lower rates.

As far as we know no one has actually built such a receiver but with the continuing rapid increase in computer throughput it is again receiving attention [Ref 5].

3.0 Loosely Coupled vs Tightly Coupled Performance Comparison

This section shows the jamming related performance of loosely coupled and tightly coupled GPS/INS navigation systems in several hypothetical situations. In addition to comparing navigation architectures, the performance of inertial systems of varying quality was evaluated. The analysis considered only at the performance of the combined GPS/INS solution and is thus appropriate to either of the loosely coupled architectures as they share the same GPS/INS solution. This particular example of a GPS/INS loosely coupled system has been the subject of numerous published studies [e.g. Ref. 10]. The tightly coupled system did not necessarily correspond to any particular existing system.

Several jamming scenarios were considered. The first scenario was designed to simply show the behavior of GPS/INS systems when GPS satellites are lost and reacquired one at a time. That is there will be 4 satellites in track, then 3, 2, 1, and finally 0. Then they were reacquired one at a time. For one of the scenarios the navigation system was augmented with a doppler ground speed measuring device.

3.1 Loosely Coupled System Definition

The loosely coupled GPS system consisted of a GPS receiver, an inertial navigation system and an integration filter. The PVA solution, from a typical receiver like the MAGR, was used as the input to the GPS/INS integration Kalman filter. In order to avoid the problem

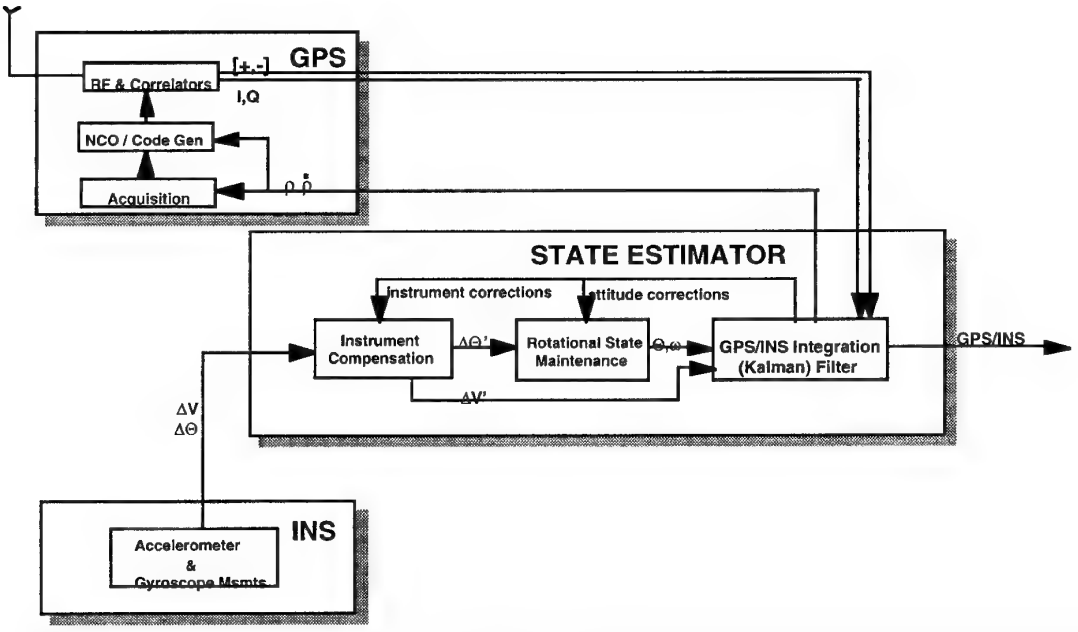

Figure 2.7. Deeply integrated GPS/INS systems feature a single estimator for both detection and navigation.

of dealing with correlated measurements the integration filter only used the position from the PVA solution and this only once every 10 seconds and only if the expected horizontal error (EHE), a receiver output and measure of horizontal navigation quality, was less than 100 m. The receiver did not compute a solution if there were fewer than four satellites in track. The state elements for the GPS receiver are shown in Table 3.1.

Table 3.1. State elements for the unaided GPS receiver.

State element	Components
position	3
velocity	3
acceleration	3
user clock bias	1
user clock drift	1
altimeter bias	1
Total	12

Since the GPS receiver solution is the result of a (Kalman) filter the velocity is correlated with the position, and both position and velocity are correlated in time. Process noise, which allows the filter to track changing acceleration, also decorrelates the output. The process noise is of such a magnitude that position solutions separated by 10 second intervals are not significantly correlated. The state elements of the integration filter which processes these measurements is shown in Table 3.2.

Table 3.2. State elements for the loosely coupled integration filter.

State element	Components
position	3
velocity	3
misalignment	3
gyro. drift	3
gyro. scale factor	3
accel. bias	3
accel. scale factor	3
altimeter bias	1
Total	22

Most Kalman filters are sub-optimal estimators. Some are less near optimal than others. The cascaded filter architecture of loosely coupled systems is certainly far from optimal. These systems are particularly sensitive to the procedure known as "tuning", in which the process noise is added and measurements are down-weighted or omitted. A considerable effort went into the tuning the loosely coupled GPS/INS system such that it could be fairly compared with the tightly coupled systems.

3.2 Tightly Coupled System Definition

The tightly coupled system consists of a receiver, inertial instruments, and an integration filter. The integration filter accepts measurements of pseudo-range and pseudo-range rate from each satellite at a 1 Hz rate. The filter state is extrapolated forward in time using inertial measurements and a model for the earth's gravity field. The state elements for this most straightforward approach are shown in Table 3.3. These same states appear in the cascaded filters of the loosely coupled system.

Table 3.3. State elements for the tightly coupled integration filter.

State element	Components
position	3
velocity	3
user clock bias	1
user clock drift	1
misalignment	3
gyro. drift	3
gyro. scale factor	3
accel. bias	3
accel. scale factor	3
altimeter bias	1
Total	24

3.3 Initial Errors, Modeling Errors, and Instrument Errors

These errors sources influence the performance of the navigation system, some more than others. The initial errors in position, velocity and misalignment in fact have very little effect on the performance of the system as long as it operates for a significant time. They are set to levels which are consistent with some kind of ground calibration and alignment mode, but are poor enough to show improvement as inflight alignment progresses - with either system architecture. Other errors can have significant effect on navigation system performance. Those errors which are independent of INS quality are given in Table 3.4. The Markov processes in this table are characterized by two numbers, a standard deviation and a distance constant.

The performance of four different IMU qualities were analyzed. The four IMU's were characterized by their navigation error after one hour of unaided (inertial only) operation. The error characteristics of actual inertial instruments whose performance was close to 10, 1, 0.5 and 0.2 nmi/hr were scaled proportionally to yield those exact values.

Table 3.4. Error values for INS independent models.

Bias Errors	Modeled Value (1σ)	No. Components
Initial position	16 m (vertical) 600 m (horizontal)	1 2
Initial velocity	0.3 m/s	3
GPS User Clock Initial offset Initial drift G-sensitive drift	 5000 ms 10^{-2} ppm 10^{-3} ppm/g	 3
GPS pseudo-range	3.0 m	4
GPS range rate	0.003 m/s	4
Gravity (Markov)	35 mg's / 37 km	3
Barometer (Markov)	150 m / 460 km	1
Noise Errors		
GPS pseudo-range	from receiver tracking loop simulation	4
GPS range rate		4
Barometer	3 m	1

The error values for each of these hypothetical instruments is shown in Table 3.5.

Note that initial misalignment is shown in this rather than the previous table. Misalignment is an "initial condition" for this analysis but was really derived from gyrocompassing each of the inertial units, so it is instrument dependent. Its values are not critical for the analysis because improvements in alignment due to inflight maneuvers soon dominate the results.

3.5 GPS Receiver Bandwidth, Loss of Lock and Reacquisition

For the loosely coupled receiver the noise bandwidths of the code and carrier loop are fixed. The carrier was a third order loop with bandwidth of 5.83 Hz. The code loop band is first order but is aided by either the carrier loop if the carrier loop is in lock, or by the INS if the carrier loop is not in lock. During carrier loop aiding the code loop bandwidth is 1.5 Hz. During inertial aiding the bandwidth is 0.5 Hz.

The bandwidths for the tightly coupled receiver were set appropriate to the quality of inertial instruments. These bandwidths are determined by the requirement that the loops stay in lock for a 10g/s jerk which lasts for 0.6 seconds. (The carrier tracking bandwidth was actually set for this study by requiring that the phase error be less than 90° for a 6 g acceleration step. This is a slightly more stringent requirement but is easier to analyze.) The next several paragraphs present the method used for setting the tracking loop bandwidths. We took maximum advantage of knowing the inertial instrument performance. Closely tuning the tracking loops to the inertial performance in this way may not always be practical for actual receivers.

The phase error in a third order loop following an acceleration step is shown in the following equation. (Note that distance has been converted to phase error in degrees using the code length of 300 m.)

$$\Delta\Phi = \frac{R}{\omega_0^2}\left[e^{-\omega_0 t} + \frac{e^{-\omega_0 t/2}}{\sqrt{3}}\left(\sin\omega_0 t\,\frac{\sqrt{3}}{2} - \sqrt{3}\cos\omega_0 t\,\frac{\sqrt{3}}{2}\right)\right]$$

where: R is the step magnitude (deg/s^2)

ω_0 is the filter natural frequency (rad/s)

$\Delta\Phi$ is the phase error in degrees

The natural frequency should be selected to keep the peak phase error less than 90°. The graph in Fig. 3.1 shows the response, $\delta\Phi$, for a natural frequency of 17.67 rad/s The maximum error is 90°.

Table 3.5. IMU error sources.

	IMU Quality (All errors except random walk are 1σ biases)			
Error Source	10 nmi./hr.	1.0 nmi/hr	0.5 nmi/hr	0.2 nmi/hr
Accel Bias	223 μg	37 μg	19 μg	4.2 μg
Accel. Scale Factor	223 ppm	179 ppm	90 ppm	21 ppm
Input Axis Misalign.	22 arcsec	3 arcsec	1.5 arcsec	0.4 arcsec
Random Walk	56 μg/√hr	56 μg/√hr	7.5 μg/√hr	4.2 μg/√hr
Gyro Bias	0.11 deg/hr	0.0045 deg/hr	0.0022 deg.hr	0.00084 deg/hr
Gyro Scale Factor	112 ppm	7.5 ppm	112 ppm.	1.67 ppm
Input Axis Misalign	22 arcsec	2.2 arcsec	1.1 arcsec	0.4 arcsec
Random Walk	0.078 deg/√hr	0.0022 deg/√hr	0.0011 deg/√hr	0.0005 deg/√hr
Initial Misalignment	2089 arcsec vertical 59 arcsec horizontal	606 arcsec vertical 59 arcsec horizontal	600 arcsec vertical 29 arcsec horizontal	600 arcsec vertical 29 arcsec horizontal

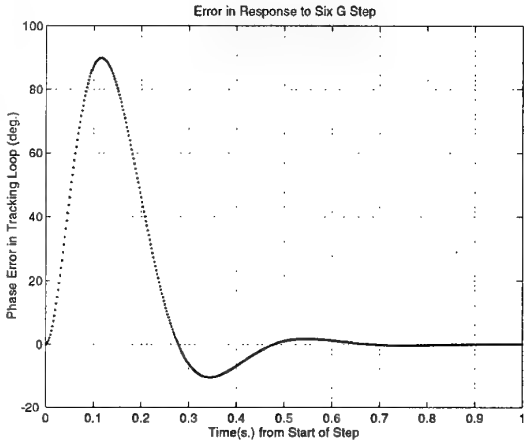

Fig. 3.1. Error in third order loop response to a 6 g step in acceleration

With inertial aiding the tracking loop will not be affected by the full magnitude of the step in acceleration. Only a residual part of the acceleration step due to imperfect inertial instruments will affect the tracking loop. The error, $\Delta\Phi$, is proportional to the step magnitude and inversely proportional to the square of the natural frequency. To maintain a 90°. peak error the natural frequency can be scaled by the square root of the ratio of aided to unaided step magnitude.

$$\omega_{0,aided} = \sqrt{\frac{R_{aided}}{R_{unaided}}}\omega_{0,unaided} \qquad (3.1)$$

The residual error (post-calibration) accelerometer scale factor and IMU misalignment cause a residual acceleration step to be seen by the tracking loop. Lag in the inertial aiding would also cause add to the acceleration seen by the tracking loop. This lag was asssumed to be negligible in this tightly coupled situation.

The residual acceleration seen by the tracking loop due to scale factor error is shown below.

$$\delta a_{sf} = \begin{bmatrix} sf_1 & 0 & 0 \\ 0 & sf_2 & 0 \\ 0 & 0 & sf_3 \end{bmatrix} a$$

IMU misalignment causes acceleration to be incorrectly rotated. The error in acceleration due to misalignment is shown below.

$$\delta a_{mis} = \begin{bmatrix} 0 & -\delta\theta_3 & \delta\theta_2 \\ \delta\theta_3 & 0 & -\delta\theta_1 \\ -\delta\theta_2 & \delta\theta_1 & 0 \end{bmatrix} a$$

The net error caused be scale factor and misalignment due to a unit acceleration step is thus:

$$\delta a = \delta a_{sf} + \delta a_{mis}$$

$$\delta a = \begin{bmatrix} 1 & 0 & 0 & 0 & -1 & 1 \\ 0 & 1 & 0 & 1 & 0 & -1 \\ 0 & 0 & 1 & -1 & 1 & 0 \end{bmatrix} \begin{bmatrix} sf_1 \\ sf_2 \\ sf_3 \\ \delta\theta_1 \\ \delta\theta_2 \\ \delta\theta_3 \end{bmatrix}$$

The covariance of residual acceleration error due to a unit acceleration step is shown below.

$$\left\langle \delta a \delta a^T \right\rangle = \begin{bmatrix} 1 & 0 & 0 & 0 & -1 & 1 \\ 0 & 1 & 0 & 1 & 0 & -1 \\ 0 & 0 & 1 & -1 & 1 & 0 \end{bmatrix} \begin{bmatrix} \sigma_{sf}^2 & c_{sf-mis} \\ c_{sf-mis} & \sigma_{mis}^2 \end{bmatrix} \begin{bmatrix} 1 & 0 & 0 \\ 0 & 1 & 0 \\ 0 & 0 & 1 \\ 0 & 1 & -1 \\ -1 & 0 & 1 \\ 1 & -1 & 0 \end{bmatrix}$$

The quantities $\sigma_{sf,}$ and σ_{mis} are the scale factor and misalignment standard deviations. The quantity $c_{sf\text{-}mis}$ is the covariance of these two quantities. This scale factor / misalignment matrix (the middle factor on the right) was taken from a covariance analysis after the aircraft had performed inflight calibration maneuvers. If the scale factor is expressed as a fraction and the misalignment is in radians, the acceleration variance (on the left) will be the variance in acceleration seen by the tracking loop for a unit acceleration step. The radius of the sphere which enclosed 90% of these acceleration errors was taken to be the acceleration magnitude to which the tracking loops were tuned. Although a 90% level may not seem very robust, it should be remembered that tracking loop errors greater than 90° do not necessarily cause loss of lock.

For the four qualities of IMU studied, the radius of the 90% sphere, and the corresponding bandwidths are shown in Table 3.6. The error due to a unit acceleration step is given in parts per million.

The quantity in the second column is the radius of the sphere which encloses 90% of the errors. The quantities in the third column are that error times the 6 g acceleration step, and the quantities in the third column are the required bandwith as determined by Eq. 3.1. For example the bandwidth for the 10 nmi/hr system was computed as shown below.

$$\omega_{0,aided} = \sqrt{\frac{.011g's}{6g's}}18rad/s = 0.77rad/s$$

For the purposes of the analysis we declared that the receiver had lost lock if the carrier phase error exceeded 90°or if the signal to noise ratio dropped below 19 dB. We declared loss of lock for the code phase if the tracking error was greater then 1/2 chip (50 ns.) or if the signal to noise ratio dropped below 18 dB. Conversely reacquisition was dependent on achieving a signal to noise ratio of at least 21 dB for the code and 22 dB for the carrier for a required amount of time. The required time depends on the uncertainty in the range and range rate to

each satellite and the rate at which each code phase and frequency combination could be searched.

At the given signal level a 20 ms integration period should be adequate for accumulating signal energy. The size of the phase shift between 20 ms search intervals was 36° corresponding to 30 m. The size of the frequency bandwidth was 50 Hz corresponding to 10 m/s. The approximate time required to search over this position-frequency space ($\pm\sigma$) is given below.

$$\Delta T = 0.020\left[\frac{2\sigma_{rng}}{30}\right]\times\left[\frac{2\sigma_{rng-rate}}{10}\right]$$

Some additional time must be added to allow for receiver moding. That is for the search process must be halted and the receiver tracking loops cycled several times with an adequate signal to noise/jammer ratio.

3.6 Navigation Performance for Four Missions

Four missions were studied. The purpose for each of these mission scenarios was to observe the effects of jamming on loosely and tightly coupled GPS/INS systems and to observe the effect of IMU quality on tightly coupled systems. For the first scenario the loss of lock and reacquisition for each of four satellites was spaced out so that the behavior of the navigation solution could be observed for extended periods of time between each loss. The other missions consisted of: 1) an aircraft flying past a jammer so that it looses lock then reacquires satellites as the jammer recedes into the distance, 2) an aircraft approaching a jammer head on, and 3) a helicopter operating in the vicinity of a jammer.

3.6.1. Sequential Outage

In this scenario the loss of lock on satellite carrier and code phase was forced at 3 minute intervals. Loss of code lock began after the fourth carrier tracking loop lost lock. Thus the sequence began with loss of lock on a single carrier signal and ended with the loss of lock of the fourth code loop. Two variations in the study were considered at this point. In one of these the signals were reacquired in inverse order after a total outage of 20 minutes. In the other variation the mission was continued for 84 minutes using inertial measurements without the aid of GPS.

The behavior of the horizontal velocity error for the loosely and tightly coupled systems is shown in Figures 3.2 and 3.3.

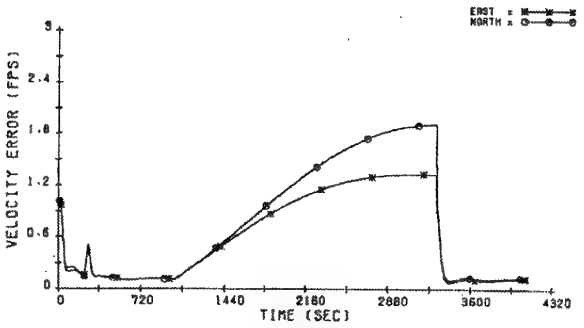

Fig. 3.2. Horizontal velocity error for the loosely coupled navigation systems.

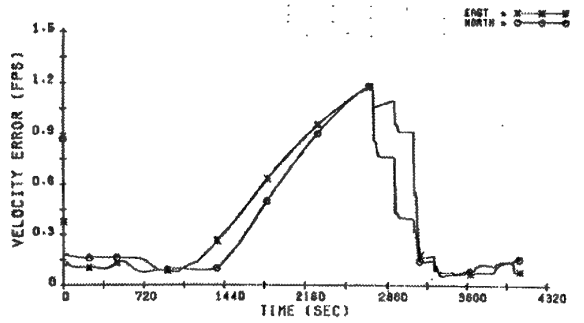

Fig. 3.3. Horizontal velocity error for the tightly coupled navigation systems.

The first loss of carrier tracking occurs at 360 seconds. The first loss of code at 1020 seconds. One feature of this loosely coupled system is that it does not form a navigation solution if fewer than four satellites are in lock. Thus the immediate rise in velocity error begins at this point for in the bottom graph (loosely coupled system). In contrast the increase in velocity error for the tightly coupled system is somewhat delayed. The sequence of code reacquisition begins at 2760 seconds. Since the tightly coupled system makes immediate use of the first code measurement the step improvement in velocity is seen at that time. The correlations between

Table 3.6. The residual acceleration error and corresponding bandwidth for the carrier tracking loop for four IMU qualities.

IMU	Residual Error (90%) Due to Scale Factor and Misalignment (ppm)	Acceleration Seen by Tracking Loop Due to 6 g Acceleration Step	Required Carrier Tracking Loop Bandwidth
No inertial aiding	not applicable	6 g	18 rad/s
10 nmi/hr	1880	0.011 g	0.77
1 nmi/hr	431	0.0026 g	0.37
0.5 nmi/hr	311	0.0019 g	0.32
0.2 nmi/hr	225	0.0014 g	0.27

position and velocity in the Kalman filter cause the decrease in velocity error even though it is a range measurement which has been made. Each successive code loop reacquisition causes a step improvement in the velocity accuracy. In contrast the loosely coupled system does not get the benefit of the recently reacquired code phase until four satellites are in lock. At this point (in the lower graph) the improvement in velocity accuracy is easily recognized.

With four satellites in lock the loosely coupled system yields perfectly acceptable navigation performance. The response to jamming of the tightly coupled system is somewhat better. The maximum horizontal position error for each system studied is shown in Fig. 3.4.

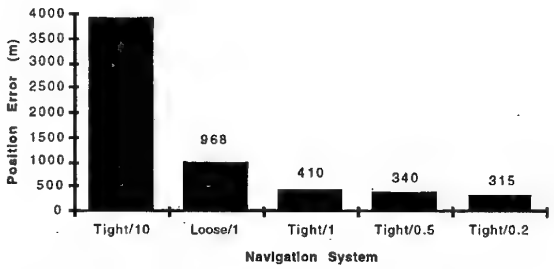

Fig. 3.4. Horizontal position error at time of reacquisition

If the navigation system is denied GPS measurements for eighty four minutes the horizontal position errors grow to the levels shown in Fig. 3.5

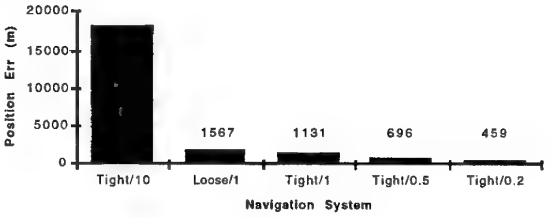

Fig. 3.5. Horizontal position errors 1 Schuler period after loss of last satellite.

In addition to the obvious correlation of navigation error to IMU quality, we can make the following general observations about these results. The tightly coupled 1.0 nmi/hr system does perform better than the loosely coupled system. This is due to two factors: 1) the tightly coupled system makes use of measurements even when fewer than four satellites are in lock, and 2) the calibration of the inertial instruments is somewhat better with the tightly coupled system. This performance difference diminishes with time. A very long time after the last GPS measurement the performance of the tightly coupled and loosely coupled systems would be identical - that of a 1 nmi/hr system. The performance of the 1.0 nmi/hr system is about 10 times better than that of the 1.0 nmi/hr system at the end of the 20 minute blackout interval. However, at the end of eighty four minutes the 1.0 nmi/hr system has only drifted to a 0.6 nmi error. The 10 nmi/hr system however has drifted to close to 10 nmi. This simply reflects the fact that the major source of error for the 10 nmi/hr system is uncalibratable random errors.

3.6.2. Jammer Flyby

For this scenario an aircraft flies by a jammer, thus loosing and regaining lock in a somewhat more realistic fashion. A jammer was on the ground near the midpoint of the trajectory was placed so as to cause an approximate 20 minute outage. In contrast to the previous situation in which the period of the outage was specified, in this scenario the actual loss of lock will be determined by the signal to noise ratio for each satellite. Reacquisition will be determined by the growing uncertainty in range and range rate to each satellite. The period of outage will also be a function of the bandwidth of the carrier tracking loops for each of the receivers. We will, again, observe position and velocity error growth as GPS measurements are lost.

Table 3.7 shows the number of range intervals to be searched for each satellite at the time the signal to noise threshold rose above 21 dB. In no case did the error growth in velocity cause the range rate uncertainty to any satellite to be greater than 10 m/s (one doppler shift interval).

Table 3.7. Search for range phase as a function of IMU quality.

Navigation System	Range (Code Phase) Intervals to be Searched Satellite Identification						
	3	11	12	15	17	18	21
Tightly Coupled 10 nmi/hr	73	64	70	42	82	70	43
Loosely Coupled 1.0 nmi/hr	8	8	8	6	9	8	6
Tightly Coupled 1.0 nmi/hr	7	6	6	5	7	6	5
Tightly Coupled 0.5 nmi/hr	6	6	6	5	6	6	5
Tightly Coupled 0.2 nmi/hr	6	5	6	5	6	5	5

For a search time of 20 ms per chip (code phase interval) the better IMU's hold the search time to 0.2 seconds. The 10 nmi/hr inertial system holds the search time to about 0.8 to 1.6 seconds. These number only reflect the error growth in position (and velocity) uncertainty and assume that the entire 1σ search area must be searched before lock on is achieved. Sometimes the signal will be found sooner, and of course 32% of the time it will be outside of the 1σ bounds and require a longer search. We would also like to state that these results cannot be generalized. The placement of the jammer, its signal strength, the antenna orientation and gain pattern are unique to the scenario and can only be considered typical.

The blackout period as a function of IMU architecture and IMU quality is shown in Fig. 3.6.

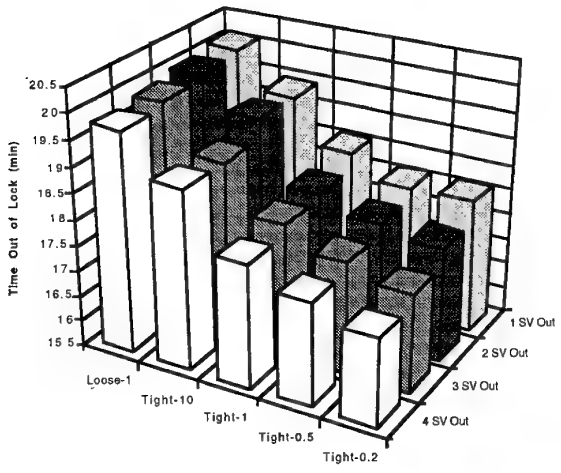

Fig. 3.6. GPS loss of lock as a function of IMU architecture and quality

(Note the vertical scale does not begin at zero. The difference is not so striking as the graph seems to indicate.) For this particular scenario the performance difference is due to better calibration of the inertial instruments rather than jamming resistance. Even for the best IMU the blackout time is reduced by only about 2 minutes from the 20 minute blackout experienced by the loosely coupled receiver with full (unaided) bandwidth. Once again we are reluctant to generalize from these results.

For this jammer flyby scenario the horizontal position errors (RSS 1σ) just prior to reacquisition are shown in Fig. 3.7.

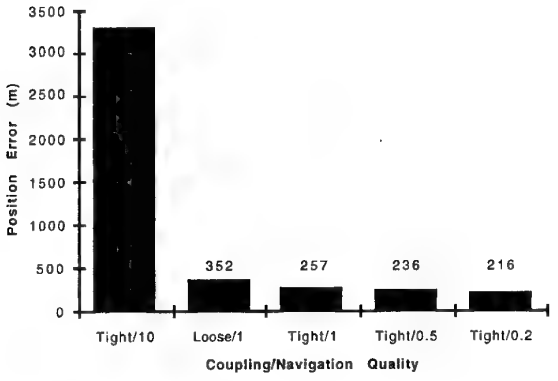

Fig. 3.7 Horizontal position error just prior to reacquisition.

The ratio of error level between the 10 nmi/hr and the 1nmi/hr tightly coupled systems (3300:260) is greater than the 10 to 1 ratio implied by their charcterization. Noise is a big error source in the 10 nmi/hr system and cannot be calibrated by the GPS measurements as can biases and scale factor errors. Thus the better IMU's perform better yet when they are continuously calibrated by inflight GPs measurements. The tightly coupled 1nm/hr system benefits somewhat more by the GPS inflight calibration than the loosely coupled system.

3.6.3 Headon Approach to Jammer

This scenario is meant to simulate the navigation performance of a fighter-bomber mission in which there is a jammer at the target. After take-off the aircraft climbs to 40,000 ft, dodges a surface to air missile then dives down to 200 ft to get below radar detection and to avoid GPS jamming. On approaching the target area the aircraft then climbs to a few thousand feet to locate the target then releases the bomb. The jammer at the target overwhelms all variations of IMU quality and architecture as soon as the aircraft climbs above its horizon. The time interval between loss of lock and bomb release is about 159 seconds. for the loosely coupled system and 153 seconds for the tightly coupled systems. Fig. 3.8 shows the position error at bomb release for the five navigation systems.

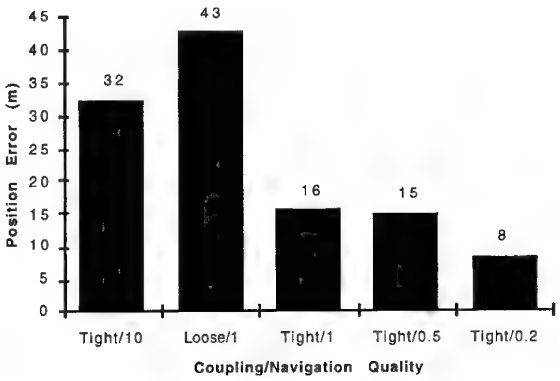

Fig. 3.8. Position error at bomb release after about 2.7 minutes of free inertial navigation.

In contrast to the previous scenarios we see here the IMU performance shortly after loss of lock. The tightly coupled system 10 nmi/hr system has better performance than this particular loosely coupled system when GPS measurements are available. After this short a time, 2.7 minutes, this advantage has not yet been lost. Another contributor to the difference is that the tightly coupled systems resisted the jamming for about 6 seconds longer than did the loosely coupled system.

3.6.4. Helicopter Performance in Jammer Vicinity

This scenario is meant to depict a helicopter on a scouting mission. The helicopter closely follows the terrain in order to avoid detection. The resulting flight profile has high levels of acceleration and jerk which caused occasional momentary loss of carrier lock. No effect on mission performance can be seen.

The jamming scenario was simplified for this mission. GPS measurements were available until on-board estimates of IMU calibration and alignment had reached steady-state. At that point GPS was assumed to be jammed. The mission continued for another 19 minutes.

In a variation from the previous scenarios the navigation system of the helicopter was augmented with ground speed doppler measurements. These doppler measurements yield velocity in body coordinates. It will be seen that these measurements make a considerable difference in navigation performance after GPS is lost. The error model for the Doppler measurements is given in Table 3.8.

Table 3.8. Error model for Doppler ground speed measurements.

Error Source	Vertical (1σ)	Horizontal (1σ) (two components)
Bias	0.05 nmi/hr	0.1 nmi/hr
Scale Factor	0.1%	0.25%
Misalignment	2.0 mr	2.0 mr

At the end of the mission the task of the helicopter is to define coordinates of a target at some distance (8 km) from its own position. The error in target coordinates, δr_{tgt}, is thus due to a combination of helicopter location error, $\delta r_{helicopter}$, and IMU misalignment, $\delta\alpha$.

$$\delta r_{tgt} = \delta r_{helicopter} + \delta\alpha \times r$$

where r is the vector from helicopter to target.

Fig. 3.9 shows the error in helicopter position and target location as a function of two IMU qualities when no ground speed Doppler measurements are included in the navigation solution.

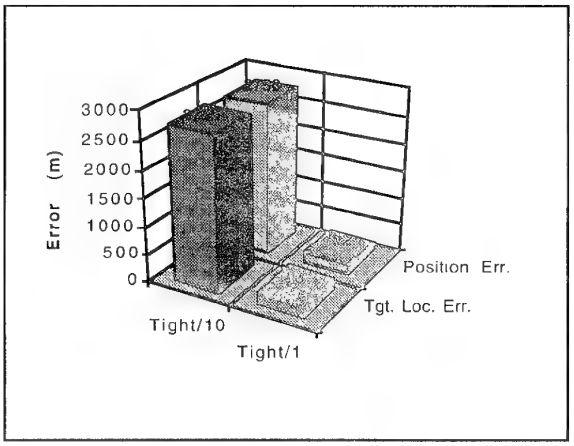

Fig. 3.9. Position and target location error for a helicopter 19 minutes after GPS loss of lock without the aid of Doppler ground speed measurements.

As seen in an earlier scenario the ratio of the errors between the 10 nmi/hr and the 1 nmi/hr navigation system, 2750:192 in this case, is greater than the characterization ratio, 10:1. The pointing error is negligible compared to the position error so that the target location errors and the aircraft position errors are essentially the same.

Fig. 3.10 shows the same errors when the navigation solution is aided with ground speed Doppler measurements. Results for both a GPS/INS system and for a GPS/INS system supplemented with Doppler ground speed measurements are shown.

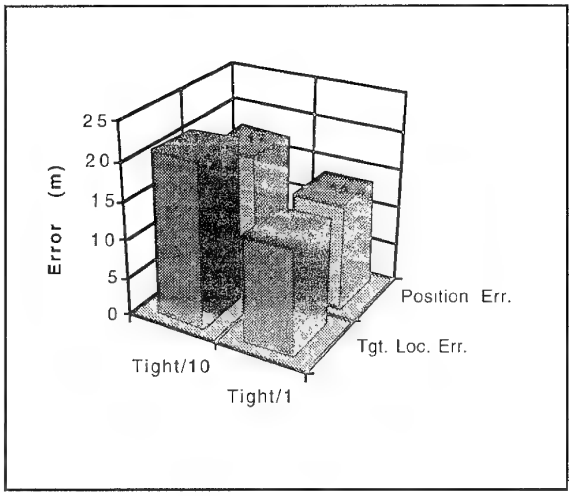

Fig. 3.10. Position and target location error for scout helicopter 19 minutes after GPS loss of lock with the aid of Doppler ground speed measurements.

As expected the Doppler ground speed measurements slow the error growth that is seen with the free inertial system. These errors in these velocity measurements integrate into growing position errors so they are not equivalent to GPS which provides position as well as velocity. But they provide much better results than the inertial instruments whose measurements must be integrated twice before yielding position. The improvement with the Doppler ground speed sensor is dramatic. Note that when aided by these measurements the performance of the 10 nmi/hr system is nearly the same (50% greater target location errors) as that of the 1 nmi/hr system.

3.7 Summary and Conclusions

This study illustrates several features of GPS/INS systems which are true in many cases. We should be careful about drawing general conclusions because the flight profiles and jamming scenarios are quite specific. A particular flight profile may allow more or less inflight calibration depending on aircraft maneuvers. These differences can be minimized by including maneuvers whose specific purpose is inflight calibration and alignment. Jamming scenarios however are more difficult to characterize in a general way. Jammers can be on the ground in which case they are shadowed by the terrain for low altitude approaches. They could also be airborne, in which case their effective range will be greater, but for which their signal strength will grow with closing distance uncomplicated by shadowing considerations. Furthermore there may be focussed jammers and as a countermeasure to jamming, receiver antennas whose gain can be made a function of direction. All these variables make it difficult to generalize about how much longer a tightly coupled system will be able to maintain lock on

the GPS signals. Perhaps the most general statement that can be made is to state the improvement in decibels in signal to noise(jammer) ratio that inertially aided receivers achieve.

The inflight calibration and alignment of the tightly and loosely coupled receivers is simpler to assess. As in this study, loosely and tightly coupled architectures can be proposed. The resulting performance after loss of lock can then be assessed by either Monte Carlo techniques or, as in this study, by linearized covariance analysis.

After doing the analysis and observing simulation results we make the following cautious assertions.

1. When GPS is available its measurements dominate navigation performance. The steady state navigation error will be reduced by inertial aiding which simply considered allows GPS measurement noise to be "averaged out". Improvement of steady state error with improving inertial quality is not as dramatic.
2. Tight coupling is superior to loose coupling for maintaining lock in a jamming environment, but the gain is hard to quantify except by improvement in signal to noise(jammer) ratio.
3. Better inertial instruments gain more from inflight alignment and perform better after GPS is lost. This is because poorer instruments in general have larger proportions of uncalibratable noise.
4. For short time intervals after GPS loss coupling architectures can make a difference in performance (because they affect calibration and alignment quality).
5. In the long run basic IMU quality will dominate navigation accuracy due to instrument noise and loss of calibration accuracy.

Finally we saw a dramatic difference in jammed performance if Doppler ground speed measurements were to be available.

References:

1. Cox, D.B., Kriegsman, B.A., Stonestreet, W.M., Kishel, J. , and Calicchia, L.V. "Feasibility Study of GPS-Inertial Navigation for Helicopters and Study of Advanced GPS Signal Processing Techniques", Draper Report R-981, Cambridge, MA. March 1978.

2. Cox, D.B. "Inertial Integration of GPS", Global Position System - Papers Published In Navigation, Vol. 1, Institute of Navigation, Alexandria, VA., 1980

3. Copps, E. M., Geier, G. J. Fidler, W. C., and Grundy, P. A. "Optimal Processing of GPS Signals", Navigation: Journal of the Institude of Navigation, Vol. 27, No. 3, Fall 1980.

4. Denaro, Robert P. and Geier, G. Jeffrey, "GPS/Inertial Navigation System Integration for Enhanced Navigation Performance and Robustness", AGARD-LS-161, Advisory Group for Aerospace Research and Development, Neuilly-sur-Seine, France, September 1988.

5. Sennott, James W. and Senffner, "Navigation Receiver with Coupled Signal Tracking Channels", U.S. Patent 5,343,209, Aug. 1994

6. Greenspan, R.L., "GPS/Inertial Integration Overview", Aerospace Navigation Systems, AGARD-AG-331, Advisory Group for Aerospace Research and Development, Neuilly-sur-Seine, France, June 1995

7. Lipman, Jerome S., "Tradeoffs in the Implementation of Integrated GPS Inertial Systems", Proceedings of the Institute of Navigation GPS-92 Technical Meeting, The Institute of Navigation, Alexandria, VA.

8. Moya, David C., Elchynski, Joseph J., "Evaluation of the World's Smallest Integrated Embedded GPS/INS, the H-764G", Proceedings of the National Technical Meeting of the Institute of Navigation 1993, The Institute of Navigation, Alexandria, VA, pp. 275-286.

9. "Systems Requirement Document for an Embedded Global Positioning System (GPS) Receiver in an Inertial Navigation System (INS) EGI", ASC/SMEV Wright Patterson AFB, Ohio 45433-6503

10. Johnson, Gregory B., Lewantowicz, Zdzislaw H. "Closed Loop Operation of GPS Aided INS", Third International Technical Meeting of the Satellite Division of the Insititute of Navigation Proceedings, The Institude of Navigation, Washington, D.C. pp. 461-470.

ATTITUDE DETERMINATION

Dr. Gérard Lachapelle
Department of Geomatics Engineering
The University of Calgary
2500 University Drive, N.W.
Calgary, Alberta, T2N 1N4, Canada
Tel: 403 220 7104; fax: 403 284 1980
e-mail: lachapel@ensu.ucalgary.ca

ABSTRACT

The fundamental concept of precise attitude determination with multi-antenna Global Positioning System (GPS) receiver technology is described. The characteristics of the observable used for this purpose, namely the carrier phase, are summarized, with emphasis on phase noise and multipath which constitute the major error sources. Given a multi-antenna configuration mounted on a rigid platform, the procedure to successively fix the double difference integer carrier phase ambiguity between the nearby antennas, obtain sub cm-level tridimensional relative position vectors and transform them into the attitude components, namely roll, pitch and heading, is described. The two-antenna case, which allows pitch and heading determination, is presented as a special case. Integer ambiguity resolution between the antennas turns out to be relatively easy to achieve with single frequency (L_1) data because the differential orbital and atmospheric errors are negligible and the fixed distances can be used as constraints to speed up the ambiguity resolution process. The use of various antenna configurations to recover the carrier phase ambiguities instantaneously is mentioned. The attitude accuracy is a function of several parameters, namely satellite configuration, inter-antenna separation, phase noise and prevailing multipath conditions. Two multi-antenna hardware approaches to the problem of attitude determination are described using various case studies, namely a dedicated multi-antenna receiver approach which allows real-time operation and a multi-GPS sensor approach which can be used in real-time only if the data from each sensor is transferred to a central processor as the measurements are made. If post-mission results only are required, no data links involving the sensors are required since the phase measurements can be precisely synchronized using the time obtained from the code measurements. The effect of signal masking on attitude determination, which is relatively severe due to the carrier phase ambiguity problem, is discussed. The effect of relative platform motion, e.g., wing flexure in the case of an aircraft, on attitude determination performance is discussed. The case studies used deal with shipborne, aircraft and land cases. The results with several multi-antenna systems deployed in various configurations are presented.

INTRODUCTION

The concept of attitude determination with GPS is straightforward. At least three antennas relatively close to each other and in an adequate relative geometry are mounted on a rigid platform. The high accuracy carrier phase measurements are used to obtain the tridimensional vectors between the antennas in a specified coordinate system, e.g., in the WGS84 cartesian geocentric reference system. Through proper coordinate rotation, the heading, pitch and roll components with respect to WGS84 can be derived. The azimuth (heading) is therefore geodetic and different from the astronomic azimuth by the Laplace correction $\eta \tan\phi$, where η is the deflection component in the prime vertical and ϕ, the longitude. η can reach 1 arcmin in extreme cases.

The concept of attitude determination with satellite observations was initially proposed in the mid 70s for the Transit system. By the early 80s, many investigators were proposing the use of GPS (e.g., Brown et al 1982) and, by the mid 80s, experiments with a single antenna were initiated (Evans 1986). By the late 80s, many multi-antenna experiments were underway (e.g., Kruczynski et al 1989, Nesbø 1988, Purcell et al 1989, Rath & Ward 1989). In the early 90s, the first dedicated multi-antenna commercial system, namely the Ashtech 3DF, became available (Ferguson et al 1991). Many successful aircraft attitude determination experiments were being reported by 1992 (e.g., van Graas & Braasch 1991, Cohen & Parkinson 1992, Cohen et al 1993). The testing of low cost, non-dedicated, GPS sensors to obtain the attitude parameters was also initiated during that period (e.g., Cannon et al 1992, Lu et al 1993).

Paper presented at the AGARD MSP Lecture Series on "System Implications and Innovative Applications of Satellite Navigation", held in Paris, France from 1-2 July 1996; Rome, Italy from 4-5 July 1996; Madrid, Spain from 8-9 July 1996 and St. Petersburg, Russia from 11-12 July 1996, and published in LS-207.

CARRIER PHASE OBSERVABLE

The carrier phase observable can be written as

$$\Phi = \rho + d\rho + c(dt-dT) + \lambda N - d_{ion} + d_{trop} + \varepsilon(\Phi)$$

where

$\Phi_{length} = (-)\lambda\phi_{cycles\ (integer+\ fract)}$ (sign depends on rx)
$\rho = \| \mathbf{r} - \mathbf{R} \|$
$\mathbf{r}$ ... position vector of the satellite (known)
$\mathbf{R}$ ... position vector of the receiver (unknown)
$d\rho$ ..... orbital errors
dt, dT... satellite & receiver clock errors
N ... cycle ambiguity (integer number)
$\varepsilon(\Phi)$... $f\{\varepsilon(\Phi_{rx}), \varepsilon(\Phi_{mult})\}$
$\varepsilon(\Phi_{rx})$... receiver measuring noise
$\varepsilon(\Phi_{rx}) = f$ (rx, tracking bandwidth)
$\varepsilon(\Phi_{rx}) \approx 0.5$ - a few mm;
$\varepsilon(\Phi_{mult}) \leq 0.25\ \lambda$ (< 5 cm at L_1)

The carrier phase observables are double differenced between receivers and atellites and the satellite and receiver clock errors are eliminated in the process. Since the inter-antenna distances are relatively small (≤ 100 m), the orbital and atmospheric errors are also practically eliminated. The effect of Selective Availability (δ or ε type) is therefore eliminated. The L_1 carrier phase integer ambiguities are resolved using a standard search technique (e.g., Cannon & Lachapelle 1994) and, in double difference mode, the carrier phase observation equation reduces to

$$\Delta\nabla\Phi = \Delta\nabla\rho + \varepsilon_{\Delta\nabla\Phi}.$$

The only errors affecting the carrier phase measurements are therefore the carrier phase receiver noise and multipath, the latter being larger by one to two orders of magnitude. Instantaneous attitude determination with GPS is at this time limited by carrier phase multipath. Under dynamic conditions, multipath tends to average out and it effect on the 3D vector is ususally below the cm level. The integer ambiguities on L_1 (single lane) can easily be resolved because the inter-antenna distances are small and, as a consequence, the differential errors practically cancel out, and the known inter-antenna vector lengths (scalar) can be used as a constraint. As a result, the integer ambiguities can usually be resolved in intervals of seconds to tens of seconds. This is based on the assumption that the carrier phase measurements are free from cycle slips and that the satellite geometry is relatively good. If cycle slips occur, new ambiguities have to be determined. Carrier phase observables under signal masking (e.g., foliage) are therefore of limited use, a limitation of signifance for certain applications, such as artillery. The Geometric Dilution of Precision (GDOP) is often used to quantify the satellite geometry. More appropriate DOP's exist however to quantify the geometry for attitude determination, e.g., the Attitude DOP or ADOP (Cohen 1996).

If the time to ambiguity resolution is too long for the application at hand, the antennas or a subset thereof can be mounted close to each other to permit instantaneous resolution (e.g., Diefes et al 1994, El-Mowafy & Schwarz 1995).

If only two antennas are used, the heading and pitch components can be determined, even under roll conditions (e.g., Lu et al 1994). In principle, a single antenna receiver in periodic motion is sufficient if no SA affects the measurements (e.g., Evans 1986, Ulmer et al 1995). The tridimensional vector between successive positions can be obtained with a resonable accuracy is the time interval is short (< a few seconds). The heading acucracy is however lower than that achievable with a twin-antenna system.

The accuracy of the attitude components is largely a function of the inter-antenna distances. An example of heading and pitch accuracy versus inter-antenna distance in given in Figure 1 for a two-sensor system (Sun & Cannon 1995). The two sensors in this case are two low cost 8-channel Motorola Oncore receivers. The configuration was in static mode and the accuracies are those obtained for single epoch (i.e., instantaneous) heading and pitch components.

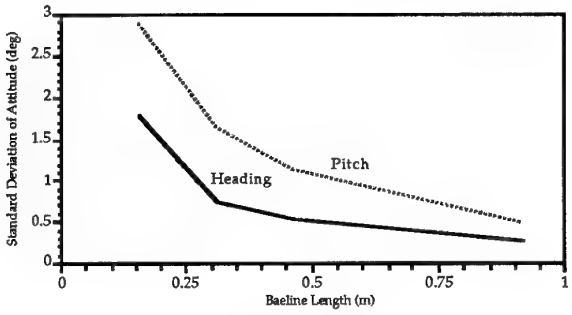

Figure 1
Relationship Between Inter-Antenna Distance and Heading and Pitch Accuracy

REFERENCE FRAME CONSIDERATIONS AND ATTITUDE PARAMETER COMPUTATION

The attitude of a rigid body platform is determined by the orientation of the specified body frame coordinate system with respect to the reference coordinate system (e.g., Lu et al 1993). In the GPS

case, the reference system is usually the *local-level* coordinate system with the z-axis pointing upward along the ellipsoidal normal, the x-axis pointing towards the ellipsoidal east and y-axis pointing towards ellipsoidal north. The body frame platform is usually formed by choosing three GPS antennas, since three points in space define a plane. Once the body platform or the plane is defined, a body frame coordinate system can be specified within the chosen platform. For example, assuming the three antennas shown in Figure 2 form a plane, Antennas 1 to 2 can be chosen as the body frame y^b-axis. The body frame x^b-axis is lying in the plane defined by Antennas 1, 2 and 3 and pointing right of the y^b-axis. The body frame z^b-axis then forms a right-handed system with the x^b and y^b axes. If the distances between the antennas are known precisely, the GPS antenna coordinates in the body frame coordinate system can be calculated immediately. This is shown for Antennas 2 and 3 in Figure 2. These body frame coordinates remain unchanged during all kinematic movements for a rigid body antenna configuration.

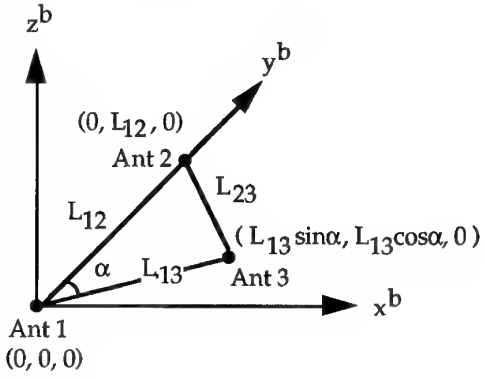

Figure 2
Body Frame Coordinate System Defined by the Three Antennas and Their Body Frame Coordinates

The geocentric coordinates of Antennas 2 and 3 relative to Antenna 1 are determined very precisely using carrier phase observables. These geocentric coordinates can then be easily transformed into the local-level system with the origin at Antenna 1. Therefore, two sets of coordinates are associated with each GPS antenna. One set is the body frame system coordinates, the other set is the GPS-derived local-level coordinates. However, the local-level coordinates can be rotated to the body frame system by three consecutive right-hand rotations about the three local-level axes (e.g., Wertz 1978). The first rotation about local-level z-axis is the yaw of the platform. The second rotation made about the rotated local-level x-axis is the pitch.. The third rotation about the rotated y-axis is the roll . The rotations can be written as (Wertz, 1978)

$$\begin{pmatrix} x^b \\ y^b \\ z^b \end{pmatrix} = R_2(r)R_1(p)R_3(y)\begin{pmatrix} x \\ y \\ z \end{pmatrix} \quad (1)$$

$$R_2(r)R_1(p)R_3(y) = R(y,p,r) = \begin{pmatrix} c(r)c(y)-s(r)s(p)s(y) & c(r)s(y)+s(r)s(p)c(y) & -s(r)c(p) \\ -c(p)s(y) & c(p)c(y) & s(p) \\ s(r)c(y)+c(r)s(p)s(y) & s(r)s(y)-c(r)s(p)c(y) & c(r)c(p) \end{pmatrix} \quad (2)$$

where R(y, p, r) is the orthogonal rotation matrix which rotates the GPS-derived local-level coordinates $(x, y, z)^T$ of an antenna to its corresponding body frame coordinates $(x^b, y^b, z^b)^T$. The functions s() and c() denote sine and cosine, respectively. The GPS-derived local-level coordinates $(x, y, z)^T$ of all the antennas are first derived from the carrier phase observables. The yaw, pitch and roll of the platform defined by the specified GPS antennas are needed.

A number of formulas have been given for the computation of yaw, pitch and roll based on both the antenna's local-level coordinates and its corresponding body frame coordinates (e.g., Wertz 1978, Shuster & Oh 1981). Generally speaking these formulas can be classified into two categories. The first category is the direct computation method which does not require knowledge of the antenna's body frame coordinates and only uses the local level coordinates of the three antennas that define the platform. The second category is the least-squares estimation procedure that make full use of all the position information of multiple antennas in the local level as well as in body frame and takes into consideration the dependence of the terms in the nine parameter matrix given in Eqn. (2).

Direct Computation of Yaw, Pitch and Roll

Let us assume that GPS antennas 1, 2 and 3 from Figure 2 form the platform, and antennas 1 - 2 define the heading. The body frame coordinates for antenna 2 and 3 can then be expressed as $(0, L_{12}, 0)^T$, $(L_{13}\sin(\alpha), L_{13}\cos(\alpha), 0)^T$, respectively. The corresponding GPS-derived local level coordinates for these two antennas are $(x_2, y_2, z_2)^T$ and $(x_3, y_3, z_3)^T$. Mathematically, the body frame coordinates and their corresponding local level system coordinates for each antenna must satisfy Eqn. (1). Thus, substituting the Antenna 2 coordinates $(0, L_{12},$

$0)^T$ and $(x_2, y_2, z_2)^T$ into Eqn. (1) and using the orthogonality of matrix $R(\psi, \theta, \phi)$, we immediately obtain the formulas for computing yaw and pitch as

$$\psi = -\tan^{-1}(x_2 / y_2) \tag{3}$$

$$\theta = \tan^{-1}(z_2 / \sqrt{x_2^2 + y_2^2}) \tag{4}$$

It can be seen from the formulas that the baseline between Antennas 1 to 2 actually determines the yaw and pitch of the platform. Once the yaw and pitch are obtained, the local-level coordinates $(x_3, y_3, z_3)^T$ of Antenna 3 can be first rotated around the local level z-axis by an amount ψ, and then rotated again around the rotated local level x-axis by an amount θ. The resultant coordinates of Antenna 3 after these two rotations are denoted by (x_3'', y_3'', z_3''). A third rotation, $R_2(\phi)$, rotates (x_3'', y_3'', z_3'') to its body frame coordinates $(L_{13}\sin(\alpha), L_{13}\cos(\alpha), 0)^T$, namely

$$\begin{pmatrix} L_{13}\sin(\alpha) \\ L_{13}\cos(\alpha) \\ 0 \end{pmatrix} = \begin{pmatrix} \cos(\phi) & 0 & -\sin(\phi) \\ 0 & 1 & 0 \\ \sin(\phi) & 0 & \cos(\phi) \end{pmatrix} \begin{pmatrix} x_3'' \\ y_3'' \\ z_3'' \end{pmatrix} \tag{5}$$

From the third row in Eqn. (5), roll can be computed as

$$\phi = -\tan^{-1}(z_3'' / x_3'') \tag{6}$$

Eqns. (3), (4) and (6) are the direct computation formulas for yaw, pitch and roll. They only use GPS-derived local-level coordinates from three GPS antennas which define the platform and thus are not dependent on *a priori* body frame coordinates. The accuracy of the computed yaw, pitch and roll can be easily derived based on error propagation laws. For instance, by differenciating Eq. (4), we get

$$d\theta = \frac{(x_2^2+y_2^2)dz_2 - z_2x_2dx_2 - z_2y_2dy_2}{\sqrt{x_2^2+y_2^2}\,(x_2^2+y_2^2+z_2^2)} \tag{7}$$

Applying the error propagation law to the above equation and neglecting the correlation among the coordiante components, we obtain

$$\sigma_\theta \le \sigma_{max} / \sqrt{x_2^2 + y_2^2 + z_2^2} = \sigma_{max} / L_{12} \tag{8}$$

where σ_{max} is the maximum standard deviation of the GPS-derived coordinates for Antenna 2, i.e. $\sigma_{max} = \max(\sigma_{x2}, \sigma_{y2}, \sigma_{z2})$. It can be seen that the pitch accuracy is inversely proportional to the baseline length that defines the heading.

Least Squares Estimation of Yaw, Pitch and Roll

From Eqn. (2) it can be seen that the rotation matrix is solely defined by the three elements, i.e. yaw, pitch and roll. Therefore, only three elements in the orthogonal rotation matrix are independent. If the precise body frame coordinates for each antenna are known *a priori*, a least squares estimation of yaw, pitch and roll can be made based on Eqns. (1) and (2). Suppose $\Theta_i^b = (x_i^b, y_i^b, z_i^b)^T$ and $\Theta_i = (x_i, y_i, z_i)^T$ are the body frame coordinates and its corresponding local level coordinates for Antenna i. Based on Eqn. (1), for all the GPS multi-antenna positions we have the following relation

$$\begin{pmatrix} \Theta_2^b \\ \Theta_3^b \\ \vdots \\ \Theta_n^b \end{pmatrix} = R(\psi, \theta, \phi) \begin{pmatrix} \Theta_2 \\ \Theta_3 \\ \vdots \\ \Theta_n \end{pmatrix} \quad \text{or} \quad \Theta^b = R(\psi, \theta, \phi)\,\Theta \tag{9}$$

with $\Theta^b = (\Theta_2^b, \Theta_3^b, \cdots, \Theta_n^b)^T, \Theta = (\Theta_2, \Theta_3, \cdots, \Theta_n)^T$.

In Eqn. (9), Θ^b is known *a priori* with a covariance matrix $Var(\Theta^b)$. Θ is treated as our observations which are derived from GPS carrier phase measurements with the covariance matrix $Var(\Theta)$. The unknown parameters to be resolved are (y, p, r).

From a statistical aspect, the least -squares estimation of yaw, pitch and roll gives the best estimates based on all the position information contained in a multiple GPS antenna array. Another advantage of least squares estimation over direct computation is that the least squares solution is less affected by multipath on a single antenna since the solution is the best fit over all antenna positions.

CASE STUDIES

The following shipborne, aircraft and land cases serve as exemples of the level of performance achievable as a function of equipment, antenna configuration and platform dynamics.

Survey Launch Test - Ashtech 3DF versus Non-Dedicated GPSCard™ Sensors

This test was conducted in a survey launch in September 1992 (Lu et al 1993). A 4-antenna 3DF system and a 3-GPSCard™ system were set up on a

12-m survey launch as shown in Figure 3. The GPSCard™ units were not interconnected and the data was post-processed. The time tags for the carrier phase measurements were provided by the single point code solutions at each unit. The inter-antenna distances were measured with an accuracy of 1 cm.

The launch cruising speed was 10 to 15 knots. The roll reached several degrees. One hour of data during which six satellites above an elevation of 15° and with a GDOP < 3 were tracked was selected for the analysis. The measurements were reducted using The University of Calgary's MULTINAV™ software. The integer ambiguities between the antennas were resolved in less than 15 seconds. The orientation differences between the two body frames defined by the two sets of antennas were resolved using a sequence of some 45 minutes of data in batch mode.

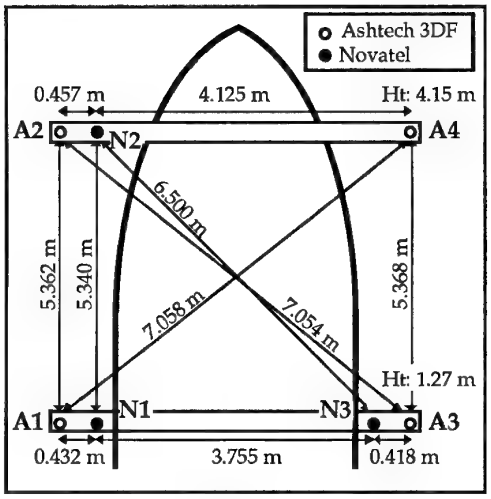

Figure 3
Survey Launch GPS Antenna Configuration

Table 1
Agreement Between the 3DF and the GPSCard™ Systems

Attitude	LS Solution		Direct Computation	
	Mean (arcmin)	RMS (arcmin)	Mean (arcmin)	RMS (arcmin)
Yaw	3.975	5.402	5.349	6.587
Pitch	-0.426	6.681	2.194	8.089
Roll	-11.993	14.838	-12.626	16.215

Shown in Table 1 are the mean and RMS differences between the two systems using the two computation approaches desbribed earlier. The RMS agreement ranges from 5 arcmins (0.08°) to 15 arcmins (0.25°). The agreement of the least-squares estimates is slightly better than that for the direct computation. This is because the additional information of the antenna's body frame coordinates is used in least-squares estimation. If one assumes that both systems deliver a similar level of accuracy, the attitude component accuracy (1σ) is RMS/√2, e.g., 3.9 arcmins in yaw, 4.74 arcmins in pitch and 10.50 arcmins in roll.

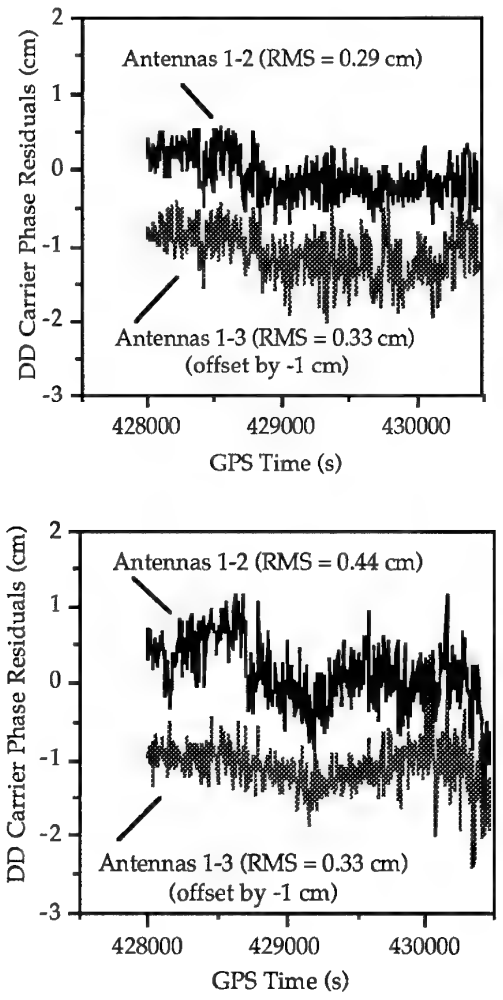

Figure 4
Double Difference Carrier Phase Residuals of SVs 23- 21 for the 3DF (above) and the GPSCard™ (below) Systems

Shown in Figure 4 are the SVs 23-21 carrier phase double difference residuals with fixed integer ambiguities for the 3DF and GPSCard™ systems, respectively. Note that the residuals for Antennas 1-3 have been offset by -1 cm for clarity. The residuals are < 5 mm, as expected. GPSCard™ antenna #2 had no chokering groundplane and slightly higher multipath effect onn the residuals is evident for the baseline connecting GPSCard™ antennas 1 and 2. The different multipath signatures for the two

systems arises from the use of antennas with different vertical response pattern.

Accuracy Performance Versus Inter-Antenna Distances - Shipborne Case

A series of tests using a (Canadian) Department of National Defence 1,600 ton research vessel was conducted in 1992 and 1993 with three different GPS attitude reference systems, namely an Ashtech 3DF, a Trimble Vector and a configuration of four NovAtel GPSCard™. The antenna configuration of each system is shown in Figure 5. A cursory analysis of these configurations leads to the conclusion that, the greater the inter-antenna distance, the higher the accuracy. A high performance dual inertial navigation system (INS) system was available to assess independently the GPS-derived attitude components (McMillan et al 1994). The results are summarized in Table 2. As expected, the accuracy is directly related to the inter-antenna distance along the relevant direction.

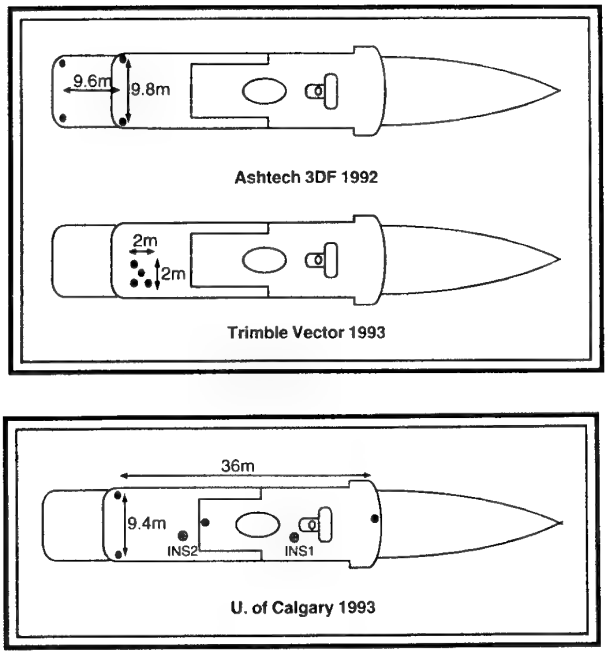

Figure 5
3DF, Vector and GPSCard™ Shipborne Antenna Configuration

Table 2
Agreement between INS and GPS-Derived Attitude Components

Attitude Component		Percentile (°)	
		68%	95%
3DF:	Heading	0.04	0.08
	Pitch	0.05	0.11
	Roll	0.05	0.11
Vector:	Heading	0.15	0.39
	Pitch	0.16	0.42
	Roll	0.15	0.31
GPSCard™ Configuration	Heading	0.026	0.052
	Pitch	0.040	0.084
	Roll	0.048	0.097

Hydrographic Survey Vessel Attitude Determination

In order to evaluate the level of accuracy achievable with GPS to provide attitude parameters for multi-beam acoustic depth determination, Lachapelle et al (1994a) tested a configuration of four GPSCard™ units on a 50-m hydrographic survey vessel of the Canadian Hydrographic Service in June 1993. A Honeywell HG1050 INS provided independent attitude parameters with an estimated accuracy of the order of 6 arcmins initially and 2 arcmins subsequently in heading and about 15 arcsecs in roll and pitch. The antenna separation ranged from 12 to 42 m, as shown in Figure 6. The carrier phase data was collected at a rate of 10 Hz. The roll component reached 10° during manoeuvres and roll variations reached 2.5° per second. During the manoeuvres, loss of carrier phase lock occurred occasionally on low satellites but this resulted in no discontinuities in GPS-derived attitude parameters. The RMS agreement between the INS and GPS derived attittude parameters is summarized in Table 3. The agreement is better than 1 arcmin in the case of the heading and pitch components due to the long inter-antenna distance along that axis (42 m). The GPS results were shown to be sufficiently accurate for multi-beam acoustic depth determination.

Table 3
Agreement between INS and GPS-Derived Attitude Components - Hydrographic Vessel

Attitude Component	RMS Differences	
	degrees	arcmins
Heading	0.015	0.87
Pitch	0.013	0.80
Roll	0.044	2.65

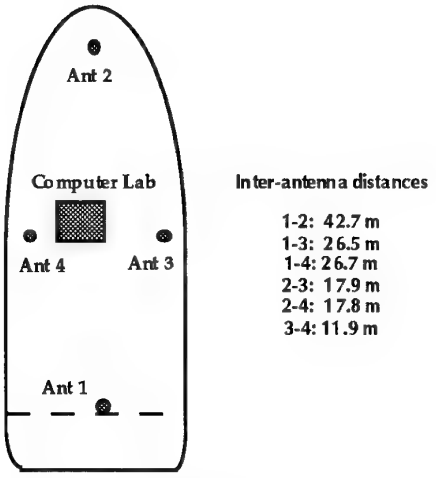

Figure 6
GPSCard™ Antenna Configuration - Hydrographic Vessel

Aircraft Attitude Determination and Wing Flexing

Several flight tests were conducted during recent years to assess the capability of a multi-antenna GPS system to measure aircraft attitude parameters (e.g., van Graas & Braasch 1991, Cohen et al 1993). The case study reported here is that reported by Cannon et al (1994).

A series of flight tests with a configuration of four GPSCard™ units were conducted by The University of Calgary and Sandia National Laboratories in February 1994 near the SNL facility located on Kirtland Air Force Base in Albuquerque, New Mexico. A de Havilland Twin Otter aircraft was used. The location of the four antennas are shown in Figures 7 and 8. A high performance Honeywell ring laser gyro INS was also used to provide an independent system for the measurement of the attitude parameters.

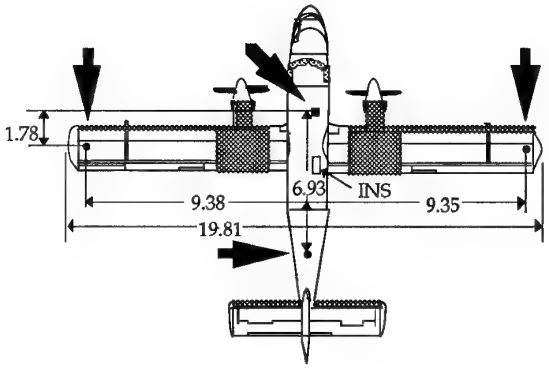

Figure 7
Aircraft Antenna Locations

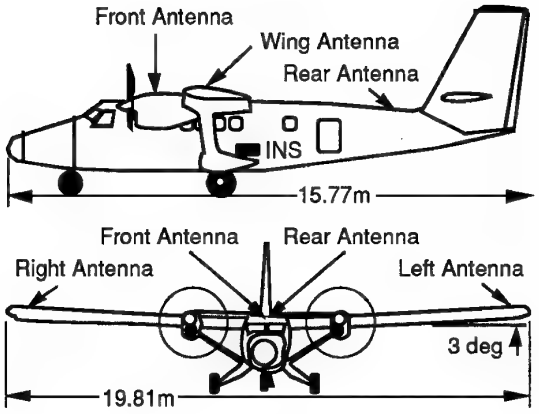

Figure 8
Aircraft Installation

The tests were carried out over a four day period under various dynamic conditions. On the first day, the aircraft was flown under low dynamic conditions to assess the nominal performance of the receivers in the flight environment. During this flight, the maximum pitch of the aircraft was about 10° while the absolute maximum roll of the aircraft was about 40 °. On the second day, pitch maneuvers of ranging between -20 to 35° and roll maneuvers of ± 60° were undertaken. The other two days had conditions that ranged between these scenarios.

The body frame, which is needed for definition of the aircraft attitude, was realized by three antennas, namely the aft, forward and port antennas. The body frame was determined through a two hour static GPS survey when the aircraft was located on the tarmac prior to take-off. Distances between the GPS antenna pairs were estimated to about the 1 cm level using the static data and were used as constraints in the attitude determination algorithm to eliminate incorrect carrier phase integer ambiguities during the search phase.

In order to obtain attitude with respect to one fixed coordinate frame, the wing flexure effect on the roll component has to be removed prior to attitude computatio, as described by Cohen et al (1993). The accuracy of the INS-derived roll and pitch reference values are at the level of 1 arcmin and the heading accuracy at the level of 4 to 5 arcmins. It should be noted that the heading error is generally a bias and is removed when comparison with the GPS heading is done. Alignment errors of the GPS and INS systems were also taken into account.

In order to assess the impact of wing flexure modelling, comparisons are first made between the INS and GPS attitude parameters without a flexure

model. Data from February 4 was selected for this analysis. Figure 9 gives the differences in roll between the two systems for the entire mission and shows two discontinuities which occur when the aircraft takes off and lands, and thus is due to wing flexure.

The GPS attitude data was then re-processed with the flexure model implemented. Estimated wing flexure from the model is shown in Figure 10 and demonstrates flexure of the order of 12 cm. The flexure is highly correlated to the roll differences shown in Figure 9, as expected.

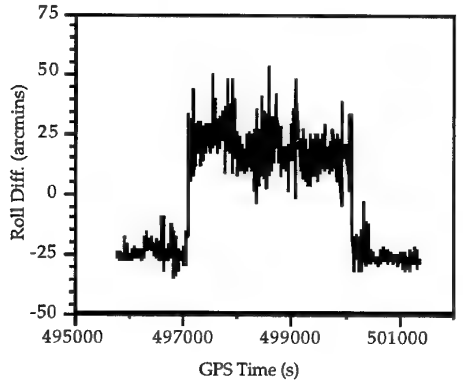

Figure 9
Roll differences between GPS and INS without wing flexure model

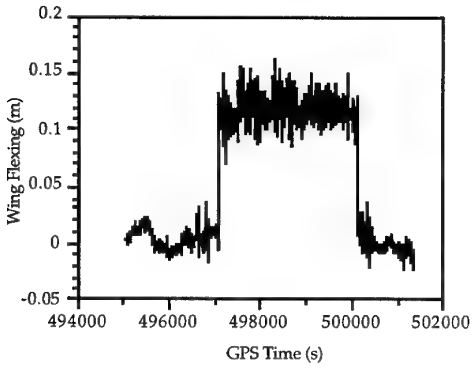

Figure 10
Estimated Wing Flexure o

The discontinuities are eliminated once the wing flexure is accounted for, and the remaining errors are carrier phase noise and multipath. Noise is evident mainly as a high frequency component, while multipath typically has a period of several tens of seconds. The effect of multipath on roll has an amplitude of 10 to 12 arcmins. Additional errors are due to high frequency wing vibration and small time tagging errors between the GPS and INS systems. Table 4 summarizes the statistics of the GPS-INS differences for the four test days. The RMS agreement is at the level of 3.1 to 6.6 arcmins for the three components which agrees well with previous results obtained by other investigators.

Table 4
RMS Differences Between GPS and INS Attitude

Session	RMS (arcmins)		
	Roll	Pitch	Heading
February 1	4.1	5.3	4.9
February 2	6.0	6.1	4.3
February 3	3.6	5.0	3.1
February 4	5.0	6.6	3.9

Fuselage Deformation with Twin-Antenna System

A by-product of a multi-antenna system mounted on a moving platform is the ability to measure platform deformations other than wing flexure. This was tested in 1993 for the case of a P-3 Orion aircraft (Lachapelle et al 1994b). Two antennas were mounted on a P-3, as shown in Figure 11. The distance between the two antennas was 20 m. The receivers wer NovAtel GPSCard™ units. The altitude of the aircraft during the flight test is shown in Figure 12. The epoch-to-epoch computed minus the known distance between the two antennas during the flight is shown in Figure 13. The distance variation of about 2.5 cm which occurs when the altitude decreases is due to the aluminium fuselage expansion caused by a temperature variation of 30°C (environmental lapse rate of -6.5°C/1,000m).

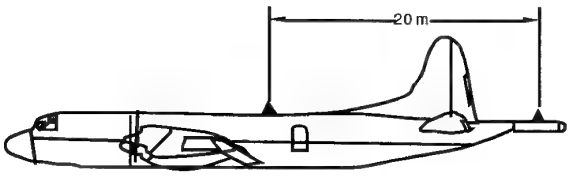

Figure 11
Twin-Antenna System on P-3 Aircraft

Heading Determination for Artillery

The artillery heading requirements specified by NATO (STANAG 2373, 1989) are summarized in Table 5. The question as to how GPS could meet these requirements was recently studied by Cannon et al (1996). It is evident based on the results described above, that a multi-antenna (a twin-antenna system is sufficient in this case) system can meet the specifications, provided that the inter-antenna distance is sufficient, namely a few tens of metres, and that unobstructed visibility to the satellite is available. A dual PLGR+GLS (Gun Laying System) system consisting of two

interconnected receivers, to be available from Rockwell by the end of 1996, will provided an orientation accuracy (1σ) of the order of 0.2 mil in a period of a few minutes, including set-up and ambiguity resolution time. The system will be available in both the SPS and PPS mode

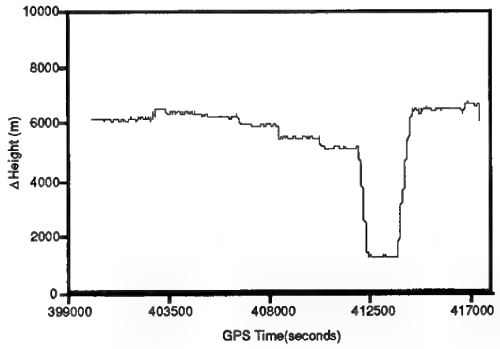

Figure 12
P-3 Aircraft Altitude

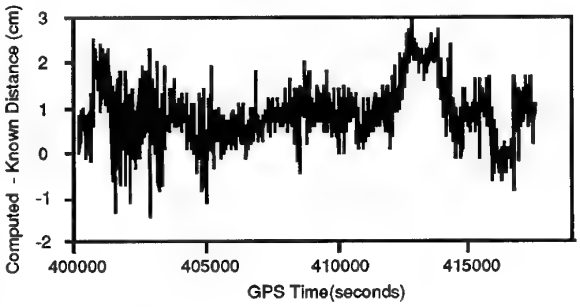

Figure 13
Computed Minus Known Distance Between the two Antennas

A single-antenna PLGR+GLS system is also available. The one antenna is moved from one point to another in a very short period of time (to limit differential errors). Test results reported by Ulmer et al (1995) show that an accuracy (1σ) of 1.1 to 2.5 mils is achievable within 30 seconds over a baseline of 50 m. Although these accuracies are sufficient for many applications, e.g., 60 and 81 MM mortars, they fail to meet the most stringent NATO STANAG 2373 accuracy of 0.3 mil for the 155MM HOW .

One of the major limitations of GPS heading determination for artillery is the need for concealment and the susceptibility of carrier phase measurements to losses of phase lock under such conditions. A potential solution to this problem would be to determine the heading with GPS where signal availability is satisfactory and transfer the heading to the gun battery fire control system with a theodolite, as shown in Figure 14.

Table 5: Artillery Heading Requirements

(NATO STANAG 2373, 1989)

Equipment	Orientation (PE) (mils†)	Time to achieve (min)
105MM HOW	0.6	20
155MM HOW	0.3	20
AN/TPQ 36	0.4	20
AN/TPQ 37	0.4	20
Sound Ranging (external)	0.3	20

† 1 mil = 3.375 arcmins ≈ 1 mrad

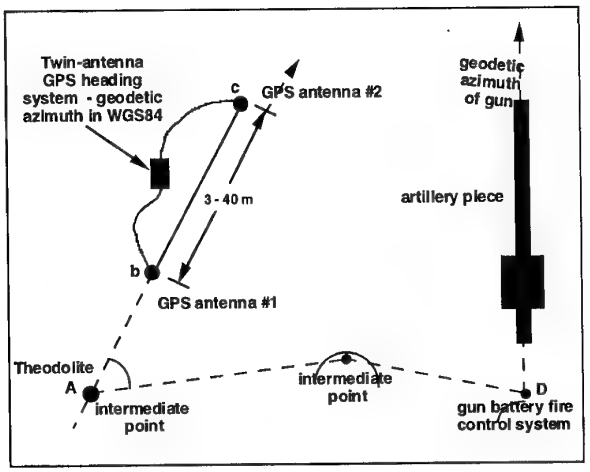

Figure 14
Orientation Transfer from Twin-Antenna GPS Heading System to Gun Battery Fire Control System with a Theodeolite

REFERENCES

Brown, A.K., W.M. Bowles, and T.P. Thorvaldsen (1982) Interferometric Attitude Determination Using the Global Positioning System: A New Gyrotheodolite. Proc. of the Third Intern. Geodetic Symp. on Satellite Doppler Positioning (Las Cruses, N.M., Feb 8-12), DMA/NOS, pp. 1289-1302.

Cannon, M.E., J.B. Schleppe, J.F. McLellan and T.E. Ollevier (1992) Real-Time Heading Determination Using an Integrated GPS-Dead Reckoning System, Proceedings of ION GPS-92, Institute of Navigation, 767-773.

Cannon, M.E., and G. Lachapelle (Convenors) (1994) Proceedings of KIS94, Dept Geomatics Eng., The Univ. of Calgary.

Cannon, M.E., H. Sun, T.E. Owen and M.A. Meindl (1994) Assessment of a non-dedicated GPS receiver system for precise airborne attitude determination. Proceedings of the ION GPS-94, Salt Lake City, September 20-23, 645-654.

Cannon, M.E., G. Lachapelle, and J. Bird (1996) Evaluation of GPS-Aided Artillery Positioning and Orientation Methods. Presented at Biennal Canadian Navigation Society Symposium, 43rd Annual Conference, Canadian Aeronautics and Space Institute, Ottawa, April 29 - May 1.

Cohen, C.E. (1996) Attitude Determination. In Global Positioning System: Theory and Applications, Vol 2, Series on Progress in Astronautrics and Aeronautics, American Institute of Aeronautics and Astronautics, Washington, D.C.

Cohen, C.E. and B.W. Parkinson (1992) Aircraft applications of GPS-based attitude determination. Proceedings of ION GPS-92, Albuquerque, September 16-18, 775-782.

Cohen, C.E., B.D. McNally and B.W. Parkinson (1993) Flight tests of attitude determination using GPS compared against an inertial navigation unit. Navigation, Journal of the Institute of Navigation, 41, 1, 83-97.

Diefes, D., G. Hazel and G. Greenlee (1994) Test Results of GPS Based Attitude Determining System for Marine Navigation. Proceedings of National Technical Meeting, The Institute of Navigation, Alexandria, VA., 893-899.

El-Mowafy, A., and K.P. Schwarz (1995) Epoch-to-Epoch Ambiguity Resolution for Real-Time Attitude Determination Using a GPS Multi-antenna system. Navigation, The Inst. of Navigation, Alexandria, VA, 42, 2, 391-408.

Evans, A.G. (1986) Roll, Pitch, and Yaw Determination Using a GPS Receiver and an Antenna periodically moving in a plane. Marine Geodesy, 10, 1, 43-52.

Ferguson, K., J. Kosmalska, M. Kuhl, J.M. Eichner, K. Kepski and R. Abtahi (1991) Three dimensional attitude determination with the ashtech 3DF 24 channel GPS measurement system. Proceedings of the ION NTM, Phoenix, January 22-24, 35-41.

Kruczynski, L.R., P.C. LI, A.G. Evans, and B.R. Hermann (1989) Using GPS to Determine Vehicle Attitude: USS Yorktown Test Results. Proceedings of GPS-89, The Institute of Navigation, Alexandria, VA, pp. 163-171.

Lachapelle, G., G. Lu, and B. Loncarevic (1994a) Precise shipborne attitude determination using wide antenna spacing. Proc. of KSI94 (Banff, August 30-September 2), Dept Geomatics Eng., The Univ. of Calgary, 323-330.

Lachapelle, G., H. Sun, M.E. Cannon, and G. Lu (1994b) Precise Aircraft-to-Aircraft Positioning Using a Multiple Receiver Configuration. Proc. of National Technical Meeting, The Institute of Navigation, Alexandria, VA., 793-799.

Lu, G., M.E. Cannon, G. Lachapelle, and P. Kielland (1993) Attitude determination in a survey launch using multi-antenna GPS technologies. Proc. of the ION National Technical Meeting, San Francisco, January 20-22, 251-260.

Lu, G., G. Lachapelle, M.E. Cannon, and B. Vogel (1994) Performance Analysis of a Shipborne Gyrocompass with a Multi-Antenna GPS System. Proceedings of PLANS'94, IEEE, New York, pp. 337-343.

McMillan, J.C., D.A.G. Arden, G. Lachapelle, and G. Lu (1994) Dynamic GPS attitude performance using INS/GPS reference, Proc. of the ION GPS94, Salt Lake City, September 21-23, 675-682.

Nesbø, I. (1988) Application of GPS Determined Attitude for Navigation. Proc. GPS88, The Institute of Navigation, Alexandria, VA, 95-100.

Purcell, G.H., J.M. Srinivasan, L.E. Young, S.J. DiNardo, E.L. Hushbeck, T.K. Meehan, T.N. Munson, and T.P. Yunck (1989) Measurement of Aircraft Position, Velocity, and Attitude Using Rogue Receivers. Proc. of 5th Intern. Geodetic Symposium on Satellite Positioning, Las Cruses, 1019-1028.

Rath, J., and P. Ward (1989) Attitude Estimation Using GPS. Proc. of National Technical Meeting (San Meteo, Jan 23-26), The Institute of Navigation, Alexandria, VA, pp. 179-178.

Shuster, M.D. and S.D. Oh (1981) Three-Axis Attitude Determination from Vector Observations. Journal of Guidance and Control, 4, 1, 70-77.

Sun, H., and M.E. Cannon (1995) Evaluation of Heading Determination with the Motorola VP Oncore Using HEAD™ Software. Internal Report, Department of Geomatics Engineering, The University of Calgary.

Ulmer, K., P. Hwang, B.A. Disselkoen, and M. Wagner (1995) Accurate Azimuth from a Single PLGR-GLS DoD GPS Receiver Using Time Relative Positioning. Proceedings of GPS-95 (Palm Springs, September 12-15), The Institute of Navigation, Alexandria, VA, 1733-1741.

van Graas, F. and M. Braasch (1991), GPS Interferometric Attitude and Heading Determination: Initial Flight Test Results, Navigation, The Institute of Navigation, Alexandria, VA, 38, 4, 297-316.

Wertz, J.R. (Ed.) (1978), Spacecraft Attitude Determination and Control, Kluwer Academic Publishers, The Netherlands.

REPORT DOCUMENTATION PAGE

1. Recipient's Reference	2. Originator's Reference	3. Further Reference	4. Security Classification of Document
	AGARD-LS-207	ISBN 92-836-1038-5	UNCLASSIFIED/ UNLIMITED

5. Originator Advisory Group for Aerospace Research and Development
North Atlantic Treaty Organization
7 rue Ancelle, 92200 Neuilly-sur-Seine, France

6. Title

System Implications and Innovative Applications of Satellite Navigation

7. Presented at/sponsored by

The Mission Systems Panel of AGARD and the Consultant and Exchange Programme of AGARD presented on 1-2 July 1996 in Paris, France, 4-5 July 1996 in Rome, Italy, 8-9 July 1996 in Madrid, Spain and 11-12 July 1996 in St. Petersburg, Russia

8. Author(s)/Editor(s)	9. Date
Multiple	June 1996
10. Author's/Editor's Address	**11. Pages**
Multiple	164

12. Distribution Statement There are no restrictions on the distribution of this document. Information about the availability of this and other AGARD unclassified publications is given on the back cover.

13. Keywords/Descriptors

Global positioning system	Technology
Navigation satellites	Utilization
Air navigation	Aircraft

14. Abstract

The Global Positioning Satellite System (GPS) is now operational and GLONASS will soon be declared operational. Meanwhile, INMARSAT has announced its intent to expand its services to include navigation signals broadcast from geostationary satellites, and several industrial organizations plan to provide commercial, satellite-based, navigation services.

With prospects for reliable worldwide service becoming a reality, the technical and financial barriers to innovative applications are being overcome. This Lecture Series will provide an appreciation of the technical, operational and performance features of satellite-based navigation including the signal-in-space and the user equipment for GPS, GLONASS, and integrated GPS/GLONASS implementations; assessment of the quality of service that has been achieved and an introduction to projected service enhancements. The introductory lecture will provide an overview of Satellite based navigation and some of the imaginative uses to which it has already been put. The application of Satellite signals to precision approach and landing for Civil Aviation and for determination of vehicle attitude (orientation) will be featured in the following lectures. Other topics include Quality monitoring of user's navigation solutions, the integration of satellite navigation with inertial measurements and high-precision relative and differential positioning.

This Lecture Series, sponsored by the Mission Systems Panel of AGARD, has been implemented by the Consultant and Exchange Programme.

AGARD

NATO OTAN

7 RUE ANCELLE • 92200 NEUILLY-SUR-SEINE

FRANCE

Télécopie (1)47.38.57.99 • Télex 610 176

DIFFUSION DES PUBLICATIONS

AGARD NON CLASSIFIEES

Aucun stock de publications n'a existé à AGARD. A partir de 1993, AGARD détiendra un stock limité des publications associées aux cycles de conférences et cours spéciaux ainsi que les AGARDographies et les rapports des groupes de travail, organisés et publiés à partir de 1993 inclus. Les demandes de renseignements doivent être adressées à AGARD par lettre ou par fax à l'adresse indiquée ci-dessus. *Veuillez ne pas téléphoner.* La diffusion initiale de toutes les publications de l'AGARD est effectuée auprès des pays membres de l'OTAN par l'intermédiaire des centres de distribution nationaux indiqués ci-dessous. Des exemplaires supplémentaires peuvent parfois être obtenus auprès de ces centres (à l'exception des Etats-Unis). Si vous souhaitez recevoir toutes les publications de l'AGARD, ou simplement celles qui concernent certains Panels, vous pouvez demander à être inclu sur la liste d'envoi de l'un de ces centres. Les publications de l'AGARD sont en vente auprès des agences indiquées ci-dessous, sous forme de photocopie ou de microfiche.

CENTRES DE DIFFUSION NATIONAUX

ALLEMAGNE
Fachinformationszentrum Karlsruhe
D-76344 Eggenstein-Leopoldshafen 2

BELGIQUE
Coordonnateur AGARD-VSL
Etat-major de la Force aérienne
Quartier Reine Elisabeth
Rue d'Evere, 1140 Bruxelles

CANADA
Directeur, Services d'information scientifique
Ministère de la Défense nationale
Ottawa, Ontario K1A 0K2

DANEMARK
Danish Defence Research Establishment
Ryvangs Allé 1
P.O. Box 2715
DK-2100 Copenhagen Ø

ESPAGNE
INTA (AGARD Publications)
Carretera de Torrejón a Ajalvir, Pk.4
28850 Torrejón de Ardoz - Madrid

ETATS-UNIS
NASA Headquarters
Code JOB-1
Washington, D.C. 20546

FRANCE
O.N.E.R.A. (Direction)
29, Avenue de la Division Leclerc
92322 Châtillon Cedex

GRECE
Hellenic Air Force
Air War College
Scientific and Technical Library
Dekelia Air Force Base
Dekelia, Athens TGA 1010

ISLANDE
Director of Aviation
c/o Flugrad
Reykjavik

ITALIE
Aeronautica Militare
Ufficio del Delegato Nazionale all'AGARD
Aeroporto Pratica di Mare
00040 Pomezia (Roma)

LUXEMBOURG
Voir Belgique

NORVEGE
Norwegian Defence Research Establishment
Attn: Biblioteket
P.O. Box 25
N-2007 Kjeller

PAYS-BAS
Netherlands Delegation to AGARD
National Aerospace Laboratory NLR
P.O. Box 90502
1006 BM Amsterdam

PORTUGAL
Estado Maior da Força Aérea
SDFA - Centro de Documentação
Alfragide
2700 Amadora

ROYAUME-UNI
Defence Research Information Centre
Kentigern House
65 Brown Street
Glasgow G2 8EX

TURQUIE
Millî Savunma Başkanliği (MSB)
ARGE Dairesi Başkanliği (MSB)
06650 Bakanliklar-Ankara

Le centre de distribution national des Etats-Unis ne détient PAS de stocks des publications de l'AGARD.
D'éventuelles demandes de photocopies doivent être formulées directement auprès du NASA Center for AeroSpace Information (CASI) à l'adresse ci-dessous. Toute notification de changement d'adresse doit être fait également auprès de CASI.

AGENCES DE VENTE

NASA Center for
AeroSpace Information (CASI)
800 Elkridge Landing Road
Linthicum Heights, MD 21090-2934
Etats-Unis

ESA/Information Retrieval Service
European Space Agency
10, rue Mario Nikis
75015 Paris
France

The British Library
Document Supply Division
Boston Spa, Wetherby
West Yorkshire LS23 7BQ
Royaume-Uni

Les demandes de microfiches ou de photocopies de documents AGARD (y compris les demandes faites auprès du CASI) doivent comporter la dénomination AGARD, ainsi que le numéro de série d'AGARD (par exemple AGARD-AG-315). Des informations analogues, telles que le titre et la date de publication sont souhaitables. Veuiller noter qu'il y a lieu de spécifier AGARD-R-nnn et AGARD-AR-nnn lors de la commande des rapports AGARD et des rapports consultatifs AGARD respectivement. Des références bibliographiques complètes ainsi que des résumés des publications AGARD figurent dans les journaux suivants:

Scientific and Technical Aerospace Reports (STAR)
publié par la NASA Scientific and Technical
Information Division
NASA Headquarters (JTT)
Washington D.C. 20546
Etats-Unis

Government Reports Announcements and Index (GRA&I)
publié par le National Technical Information Service
Springfield
Virginia 22161
Etats-Unis
(accessible également en mode interactif dans la base de données bibliographiques en ligne du NTIS, et sur CD-ROM)

Imprimé par le Groupe Communication Canada
45, boul. Sacré-Cœur, Hull (Québec), Canada K1A 0S7

AGARD

NATO OTAN

7 RUE ANCELLE • 92200 NEUILLY-SUR-SEINE

FRANCE

Telefax (1)47.38.57.99 • Telex 610 176

DISTRIBUTION OF UNCLASSIFIED

AGARD PUBLICATIONS

AGARD holds limited quantities of the publications that accompanied Lecture Series and Special Courses held in 1993 or later, and of AGARDographs and Working Group reports published from 1993 onward. For details, write or send a telefax to the address given above. *Please do not telephone.*

AGARD does not hold stocks of publications that accompanied earlier Lecture Series or Courses or of any other publications. Initial distribution of all AGARD publications is made to NATO nations through the National Distribution Centres listed below. Further copies are sometimes available from these centres (except in the United States). If you have a need to receive all AGARD publications, or just those relating to one or more specific AGARD Panels, they may be willing to include you (or your organisation) on their distribution list. AGARD publications may be purchased from the Sales Agencies listed below, in photocopy or microfiche form.

NATIONAL DISTRIBUTION CENTRES

BELGIUM
Coordonnateur AGARD — VSL
Etat-major de la Force aérienne
Quartier Reine Elisabeth
Rue d'Evere, 1140 Bruxelles

CANADA
Director Scientific Information Services
Dept of National Defence
Ottawa, Ontario K1A 0K2

DENMARK
Danish Defence Research Establishment
Ryvangs Allé 1
P.O. Box 2715
DK-2100 Copenhagen Ø

FRANCE
O.N.E.R.A. (Direction)
29 Avenue de la Division Leclerc
92322 Châtillon Cedex

GERMANY
Fachinformationszentrum Karlsruhe
D-76344 Eggenstein-Leopoldshafen 2

GREECE
Hellenic Air Force
Air War College
Scientific and Technical Library
Dekelia Air Force Base
Dekelia, Athens TGA 1010

ICELAND
Director of Aviation
c/o Flugrad
Reykjavik

ITALY
Aeronautica Militare
Ufficio del Delegato Nazionale all'AGARD
Aeroporto Pratica di Mare
00040 Pomezia (Roma)

LUXEMBOURG
See Belgium

NETHERLANDS
Netherlands Delegation to AGARD
National Aerospace Laboratory, NLR
P.O. Box 90502
1006 BM Amsterdam

NORWAY
Norwegian Defence Research Establishment
Attn: Biblioteket
P.O. Box 25
N-2007 Kjeller

PORTUGAL
Estado Maior da Força Aérea
SDFA - Centro de Documentação
Alfragide
2700 Amadora

SPAIN
INTA (AGARD Publications)
Carretera de Torrejón a Ajalvir, Pk.4
28850 Torrejón de Ardoz - Madrid

TURKEY
Millî Savunma Başkanliği (MSB)
ARGE Dairesi Başkanliği (MSB)
06650 Bakanliklar-Ankara

UNITED KINGDOM
Defence Research Information Centre
Kentigern House
65 Brown Street
Glasgow G2 8EX

UNITED STATES
NASA Headquarters
Code JOB-1
Washington, D.C. 20546

The United States National Distribution Centre does NOT hold stocks of AGARD publications.
Applications for copies should be made direct to the NASA Center for AeroSpace Information (CASI) at the address below.
Change of address requests should also go to CASI.

SALES AGENCIES

NASA Center for
AeroSpace Information (CASI)
800 Elkridge Landing Road
Linthicum Heights, MD 21090-2934
United States

ESA/Information Retrieval Service
European Space Agency
10, rue Mario Nikis
75015 Paris
France

The British Library
Document Supply Centre
Boston Spa, Wetherby
West Yorkshire LS23 7BQ
United Kingdom

Requests for microfiches or photocopies of AGARD documents (including requests to CASI) should include the word 'AGARD' and the AGARD serial number (for example AGARD-AG-315). Collateral information such as title and publication date is desirable. Note that AGARD Reports and Advisory Reports should be specified as AGARD-R-nnn and AGARD-AR-nnn, respectively. Full bibliographical references and abstracts of AGARD publications are given in the following journals:

Scientific and Technical Aerospace Reports (STAR)
published by NASA Scientific and Technical
Information Division
NASA Headquarters (JTT)
Washington D.C. 20546
United States

Government Reports Announcements and Index (GRA&I)
published by the National Technical Information Service
Springfield
Virginia 22161
United States
(also available online in the NTIS Bibliographic
Database or on CD-ROM)

Printed by Canada Communication Group
45 Sacré-Cœur Blvd., Hull (Québec), Canada K1A 0S7

ISBN 92-836-1038-5